

# **PERFORMANCE EVALUATION OF FLEXIBLE JUTE-NATURAL RUBBER COMPOSITES FOR IMPACT BEHAVIOUR**

Thesis

Submitted in partial fulfilment of the requirements for the degree of

**DOCTOR OF PHILOSOPHY**

by

**VISHWAS M.**



**DEPARTMENT OF MECHANICAL ENGINEERING  
NATIONAL INSTITUTE OF TECHNOLOGY KARNATAKA  
SURATHKAL, MANGALORE-575 025**

**AUGUST, 2020**



## DECLARATION

I hereby declare that the Research Thesis titled “**PERFORMANCE EVALUATION OF FLEXIBLE JUTE-NATURAL RUBBER COMPOSITES FOR IMPACT BEHAVIOUR**” which is being submitted to the **National Institute of Technology Karnataka, Surathkal** in partial fulfillment of the requirements for the award of the degree of **Doctor of Philosophy** in **Department of Mechanical Engineering** is a *bonafide report of the research work carried out by me*. The material contained in this Research Thesis has not been submitted to any other Universities or Institutes for the award of any degree.

Register Number: 177051ME024

Name of the Research Scholar: **VISHWAS M.**

Signature of the Research Scholar:



Department of Mechanical Engineering

Place: NITK-Surathkal

Date: 26/08/2020



## CERTIFICATE

This is to certify that the Research Thesis titled “**PERFORMANCE EVALUATION OF FLEXIBLE JUTE-NATURAL RUBBER COMPOSITES FOR IMPACT BEHAVIOUR**” submitted by **Mr. Vishwas M. (Register Number: 177051ME024)** as the record of the research work carried out by him, *is accepted as the Research Thesis submission* in partial fulfillment of the requirements for the award of the degree of **Doctor of Philosophy**.

 27/08/2020

**Dr. Sharnappa Joladarashi**  
Research Guide

 27/08/2020

**Dr. S M Kulkarni**  
Research Guide



**Chairman-DRPC**

Date: 27/08/2020









## ACKNOWLEDGEMENT

It provides an immense pleasure to acknowledge all the people who have helped, encouraged and supported throughout my dissertation. It is my humble appreciation towards everyone who has sacrificed their comfort in some form or other on the successful completion of my doctoral studies.

I am highly indebted to almighty **Lord Veerabhadra Swamy** and **Lord Shiva** who always blessed me to overcome every hurdles of my life and accomplish the goals with ease. I express my sincere pranams to His Holiness late **Dr. Sri Sri Sri Shivakumara Swamigalu** and **Sri. Siddalinga Swamigalu** for their blessings.

I would like to express my sincere gratitude and heartiest thanks to my supervisors **Dr. Sharnappa Joladarashi**, Associate Professor and **Dr. S M Kulkarni**, Professor, Department of Mechanical Engineering, National Institute of Technology Karnataka (N.I.T.K), Surathkal, for considering me worthy of working under their esteemed guidance. This research outcome is a result of their excellent guidance and support throughout the work. This thesis could not have attained its present form, both in content and presentation without their active interest, timely support, direction and valuable guidance. My professional ethics, problem solving skills and knowledge level have received the professional boost through all those days I was able to spend in their proximity. Their vast knowledge and insight into the area of the composite materials have helped me to overcome the hurdles throughout my dissertation. The words are insufficient to express my deep feeling and heartfelt thanks to my supervisors for their un hesitated guidance throughout my doctoral work. For all this, I will remain grateful to them throughout my career.

I take this opportunity to thank **Dr. Narendranath S**, Professor, Department of Mechanical Engineering and **Dr. Shrikantha S. Rao**, Professor and Head, Department of Mechanical Engineering for their continuous and timely support. I would like to express the deepest appreciation to the members of research progress assessment committee **Dr. Subhaschandra Kattimani** and **Dr. Subhash C. Yaragal** for their valuable remarks, suggestions and technical advices during the length of my research.

I wish to express my sincere gratitude to all the faculty members of Department of Mechanical Engineering, of N.I.T.K Surathkal for their unbiased appreciation and support all through this research work. I take this opportunity to thank all my friends and colleagues of both N.I.T.K and S.I.T, Tumakuru along with all my students of S.I.T, Tumakuru who have supported directly or indirectly to expedite towards my goal.

I would like to take this opportunity to express my gratitude to my family. Words cannot express how grateful I am to my father **Mr. T G Mahesh** and mother **Mrs. Sunitha Mahesh** for their blessings, love, support and all the sacrifices that they have made on my behalf. I express my special gratitude towards my younger brother **Dr. Vinyas Mahesh** for the timely suggestions and support that he has rendered during my entire life.

It gives me immense pleasure to express my sincere gratitude to my wife **Smt. Chandrika Vishwas** and my son **Master Viaan V. Aradhya** for their unmatched sacrifice, love and support towards me. I express my sincere thanks towards **Manjunath Rubbers**, Baikampady, Mangaluru, **Dr. Chittappa H C.**, Professor, UVCE, Bengaluru, **Dr. Guled F D.** for providing the materials and testing facilities. I am grateful to **Dr. G R Bharath Sai Kumar**, **Nagaraj G.**, **Koppal Nagaraj**, **Kiran V C S.**, **Shashidhara N.**, **Nandeesh**, **Dr. Vasu M**, **Dr. Pradeep V Badiger**, **Jagadeesh**, **Chetan H C**, **Vinayak Kallannanavar**, **Gangadhar**, **Mr. and Mrs Naveen Kumar H S**, **Mr. and Mrs Deepak Raj** who stood by me during my difficult days and supported me by being a source of my courage. Last but not the least, I am very much thankful to **Dr. Shivakumaraiah**, CEO, SIT, Tumakuru, **Sri T K Nanjundappa**, Secretary, Sree Siddaganga Education Society, Tumakuru and management of **Siddaganga Institute of Technology**, Tumakuru who deputed me under QIP to pursue my Ph.D.

**VISHWAS M.**

National Institute of Technology Karnataka, Surathkal

Date: 26/08/2020

## ABSTRACT

A composite material is made from two or more constituent materials with significantly different physical or chemical properties which are combined to produce a material with characteristics different from the individual components. 'Flexible composites' is a term coined to identify the composites making use of elastomeric polymers as matrix. These flexible composites exhibit usable range of deformations which are much larger than conventional stiff composites. The ability of flexible composites to undergo larger deformation and still provide high load carrying ability makes them suitable for many engineering applications. Flexible composites are better energy absorbers compared to conventional stiff composites subjected to impact loading.

The objectives and scope of the present study includes proposing, developing and characterizing the flexible 'green' composite for impact applications. An extensive literature review was carried out to explore the potential constituent materials for impact applications and accordingly the present study is carried out to explore the possible use of jute and rubber for impact applications. Initially, the feasibility of using natural rubber (NR) as a constituent material in composite is studied using commercially available finite element (FE) package. Further different stacking sequences of the flexible green sandwich composite are optimized and the three stacking sequences are selected for experimental study. These three optimized stacking sequences of the proposed flexible green sandwich composite are prepared using compression moulding technique and are characterized for their physical and mechanical properties. Further, the proposed flexible green composites are studied for their abrasive behaviour under two body environments and erosive behaviour under slurry environment. Finally, the impact behaviour of the proposed flexible composites is studied under low velocity impact (LVI) and lower ballistic impact.

The mechanical characterization of the proposed flexible composites revealed that the composite with jute/rubber/jute (JRJ) exhibits better tensile and tear strength compared to jute/rubber/rubber/jute (JRRJ) and jute/rubber/jute/rubber/jute (JRJRJ) with JRJ exhibiting 57.7% and 64.47% higher tensile strength compared to JRRJ and JRJRJ respectively. Also, the tear strength of JRJ is found to be 0.4% and 2.38%

higher than JRRJ and JRJRJ respectively. The interlaminar shear strength (ILSS) studies shows that short beam strength of JRJRJ is better compared to JRRJ and JRJ with JRJRJ exhibiting nearly 2.1 times and 2.75 times better ILSS compared to JRRJ and JRJ respectively.

The proposed flexible green composites are further studied for their abrasive behaviour under two body environments and erosive behaviour under slurry environment, the outcome of which reveals that JRJ provides better results compared to its counterpart JRRJ and JRJRJ. Various factors affecting the wear behaviour of the flexible composites are also studied from which it is clear that abrading distance and sand concentration affects the weight loss of the proposed flexible green composite in case of two body wear and slurry erosion respectively.

Flexible 'green' composites of different stacking sequences are further subjected to impact tests at low velocity and lower ballistic velocity at different impact energies. The results of low velocity impact reveals that flexible green composite with JRJ stacking sequence exhibit better energy absorption and the stacking sequences JRJRJ exhibit better resistance to damage with no appreciable variation in specific energy absorption of the composites. The lower ballistic impact study reveals that the flexible composites are better energy absorbers with JRJRJ exhibiting better lower ballistic response compared to JRJ and JRRJ. The ballistic limit of JRJRJ is enhanced by 39.7% and 6% compared to JRJ and JRRJ respectively. The energy absorption at ballistic limit of JRJRJ is more compared to JRJ and JRRJ by 97.7% and 12.7% respectively. The energy absorption of JRRJ is enhanced by 75.5% compared to JRJ. The specific energy absorption (SEA) of JRJRJ is enhanced by 52% and 2.7% compared to JRJ and JRRJ respectively. The proposed flexible green composite can be a potential material for sacrificial structures in order to protect the primary structural components.

**KEYWORDS:** Flexible composite; Natural rubber; Jute; Impact; Two body abrasion; Slurry erosion; Design of experiments; Multi attribute decision making.





## TABLE OF CONTENTS

1	INTRODUCTION .....	1
1.1	Composites and its classification .....	2
1.2	Sandwich composite.....	4
1.2.1	Core materials for sandwich structure .....	6
1.2.2	Skin materials for sandwich structure.....	8
1.2.3	Adhesives.....	10
1.2.4	Characteristics of flexible sandwich composite.....	11
1.2.5	Advantage and disadvantages of flexible sandwich composites .....	12
1.2.6	Applications of flexible composites.....	13
1.3	Approches for evaluating the mechanical properties of composites .....	13
1.3.1	Theoretical approach.....	14
1.3.2	Finite element approach.....	15
1.3.3	Experimental approach .....	17
1.3.4	Optimization methods.....	21
2	LITERATURE REVIEW .....	24
2.1	Reinforcement material .....	24
2.2	Matrix material.....	38
2.3	Core materials used in polymer matrix composites for impact applications	46
2.4	Impact of composites .....	50
2.4.1	Analytical and finite element modeling approach .....	54
2.4.2	Experimental approach .....	57
2.5	Wear characterization.....	63
2.6	Material selection approaches .....	73
2.7	Research gap and motivation for the work.....	80
2.8	Objectives of proposed work .....	80

2.9	Scope of proposed work .....	81
3	METHODOLOGY .....	83
3.1	Raw materials and processing methods .....	84
3.1.1	Reinforcement (Jute).....	84
3.1.2	Natural rubber .....	85
3.1.3	B stage cured pre peg .....	86
3.1.4	Processing techniques .....	86
3.2	Analytical approach.....	88
3.2.1	Analytical approach for lower ballistic impact .....	88
3.3	Finite element analysis .....	93
3.3.1	Comparative study of impact behaviour of jute-epoxy composite laminate and jute-epoxy-rubber sandwich composite .....	94
3.3.2	Comparative study on stiff and flexible composites.....	98
3.3.3	Identification of different stacking sequences of flexible composite ....	99
3.3.4	Determining optimum configuration of flexible composite .....	100
3.3.5	Finite element analysis of lower ballistic impact.....	101
3.4	Testing.....	103
3.4.1	Curing characteristics of natural rubber based pre peg.....	103
3.4.2	Determining the peel strength of the constituents.....	103
3.4.3	Physical and mechanical characterization .....	105
3.4.4	Erosion and abrasion testing .....	108
3.4.5	Impact testing.....	113
3.5	Optimization using multi attribute decision making approach .....	117
3.5.1	VIKOR method.....	118
3.5.2	PSI method.....	120
4	RESULTS AND DISCUSSIONS .....	123



4.1	Analytical approach.....	123
4.2	Finite element analysis .....	123
4.2.1	Results of comparative study on impact behaviour of jute-epoxy composite laminate and jute-epoxy-rubber sandwich composite.....	123
4.2.2	Results of comparative study on stiff flexible composite .....	131
4.2.3	Results of identification of different configurations of flexible composite.....	131
4.2.4	Results of determining optimum configuration of flexible composite	132
4.3	Testing.....	136
4.3.1	Results of curing characteristics of natural rubber based pre peg .....	136
4.3.2	Results of determining peel strength of constituents .....	137
4.3.3	Results of physical and mechanical characterization.....	139
4.3.4	Results of erosion and abrasive study .....	153
4.3.5	Results of impact testing.....	164
4.4	Optimization using multi attribute decision making approach .....	195
4.4.1	Results of VIKOR method.....	195
4.4.2	Results of PSI method.....	199
5	CONCLUSION AND FUTURE SCOPE.....	203
5.1	Conclusion.....	203
5.2	Future scope .....	208
	REFERENCE.....	209
	LIST OF PUBLICATIONS BASED ON PH.D. RESEARCH WORK .....	254
	<b>LIST OF FIGURES</b>	
	Figure 1.1 Classification of composites based on reinforcements (Otani et al. 2014) ..	3
	Figure 1.2 Analogy between (a) I-Beam and (b) Sandwich .....	5
	Figure 2.1 Classification of fibers (Sathishkumar et al. 2014) .....	25
	Figure 2.2 Popular natural fibers extracted from different parts of plant .....	26

Figure 2.3 Structure of natural fiber (Rong et al. 2001) .....	28
Figure 2.4 Criteria affecting natural fiber selection in composite (AL-Oqla and Sapuan 2014) .....	34
Figure 2.5 Physical and mechanical properties of Polymer matrix .....	43
Figure 2.6 Classification of core based on their structures (Pflug et al. 2002).....	47
Figure 2.7 Structure of cores.....	47
Figure 2.8 Stages of development of impact analysis (Bogenfeld et al. 2018) .....	50
Figure 2.9 Damage propagation in (a) flexible composite and (b) stiff composite(Saghafi et al. 2019) .....	62
Figure 2.10 Approach to design the optimum configuration of polymer matrix composites for wear application (Friedrich et al. 2002) .....	64
Figure 2.11 Classification of different tests available for tribological characterization .....	65
Figure 2.12 Interaction of bio tribo system towards global sustainable development (Nirmal et al. 2015; Tzanakis et al. 2012) .....	66
Figure 2.13 Parameters affecting wear behaviour of polymer matrix composites .....	67
Figure 2.14 Classification of polymers for wear applications (Friedrich 2018).....	68
Figure 2.15 Sequence of wear classification (Stachowiak and Batchelor 2011).....	69
Figure 2.16 Variation of wear rate for steel and rubber for different erodent (Sare et al. 2001) .....	72
Figure 2.17 Steps involved in decision making (Bhushan 2004; Jackson and Pascual 2008).....	73
Figure 2.18 Classification of ranking methods for material selection (Jahan et al. 2010).....	75
Figure 3.1 Methodology of proposed work .....	83
Figure 3.2 Jute woven fabric.....	84
Figure 3.3 Natural rubber sheet .....	85
Figure 3.4 B stage cured pre peg .....	86
Figure 3.5 Steps involved in processing of flexible composites.....	87
Figure 3.6 Cone formation at the back face of the target.....	88
Figure 3.7 Schematic representation of (a) normal and (b) oblique impact of jute epoxy composite .....	95

Figure 3.8 Schematic representation of (a) normal and (b) oblique impact of jute epoxy-rubber-jute epoxy sandwich composite .....	95
Figure 3.9 Modeling of (a) jute epoxy and (b) jute epoxy-rubber-jute epoxy composite .....	96
Figure 3.10 Meshing of (a) jute epoxy and (b) jute epoxy-rubber-jute epoxy composite .....	96
Figure 3.11 Boundary conditions applied to (a) jute epoxy and (b) jute epoxy-rubber-jute epoxy composite .....	97
Figure 3.12 Assembled view of jute epoxy laminate and jute/rubber/jute sandwich along with boundary condition and meshing .....	98
Figure 3.13 Assembled view of jute/rubber/jute configuration and boundary condition applied.....	101
Figure 3.14 Meshing of jute/rubber/jute composite and impactor.....	101
Figure 3.15 Modeling of proposed flexible composite laminates and projectile.....	102
Figure 3.16 T-Peel specimens of (a) Jute-Rubber gum and (b) Rubber-Rubber gum .....	104
Figure 3.17 Initial separation obtained in T-Peel specimens .....	104
Figure 3.18 Peel specimen mounted on universal testing machine .....	105
Figure 3.19 Tensile test specimen.....	107
Figure 3.20 Tear test specimen .....	107
Figure 3.21 Specimens used for interlaminar shear strength testing along with its cross section and (b) its loading in universal testing machine .....	108
Figure 3.22 Specimen used for slurry erosion test.....	110
Figure 3.23 Slurry erosion setup.....	110
Figure 3.24 Sand used as abrasive medium .....	110
Figure 3.25 Samples, schematic and DIN abrader.....	112
Figure 3.26 Drop weight impact set up and specimen used .....	114
Figure 3.27 Gas gun arrangement used to carry out high velocity impact test.....	116
Figure 3.28 (a) Specimen clamped in fixture and (b) projectile used.....	116
Figure 3.29 Flowchart of the proposed (a)VIKOR and (b)PSI methods .....	118
Figure 4.1 Variation of contact force with time for (a) jute epoxy and (b) jute epoxy-rubber-jute epoxy composite.....	124

Figure 4.2 Variation of kinetic energy with time for (a) jute epoxy and (b) jute epoxy-rubber-jute epoxy composite.....	126
Figure 4.3 Variation of deflection with time for (a) jute epoxy and (b) jute epoxy-rubber-jute epoxy composite.....	128
Figure 4.4 Von Mises stress patterns in jute epoxy laminate and jute epoxy-rubber-jute epoxy sandwich.....	129
Figure 4.5 Schematic representation of damage progression in (a) jute epoxy and (b) jute epoxy-rubber-jute epoxy composite .....	130
Figure 4.6 Variation in (a) kinetic energy and (b) contact force for different configurations .....	132
Figure 4.7 Comparison of sp. energy absorption and contact force for different configurations .....	133
Figure 4.8 Damage behavior of various configurations of flexible composite.....	134
Figure 4.9 Oscillating disk rheometer graph representing curing behaviour of natural rubber based B stage cure pre peg .....	137
Figure 4.10 Force vs displacement plot for jute and rubber .....	138
Figure 4.11 Water absorption of the composites over a period of time.....	142
Figure 4.12 Tensile specimens of (a) jute/rubber/jute (b) jute/rubber/rubber/jute and (c) jute/rubber/jute/rubber/jute after fracture .....	143
Figure 4.13 Stress v/s strain plots of proposed flexible composites .....	144
Figure 4.14 Fractography of (a) jute/rubber/jute (b) jute/rubber/rubber/jute and (c) jute/rubber/jute/rubber/jute after tensile test .....	145
Figure 4.15 Fractured specimens of (a) jute/rubber/jute (b) jute/rubber/rubber/jute and (c) jute/rubber/jute/rubber/jute after tear test .....	146
Figure 4.16 Force v/s displacement plots of proposed flexible composites .....	147
Figure 4.17 Fractography of (a) jute/rubber/jute (b) jute/rubber/rubber/jute and (c) jute/rubber/jute/rubber/jute after tear test .....	147
Figure 4.18 (a) Load-displacement graphs and (b) normalized interlaminar shear strength graph for flexible composites.....	148
Figure 4.19 Variation of interlaminar shear strength for flexible composites.....	150
Figure 4.20 Short beam failure pattern of jute/rubber/jute .....	150
Figure 4.21 Short beam failure pattern of jute/rubber/rubber/jute.....	151

Figure 4.22 Short beam failure pattern of jute/rubber/jute/rubber/jute.....	151
Figure 4.23 Fractography analysis of flexible composite.....	153
Figure 4.24 Main effect plot for means and signal to noise ratio for slurry erosion study.....	155
Figure 4.25 Interaction effect plot for weight loss during slurry erosion study .....	156
Figure 4.26 Comparison of experimental and calculated weight loss for slurry erosion study.....	158
Figure 4.27 Main effect plots for means and signal to noise ratios (Two body wear) .....	160
Figure 4.28 Interaction plots for means and signal to noise ratios for two body abrasion study .....	160
Figure 4.29 Comparison of experimental and predicted specific wear rate for two body abrasion study .....	163
Figure 4.30 Surface morphology of composite at different stages of wear.....	164
Figure 4.31 Energy absorbed by proposed flexible composite at various energy levels .....	166
Figure 4.32 Variation of energy absorption ratio of flexible composites at different impact energies .....	168
Figure 4.33 Force-Time history of proposed flexible composites at impact energy of 10.24 J and variation of peak force at different impact energies .....	169
Figure 4.34 Enlarged View of the damages on the front face of the flexible composites subjected to low velocity impact at different energy levels.....	174
Figure 4.35 Variation of depth of damage against (a) energy absorption ratio and (b) coefficient of restitution.....	176
Figure 4.36 Schematic representing the relation between rebound velocity and extent of damage for (a) jute/rubber/jute and (b) jute/rubber/jute/rubber/jute in case of low velocity impact.....	176
Figure 4.37 Internal damage mechanism in jute/rubber/jute flexible composite subjected to low velocity impact at (a) 10.24 J (b) 23.95 J and (c) 37.67 J.....	177
Figure 4.38 Internal damage mechanism in jute/rubber/rubber/jute flexible composite subjected to low velocity impact at (a) 10.24 J (b) 23.95 J and (c) 37.67 J.....	178

Figure 4.39 Internal damage mechanism in jute/rubber/jute/rubber/jute flexible subjected to low velocity impact composite at (a) 10.24 J (b) 23.95 J and (c) 37.67 J .....	178
Figure 4.40 Schematic of damage resistance distribution in flexible composite in case of lower ballistic impact.....	190
Figure 4.41 Proposed damage mechanism validated with experimental and finite element approach .....	191
Figure 4.42 Damage mechanism of flexible composites at (a) ballistic limit; (b) 80 m/s; (c) 100 m/s and (d) 120 m/s. ....	192
Figure 4.43 Scanning electron microscope images exhibiting the damage mechanism involved.....	193
Figure 4.44 Damage mechanism of flexible composites for no complete penetration .....	194

## LIST OF TABLES

Table 2.1 Comparison between natural and synthetic fibers .....	27
Table 2.2 Chemical composition of natural fibers.....	30
Table 2.3 Physical and mechanical properties .....	32
Table 2.4 Natural fibers used for impact applications .....	34
Table 2.5 Characteristics of thermoset and thermoplastic .....	38
Table 2.6 Polymer matrix composites resulting from thermoset and thermoplastic matrix systems .....	39
Table 2.7 Applications of polymer matrix composites .....	41
Table 2.8 Matrix materials used in impact applications .....	44
Table 2.9 Core materials used in polymer matrix composites.....	47
Table 2.10 Reported research on polymer matrix composites subjected to impact.....	51
Table 2.11 Natural fibers in polymer matrix composites for low velocity impact applications .....	63
Table 2.12 Fibers and Polymers used in polymer matrix composites for tribological application.....	66
Table 2.13 Temperature range and abrasion resistance of various elastomers.....	72
Table 2.14 Multi criteria decision making methods used for material selection.....	77

Table 3.1 Properties of jute .....	84
Table 3.2 Properties of natural rubber sheet .....	85
Table 3.3 Properties of NR based B stage cured pre peg.....	86
Table 3.4 Material properties of structural steel and rubber .....	97
Table 3.5 Material properties of jute epoxy .....	97
Table 3.6 Element and mesh details used in finite element analysis .....	97
Table 3.7 Material properties used for jute epoxy and jute/rubber/jute composite .....	99
Table 3.8 Details of element type used in finite element analysis .....	99
Table 3.9 Configurations of composite considered .....	100
Table 3.10 Type of elements and number of elements used in composite plate and projectile .....	102
Table 3.11 Material properties used in finite element analysis .....	103
Table 3.12 Stacking sequences and fiber weight percentage.....	105
Table 3.13 Factors and levels used .....	109
Table 3.14 Factors and levels for two body wear .....	113
Table 3.15 Impact test conditions .....	114
Table 4.1 Contact force variation at various loading conditions .....	125
Table 4.2 Kinetic energy and internal energy for jute epoxy laminate and jute epoxy-rubber-jute epoxy sandwich.....	127
Table 4.3 Deflection for jute epoxy laminate and jute epoxy-rubber-jute epoxy sandwich .....	129
Table 4.4 Energy absorption of jute epoxy and jute epoxy/rubber/jute epoxy composite .....	131
Table 4.5 Configurations of composite considered in the present study .....	131
Table 4.6 Summary of energy absorbed and contact force during impact behaviour of different configurations of flexible composites through finite element approach.....	135
Table 4.7 Cure characteristics of natural rubber based B stage cure pre peg matrix.	137
Table 4.8 Summary of peel strength of rubber and jute when bonded with natural rubber based B stage cured pre peg .....	138
Table 4.9 Summary of physical and mechanical characterization.....	139
Table 4.10 Average experimental interlaminar shear strength values of flexible composites.....	149

Table 4.11 Response, signal to noise ratio and mean for various combinations of control factors for different stacking sequence for slurry erosion study .....	154
Table 4.12 Response table for signal to noise ratio of all three stacking sequences for slurry erosion study.....	154
Table 4.13 Analysis of variance for weight loss during slurry erosion study.....	156
Table 4.14 Comparison on experimental and calculated weight loss for slurry erosion study.....	157
Table 4.15 Response and signal to noise ratio for the trials during two body abrasion study.....	159
Table 4.16 Response table for signal to noise ratio for two body abrasion study .....	159
Table 4.17 Analysis of variance for weight loss during two body abrasion study ....	161
Table 4.18 Comparison of experimental and predicted values of specific wear rate for two body abrasive study.....	162
Table 4.19 Summary of energy absorption, impact damage initiation and peak force during low velocity impact .....	165
Table 4.20 Specific energy absorption of proposed flexible composites subjected to low velocity impact.....	167
Table 4.21 Coefficient of restitution and energy loss percentage of the flexible composites subjected to low velocity impact.....	172
Table 4.22 Depth of damage of the proposed flexible composite .....	173
Table 4.23 Ballistic limits of proposed flexible composites determined analytically, through FE approach and experimentally .....	180
Table 4.24 Residual velocities of the proposed flexible composites at different lower ballistic impact velocities.....	181
Table 4.25 Energy absorption of the proposed flexible composites at the ballistic limit .....	182
Table 4.26 Energy absorption at lower ballistic impact velocity of 80m/s, 100m/s and 120m/s.....	183
Table 4.27 Energy absorption percentage of proposed flexible composites .....	185
Table 4.28 The areal density of the flexible composite .....	187
Table 4.29 Specific energy absorption of the proposed flexible composites at the ballistic limit .....	187



Table 4.30 Specific energy absorption of the proposed flexible composites at impact velocity of 80 m/s, 100 m/s and 120 m/s .....	188
Table 4.31 Performance defining attributes description used in MADM.....	195
Table 4.32 Decision matrix for VIKOR .....	196
Table 4.33 Normalized matrix for VIKOR.....	196
Table 4.34 Weights calculated from the entropy method .....	197
Table 4.35 Weighted normalized matrix for VIKOR .....	198
Table 4.36 Positive and negative ideal solution for VIKOR .....	198
Table 4.37 Utility and regret measures for VIKOR.....	199
Table 4.38 Vikor index for $\alpha = 0.5$ .....	199
Table 4.39 Normalized matrix and mean values of normalized data for PSI.....	200
Table 4.40 Preference variation value, deviation in preference value and overall preference value .....	200
Table 4.41 PSI values and ranking of alternatives.....	201
Table 4.42 Results of VIKOR and PSI methods.....	201

## NOMENCLATURE

### ABBREVIATIONS

ANOVA	:	Analysis of Variance
CoR	:	Coefficient of Restitution
DOE	:	Design of Experiments
ELP	:	Energy Loss Percentage
FE	:	Finite Element
HVI	:	High Velocity Impact
ILSS	:	Interlaminar Shear Strength
JE	:	Jute-Epoxy
JE-R-JE	:	Jute Epoxy-Rubber-Jute Epoxy
JRJ	:	Jute/Rubber/Jute
JRJRJ	:	Jute/Rubber/Jute/Rubber/Jute
JRRJ	:	Jute/Rubber/Rubber/Jute
LVI	:	Low Velocity Impact
MADM	:	Multi Attribute Decision Making
MCDM	:	Multi Criteria Decision Making
NR	:	Natural Rubber
PSI	:	Preferential Selection Index
SEA	:	Specific Energy Absorption
SN	:	Signal to Noise
VIKOR	:	Vlise Kriterijumska Optimizacija Kompromisno Resenje

### NOTATIONS

$E_a$	:	Absorbed Energy
$E_i$	:	Impact Energy
$E_a^{bl}$	:	Energy Absorbed at Ballistic Limit
$E_{TF}$	:	Energy Absorption During Tensile Failure of Primary Yarns
$E_{eds}$	:	Total Energy Absorption by Elastic Deformation of Secondary Yarns
$E_t$	:	Energy Absorption by Matrix/Interleaved NR Tearing Mechanism
$E_{KE}$	:	Kinetic Energy Of Moving Projectile
$E_j$	:	Entropy of Index j

$F_{sbs}$	:	Short Beam Strength
$K_s$	:	Specific Wear Rate
$P_{ij}$	:	Proportion of the Index
$P_s$	:	Peel Strength
$PSI_i$	:	Preferential Selection Index Value
$Q_i$	:	VIKOR Index
$R_i$	:	Regret Measure
$S_i$	:	Utility Measure
$T_s$	:	Tear Strength
$t_{s2}$	:	Scorch Time
$t_{c90}$	:	90% Cure Time
$v_i$	:	Impact Velocity
$v_r$	:	Residual Velocity
$v_{bl}$	:	Ballistic Limit Velocity
$v_{ij}$	:	Standardized Value of Weight
$V_l$	:	Volume Loss
$w_j$	:	Entropy Weight of Index j



## **CHAPTER 1**

### **1 INTRODUCTION**

Advancement in the area of materials defines the evolution of mankind. Extent of usage of materials decides the development of any country in this world. Usage of wide variety of materials in different engineering equipments to satisfy the purpose is mainly due to industrial revolution. The past few decades have witnessed a significant development in the field of materials, particularly in the field of composites. Composites have made it possible for designers to extend their material selection possibilities to suit to a particular need. Usually a common man does not notice beyond the architecture and fine finishing of the structures such as radome in aerospace, bumper in automobiles made up of glass fiber reinforced plastic (GFRP) and fuselage in aerospace, doors, hoods, fenders in automobiles made up of carbon fiber reinforced plastic (CFRP). However, there lies an appreciable amount of complexity in these structures from material aspects. In case of composites, the ingredients are integrated in a manner that their advantages are made use of righteously while minimizing their flaws. Extending this principle to mechanical, physical and chemical properties that can lead to Pandora's Box where the variety of combinations used for optimizing the above properties are obtained by one's imagination (Kulkarni 2002). This can help the designer overcome the constraints associated with selection and manufacturing of the conventional materials and has made it possible to tailor the material according to the requirement of the application.

Composite is not a new invention, instead it has a history of more than 3000 years. There are composites existing in nature such as bone, teeth and wood. The ancient civilization made use of bricks made of straw reinforced with mud which are also natural composites. Presently the area of application of composites are wide spread in the areas of automobile, aerospace, construction, marine, sports and so on owing to their light weight and high specific strength. The requirement of the customer changes day by day with respect to the performance of the product leading to development of newer materials. Also, the concerns about the environment and energy leads to

increasing demand for light weight materials yet strong. Composites are the potential materials which are constantly meeting these needs (Krishan K Chawla 2012). The difficulty of achieving higher performance in monolithic materials can be easily overcome by composites obtained by combining two or more materials together. Composites provide unique properties which are impossible to be obtained from any of the constituent materials individually.

### **1.1 Composites and its classification**

According to ASTM D3878 standard, *composite is a macroscopic combination of two or more distinct materials, having a recognizable interface between them.* Apart from this, composites are defined as those which is manufactured or manmade, consisting of two or more physically and/ or chemically distinct, suitably arranged or distributed phases with an interface separating them and has the characteristics which are not depicted by any of the constituents individually (Krishan K Chawla 2012).

‘Composites’ are extracted from Latin word ‘Compositus’ having a meaning ‘put together’. Composite materials are made from two or more constituent materials with significantly different physical or chemical properties that, when combined, produce a material with characteristics different from the individual constituents. Composite materials consist of two phases namely continuous and discontinuous phase. Continuous phase is usually called as matrix. Reinforcements which are much stronger and harder than matrix are discontinuous in nature. Matrix assumes a crucial part in keeping the aggregates of reinforcement in bound form and without matrix the reinforcement are of no use. Comparing the mechanical properties, the matrix is inferior compared to reinforcement and plays a role of transferring the load to the reinforcement. Along with these functionalities, the matrix also acts as a barrier against environmental effects, mechanical and chemical degradation such as abrasion and corrosion. The main functionality of the reinforcement is to bear the load as the load transfers from the matrix to reinforcement (Sanjay K 2002).

Composites are classified based on their constituents, matrix or reinforcement. Based on the matrix used, composites are classified as metal matrix composite (MMC),

polymer matrix composite (PMC), ceramic matrix composite (CMC). Similarly based on the reinforcement used, the composites are classified as particle reinforced composite, fiber reinforced composite and structural composite which are further classified as shown in Figure 1.1 (Otani et al. 2014).

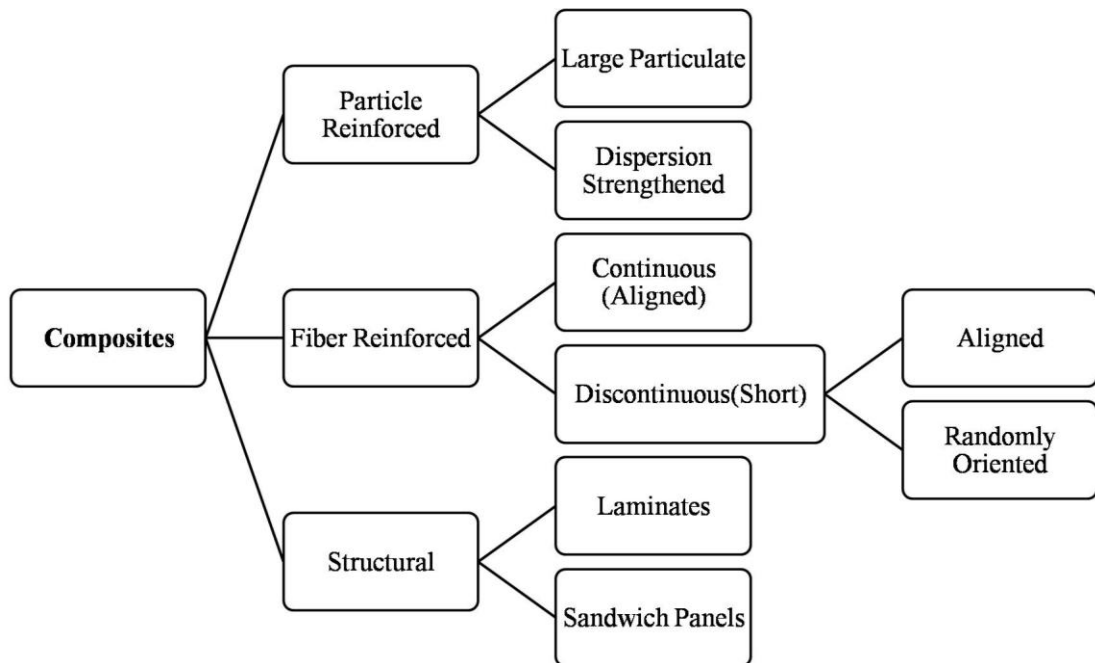


**Figure 1.1** Classification of composites based on reinforcements (Otani et al. 2014)

PMC's are popularly used in various engineering applications as the substitutes for metals and alloys owing to numerous advantages that they possess over metals and alloys. Compared to MMC's and CMC's, PMC's are easy to fabricate and economical. MMC's and CMC's find their application where high performance is demanded. However, PMC's have gained popularity in almost all fields of engineering due to the edge they have in terms of cost, fabrication, density, corrosion resistance and desirable electrical and thermal properties.

Various types of reinforcements such as fibers, fabrics particles or whiskers can be used in PMC's. Fibers are essentially characterized by one axis along the length of fiber and cross section area. Particles have no preferred orientation and so does their shape. Whiskers have a preferred shape but are small both in diameter and length as compared to fibers. Fibers are the principal constituents in a fiber reinforced

composite material. They occupy the largest volume fraction in a composite laminate and share the major portion of the load acting on a composite structure. Proper selection of the fiber type, fiber volume fraction, fiber length, and fiber orientation is very important, since it influences the characteristics of a composite laminate such as density, tensile, compressive and fatigue strength and cost (P.K. Mallik 2008).

Two main classes of polymers, namely thermosetting and thermoplastic polymers are used as matrix in PMC's. Thermoplastic polymers soften/melt upon heating and further hardens upon cooling to room temperature. Typical examples of thermoplastic polymers are polyethylene and polystyrene. Whereas, Thermosetting polymers decompose on heating. Cross linking makes sliding of molecules past one another difficult, making the polymer strong and rigid. A typical example is vulcanized rubber, epoxy, polyester and vinylester. Curing in case of thermosets involves cross-linking of polymeric chains which is initiated by addition of chemical agents or application of heat and pressure (Krishan K Chawla 2012).

## **1.2 Sandwich composite**

Sandwich composites belong to special class of composite materials having a light weight core in between two stiff composite layers (skins). The skins are attached to the core to achieve load transfer between the components. Sandwiches are designed based on the principle of I-beam. In case of I-beam, most of the material is provided in the flanges situated away from neutral axis and sufficient amount of material is provided in web to make the flanges act in concert and to resist shear and buckling loads. Comparing the sandwich structure with I-beam, the skin of the sandwich acts as flanges of I-beam and core acts a web. The only difference is in the materials used. In case of sandwich structures the materials used for skin and core are different. Whereas, in case of I-beam the material remains same for flange and web. The core used in sandwich resists the shearing load and avoids buckling of skins. In order to resist the shear and tensile stresses between core and skins, the bonding between them should be sufficiently strong and thus the adhesive that bonds the core and skin plays an important role. Analogy between I-Beam and sandwich is presented in Figure 1.2



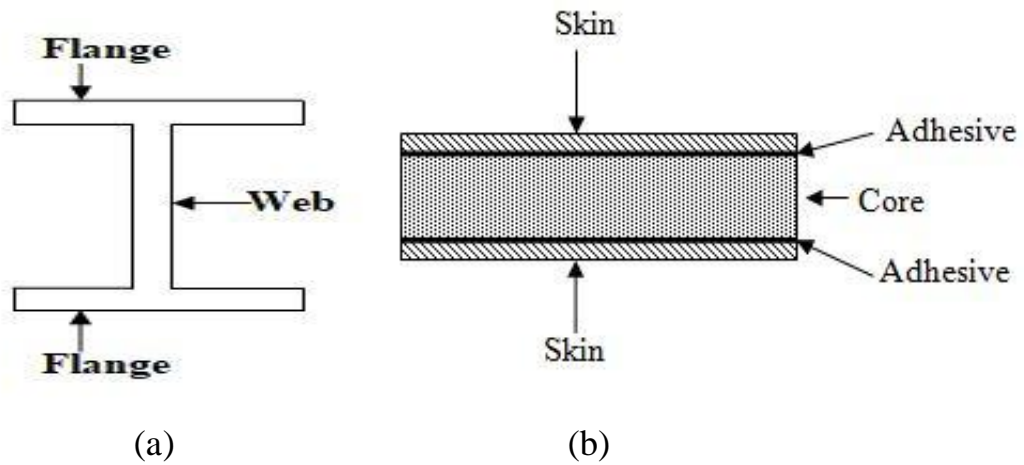


**Figure 1.2** Analogy between (a) I-Beam and (b) Sandwich

‘Flexible composites’ is a term coined to identify the composites making use of elastomeric polymers as matrix. These flexible composites exhibit usable range of deformations which are much larger than conventional stiff composites. The ability of flexible composites to undergo larger deformation and still provide high load carrying ability makes them suitable for many engineering applications such as tire and conveyor belt constructions (Chou 1989). Understanding the basic characteristics of the flexible composites is very much essential to assess its real potential (Chou and Takahashi 1987). Apart from being used in tires and conveyor belts, flexible composites also find their applications in the form of coated fabrics used in hoses, flexible diaphragms, inflated structures, surgical replacements and bullet proof vests.

The large deformations in the flexible composites are mainly due to matrix or fiber. In order for the matrix to undergo larger deformation, the associated fiber must deform accordingly. This is possible by using:

1. Fibers in the form of woven knitted or braided form.
2. Short fibers
3. Continuous fibers with an appropriate arrangement such that as the load increases, the fibers are allowed to rotate.

Out of all the options mentioned above, the option of using fibers in the form of woven knitted or braided form has greatest potential. It is possible to enhance the

stiffness with increased deformation by straightening the crimped region in textile composite with external loading.

Similar to conventional stiff composites, the flexible composites also has two primary components namely skin and core with an adhesive layer acting as the third component that is used to bind the skin and core together. The material used for skin, core and their relative thickness and bonding between them decides the overall characteristic of the flexible composite (Gupta 2003).

The advance in the field of composites with fiber reinforced elastomers (FRE) has opened up an opportunity for wide range of applications in the field of automobiles, aerospace, robotics and bio medical. The main advantage of flexible composite is the ability to modify the various physical characteristics over a wider range when compared to stiff composites, metals, alloys and plastics. Flexible composites are useful in applications like acoustics, automobile cladding, and interiors of aerospace and automobile where flexibility is much needed than stiffness, the flexible composites are useful as they can be tailor made to the requirement (Peel and Jensen 2001).

#### 1.2.1 Core materials for sandwich structure

Particulate composites are popularly used as core materials in sandwich structures next to honeycomb cores due to the advantage of tailored mechanical, electrical and magnetic properties that can be achieved. Hence, they find wide application in weight sensitive structural applications such as aircrafts, automobiles, and sport goods and so on. Sandwiches making use of particulate composites as core materials possess high specific compressive strength and bending stiffness (Chittineni 2009).

Depending on the desired performance of the sandwich composites, wide variety of core materials are available (Vinson 1999). Few among them are:

1. Low density solid materials such as structured foams, balsa and other woods.
2. Expanded high density materials in cellular form such as honeycomb.
3. Expanded high density materials in corrugated form such as truss and corrugated sheets

The interfacial contact between the skin and the core is affected by the structure of the core material used in the composite. Low density solid materials usually provide larger and continuous contact area of the core with the skin as opposed to expanded high density core materials where the area of contact of the core with the skin is minimal. The selection of appropriate core material also depends on various other design parameters as per the requirement.

Making use of cores such as closed cell structures foams provides some advantage over the open cell structured foams in terms of specific compressive strength. The specific compressive strength of closed cell is higher compared to open cell and also closed cell absorbs less moisture compared to open cell (Gupta 2003).

Although the polymers exhibit disadvantage of limited usage temperature, their ease of manufacture has made them as the popular core material for sandwiches (Seymour 1990). Polymers may be thermoplastic or thermosetting. Thermosetting polymers do not dissolve in solvent and do not get softened on heating unlike thermoplastic polymers. Instead, thermosetting polymers are permanently hardened when heated. Thus thermosetting polymers are harder, stronger and brittle compared to thermoplastic polymers thereby exhibiting better dimensional stability. Other class of polymers are 'elastomer' which exhibit rubberlike elasticity. Natural rubber (NR), Acrylonitrile butadiene rubber (ABR) and Styrene butadiene rubber (SBR) are few elastomers which belong to this class. Elastomers are used for specific applications where large deformations are required.

Elastomers are being considered as the most useful substance in modern world (Chandra and Mishra 1995) and are widely used by engineers especially in the field of vibrations to minimize the vibrations and shocks (Andre 1945). NR can be isolated from more than 200 different species of plant; including surprising examples such as dandelions. Only one tree source, *Hevea Brasiliensis*, is commercially significant. Latex is an aqueous colloid of NR, and is obtained from the tree by tapping into the inner bark and collecting the latex in cups. The latex typically contains 30-40% dry rubber by weight. It is coagulated with the help of formic acid and water content is removed. Later the NR is rolled into sheets and dried in sunlight which is used for

further processing. Sheet rubber, prepared by deliberate coagulation of fresh natural rubber latex, properly dried and smoked is used in making these grades. Lump, cuttings or other scrap or frothy sheets, weak, heated or burnt sheets, air dried or smooth sheets are not permissible. Wet, bleached, under-cured and virgin rubber and rubber that are not completely visually dry at the time of buyer's inspection is not acceptable.

Rubber phase consists of billions of rubber globules along with layer of soapy substance comprising of proteins and phospholipids. Additional stabilizers are added and the latex is centrifuged to remove water content and enhance the rubber content present in latex. The material obtained after centrifugal process is known as latex concentrate containing roughly 60% of solid rubber and 40% of water and other stuff resulting in NR (Blackley 1997). The vulcanization process is then carried out to solidify the rubber in the presence of sulphur. Owing to the excellent energy absorbing characteristics, enhanced flexibility, high puncture and tear resistance along with good adhesion to fabrics, NR is considered as the potential core material for sandwich composites (Baarle 2003).

### 1.2.2 Skin materials for sandwich structure

There are wide varieties of materials ranging from metals, alloys and fiber reinforced plastics that are used as a skin material in sandwich structure. Selecting an appropriate skin material mainly depends on the working environment of the proposed composite as in the composite; the skin is the constituent that is directly exposed to working environment. Tribological, corrosive, thermal, water absorption and other mechanical properties of the proposed sandwich composite can be tailored by appropriate selection of the skin material. In most of the cases, the upper and lower skins of the sandwich composite are identical but at the same time it is not mandatory also. Depending on the requirement, it is admitted to different types of the upper and lower skins (Satapathy et al. 2010). The difference may be in terms of materials, fiber orientation, thickness, volume fraction and so on. One of the most popularly used skin is fiber reinforced polymers (FRP) owing to their favourable properties such as reduced density and enhanced specific strength (Patil 2006).

Out of the different types of composites available for engineering applications, PMC/FRP are widely used and are considered as substitutes for many metals and alloys in various engineering applications due to their inherent advantages such as low density, high specific strength, corrosion and impact resistance, ease of fabrication and design flexibility. PMC find their usage in various engineering applications such as aerospace, automobile, marine, sport goods and so on.

PMC are comprised of mainly two constituents: a fiber bonded to a polymer matrix. The reasons why they are the most common composites include their low cost, high strength, and simple manufacturing principles. The main drawbacks of PMCs include low operating temperatures, high coefficients of thermal and moisture expansion and low elastic properties in certain directions (Autar K. Kaw 2006). Reinforcing the woven fabric with a different kind of matrices results in varied impact behavior of the PMCs. Depending on the matrix used, the mechanical behavior and damage characteristics of the PMCs vary (Khodadadi et al. 2019b).

Fibers normally exhibit higher strength and function as primary load bearing member, whereas the role of the matrix is to transfer the load on to the fibers. Fibers are protected by the matrix both before and after processing and also during service life of the composite. Wide varieties of fibers are available for use in the composites and can be classified as synthetic and natural fibers. The most commonly used synthetic fibers include carbon, glass and aramid and jute, flax, hemp, remi, sisal, coconut fiber (coir), and banana fiber (abaca) are some examples of natural fiber. All these fibers are grown as agricultural plants in various parts of the world and are commonly used for making ropes, carpet backing, bags, and so on. The components of natural fibers are cellulose micro fibrils dispersed in an amorphous matrix of lignin and hemicelluloses. Depending on the type of the natural fiber, the cellulose content is in the range of 60–80 wt% and the lignin content is in the range of 5–20 wt%.

In addition, the moisture content in natural fibers can be up to 20 wt%. Recently, natural fiber-reinforced polymers have created interest in the automotive industry. The applications in which natural fiber composites are now used include door inner

panel, seat back, roof inner panel, and so on. Some of the properties of natural fibers are:

1. They are eco friendly exhibiting biodegradability and the energy utilized in producing natural fibers are negligible compared to synthetic fibers such as glass and carbon fibers.
2. Natural fibers exhibit lesser density compared to synthetic fibers leading to lighter components.
3. Few natural fibers exhibit better specific modulus compared to E-glass fibers indicating that such natural fibers can be potential substitutes for E-glass fibers.
4. Natural fiber composites are more suitable for noise attenuation applications such as automotive interiors since they exhibit better acoustic damping properties compared to carbon and glass fibers.
5. Natural fibers are economical than glass and carbon fibers. However, there are few constraints of natural fibers such as low tensile strength, low melting point, susceptibility to water absorption and degradability.

When matrix and the fibers are appropriately selected, it leads to a composite that is having the desired property comparable to or even better than the conventional metals and alloys. Apart from the fibers and the matrix used, the overall performance of the sandwich composite also depends on the adhesive bonding between skin and core. It is very much essential to select a proper and compatible adhesive so that the desired strength is achieved and at the same time, the adhesion is unaffected by the working environment.

### 1.2.3 Adhesives

Adhesively bonding of the constituents used to make composite has emerged as one of the most promising joining technology since they induce lower stress concentrations compared to conventional fasteners resulting in increased efficiency of the joint in terms of strength-to-weight ratio (Freitas et al. 2018). The strength and the failure behaviour of adhesively bonded structures mainly depend on the mechanical

properties of the adhesive material and stress concentration in bonded structures (Afendi et al. 2011). Adhesives of different types and with a wide range of mechanical properties are available. However, selecting an appropriate adhesive mainly depends on the adherand, working environment and nature of application (Yablokov et al. 2015).

The primary function of the adhesive in a sandwich composite is to bind the skin and core properly. The adhesives available for use can be classified as synthetic adhesives and natural adhesives. Wide variety of synthetic adhesives such as epoxy resins, polyester, polyurethane, vinyl resins, phenolics etc. are widely used in processing the PMC. Similarly there are few naturally available adhesives such as cashew nut shell resin and NR. Adhesives based of NR provides flexibility to the composite and are suitable for processing of flexible composites. These flexible adhesives provide joints with a more uniform stress distribution and less of a difference between average and maximum stress. These adhesives distribute peel and shear stresses over a larger area, thereby improving joint efficiency. However, as adhesives with high flexibility and elongation typically have lower cohesive strength than more rigid adhesives, the advantage of flexibility and high elongation is usually compromised. In order to transfer the same load, a much larger overlap is needed (Kwakernaak et al. 2012). NR mixes usually have good inherent tack and thus added to less tacky materials like synthetic rubbers to enhance their tack property (Basak et al. 2010). Numerous scientific literature are published regarding tackifier mediated adhesion between polymers covering different aspects (Bhowmick and Gent 1984; Bhowmick et al. 1989; Loha et al. 1987; Mahmood and Busse 2006; Purnima et al. 2006; Sa et al. 2008; Thurston et al. 2007; Wool 2006; Zanini et al. 2009), but studies involving fabric made of naturally available plant fiber and natural rubber are comparatively less.

#### 1.2.4 Characteristics of flexible sandwich composite

The main advantage of the composite lies in tailoring its properties according to the particular application. Appropriate selection of the skin, core and adhesive material results in a sandwich composite which is capable of adapting itself to wide variety of

applications and environmental conditions. Some of the general characteristics of flexible composites are as follows:

1. Low density: The general advantage of any PMC lies in its low density. Using a light weight core results in a sandwich composite whose overall density is reduced considerably since volume of the core is appreciable in sandwich compared to the skin. Thus any reduction in the density of the core directly results in reduction of density of the sandwich appreciably.
2. Deformation: Flexible composite exhibit larger deformation owing to their flexibility.
3. Energy absorption: Flexible composite are known for their better energy absorption characteristics compared to conventional stiff composites and thus are widely used in body armour applications.
4. Damage resistance: Use of flexible core results in highly damage resistant sandwich composite. Thus flexible materials are used in packaging applications.
5. Tear strength: Flexible composite exhibit better tear strength.
6. Tribological properties: The range of working temperature of flexible composites for wear resistant applications is small.

#### 1.2.5 Advantage and disadvantages of flexible sandwich composites

The advantages of composites include:

1. Excellent strength to weight ratios compared with traditional materials.
2. Resistant to corrosion.
3. Allows a greater flexibility with designs.
4. Low density
5. Reliability in manufacturing and usage.
6. Non-magnetic
7. Better vibration and tribological properties



The disadvantages of composites include:

1. Expensive to manufacture.
2. Higher thickness.
3. Difficult to reshape.
4. When damaged they are difficult to repair due to the fibers being mixed in the matrix.
5. Difficult to produce to required properties requiring extensive design and testing.

#### 1.2.6 Applications of flexible composites

Flexible composites are widely used in many engineering applications. Few of the applications where flexible composites are/can used are listed below:

1. Structural applications: Hoses, Pipe linings, Hose bends, Side liners, pump casing
2. Sacrificial structural application: Claddings to protect primary structure
3. Bullet proofing: Body armors
4. Thermal and electrical insulation
5. Packaging materials

A continuous effort has been put by various researchers, engineers and designers to find a sandwich composite with new combination of skin and core material for different engineering applications. Such possible new sandwich materials need to be critically analyzed for their mechanical behaviour to assess their performance in advance.

### **1.3 Approaches for evaluating the mechanical properties of composites**

During design and development of any new material, it is very much essential to assess the material for its mechanical properties. There are three main approaches available for acquiring the mechanical properties of such newer material namely theoretical approach, analysis using finite element (FE) software and experimental

methods. Following section focuses on the discussion of all the three approaches available to characterize the material for the mechanical properties.

### 1.3.1 Theoretical approach

During the design of the composite for any particular application, one needs to understand the micromechanical and macro mechanical behaviour of the composite to arrive at the optimal design solution. Mechanical characterization of composite materials are complicated when compared to metals as composite are not isotropic. The mechanical properties of the composites can be assessed as follows:

1. The individual properties of the ingredients used to prepare composites are used to determine the properties of the composites making use of rule of mixture. Here, it is assumed that the plies are homogeneous. During this stage it is possible to optimize the properties and this is called as micromechanics of lamina.
2. Stress strain relationships are developed for lamina based on which the relationships for various properties are derived. This is called macro mechanics of lamina. Develop the stress-strain relationships for a unidirectional/

A structure made of composite materials is generally a laminate structure made of various laminas stacked on each other. Knowing the macro mechanics of a single lamina, one develops the macro mechanics of a laminate. Stiffness, strengths, and thermal and moisture expansion coefficients can be found for the whole laminate. Laminate failure is based on stresses and application of failure theories to each ply. This knowledge of analysis of composites can then eventually form the basis for the mechanical design of structures made of composites. Numerous equations have been postulated by many researchers (Feringo 1978; Ishai and Cohen 1967; Pal 2005; Wong and Truss 1994) in the past to predict modulus depending on many theories.

A detailed literature on the modelling of compliant flexible materials like rubber is available (Bloch 1976; Christensen 1982; Schapery 1969). Many constitutive models have also been developed by various researchers (Liu 2010; Liu and Hoo Fatt 2011)

for dynamic response and cyclic loading of rubber. The non linear elastic behaviour of rubber is described by hyper elastic constitutive models in which non linear stress strain relationship is represented independent of prior strain history. The stress strain behaviour of rubber is been studied by many researchers with the help of different hyper elastic constitutive models (Bloch 1976; Gent 1996; Liu 2010; Mooney 1940; Mullins 1947; Odgen 1997; Rivlin 1992). Though rubber is most popularly used in many engineering applications, there is still a gap in understanding its mechanical behaviour completely and also there is lack of constitutive models to simulate some of the responses of the rubber exactly. The drawback of the theoretical approach lies in its inability to deal with materials having flaws such as cracks, voids, manufacturing defects and inhomogeneity. Finite element approach using commercially available simulation packages has been proved to be better than analytical approach (Gupta and Woldesenbet 2009).

### 1.3.2 Finite element approach

As discussed earlier, designing a composite for a particular engineering application demands the thorough understanding of its behaviour under the intended load. Material and proposition geometrical non linearity can be easily generated using finite element packages and thus appears to be the better approach in hand compared to theoretical approach. Finite element method (FEM) has proven its usefulness in the area of engineering applications over the past few years. Originated from structural analysis, FEM has now expanded to almost all fields of engineering including mechanical design and recently in the modelling of composites. Modelling and simulating the behaviour of composite at macro and micro scale level can be easily carried out using FEM. The three basic steps of analysis are:

1. Pre-processing
2. Solution
3. Post-processing

Pre processing aims at allocating suitable material properties, meshing, and boundary conditions. Meshing is a process of dividing the entire geometry into smaller elements

which further creates nodes where the boundary conditions are applied. The elements used in meshing may be 2dimensional (2D) or 3 dimensional (3D). Shell elements represent a 2D element. In case of 3D elements, the element will be having the thickness in all the directions. Some of the examples of 3D elements are brick and tetrahedral element. The degrees of freedom (DOF) which defines the movement are defined at the nodes. Meshing is the most difficult task involved in FEM. Depending on the nature of the analysis, the various material properties of the related material has to be defined. Elastic modulus poissons ratio and density is essential for performing linear static analysis. In case if it is essential to analyse the thermal behaviour of the material, it is essential to assign the thermal properties such as coefficient of thermal expansion and so on. Boundary conditions involve assigning the loads and constraints for the desired problem. Loads can be force, pressure, velocity, temperature and heat flux. Whereas, the constraints are those which suppress the DOF of the nodes.

Solution phase involves obtaining the solution for the model that has completed all the pre-processing requirements. The numerical methods that form the basics of solver perform following functions:

1. Approximation of unknown variable by means of simple functions.
2. Discretisation of domain (model) to be analyzed.
3. Solution to the set of algebraic equations.

Post processing phase provides the results on model as contours and vector plots to provide summaries of the results (like min/max values and locations). Powerful and intuitive slicing techniques allow the user to get more detailed results over given parts of the geometries. All the results can be exported as text data or to a spreadsheet for further calculations. Animations are provided for static cases as well as for nonlinear or transient histories. Any result or boundary condition can be used to create customized charts. Availability of such user friendly packages has attracted many engineers and designers to adopt them in material modelling, especially for composites (Kulkarni 2002). To minimize the high cost and time involved in manufacturing and testing of the proposed material in the initial stage, finite element

method (FEM) is adopted to check for its suitability and optimizing the parameters before proceeding with actual fabrication.

Though, FEM has been proven to be the better method to extract the mechanical properties with numerous advantages, it has its limitations like difficulty in modelling the sandwich exactly and requires few assumptions to be made which can affect the results. Thus, compared to both theoretical and finite element approach, experimental approach proves to be much accurate and full proof methodology as it considers all the parameters associated with material, environment, geometrical and loading non linearity into account.

### 1.3.3 Experimental approach

Experimental approach is the most appropriate approach to assess the mechanical properties of the composites compared to theoretical and finite element analysis, as it has no assumptions and carried out in real world situation if the manufacturing and testing is done as per the standard. There are various factors that affect the mechanical properties, geometrical properties and loading conditions. Experimental approach takes into account all these factors into account. Some of the aspects of experimental investigation of mechanical properties, slurry erosion testing, two body abrasion testing, low velocity impact, and lower ballistic impact are presented in this section. End of this section discusses about the statistical tools namely design of experiment (DOE) used to carry out the experiment systematically and multi attribute decision making (MADM) methods which helps in selecting the optimal configuration of the composite. It is essential to characterize the composites for their mechanical properties, tribological properties and impact responses according to respective ASTM standards wherever applicable.

Prior to finalizing any composite for any engineering application, the density of the composite is checked. Based on the density, the void content is determined. Natural fibers being hydrophilic in nature have the tendency to absorb water and thus the water absorption test on the composites becomes most essential. Water absorption of the composites can be determined using ASTM D 570-98 standard. The water

absorption percentage of the particular composite is determined by weighing its weight before and after immersing in water for a particular period of time. Characterizing the flexible composite for tensile and tear strength are most important since, these are the parameters that govern the mechanical behaviour of the flexible composites under any applied load. ASTM D 412 and ASTM D 624 standards are used to determine the tensile and tear tests respectively.

The strength and the failure behaviour of adhesively bonded structures mainly depend on the mechanical properties of the adhesive material and stress concentration in bonded structures (Afendi et al. 2011) and hence determining the peel strength of the constituents becomes critical in case of flexible composites. In order to evaluate the strength of the adhesive joint and to understand the strength of the adhesive structure, the peel test is considered to be useful. Peel strength can be determined by carrying out the peel test.

Interlaminar shear strength (ILSS) of the composite laminates is one of the important properties that play a vital role in design consideration (Byrd and Birman 2006; Fan et al. 2008; Garg et al. 2015; Wang et al. 2016a). Three factors mainly govern the strength of the PMCs namely; fiber properties, properties of matrix and interaction between matrix and fiber. The properties of the fiber and matrix can be individually improved, but the interfacial property depends on both matrix and fiber. ILSS is the one that determines the interfacial bonding strength between reinforcement and matrix (Zahid et al. 2019). Lower value of ILSS is an indication of debonding of fiber from the matrix under the influence of stress which will affect the optimal load transfer from matrix to the fibers (Mazumdar 2002). There are two ways to enhance the ILSS of PMCs. The first being modification of fibers (Carvelli et al. 2010; Dan et al. 2011; Dang et al. 2019; Senol 2012) and the second being modification of matrix (Jahan et al. 2010; Jia et al. 2015; Quaresimin et al. 2012; Zaheer et al. 2018). Interleaving method can be used in laminated composites to minimize the interlaminar stresses and improve interlaminar fracture toughness (Khan and Kim 2012; Kim and Mai 1991; Kim and Lee 2016; Wong et al. 2017) which results in resisting or arresting delamination. Materials having low modulus and high elongation was made use of as delamination resistors (Chan et al. 1986). The material with low surface energy results

in possible reduction of surface defects, resulting in higher ILSS. ILSS of the flexible composites of different stacking sequences are carried out according to ASTM D2344 which is the designated standard for determining the short beam strength of polymer matrix materials and their laminates.

There are various parameters that affect erosion rate during slurry pot testing like particle velocity, abrasive concentration, particle size and property of material (Levy and Crook 1991; Rao et al. 2016). The slurry is prepared by adding erosive medium to liquid and the mixture is stirred well. The pre weighed samples are fixed into the specimen holder. The slurry pot is fixed in its position and the specimen is rotated inside the slurry. Three to five such specimens were subjected to testing and each time new slurry concentration is prepared. The wear of the samples is measured as a function of weight loss. The samples after test are dried and cleaned using acetone and then the final weight is noted down. The difference in initial and final weight of the specimen gives the weight loss.

Abrasive wear is brought about by the hard protuberances which move against the strong surface and constrained against it (Hutchings 1992). In case of two body wear, hard projections caused wear on only one surface. Neat polymeric materials are rarely used in wear applications (P.K. Mallik 2008). Flexible composites are found to exhibit wide range of tribological properties and are useful in applications such as material handling, transportation and secondary structural applications like claddings and thus, wear studies in these areas are acquiring more importance (Friedrich et al. 1995). Two body abrasion tests of flexible composites are carried out according to ASTM D5963/ ISO4649 standards.

The composites during their service are subjected to dynamic loading rather than static loading. The impact loading is one of the critical dynamic loads the composites are subjected to. The study of energy absorption and the nature of damage that the flexible composite undergoes when it is subjected to impact load is critical before designing and finalizing the composite for a particular engineering application. Composites used in various engineering applications are prone to different types of impact loadings such as: low velocity impact (below 10 m/s), intermediate impacts

(10 m/s to 50 m/s), ballistic velocity impacts (50 m/s to 1000 m/s) and hypervelocity impacts (2 km/s to 5 km/s) (Abrate 2011). The energy absorption in the composite can happen by two different mechanism: a) by material deformation and b) by creation of new surfaces. When the initial portion of the work is stored as elastic deformation, the material deformation occurs. Further, if more amount of energy is supplied, crack initiation and propagation may happen. Thus it is clear that to enhance the energy absorption, it is essential either to enhance the material deformation or make the crack growth path curvy. Energy absorption in case of composites can be assessed by drop weight impact test for Low velocity impact (LVI) and ballistic test using gas gun for high velocity impact (HVI). In both the cases, the energy absorption can be determined by using the impact and residual velocities.

LVI tests are carried out using drop weight impact testing machine. The shape of the impactor can vary depending on the requirement. The positioning of the specimen is done in the specimen holder and the impactor is then raised to the desired height from which it is made to fall on the specimen. Different heights can be chosen so that different impact velocities could be achieved. The different energies of impact can be obtained by varying the drop height of the impactor. The potential energy of the impactor increases with an increase in the height of the drop. The energy absorption and damage mechanisms of the flexible composites under LVI are studied from this test.

Ballistic impact is one of the most adverse loading conditions that any composite structure might be subjected to, and in such structures, the fundamental importance lies in selection of an appropriate material. Prior to using the PMCs in any ballistic impact applications, it is very much essential to study their damage tolerance characteristics and ballistic resistance (Lee et al. 2001). Sacrificial structures which are used to protect the primary structures from impact loading must be capable of absorbing maximum energy. To enable this, flexible materials are widely used by designers and engineers (Khodadadi et al. 2019c; Roylance and Wang 1979; Shim et al. 2012). Energy absorbing behaviour of flexible materials are extensively studied using experimental and analytical techniques by various researchers (Mamivand and Liaghat 2010; Yang and Chen 2016). Determining the ballistic limit which is defined



as the average number of maximum partial penetration velocities and minimum complete penetration velocities of a projectile and target combination is most crucial to assess the HVI response of the composites.

#### 1.3.4 Optimization methods

Optimization aims at achieving the best outcome with a set of constraints or criteria. This may include maximizing the productivity, strength and so on. In almost all fields of engineering, the most critical task of an engineer is to identify the most appropriate design solutions and then decide the best alternative among the available. The optimization methods are classified based on variable type, type of constraint, deterministic nature variable, permissible value of design variable and the number of objective functions.

Statistical methods play an important role in design and analysis of engineering experiments (Prabhu et al. 2014). Taguchi, being one of such method provides sufficient information to optimize a process with the use of minimum number of experiments. The design of experiments (DOE, DOX, or experimental design) is the design of any task that aims to describe or explain the variation of information under conditions that are hypothesized to reflect the variation. The term is generally associated with experiments in which the design introduces conditions that directly affect the variation, but may also refer to the design of quasi-experiments, in which natural conditions that influence the variation are selected for observation. In its simplest form, an experiment aims at predicting the outcome by introducing a change of the preconditions, which is represented by one or more independent variables, also referred to as "input variables" or "predictor variables." The change in one or more independent variables is generally hypothesized to result in a change in one or more dependent variables, also referred to as "output variables" or "response variables." The experimental design may also identify control variables that must be held constant to prevent external factors from affecting the results. Experimental design involves not only the selection of suitable independent, dependent, and control variables, but planning the delivery of the experiment under statistically optimal conditions given the constraints of available resources. There are multiple approaches

for determining the set of design points (unique combinations of the settings of the independent variables) to be used in the experiment. Main concerns in experimental design include the establishment of validity, reliability, and replicability. For example, these concerns can be partially addressed by carefully choosing the independent variable, reducing the risk of measurement error, and ensuring that the documentation of the method is sufficiently detailed. Related concerns include achieving appropriate levels of statistical power and sensitivity. Correctly designed experiments advance knowledge in the natural and social sciences and engineering

The performance of the end product mainly depends on the material selected for the particular application. Thus, the process of material selection gains importance and has to be performed with utmost care by the designers and material engineers (Jahan et al. 2010; Rao 2006; Sapuan 2001). Since there does not exist a single standard method that can be adopted as a rule for material selection, it is the responsibility of the engineers to consider various criteria before finalizing a material. Out of the various approaches available for material selection, multiple criteria decision making (MCDM) method is one which takes into consideration various criteria before arriving at a conclusion (Shanian and Savadogo 2006). MCDM is further classified into multi attribute decision making (MADM) approach and multiple objective decision making (MODM) approach (Jahan et al. 2010). MADM approach can be conveniently used to select a suitable material for an application when there are multiple alternatives available (Rao 2008). Many literatures are available related to material selection based on classical MADM approaches such as Elimination Et Choix Traduisant la REalite meaning Elimination and Choice Expressing REality (ELECTRE) (Shanian and Savadogo 2006), Technique for Order Preference by Similarity to Ideal Solution (TOPSIS) (Rathod and Kanzaria 2011), Weighted Product Method (WPM) (Rathod and Kanzaria 2011), Simple Additive Weight (SAW) method (Chen 2012), Preference Selection Index (PSI) method (Maniya and Bhatt 2010), Analytic Hierarchy Process (AHP) (Jahan et al. 2010), Graph Theory and Matrix representation Approach (GTMA) (Chen 2012), Vise Kriterijumska Optimizacija Kompromisno Resenje (VIKOR) method (Jahan et al. 2010), TOPSIS-PSI approach (Yadav et al. 2019), combined DEMATEL-VIKOR (Chakraborty et al.

2018)etc. MCDM approaches are extensively utilized in different sectors such as marketing, supply chain, power plant and so on due to its ability of providing realistic results. TOPSIS which belongs to MADM method is widely used in material selection, especially in the field of composites (Patel et al. 2018; Patel and Dhanola 2016; Patel and Rawat 2017; Sandeep Kumar, Patel V K, Mer KKS, Fekete Gusztav 2018). Other popular MADM method called VIKOR also has the potential to be used in material selection applications. VIKOR method is used for improving the complicated systems by considering many criteria. In this method, weights are assigned to each criteria and then the agreeable solution is obtained. This method proves its usefulness in selecting and ranking the alternatives when there is a conflict among the criteria (Gangil and Pradhan 2018). PSI approach tackles multi attribute issues with minimal effort and also more effectively (Maniya and Bhatt 2010). As compared to VIKOR and TOPSIS methods, there is no necessity of assigning weight in case of PSI method which makes this approach simple.

In this chapter, the basics of composites, their advantages and limitations, characteristics of flexible composites and their applications along with various approaches for assessing the mechanical behaviour of the composites and application of optimization methods in material selection are discussed. The next chapter deals with the extensive literature review concentrating on selecting the constituents of the composites, identifying the research gap and motivation along with fixing the objectives of the present study.

## **CHAPTER 2**

### **2 LITERATURE REVIEW**

In the past few decades, reasonable amount of research work has been carried out on impact behaviour of PMC's. Present study is concerned with development of jute/natural rubber based flexible composite to serve as a sacrificial structure, carry out the physical, mechanical and tribological characterization of the proposed flexible 'green' composite along with studying the low and lower ballistic velocity impact response of the proposed composite. A brief review of recent literature concerned with characterization and impact response of composites is discussed below under following sections:

1. Reinforcement material
2. Matrix material
3. Core materials used in PMC for impact applications
4. Impact of composites
5. Wear characterization
6. Material selection approaches

#### **2.1 Reinforcement material**

Composites mainly make use of two different types of fibers as reinforcements: manmade synthetic fibers and naturally available fibers. The classification of synthetic and natural fibers is shown in Figure 2.1. Plant based natural fibers are most commonly used in natural fiber reinforced PMC. Plant based fibers are extracted from different parts of the plant and the Figure 2.2 illustrates the major fibers extracted from different parts of plant.

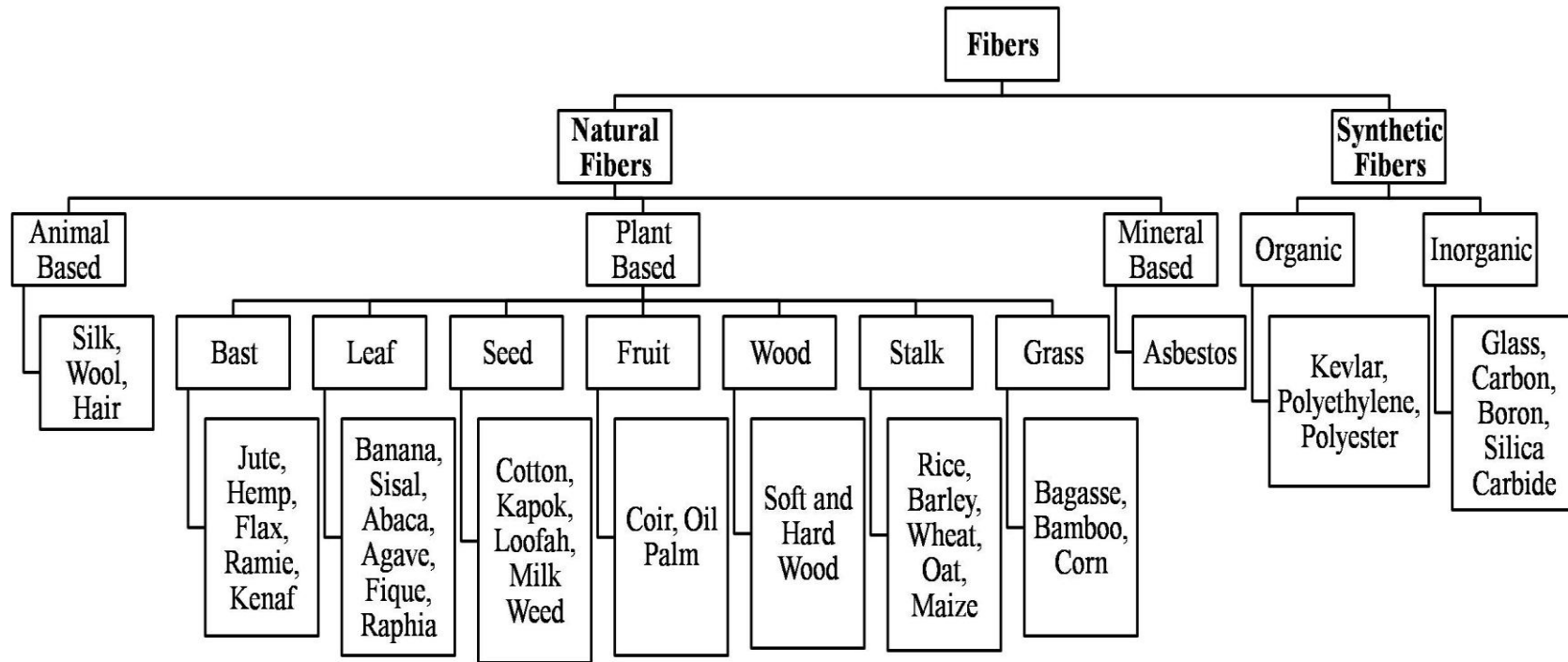


**Figure 2.1** Classification of fibers (Sathishkumar et al. 2014)

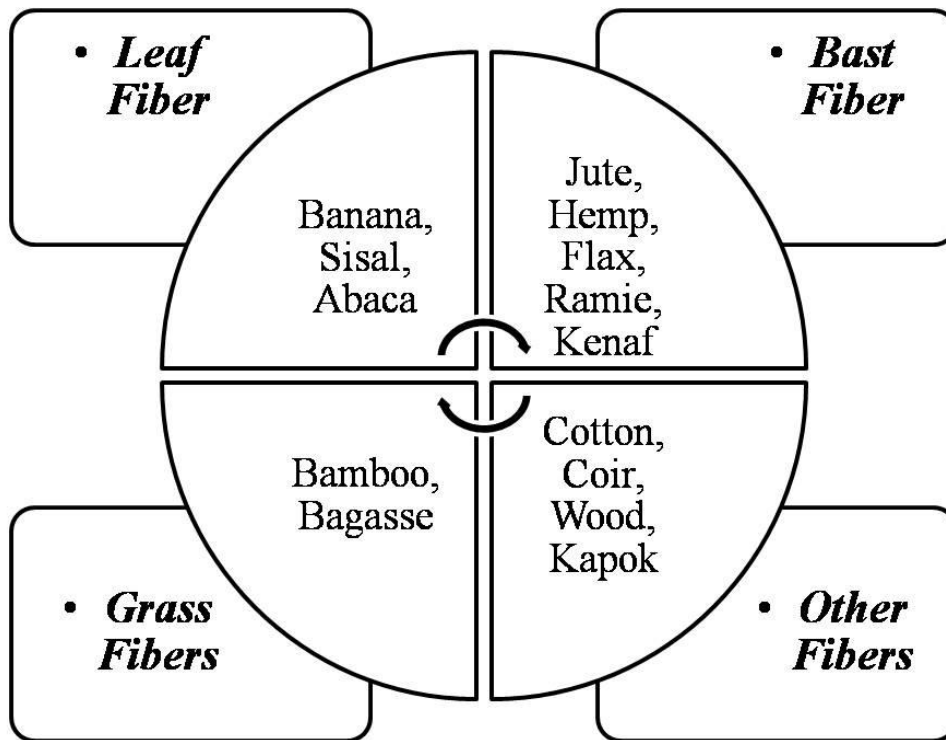


**Figure 2.2** Popular natural fibers extracted from different parts of plant

In order to reduce the weight of the final product made of composites, synthetic fibers are more commonly used (Kling and Czigány 2014; Wang et al. 2017b). Synthetic fibers are popular choice for reinforcement in composites used for various engineering applications; but are expensive. However, the recent trend in the composites have shifted towards using the natural fibers in place of synthetic fibers keeping in mind the advantages of natural fibers over synthetic fibers such as environmental friendliness (Monteiro et al. 2009; Wambua et al. 2003). Natural fibers also possess numerous advantages over the synthetic fibers in terms of acceptable physical, mechanical, corrosive and thermal properties (Katabchi et al. 2016; Khalil et al. 2017; Liu et al. 2018b; Patel et al. 2018; Vignesh 2018). Despite the favourable circumstances the natural fibers provide, the available literature also shows that contrasted with synthetics fibers, natural fibers has more water take-up capacity and lower mechanical properties (Judawisastra et al. 2017; Nurazzi et al. 2018). In order to convert this unfavourable condition of the natural fiber, many researchers have

come up with an approach of modification techniques (Azghan and Eslami-farsani 2018; Sapiai et al. 2018).

Nowadays it can be extensively found that composites made out of natural fibers are popularly used in the interiors of the automobiles (Holbery and Houston 2006; S. Thomas, S. A. Paul, A. Pothen 2011). Based on their origin, natural fibers can be classified as plant fiber, animal fibers and mineral fibers (Sparmins 2009). The sources of natural fibers are vast and accordingly natural fibers are found in wide varieties. Natural fibers when compared to synthetic fibers are lighter in weight and also exhibit acceptable mechanical properties (Safri et al. 2018). The comparison between natural and synthetic fibers are tabulated in Table 2.1 (Sanjay et al. 2016).

**Table 2.1** Comparison between natural and synthetic fibers

<b>Criteria</b>	<b>Synthetic fiber</b>	<b>Natural fiber</b>
Density	High	Low
Structure of fiber	Can be modified	Cannot be modified
Nature	Hydrophobic	Hydrophilic
Durability, usage and cost	High	Low
Renewable and recyclable	No	Yes
Biodegradability	No	Yes
Specific strength and modulus	Low	High
Strength and modulus	High	Low

The structure and constituents of the natural fiber are well defined (Rong et al. 2001). Plant based natural fibers consists of cellulose, hemicelluloses, lignin, pectin and other materials and based on these contents, the characterization of plant based natural fibers are carried out. Natural fiber is comprised on one thin primary wall and three thick secondary walls as shown in Figure 2.3.

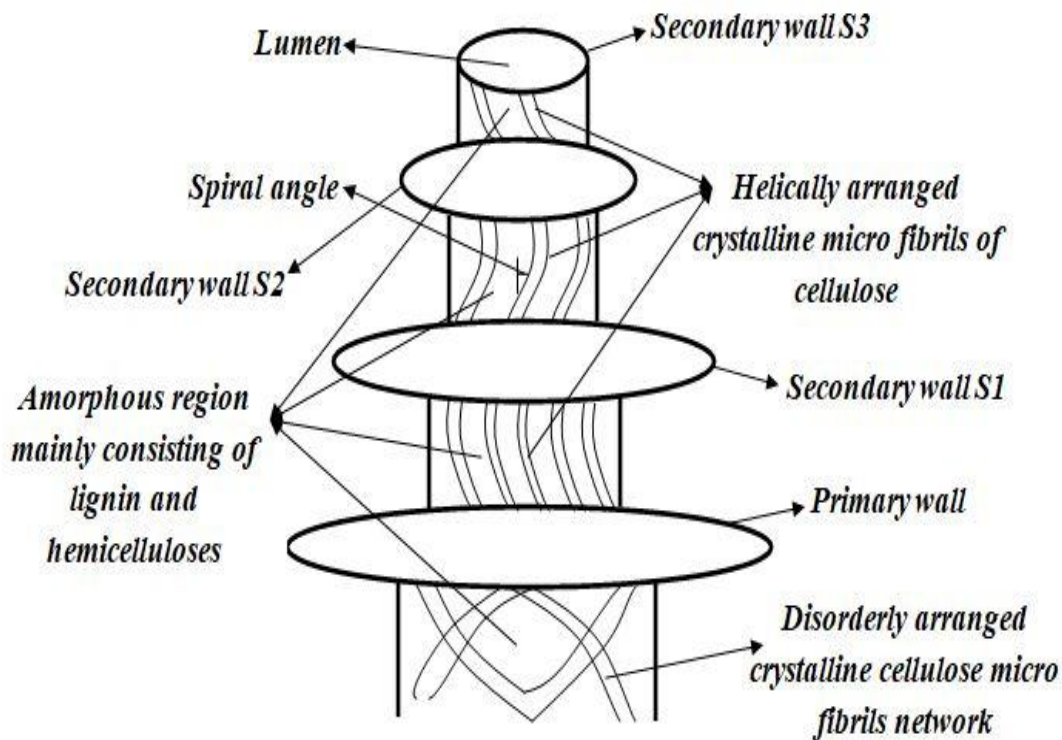


**Figure 2.3** Structure of natural fiber (Rong et al. 2001)

Secondary wall is surrounded by primary wall which is deposited during the cell growth. Three layers are present in the secondary wall and the mechanical property of the fiber is controlled by the middle layer (MJ and Anandjiwala 2008). It is found that when the micro fibrils are parallel to the fiber axis, the fiber strength will be more (Kozłowski and Władyska-Przybylak 2008).

The properties of the fiber are mainly dependant on cellulose which is the major constituent of fiber (Kabir et al. 2011). Hemi cellulose comprises a group of polysaccharides consisting of five to six carbon ring sugars and is hydrophilic in nature (Céline et al. 2014).

Lignin is amorphous in nature which is also cross linked polymer network consisting of irregular array of variously bonded hydroxy and methoxy substituted phenylpropane units which acts as a chemical adhesive within and between fibers (Xanthos 2010). Toughness of the fiber depends on the lignin and hemicelluloses



content and is directly proportional to each other. At the same time, the strength and stiffness of the fiber is found to increase up to a certain limit (Mwaikambo 2009).

Pectins are rich in D-galacturonic acid residues. The hemicelluloses, pectin polysaccharides and aromatic polymer lignin, interact with the cellulose fibrils, forming a rigid structure strengthening the plant cell wall (Rasmussen 2011). Natural fibers are currently gaining the attention of many researchers as a reinforcement in the composite owing to several advantages they possess such as low density and cost, ease of availability and high specific strength (Khalil et al. 2017; Liu et al. 2018b; Patel et al. 2018; Vignesh 2018). Also, the structure of natural fibers is unique compared to synthetic fibers as they exhibit non uniform and irregular cross sections.

Out of the widely available natural fibers, the chemical composition of the most commonly used natural fibers are provided in Table 2.2 and the physical and mechanical properties are provided in Table 2.3 (MJ and Anandjiwala 2008; De Rosa et al. 2010; Sahu and Gupta 2017; Sathishkumar et al. 2013; Tong et al. 2014).

**Table 2.2** Chemical composition of natural fibers

<b>Fiber</b>	<b>% of cellulose</b>	<b>% of hemi cellulose</b>	<b>% of lignin</b>	<b>% of pectin</b>	<b>% of moisture</b>	<b>Micro fibril angle (degrees)</b>	<b>% of wax</b>	<b>Reference</b>
Jute	61 -71.5	12-20	11.8-13	0.2	12.5-13.7	-	0.5	(De Rosa et al. 2010)
Hemp	70-74.5	18-22.5	3.7-5.7	0.9	6-12	2-6	0.8	(MJ and Anandjiwala 2008)
Ramie	68.5-76	13-16.5	0.5-0.7	1.9	7.5-17	7.5	0.3	(MJ and Anandjiwala 2008)
Flax	64-72	16.5-20.5	2-2.2	1.8-2.3	8-12	5-10	1.7	(De Rosa et al. 2010)
Kenaf	31-39	21.4	15-19	-	-	11	-	(De Rosa et al. 2010)
Cotton	82.5-90	5.6	-	1	7.7-8.5	-	0.6	(De Rosa et al. 2010)
Kapok	64	23	13	23	-	-	-	(Sathishkumar et al. 2013)
Coir	31.9-42.9	0.16-0.25	40-45	3-4	8	8	-	(De Rosa et al.

<b>Fiber</b>	<b>% of cellulose</b>	<b>% of hemi cellulose</b>	<b>% of lignin</b>	<b>% of pectin</b>	<b>% of moisture</b>	<b>Micro fibril angle (degrees)</b>	<b>% of wax</b>	<b>Reference</b>
Luffa	62	20	11	-	-	-	-	(Tong et al. 2014)
Pineapple	70-81.8	-	5-12.5	-	11.6	-	14	(MJ and Anandjiwala 2008)
Sisal	66-78	10-14	7.9-10.9	10	-	-	-	(Sahu and Gupta 2017)
Palm	70-82	-	5-12.5	-	11.6	-	-	(Sathishkumar et al. 2013)
Abaca	55-62.8	14.8-16.9	7.1-8.9	7.1-8.9	-	-	3	(Sathishkumar et al. 2013)
Banana	64	10.1-19	5	-	9.9-11.9	-	-	(MJ and Anandjiwala 2008)
Agave	68	4.8	4.8	-	7.7	-	0.25	(Sathishkumar et al. 2013)
Wheat	51	26	16	-	-	-	-	(Sathishkumar et al. 2013)

<b>Fiber</b>	<b>% of cellulose</b>	<b>% of hemi cellulose</b>	<b>% of lignin</b>	<b>% of pectin</b>	<b>% of moisture</b>	<b>Micro fibril angle (degrees)</b>	<b>% of wax</b>	<b>Reference</b>
Rice	45	20	-	-	-	-	-	(Sathishkumar et al. 2013)
Bamboo	25-43	29.8	20.9-30.9	-	-	-	-	(Sahu and Gupta 2017)
Bagasse	55.1	18.7	25.2	-	-	-	-	(Sathishkumar et al. 2013)

**Table 2.3** Physical and mechanical properties

<b>Fiber</b>	<b>Diameter (<math>\mu\text{m}</math>)</b>	<b>Density (<math>\text{g/cm}^3</math>)</b>	<b>Tensile strength (MPa)</b>	<b>Tensile modulus (GPa)</b>	<b>Elongation (%)</b>	<b>Reference</b>
Jute	25-250	1.3-1.49	390-800	13-27	1.1-1.5	(Sahu and Gupta 2017)
Hemp	25-600	1.469	685	69	1.9-4.1	(Madeed-Al and Labidi 2014)
Ramie	20-80	1.49	398-937	61.3-127.9	3.59-3.79	(Madeed-Al and Labidi 2014)
Flax	24.9	1.49	499-1501	27.5	2.6-3.1	(Yan et al. 2014)

<b>Fiber</b>	<b>Diameter (<math>\mu\text{m}</math>)</b>	<b>Density (<math>\text{g}/\text{cm}^3</math>)</b>	<b>Tensile strength (MPa)</b>	<b>Tensile modulus (GPa)</b>	<b>Elongation (%)</b>	<b>Reference</b>
Kenaf	39.9-89.9	1.21-1.39	294-929	21.9-53	3.69-6.89	(Sathishkumar et al. 2013)
Cotton	-	1.59	285-595	5.4-12.5	6.9-7.9	(Sahu and Gupta 2017)
Kapok	21.9-64	1.46	44.9-64.1	1.72-2.54	1.95-3.96	(Madeed-Al and Labidi 2014)
Coir	149.5-249.8	1.19	174.8	4-6	29.85	(Sahu and Gupta 2017)
Pineapple	50	1.52	169.5-1626	60-81.8	2.39	(Yan et al. 2014)
Sisal	100-300	1.3-1.5	500-1000	9.9-27.8	1.9-2.89	(Sahu and Gupta 2017)
Palm	402-491	1	375	2.7	13.5	(Madeed-Al and Labidi 2014)
Abaca	10-30	1.5	425-815	31-33	2.85	(Madeed-Al and Labidi 2014)
Banana	95-245	0.75	161	8.5	2	(Yan et al. 2014)
Bamboo	240-330	0.9	440	36	1.5	(Sahu and Gupta 2017)
Bagasse	200-400	1.25	96.5	6.5	4	(Sahu and Gupta 2017)

Many researchers have studied the use of natural fibers in PMC. Selection of natural fibers for any particular application depends on various factors (AL-Oqla and Sapuan 2014) and are represented in Figure 2.4 .

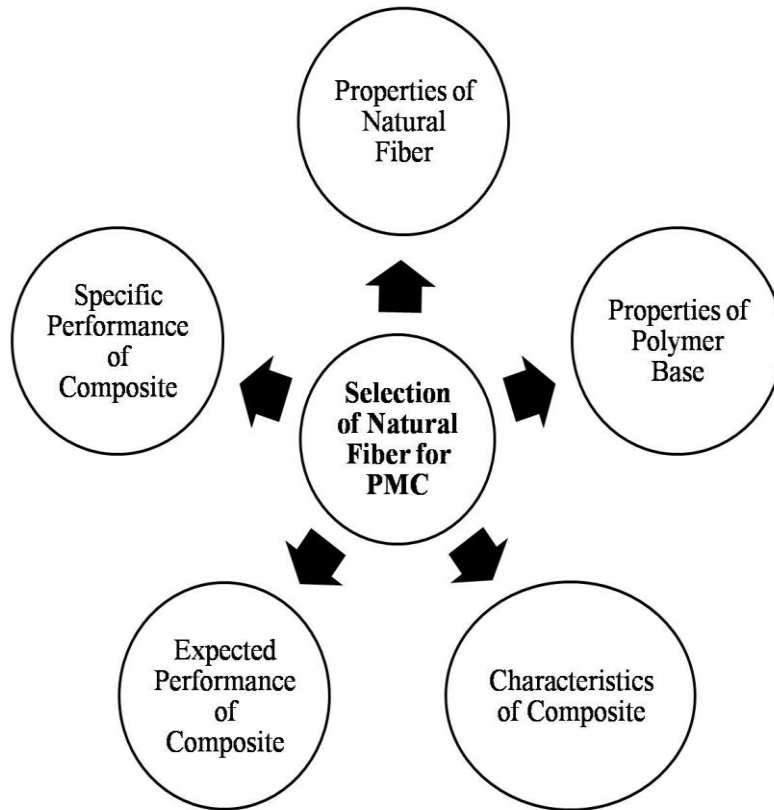


**Figure 2.4** Criteria affecting natural fiber selection in composite (AL-Oqla and Sapuan 2014)

The natural fibers used in the PMC for impact applications are presented in Table 2.4.

**Table 2.4** Natural fibers used for impact applications

<b>Fiber</b>	<b>Hybrid/ Non Hybrid</b>	<b>Impact application</b>	<b>Reference</b>	<b>Year</b>
Flax	Non Hybrid	Low velocity impact	(Nisini et al. 2017)	2017
	Non Hybrid		(Habibi et al. 2018)	2018
	Non Hybrid		(Ravandi et al. 2017)	2017
Flax	Non Hybrid	Low velocity	(Bensadoun et al. 2017)	2017

<b>Fiber</b>	<b>Hybrid/ Non Hybrid</b>	<b>Impact application</b>	<b>Reference</b>	<b>Year</b>
	Non Hybrid	impact	(Bax and Müssig 2008)	2008
	Non Hybrid		(Rahman et al. 2017)	2017
	Non Hybrid		(Singleton et al. 2003)	2003
	Hybrid with Carbon		(Flynn et al. 2016; Sarasini et al. 2016)	2016
	Hybrid with Glass		(Cerbu and Botiș 2017; Saidane et al. 2016)	2017, 2016
Caraua	Non Hybrid	Ballistic velocity impact	(Braga et al. 2017)	2017
	Hybrid with Glass	Low velocity impact	(Angrizani et al. 2017)	2017
Hemp	Non Hybrid	Low velocity impact	(Caprino et al. 2015)	2015
	Non Hybrid	impact	(Scarponi et al. 2016)	2016
	Hybrid with Glass		(Hajiha and Sain 2015)	2015
Abaca	Non Hybrid	Low velocity impact	(Bledzki et al. 2009)	2009
	Non Hybrid	impact	(Bledzki et al. 2010)	2010
Agave	Non Hybrid	Low velocity impact	(Langhorst et al. 2018)	2018
Banana	Non Hybrid	Low velocity impact	(Liu et al. 2009)	2009
Bamboo	Non Hybrid	Low velocity impact	(Lee et al. 2009)	2009
	Non Hybrid	impact	(Mohanty and Nayak 2010)	2010
	Hybrid with Glass		(Zuhudi et al. 2016)	2014

<b>Fiber</b>	<b>Hybrid/ Non Hybrid</b>	<b>Impact application</b>	<b>Reference</b>	<b>Year</b>
Coir	Non Hybrid	Low velocity impact	(Haque et al. 2012)	2012
Hemp	Non Hybrid	Low velocity impact	(Guo et al. 2010)	2010
Jute	Non Hybrid	Low velocity impact	(Mohanty et al. 2006)	2006
	Non Hybrid		(Rahman et al. 2010)	2010
	Non Hybrid		(Dhakal et al. 2014)	2014
	Non Hybrid		(Papa et al. 2017)	2017
	Hybrid with Glass		(Johnson et al. 2016)	2016
Kenaf	Non Hybrid	Low velocity impact	(Anuar and Zuraida 2011)	2011
	Hybrid with Kevlar	Low and High velocity impact	(Yahaya et al. 2014, 2015)	2014,2015
Oil palm	Non Hybrid	Low velocity impact	(Nordin et al. 2017)	2017
Ramie	Non Hybrid	Low velocity impact	(Li et al. 2012)	2012
Sisal	Non Hybrid	Low velocity impact	(Oksman et al. 2009)	2009
	Hybrid with Glass		(Rana et al. 2017)	2017
Basalt	Hybrid with Carbon	Low velocity impact	(Sarasini et al. 2014)	2017
	Hybrid with Kevlar		(Bandaru et al. 2016b)	2016

Concerned to natural fiber reinforced PMC subjected to impact, various researchers have tried with different fibers as reinforcements in composites. The hybrid composites comprising of carbon, basalt and flax fibers are characterized for their



mechanical and impact properties (Nisini et al. 2017). This study shows that intercalation of basalt with flax layers proved beneficial. The Influence of low-velocity impact on residual tensile properties of nonwoven flax/epoxy composite was studied using different shaped impactors (Habibi et al. 2018). LVI response of stitched flax epoxy PMC was studied with an intention of using the proposed composite for high performance applications (Ravandi et al. 2017). The outcomes led to the conclusion that stitching of the fiber leads to propagation of in-plane cracks leading to lower energy absorption per area of damage. The LVI response of flax reinforced PMC with two different types of matrices (epoxy and MAPP) was studied whose outcome concluded that flax fiber reinforced with ductile matrix MAPP results in better energy absorption compared to flex fiber reinforced epoxy composite (Bensadoun et al. 2017). The comparative study on impact response of flax reinforced PLA composite and cordenka reinforced PLA composite showed that flax reinforced PLA composite is inferior in impact performance compared to cordenka reinforced PLA composite (Bax and Müssig 2008).LVI behaviour of hybrid basalt/ carbon epoxy PMC was studied where it was found that due to the use of basalt fiber, the damage resistance of the laminate was increased (Sarasini et al. 2014). Due to the higher ductility of the basalt fiber, laminate was allowed to undergo larger deformation thus having wider area of damage and higher energy absorption. The ballistic impact performance of the natural curaua fiber-reinforced polyester composites was studied for personal protection (Braga et al. 2017). The curaua natural fiber with 30% volume fraction opened up interesting results for multi hit applications under ballistic impact. Hemp fibers are another type of natural fibers which can be used along with epoxy resin as a PMC. The LVI response of such PMC concluded that hemp fiber have the potential to replace glass fibers in PMC subjected to LVI loading (Caprino et al. 2015). A study regarding usage of natural fibers for structural engineering applications was attempted. The outcome of this work showed that selecting an appropriate manufacturing method along for natural fiber reinforced PMC can lead to better performance of composites (Lau et al. 2018). Flax reinforced PMC for impact application was studied along with two different types of matrices and the major conclusion from this study showed that the ductility of the matrix largely affects the energy absorption capability of the composite (Bensadoun et al. 2017).

## 2.2 Matrix material

Matrix materials used in the PMC can be classified as thermoplastic and thermoset based resin system. Selection of appropriate matrix system for the PMC based on the intended application is a critical task since the final property of the composite is directly influenced by the matrix used (Wang et al. 2011). Though the tensile property of the composite in longitudinal direction depends on the reinforcement used, the other properties such as tensile property in transverse direction, shear strength, compressive strength, resistance to heat and environment are related to the matrix used. During the initial days of development of PMC, thermoset based matrix systems were extensively used for the development of composites in military aircraft applications. Although, it was possible to obtain superior mechanical properties with the thermoset matrix based composites, many flaws were discovered with the use of epoxy based composites. This led to the invention of thermoplastic based matrices for use in PMC (Chang and Lees 1988). Nowadays, though it is found that thermoplastics are being used as the matrices in PMC, thermoset still find their application in PMC. The differences in the characteristics of thermoset and thermoplastic matrix systems are tabulated in Table 2.5 (Plummer et al. 2016).

**Table 2.5** Characteristics of thermoset and thermoplastic

<b>Property</b>	<b>Thermoset</b>	<b>Thermoplastic</b>
Modulus	High	Average
Service temperature	High	Average
Toughness	Average	High
Viscosity	Low	High
Processing temperature	Low	High
Recyclability	Average	Good

Wide variety of thermoset resins are found to be used in PMC (Charrier 1990). Epoxy, ethylene co-vinyl-acetate (EVA), polyester, vinyl-acetate, phenolic, unsaturated polyester, Unsaturated and accelerated orthophthalic polyester, Unsaturated isophthalic Polyester and Phenol Formaldehyde are most commonly used

thermoset based resins. Similarly, there are many thermoplastic based resins available for use in PMC namely natural rubber, high density polyethylene (HDPE), Polystyrene, Acrylonitrile butadiene rubber, poly methyl methacrylate, polyvinylchloride, low density polyethylene (LDPE) and polypropylene (PP). The PMC resulting from the thermoset and thermoplastic matrix systems are presented in Table 2.6.

**Table 2.6** Polymer matrix composites resulting from thermoset and thermoplastic matrix systems

<b>Reinforcement</b>	<b>Matrix</b>	<b>Reference</b>
Ramie fiber	Epoxy	(Margem et al. 2010)
Cellulose microfiber	EVA	(Sonia et al. 2013)
Banana fiber	Polyester (PE)	(Laly et al. 2003)
Untreated and alkali-treated jute fibre	Vinyl-ester	(Ray et al. 2002)
Sansevieria cylindrical fibre	Polyester (PE)	(Sreenivasan et al. 2015)
Eucalyptus wood cellulose fibre	Phenolic	(Rojo et al. 2015)
Oil palm empty fruit bunch fibre	Epoxy	(Jawaid et al. 2013)
Phormium tenax leaf fibre	Epoxy	(De Rosa et al. 2010)
Untreated and treated coconut sheath fibre	Epoxy	(Suresh Kumar et al. 2014)
Treated and untreated agave continuous fibre	Epoxy	(Mylsamy and Rajendran 2011)
Piassava fibre	Polyester (PE)	(D'Almeida et al. 2011)
Jute fibre	Polyester (PE)	(Saha et al. 1999)
UD and twill 2/2 flax fibre	Epoxy	(Duc et al. 2014a)
Sisal fibre	Epoxy	(Towo and Ansell 2008)
Pultruded kenaf fibre	Unsaturated PE	(Mazuki et al. 2011)
Short coir fibre	Natural rubber	(Geethamma et al. 2005)

<b>Reinforcement</b>	<b>Matrix</b>	<b>Reference</b>
Kenaf fibre	HDPE	(Salleh et al. 2014)
Short hemp fibre	Polypropylene (PP)	(Etaati et al. 2014b)
Short sisal fibre	Polystyrene (PS)	(Manikandan Nair et al. 2001)
Wood flour	Polypropylene (PP)	(Guo et al. 2006)
Pineapple leaf fibre	Polypropylene (PP)	(Arib et al. 2006)
Short hemp fibre	Polypropylene (PP)	(Etaati et al. 2014a)
Hemp fibre	Polypropylene (PP)	(Tajvidi et al. 2010)
Jute fibre	Polypropylene (PP)	(Doan et al. 2007)
Sisal fibre	Rubber seed oil polyurethane	(Bakare et al. 2010)
Short jute fibre	Polypropylene (PP)	(Rana et al. 1999)
Oil palm microfibril	Acrylonitrile butadiene rubber	(Joseph et al. 2010a)
Oil palm microfibril	Natural rubber	(Joseph et al. 2010b)
(MAPE) modified jute fibre	HDPE	(Mohanty et al. 2006)
Doum palm fibre	Polypropylene (PP)	(Essabir et al. 2013)
Chicken feathers	Poly(methyl methacrylate)	(Martínez-Hernández et al. 2007)
Alfa fibre	Polyvinylchloride (PVC)	(Hammiche et al. 2013)
Short henequen fibre	Polyethylene	(Herrera-Franco and Valadez- González 2005)
Unidirectional and twill 2/2 Flax fibre	Polypropylene (PP)	(Duc et al. 2014b)
Modified jute fibre	Polypropylene (PP)	(Karaduman et al. 2014)
Oil palm fibre	Linear LDPE	(Shinoj et al. 2011)
Treated argan nut shell particles	HDPE	(Essabir et al. 2015)

<b>Reinforcement</b>	<b>Matrix</b>	<b>Reference</b>
Pineapple fibre	Polyethylene	(George et al. 1996)

It is evident from the Table 2.6 that various thermoset and thermoplastic matrix systems have led to different PMC. Various engineering applications make use of PMC for structural applications as listed in Table 2.7.

**Table 2.7** Applications of polymer matrix composites

<b>Engineering applications</b>	<b>Component making use of PMC</b>	<b>Reinforcement and matrix used</b>	<b>Reference</b>
Automobile	Door panels	Flax/sisal with thermosets resin	(Chandramohan and Bharanichandar 2013)
	Seat backrest	Coconut fibre/natural rubber	(Mohammed et al. 2015)
	Floor panels	Flax mat with polypropylene	(Mohammed et al. 2015)
Aircraft	Radome	Kenaf/glass fibre epoxy composite	(Karus et al. 2006)
Building materials	Panel	Sisal jute sandwich composites	(Saxena et al. 2011)
	Door panel	Bamboo mat composite	(Mohammed et al. 2015)
	Roof	Jute coir composite	(Mohammed et al. 2015)
	Wardrobes	Natural fibre reinforced boards	(Peças et al. 2018)
Sport	Tennis racket	Flax and hemp epoxy composite	(Peças et al. 2018)
	Bicycle frame	Flax fibre composite	(Peças et al. 2018)

<b>Engineering applications</b>	<b>Component making use of PMC</b>	<b>Reinforcement and matrix used</b>	<b>Reference</b>
Acoustic	Acoustic absorber	Cotton fibre-rubber granulate composites	(Mamtaz et al. 2016)
Furniture	Chair	Coir fibre polyester composite	(Sahu and Gupta 2017)
	Table	Oil palm based biocomposite	(Sahu and Gupta 2017)
Naval	Boat building	Woven glass/sugar palm fibres reinforced unsaturated polyester hybrid composite	(Karus et al. 2006)
Packaging	Food packaging	Wood fibers with Poly lactic acid	(AG 2017)
	Container for perfume	Curaua fibre wood flour based composites	(Peças et al. 2018)

The physical and mechanical properties of most popularly used thermoset and thermoplastic matrix systems studied by various researchers (Biron.M 2007; Callister 2006; Gupta et al. 2010; Mark 1999; Mohanty et al. 2005; Pilato 2010; Rout et al. 2001; Silva et al. 2010) are shown in Figure 2.5 from which it is clear that thermosets exhibit better physical and mechanical properties compared to thermoplastics.

Selection of appropriate matrix material for PMC subjected to impact loading is as important as selection of appropriate fiber material. Table 2.8 provides the various matrix materials used for impact applications.

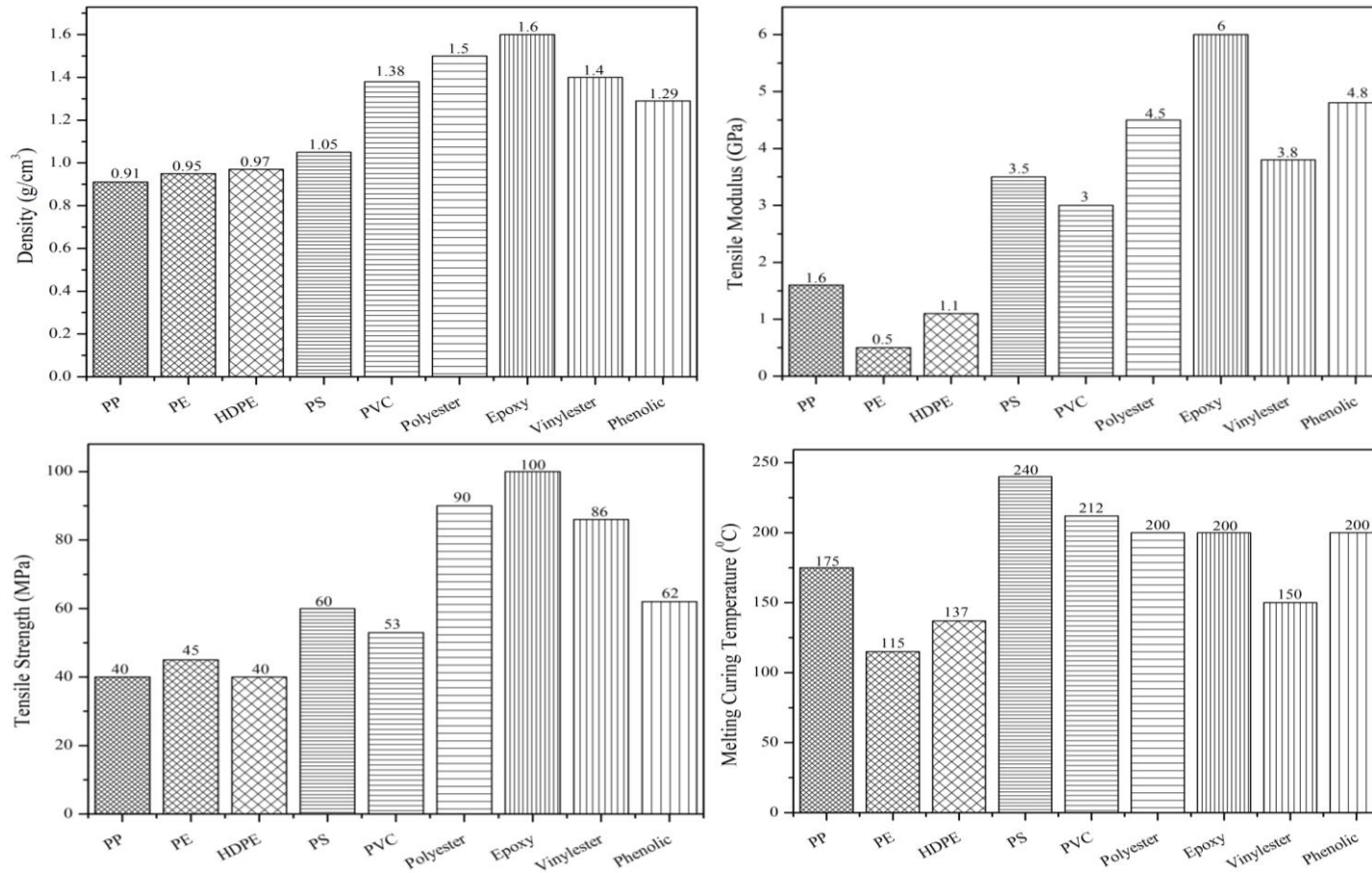


**Figure 2.5** Physical and mechanical properties of Polymer matrix

**Table 2.8** Matrix materials used in impact applications

<b>Matrix Material (Fiber)</b>	<b>Impact Application</b>	<b>Year</b>	<b>Reference</b>
PEEK (Carbon Fiber)	LVI	2014	(Xu et al. 2014)
Vinylester and Polyurethane (PE)	LVI and HVI	2001	(Lee et al. 2001)
Soft and Stiff matrix mimicking material (Kevlar)	Ballistic impact	2012	(Gopinath et al. 2012)
Epoxy, PU (Dyneema)	HVI	2017	(Wang et al. 2017a)
Polyester (Glass)	LVI	2004	(Pegoretti et al. 2004)
Shear thickening fluid (STF) (Glass)	HVI	2004	(Wetzel et al. 2004)
		2019	(Sen et al. 2019)
Epoxy (Kevlar, Glass, Flax, Glass, Glass)	LVI	2014	(Siegfried et al. 2014)
	LVI	2019	(Sreekantha Reddy et al. 2019)
	HVI	2015	(Reddy et al. 2015)
HDPE (Chonta palm wood)	HVI	2018	(Haro et al. 2018)
Rubber (Kevlar, Kevlar)	HVI	2019	(Khodadadi et al. 2019b; a)



The transfer of the load between the fibers, alignment and stabilization of the fibers depends on the type of matrix selected (Hancox 2000). Thermoplastics are more commonly used in composites reinforced by short fibers. PEEK and PPS have emerged as the potential substitutes for thermosetting polymers for impact applications. Research was concentrated on why the thermoplastics are able to resist damage during impact loading much better than thermosetting in the early part of 90's (Nash et al. 2015).

Effect of the type of matrix to resist damage during impact loading in PMC has been studied by few researchers (Reyes and Sharma 2010). It was showed that PMC with PEEK as matrix material provides excellent impact energy absorption capability while exhibiting minimal damage under LVI (Xu et al. 2014). Since PEEK is thermoplastic in nature, it also exhibits the advantage of easy and fast repair of the damaged composite. Consequently, PEEK has poor response to high velocity impact applications. Epoxy based carbon nano tubes incorporated PMC was investigated by researchers (Siegfried et al. 2014).

Polyester based resin was used to fabricate a PMC subjected to LVI (Pegoretti et al. 2004). It was found that the use of STF matrix enhances the ballistic impact response of the composites compared to neat fabrics (Sen et al. 2019). Many researchers make use of epoxy resin widely because of its remarkable mechanical properties, low shrinkage, strong adhesion, chemical stability, and dimensional stability (Siegfried et al. 2014), (Sy et al. 2019), (Sreekantha Reddy et al. 2019), (Reddy et al. 2015). In epoxy based composites subjected to low velocity impact, the transition of impact event to a stress wave dominated mode happens. The introduction of micro particles to HDPE proved to enhance the high velocity impact properties of the PMC (Haro et al. 2018).

The rubber was used as a matrix material in development of flexible composite subjected to ballistic impact loading with kevlar as reinforcement. It was compared with kevlar/epoxy PMC and it was concluded that kevlar/rubber composite exhibits better ballistic impact response compared to kevlar/ epoxy composite (Khodadadi et al. 2019b; a). Various researchers have conducted the impact study on the PMC at

different impact regimes. The matrix used decided the stiffness of the manufactured PMC. Pertaining to the role of matrix in deciding the impact property of PMC, an argument was put forth that stiff composites absorb higher energy compared to flexible composites (Lee et al. 2001). On the contrary, (Gopinath et al. 2012) showed that flexible composites are better energy absorbers compared to stiff composites.

Supporting the above argument, the study, on fabric reinforced PMCs using four different matrices showed that flexible composites have higher energy absorbing capability and undergo larger deformation compared to stiff composites (Wang et al. 2017a). The matrix used in PMCs governs the extent of deformation and thus affects local strain and impact resistance of PMCs. Though extensive literature is available for the impact studies of the composites, it is found from the literature that the application of flexible 'green' composites making use of natural rubber based matrix with natural fiber as reinforcement for impact applications is not studied by any researchers. The natural rubber being a complaint material can be a potential matrix system for flexible PMC subjected to impact. Also, natural rubber is environmental friendly, low cost and easily available.

### **2.3 Core materials used in polymer matrix composites for impact applications**

Various metallic and non metallic materials are available for use as a core in sandwich composites. The selection of appropriate core material depends on the nature of application of the sandwich composite. Cores used in sandwich composites have homogeneous or non homogeneous structures (Pflug et al. 2002) and accordingly, their classification is presented in Figure 2.6 and the core structures are presented in Figure 2.7. Various researchers have studied the application of various core materials for use in sandwich composites and different cores used are tabulated in Table 2.9.

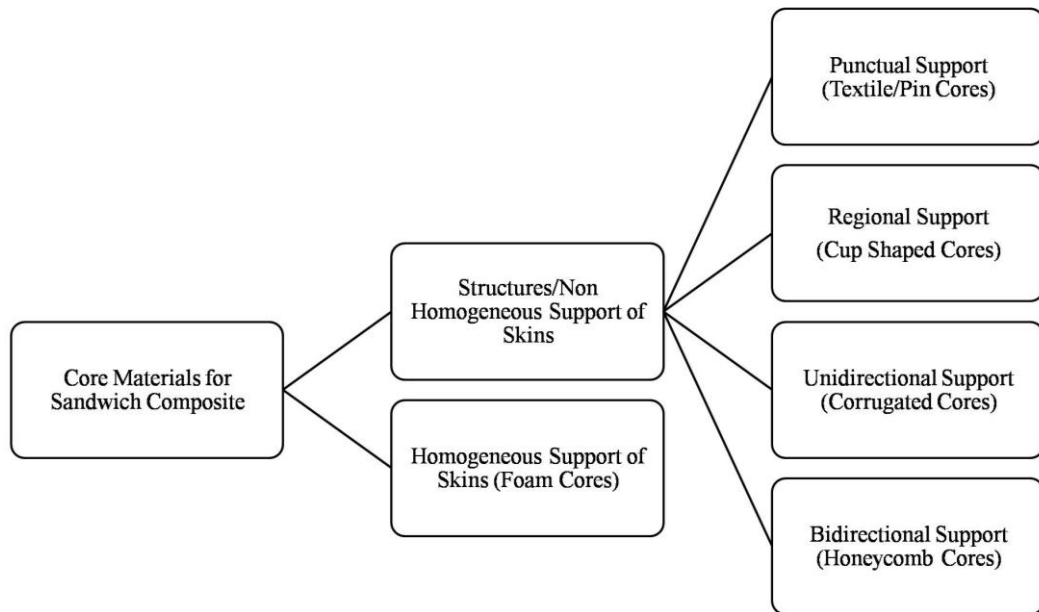


**Figure 2.6** Classification of core based on their structures (Pflug et al. 2002)

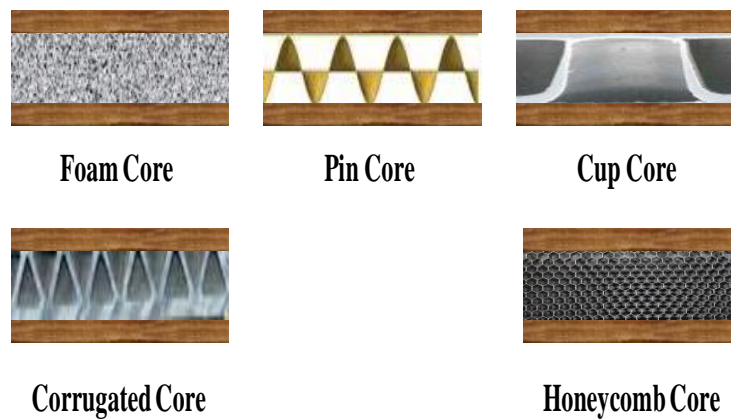


**Figure 2.7** Structure of cores

**Table 2.9** Core materials used in polymer matrix composites

Core material used in PMC	Reference
Balsa wood	(Jover et al. 2014)
Rubber	(Stellinger et al. 2016), (Liu et al. 2018a)
Low density balsa wood, high density balsa wood, cork, polypropylene honeycomb, and polystyrene foam	(Ramakrishnan et al. 2012; Wang et al. 2016b)

<b>Core material used in PMC</b>	<b>Reference</b>
Silly putty	(Xu et al. 2017)
Elastomer	(Düring et al. 2015)
Cork	(Walsh et al. 2017)
PP honeycomb	(Cabrera et al. 2008; Muzzy et al. 2001; Passaro et al. 2004)
PP foam	(Kulandaivel 2006; Kulandaivel et al. 2005; Muzzy et al. 2001)
PP nano carbon syntactic foam	(Brown et al. 2008)
Polyethylene terephthalate (PET) foam	(Pappada et al. 2010; Sorrentino et al. 2009)
Carbon foam	(Reyes and Rangaraj 2009)
Polymethacrylimide (PMI) foam	(Brown et al. 2008; McGarva and Åström 1999)
Aramid/phenolic honeycomb	(Offringa and Davies 1996)
Polyetherimide (PEI) foam	(Rozant et al. 2001)
PEI foam (in situ formed)	(Brouwer 1990; Provo Kluit 1997)

Application of balsa wood as a core material in sandwich structure was studied for ballistic impact application and concluded that the sandwich made up of balsa wood as core material is capable of with standing impacts from small projectiles such as, secondary debris from blast, hurricane, tornado and foreign object debris from roads and runways (Jover et al. 2014).

The rubber layer was integrated as core material in carbon fiber reinforced polymer matrix composite to evaluate the LVI damage resistance where it was shown effectively that a significant improvement in impact damage resistance can be achieved by integrating a rubber layer into a carbon/epoxy laminate (Stelldinger et al. 2016). The influence of rubber layer on the response of fluid-filled container due to high-velocity impact was studied. The outcome of this particular work proved that

introduction of rubber into the composite significantly affects the shock wave created in the container due to high velocity impact in a positive manner (Liu et al. 2018a).

The medium velocity impact response of the sandwich composite with different cores was studied. The sandwich panels made of aluminium face sheets with five different cores, viz., low density balsa wood, high density balsa wood, cork, polypropylene honeycomb, and polystyrene foam were studied and it was concluded that the core material plays a prominent role in deciding the impact performance of the sandwich (Wang et al. 2016b). It showed that depending on the nature of application of the composite, the particular core can be selected which directly affects the performance of the sandwich composite. Polypropylene foam core is found to be useful if the requirement of the composite is to absorb maximum energy with maximum resistance to penetration. In case, if it is essential to have minimum deformation of the rear skin in a sandwich composite, it is preferable to go for polypropylene (PP) honeycomb core. Silly putty (SP) is another potential core material whose suitability for high velocity impacts is studied. The outcomes of the particular study revealed that the inclusion of SP as core material enhances the ballistic impact response of the sandwich composite compared to kevlar composite laminate (Xu et al. 2017). Low velocity impact (LVI) response of sandwich composite with steel face sheet and elastomer core was assessed where it was proved that the minimal load required to initiate damage was increased due to addition of the rubber layer (Düring et al. 2015). Carbon fiber reinforced sandwich composite making use of cork as core material was studied for LVI response. The results obtained were encouraging since there was a significant improvement of the sandwich making use of cork core in acoustic, damping, and impact damage resistance characteristics compared to sandwich making use of synthetic foam (Walsh et al. 2017). This opened up the possibility to further investigate a sandwich composite with lighter cork as core material for its usage in energy absorption application. Thus can be very useful in the field of aerospace where high performance is demanded and at the same time protect the structure from impact loads. From the available literature pertaining to core materials used in PMC, it is clear that the possibility of using natural rubber as a core material is not explored to the fullest.

## 2.4 Impact of composites

The stages involved in the analysis of impact in composites ranges from simple analytical model to complex FE approaches as presented in Figure 2.8. With each increment in the methodology adopted for impact analysis, the capabilities related to prediction of damage is enhanced.

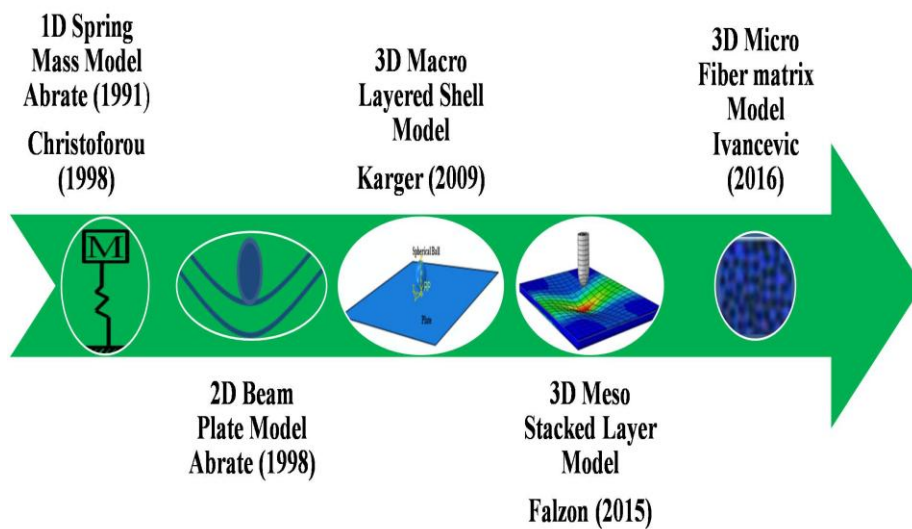


**Figure 2.8** Stages of development of impact analysis (Bogenfeld et al. 2018)

The analytical and experimental methods provide sufficient results pertaining to the damage onset and its quantitative dimensions. Whereas, FE based numerical methods are found to be useful in predicting the type and shape of damage based on the FE methodology adopted. In the early days, analytical methods based on spring mass system was adopted to assess the impact behaviour in 1991 (Abrate 1991) and 1998(Christoforou and Yigit 1998). Going further, the beam plate model was used for impact analysis in 1998 (Abrate 1998) which was able to identify the damage initiation in composites. Layered shell model was used in 2009 with the capability to identify the damage type, shape and extent of damage (Kärger et al. 2009). Further progress in the effort level led to stacked layered model in 2015 with micro damage prediction capability (Tan et al. 2015). Finally, Fiber matrix model was developed in 2016 (Ivančević and Smojver 2016). The reported research pertaining to various PMC used for impact applications at different impact regimes and the methodologies adopted to assess the impact response of the PMC are presented in Table 2.10.

**Table 2.10** Reported research on polymer matrix composites subjected to impact

<b>Material</b>	<b>Impact test</b>	<b>Method</b>	<b>Reference</b>
Glass epoxy composite	LVI	Analytical	(Whisler and Kim 2012)
Carbon epoxy composite	LVI	FE	(Panettieri et al. 2016)
Carbon fiber reinforced composite	LVI	Experimental and FE	(Topac et al. 2017)
Graphite epoxy composite	LVI	FE	(Kim et al. 2013)
Glass epoxy composite	Low to hyper velocity impact	FE	(Ansari and Chakrabarti 2016a)
Sandwich composite with facesheet as Glass, Carbon and Kevlar Fibre Reinforced polymer composite and core as Aluminium foam	HVI	FE	(Nalla Mohamed et al. 2016)
Carbon fiber+PEEK	HVI	FE	(Žmindák et al. 2016)
Shear thickening fluid impregnated with kevlar fabrics	HVI	FE	(Park et al. 2015)
Kevlar-polypropylene composite	HVI	Experimental and	(Bandaru et al.

<b>Material</b>	<b>Impact test</b>	<b>Method</b>	<b>Reference</b>
		FE	2016a)
Ceramic composite	HVI	FE	(Fawaz et al. 2004)
Napier grass fibre/polyester composites	LVI	Experimental	(Fahmi et al. 2016)
Glass fiber reinforced composite	Crash	FE	(Nasir Hussain et al. 2017)
Polyurethane foam, silicon carbide inserts/plate bonded to glass fiber composite	LVI	FE	(Akshaj et al. 2016)
3D woven composites	LVI	Experimental	(Elias et al. 2017)
Pandanus composites	LVI	Experimental	(Kuan et al. 2017)
Pultruded glass fiber reinforced composites	LVI	Experimental	(Li et al. 2017)
Carbon-silicon carbide composite	LVI	Experimental	(Mei et al. 2016)
Polypropylene based composites with fibers kevlar, basalt and hybrid combination	LVI	Experimental	(Bandaru et al. 2016b)
Sandwich composite with carbon fiber reinforced composite as skin and rubber/aluminium as core	LVI	Experimental	(Abo Sabah et al. 2017)
Jute based PMC	LVI	Experimental	(Papa et al. 2017)
ATH/epoxy core sandwich composite panels	LVI	Experimental and	(Morada et al. 2017)



<b>Material</b>	<b>Impact test</b>	<b>Method</b>	<b>Reference</b>
		numerical	
Glass fiber reinforced composites	LVI	Experimental	(Ansari and Chakrabarti 2017a)
Glass epoxy composite	HVI	Experimental	(VanderKlok et al. 2018)
Glass epoxy and Dyneema composites	HVI	Experimental	(Reddy et al. 2017)
Kevlar composites	HVI	Experimental	(Palta et al. 2018)
Carbon, Kevlar and Glass fiber reinforced composites	HVI	Experimental	(Sudhir Sastry et al. 2014)
Glass phenolic composites	HVI	Experimental	(Reddy et al. 2015)
Hemp fabric reinforced composite	LVI	Experimental	(Scarponi et al. 2016)
Glass fiber reinforced nitrile rubber modified epoxy resin	LVI	Experimental	(Ricciardi et al. 2018)

#### 2.4.1 Analytical and finite element modeling approach

In the literature we can find the analytical approaches used for solving the impact problems. Simplified analytical model was proposed to analyze the LVI response of reinforced concrete structures using energy balance and single degree of freedom models (Das Adhikary and Li 2018). LVI response of sandwich composites was analytically predicted using a new three degree of freedom spring mass damper model (Malekzadeh et al. 2006). The use of analytical approach was demonstrated to predict the effect of radius of impactor of damage of glass epoxy composite subjected to LVI (Whisler and Kim 2012). Impact response of a sandwich composite with honeycomb core was assessed using revised energy balance model (Zhang et al. 2017b). The sandwich composite beams were analysed for their LVI behaviour using analytical model (Fatt and Park 2001; Ivañez et al. 2014).

The numerical methodology was proposed to predict the ballistic impact response of composite impacted by steel sphere (Pernas-Sánchez et al. 2014b). The outcome led to conclusion that the ballistic response of composite is affected by radius of the projectile. The analytical model makes use of energy balance approach and shows that ballistic limit of composite is inversely proportional to square root of the projectile radius. The analytical approach to study the high velocity impact of composite based of woven fabric was proposed (Pasquali et al. 2015). The main mechanism for absorbing energy is found to be deformation of secondary yarns and the target was perforated due to failure of primary yarns. The drawback of the theoretical approach lies in its inability to deal with materials having flaws such as cracks, voids, manufacturing defects and inhomogeneity. Finite element approach using commercially available simulation packages has been proved to be better than analytical approach (Gupta and Woldesenbet 2009). Accurate numerical simulation of impact events can provide physical insights that cannot be captured by experiments. Currently, for impact modelling in composite structures at low and high speeds mainly Finite Element Method (FEM), Boundary Element Method (BEM), Finite Volume Method (FVM), mesh less formulations are used. Many researchers have adopted the FE approach to simulate the impact response of the composites, metals and alloys. Some of the approaches adopted and their outcomes leading to

justification of using FE approach in the initial part of the study are presented in this section.

Both experimental and FE approach to analyse the LVI impact performance of the carbon fiber reinforced composite (Topac et al. 2017). Commercially available FE software was made use of to simulate the LVI behaviour of the composite. Damage mechanisms are modelled based on continuum damage mechanics (CDM). The results showed that there is a good agreement between experimental and FE results.

Different modelling techniques for analysing the LVI response of composite plates was studied with an intention of comparing results obtained from different techniques and provide a guideline for those researchers who opt for FE simulation to study the LVI response of composites (Ibrahim 2014). Impact simulation was carried out using LS-DYNA to study the different modes of failure in composites using a 3D solid element (Jagtap et al. 2017). It was found that results vary with mesh size. Parametric study was also carried out by varying the boundary conditions and impact velocity. The validation of the obtained FE results with experimental results showed that FE method can be effectively used to simulate the LVI response of the composite to near real life situation.

The cross ply composite laminates subjected to LVI was studied using a FE approach using a CDM based method with the help of ABAQUS/ Explicit software (Zhang et al. 2017a). The results obtained led to respectable comparison of FE and experimental results. The delamination type of damage induced in composite due to LVI loading was studied using LSDYNA with the help of transient non-linear finite element code (Maio et al. 2013). The material model proposed in this study proved to be the good approach to assess the LVI behaviour of composite using FE approach for non penetrating response of composite laminates.

The progressive damage analysis of the graphite epoxy composite laminates using CDM was proposed using ABAQUS/ Explicit FE software (Kim et al. 2013). Weibull distribution of the composite strength was employed in the proposed model along with consideration of non linear shear behaviour of composite. In addition to these

considerations, the model was also incorporated with irreversible strain due to the damage. The FE results well matched with the experimental results supporting the proposed model. Impact response of the composite ranging from low to hyper velocity was studied using AUTODYN hydro code (Ansari and Chakrabarti 2016a). The results concluded that the penetration of the proposed composite by bullet is more difficult when the composite is fully restrained. In case of high velocity impact, damage of the composite plate is localized. The obtained FE results agreed well with the available literatures.

The LVI response of carbon/epoxy laminates was carried out and the results matched with the experimental results (Panettieri et al. 2016). Numerical analysis with the aid of FE software was carried out for impact analysis of steel plates and graphite/epoxy composite where the flexible nature of the composite was investigated. The results proved that flexible nature of the composite has a positive effect on the energy absorption due to impact. High velocity impact of the sandwich composite was studied using ABAQUS/ Explicit (Nalla Mohamed et al. 2016). The accuracy of the current FE approach used was assessed by comparing the obtained results with the experimental results available in literature in terms of residual velocity, ballistic limit and damage area. The conclusion of this study reveals that FE approach can be successfully adopted in the initial part of study to save time and effort. High velocity response of composite plates was studied using FE modelling and the results reveal that FE approach efficiently simulates the minute details pertaining to impact response of the composite which are difficult to obtain through experiment (Žmindák et al. 2016). Shear thickening fluid impregnated with kevlar fabrics was assessed for their high velocity impact behaviour using numerical simulation method with the help of LSDYNA (Park et al. 2015). At the time of carrying out the simulation, an assumption was made that friction between the yarns and fabric layers was the major energy absorption mechanism. The obtained results were compared with analytical results and proved that they are in agreement with each other. Similarly high velocity impact response of the kevlar-polypropylene composite was assessed using ANSYS (Bandaru et al. 2016a). The FE model was validated with experimental results. The

extension of FE simulations was used to study the influence of projectile mass of high velocity impact response of the composite.

Three dimensional FE model was adopted to assess the normal and oblique performance of the ceramic composite armours (Fawaz et al. 2004). The experimentation is done with the same conditions in which the simulation was carried out and it was found that the deviation in experimental and FE results are within acceptable range. The LVI impact response of the napier grass fibre/polyester composites was studied and it was found that there exists a relationship between the amount of fiber used and the impact properties of the composite (Fahmi et al. 2016). The incorporation of napier fiber led to increased damage resistance of the composite compared to pure polyester. The energy absorption of crash box made up of glass fiber reinforced composite was studied. It was found that the geometry of the crash box played a vital role in deciding the energy absorption of the composite (Nasir Hussain et al. 2017).

#### 2.4.2 Experimental approach

Energy absorption of polyurethane foam, silicon carbide inserts/plate bonded to glass fiber composite was assessed. The study revealed that composite with silicon carbide plate absorbs higher energy compared to composite having silicon carbide inserts (Akshaj et al. 2016). LVI impact response of 3D woven composites intended for aerospace applications are carried out and results are compared with numerical results, The outcome revealed that the model used gives exact damage mechanism and also it was possible to predict the residual depth accurately (Elias et al. 2017). The pandanus composites were assessed for their impact response which showed that pandanus fibers offer excellent impact properties. Increase in volume fraction of these fibers resulted in enhanced toughness of composite (Kuan et al. 2017).

Impact response of the pultruded glass fiber reinforced composites was studied at different impact energy levels. It was found that as the impact energy increases, the extent of damage increases in pultruded glass fiber reinforced composites. Also, when the composites are subjected to higher impact energy, a multiple shear damage mode

was found to occur (Li et al. 2017). The effect of orientation of plies in the carbon-silicon carbide composite subjected to LVI was studied. It was noted that the damage mechanisms were different on the impacted side and the rear side of the laminate. The laminate with 0/90 orientation is found to experience extreme fiber fracture, whereas the ones with 45/45 and 0/45/90/45 showed less fracture of fiber (Mei et al. 2016). The process for analysing the damage of the composite subjected to LVI was proposed where C scan methodology was adopted to assess the damage (Long et al. 2015). Based on the damage model, the numerical models were built with cohesive contact method as reference. The LVI response of three different polypropylene based composites with fibers kevlar, basalt and hybrid combination was assessed (Bandaru et al. 2016b). The outcome led to a conclusion that basalt composite has higher resistance to damage and hybrid composite exhibited better energy absorption characteristics.

Inspired by the woodpecker head, a sandwich beam was developed and analysed for LVI (Abo Sabah et al. 2017). The sandwich consisted of facesheets made of carbon fiber reinforced composite and rubber and aluminium were used as core materials. The results indicate that inclusion of rubber enhances the damage resistance with matrix cracking as the only damage mechanism observed. The sandwich composite proposed for use in trains structures were evaluated (Sakly et al. 2016). The results revealed that cavitations in core could lead to critical damage in the sandwich structure. A methodology for predicting the incipient point of impact force and related damage in the composites was proposed (Zhang and Zhang 2015). Initially potential failure modes were assessed. Later, the damage was simulated along with assessing the effect of damage mode on the stiffness of the composite. High compressive stress suppresses the delamination adjacent to the point of impact thereby resulting in negligible reduction of laminate stiffness. Damage investigation of the jute based PMC through ultrasonic method was studied (Papa et al. 2017). Special attention is given to jute fiber due to limited or nor literature available on the impact behaviour of jute based composite. Impact response of innovative sandwich composites made of core having epoxy resin filled with alumina tri hydrate particles was assessed (Morada et al. 2017). The results revealed that this type of sandwich exhibited better

performance in terms of damage resistance which is due to the nature of the core used which can undergo good amount of plastic deformation prior to failure. Thus this type of core material is suitable for sandwich composites subjected to impact loading. The fiber metal laminates subjected to LVI was studied (Bienias et al. 2016). It was found that in fiber metal laminates, with increase in impact energy, the damage area increases with delamination and matrix cracks as the major source of failures.

It was found that PMC are more susceptible to damage due to impact and this damage is generally more difficult to detect and repair and can be serious threat to the integrity of the component (Ali et al. 2017). Glass fiber reinforced composites subjected to dynamic loading was assessed (Ansari and Chakrabarti 2017a) under different shaped impactors. It was found that the shape of the impactor also plays a vital role in deciding the impact response of the laminate. Delamination is found to be the most influenced damage condition compared to others. It was also found that when glass fiber reinforced composite is sandwiched in between kevlar fiber reinforced composite, better penetration resistance is obtained. Ballistic impact performance of glass epoxy composite laminate was studied in terms of ballistic limit and was concluded that S2-glass/epoxy composite is ranked high in ballistic capability (VanderKlok et al. 2018).

New type of sandwich structure comprising aluminium foam as the core and fiber metal laminate as skin was studied (Liu et al. 2017). It was found that the energy absorption can be increased by increasing the thickness of the skin. Also it was found that blunter projectile showed greatest decrease in the velocity, followed by the hemispherical, semi-ellipsoid and conical projectiles. A comparative study on energy absorption of glass epoxy and Dyneema composites was carried out (Reddy et al. 2017). Dyneema composite emerged as better energy absorbers compared to glass epoxy composites when subjected to high velocity impact. Failure analysis shows that the nature of damage in both the composites are different with Dyneema composite undergoing plastic deformation and fiber stretching due to tension. Whereas, glass epoxy composite undergoes elastic deformation, delamination and brittle failure of fibers.

Parametric studies was carried out on single, multi layered steel plates and kevlar composites subjected to high velocity impact loading (Palta et al. 2018). The results revealed that impact performance of composites are dependent on thickness and layer configuration. High velocity impact studies on carbon, kevlar and glass fiber reinforced composites were carried out (Sudhir Sastry et al. 2014) out of which kevlar is found to absorb maximum energy compared to carbon and glass. Ballistic impact performance of composites were studied (Shaktivish et al. 2013) in terms of absorbed energy and damage mechanism. It was found that energy absorbing mechanisms are different with different target thickness.

Ballistic response of glass phenolic composites are studied with varied thickness and impact velocity (Reddy et al. 2015). A non linear relationship between thickness and energy absorption was found. Also the projectile deforms more based on the thickness of target compared to impact velocity. The post-mortem study of the laminates shows that failure mechanism is different for different thickness of laminate with more damage area for laminate with larger thickness. Tensile failure and delamination are found to be the predominant mechanism of failure in case of laminate with larger thickness. Whereas, for laminate with smaller thickness, failure is dominated by shear cutting of fibers. The influence of impact angle on the response of the composite laminates was studied (Ansari and Chakrabarti 2017b; Xie et al. 2016). The delamination type of damage occurs due to failure of matrix in tension in case of normal impact and in case of oblique impact, the interlaminar stresses leads to delamination. The fiber at the front portion of the composite laminate breaks due to shearing and no signs of crater were found in case of normal impact. Whereas in case of oblique impact, crater were formed with breakage of fiber was visible. The oblique impact response of composite was studied (Ivañez et al. 2015) and was found that 15 degree is the critical angle of impact below which no significant effects are seen in impact response of composite. The oblique impact response of sandwich structure was carried out (Navarro et al. 2012). It was found that the extent of damage is highly dependent on the firing axis or in other words on the impact angle. The effect of impactor shape on the ballistic impact response of the single, two layered steel sheet and sandwich composite was studied (Zhou and Stronge 2008). The results revealed



that layered plate lost more energy compared to single layered plate when impacted by flat nosed projectile. But no significant changes were observed for hemispherical projectile. A study on normal and oblique impact response of aluminium plates was taken up (Børvik et al. 2011). The results revealed that critical oblique angle was less than 60 degrees. As the oblique angle increased beyond 60 degrees, bullets went unpenetrated through the targets.

Experimental approach for assessing the high velocity impact response of the composites were carried out (Pernas-Sánchez et al. 2014a). Below the ballistic limit of the composites, the damage caused due to oblique impact is smaller compared to normal impact. Whereas the behaviour is found to get reversed above ballistic limit. Chopped strand mat reinforced composites were analysed for their impact performance at oblique angles (Madjidi et al. 1996). It can be concluded that the impact of obliquely inclined plates is less onerous than the impact of flat plates. Dynamic response of delaminated composite shells at oblique impact was studied (Dey and Karmakar 2014). It was found that with increase in angle of impact, resistance to damage is found to reduce.

Preliminary studies related to assessing the LVI of fiber metal laminates was assessed (Ferrante et al. 2016). The impact response is found to be dependent on the size of impactor. Damage resistance and damage tolerance post impact of the hemp fabric reinforced composite subjected to LVI was addressed (Scarponi et al. 2016). From the results it is evident that compared to standard hemp epoxy composite laminate, hemp and bio based resin resulted in superior performance. Impact test was carried out on the glass fiber reinforced nitrile rubber modified epoxy resin (Ricciardi et al. 2018). The results showed higher indentation for modified composite with lower delamination extension. It also showed that addition of nitrile rubber resulted in more difficult damage propagation. Impact response of rubber reinforced concrete (RRC) was carried out (Liu et al. 2012). Due to addition of rubber the energy absorption of RRC was found to be higher compared to normal concrete.

An argument was put forth saying that stiff composites absorb higher energy compared to flexible composites (Lee et al. 2001). On the contrary, it was showed

that flexible composites are better energy absorbers compared to stiff composites (Gopinath et al. 2012). Supporting this, the study carried, on fabric reinforced PMCs using four different matrices showed that flexible composites have higher energy absorbing capability and undergo larger deformation compared to stiff composites (Wang et al. 2017a). The matrix used in PMCs governs the extent of deformation and thus affects local strain and impact resistance of PMCs. The damage mechanisms in flexible composites also differ from that of stiff composites as shown in Figure 2.9.

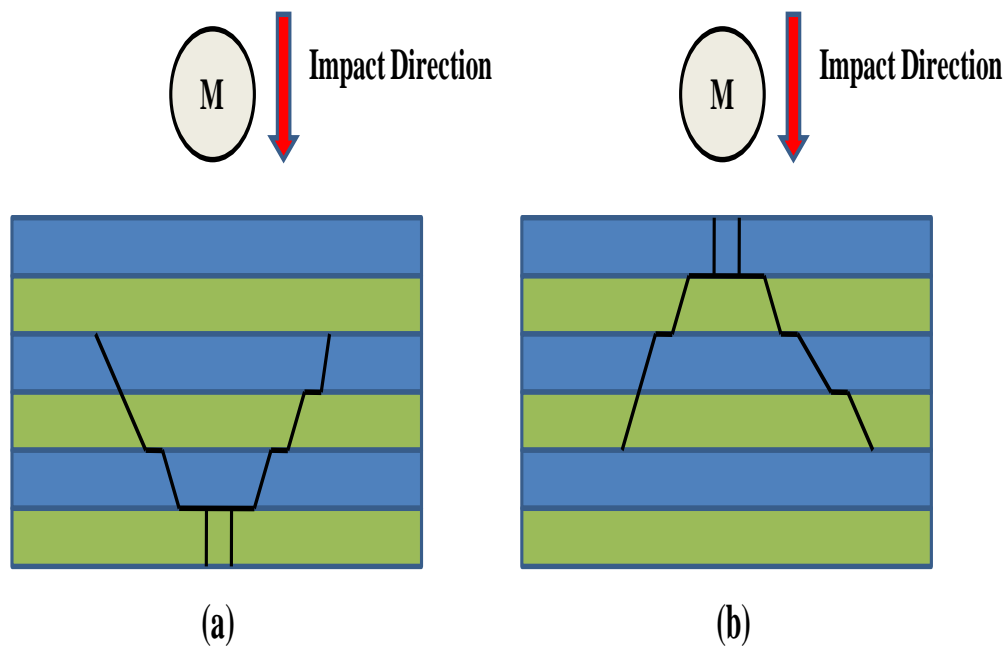


**Figure 2.9** Damage propagation in (a) flexible composite and (b) stiff composite (Saghafi et al. 2019)

The flexible composites undergo larger deflection during an impact event and due to the flexural deformation; the damage is introduced at the bottom ply; whereas in case of stiff composites, the limited deformation of the composites leads to localized stress leading to damage at the point of contact (Abrate 1998). Though extensive literature is available for the impact studies of the composites, it is found from the literature that the application of flexible green composites for impact applications are untouched.

**Table 2.11** Natural fibers in polymer matrix composites for low velocity impact applications

Natural fiber	Matrix used	References
Abaca	PLA	(Bledzki et al. 2009)
Abaca	PP	(Bledzki et al. 2010)
Agave	PP	(Langhorst et al. 2018)
Banana	PE	(Liu et al. 2009)
Bamboo	PP	(Lee et al. 2009)
Bamboo	PE	(Mohanty and Nayak 2010)
Coir	PP	(Haque et al. 2012)
Flax	PLA	(Bax and Müssig 2008)
Flax	PP	(Rahman et al. 2017)
Flax	PE	(Singleton et al. 2003)
Hemp	PP	(Guo et al. 2010)
Jute	PE	(Mohanty et al. 2006)
Jute	PP	(Rahman et al. 2010)
Kenaf	PP	(Anuar and Zuraida 2011)
Oil palm	PP	(Nordin et al. 2017)
Ramie	PP	(Li et al. 2012)
Sisal	PP	(Oksman et al. 2009)

Table 2.11 provides the details of fibers used for manufacturing PMC for impact applications. It can be seen from the Table 10 that natural fibers are used mostly with PP matrix for preparation of composites. The literature reveals that the jute which is the most popular natural fiber reinforced with natural rubber leading to flexible PMC is not studied by any researchers.

## 2.5 Wear characterization

In many engineering applications where PMC are used, assessing the tribological properties of the PMC used is a critical issue (Friedrich 2018). To meet the demand of the industry for a better wear resistant material, the new wear resistant materials are being developed and this has led to more demand for the research in this area.

Till date, researchers were focusing on the contact tribology of the metals, metals with metals or ceramics; however, polymers and PMC are emerging as the popular substitutes for metals for various engineering applications demanding the assessment of tribological characteristics of such polymers and PMC.

The composites are subjected to different kind of loading during their service and thus it becomes essential to assess the behaviour of the composite subjected to various mechanical loads prior their usage. Tribological characterization of the PMC is very much essential prior to its application in any engineering component.

An approach to design the optimum configuration of PMC for wear application is presented in Figure 2.10 and the classification of different methods available for tribological characterization is presented in Figure 2.11.

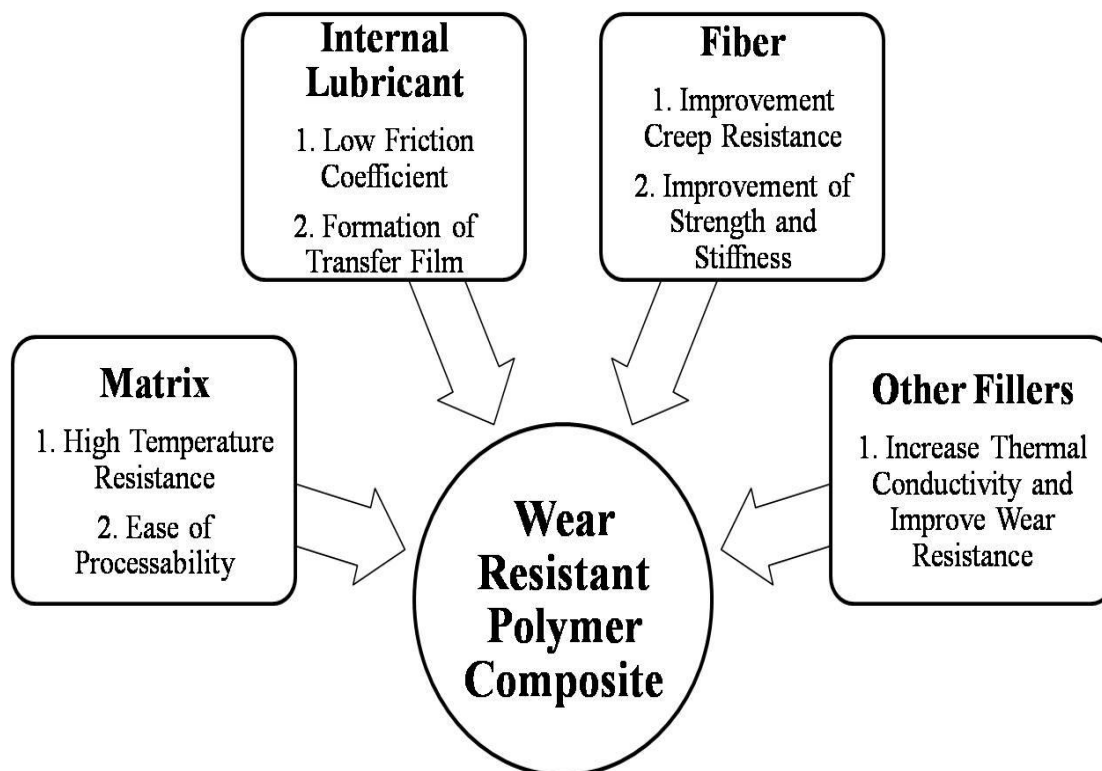


**Figure 2.10** Approach to design the optimum configuration of polymer matrix composites for wear application (Friedrich et al. 2002)

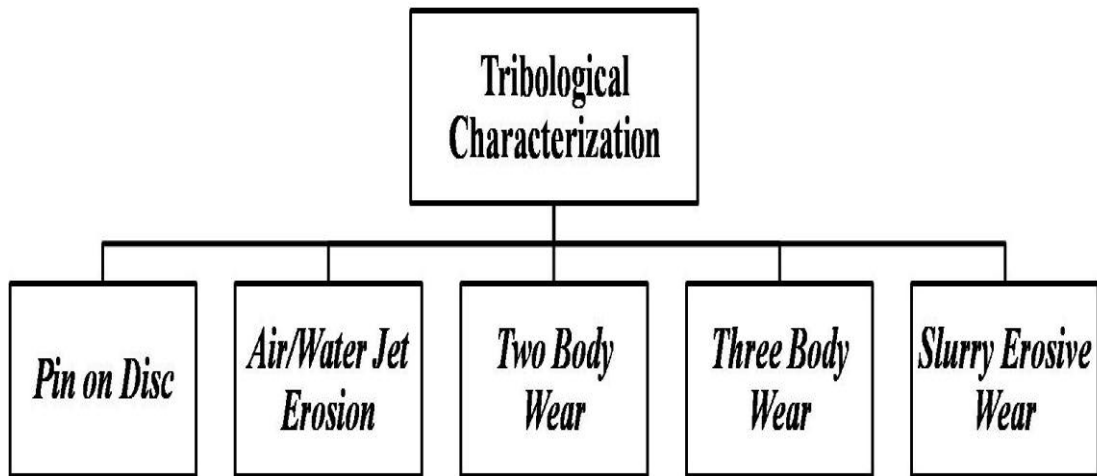


**Figure 2.11** Classification of different tests available for tribological characterization

The loss of the mass due to erosive wear by impingement of small solid particles is a critical design consideration while selecting a material for structural applications like bumpers in automobiles, cladding for armour vehicles, pipelines carrying solid particles and material handling systems (Rao et al. 2016).

The concept of ‘green tribology’ emerged during the ‘World Tribological Congress’ which concentrates on the science and technological aspects of tribology related ecological balance of environmental and biological impacts (Jost 2009). The role of designer in implementing the green tribology of a designer is to bridge the gap between the desire of energy usage and the possible environmental impacts upon introducing the equipment to the society and the need in reducing the dependency on fossil fuels and is summarized in Figure 2.12 (Nirmal et al. 2015; Tzanakis et al. 2012). This led to the usage of natural fibers and naturally available matrix materials for developing a PMC which emerged as the great potential materials for tribological applications due to their self lubricating, light weight and corrosion resistance properties.

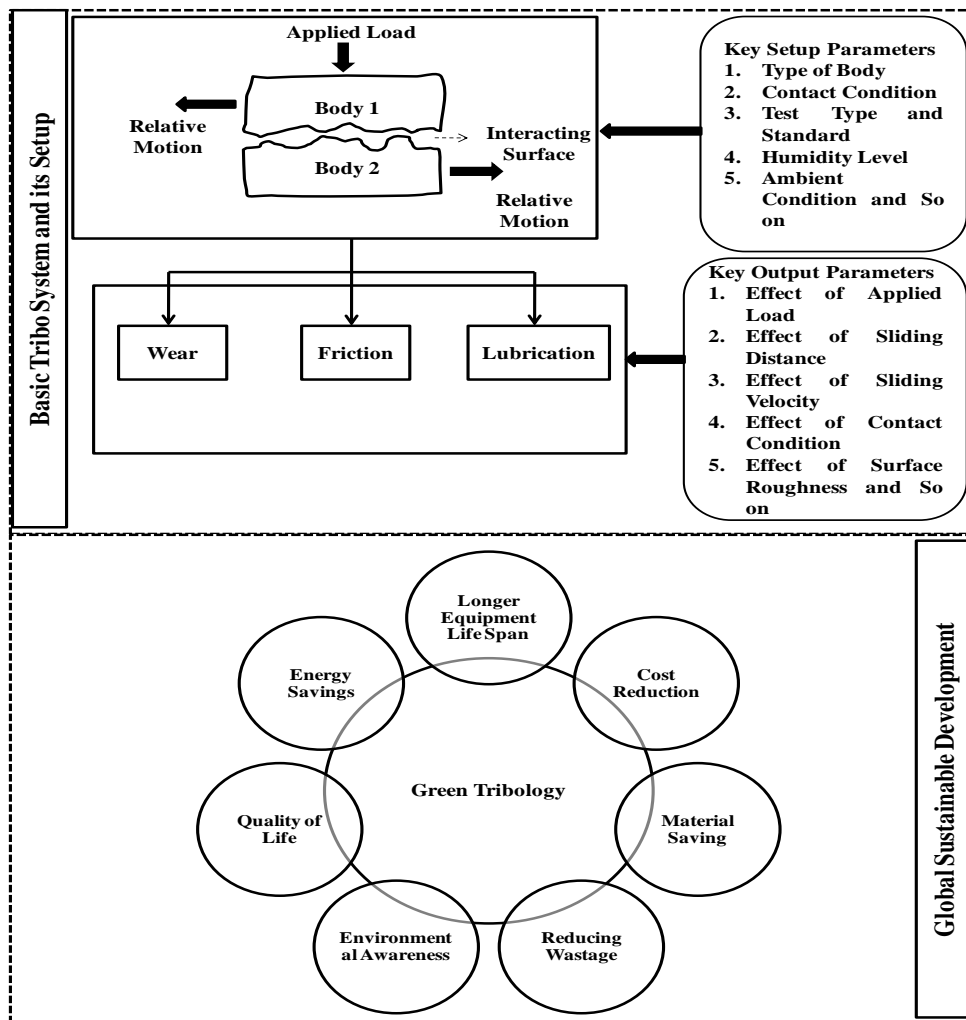


**Figure 2.12** Interaction of bio tribo system towards global sustainable development (Nirmal et al. 2015; Tzanakis et al. 2012)

The PMC with different fiber matrix combination used for tribological applications are presented in Table 2.12.

**Table 2.12** Fibers and Polymers used in polymer matrix composites for tribological application

Fiber	Matrix	Reference
Glass	Polyester	(El-Tayeb 2007; Yousif 2013)
Carbon	Epoxy	(Algbory 2011; Wan et al. 2005)
Rubber dust	Epoxy	(Mishra 2012)
Glass	Epoxy	(Basavarajappa et al. 2009; Joshi et al. 2014; Rajesh

Fiber	Matrix	Reference
		et al. 2012; Shivamurthy et al. 2009)
Kenaf	Epoxy	(Chin and Yousif 2009)
Sugarcane	Epoxy	(Mishra and Acharya 2010)
Linen and Jute	Polyester	(El-Sayed et al. 1995)
Bamboo	Epoxy	(Nirmal et al. 2012)
Bamboo	Polyester	(Dwivedi et al. 2007)
Coir	Epoxy	(Mahesh et al. n.d.; Rao et al. 2012)
Coir	Polyester	(Yousif 2009)
Kenaf	Polyurethane	(Singh et al. 2011)

Various materials and operating parameters affect the wear behaviour of the natural fiber reinforced PMC. The parameters affecting the wear behaviour of PMC are presented in Figure 2.13.

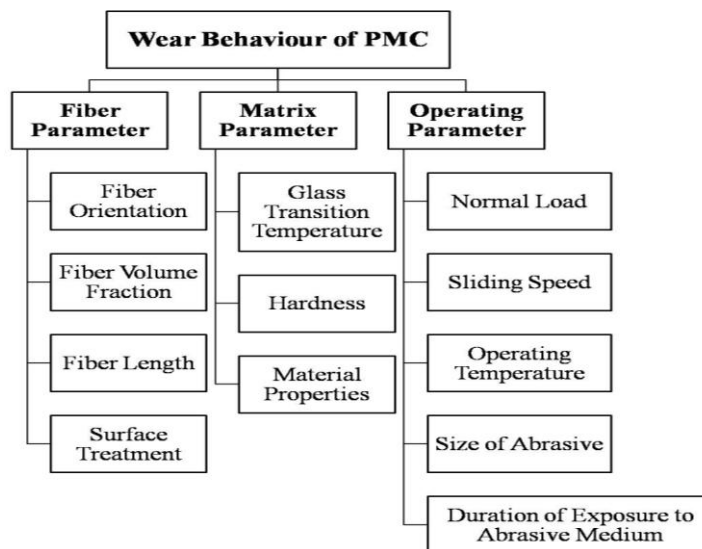


**Figure 2.13** Parameters affecting wear behaviour of polymer matrix composites

Polymers of different classes including thermosets, thermoplastics and elastomers with wide range find their application in PMC for wear applications (Fahim and Chand 2008; Friedrich 2018). Classification of such polymers based on application, cost and properties are presented in Figure 2.14.

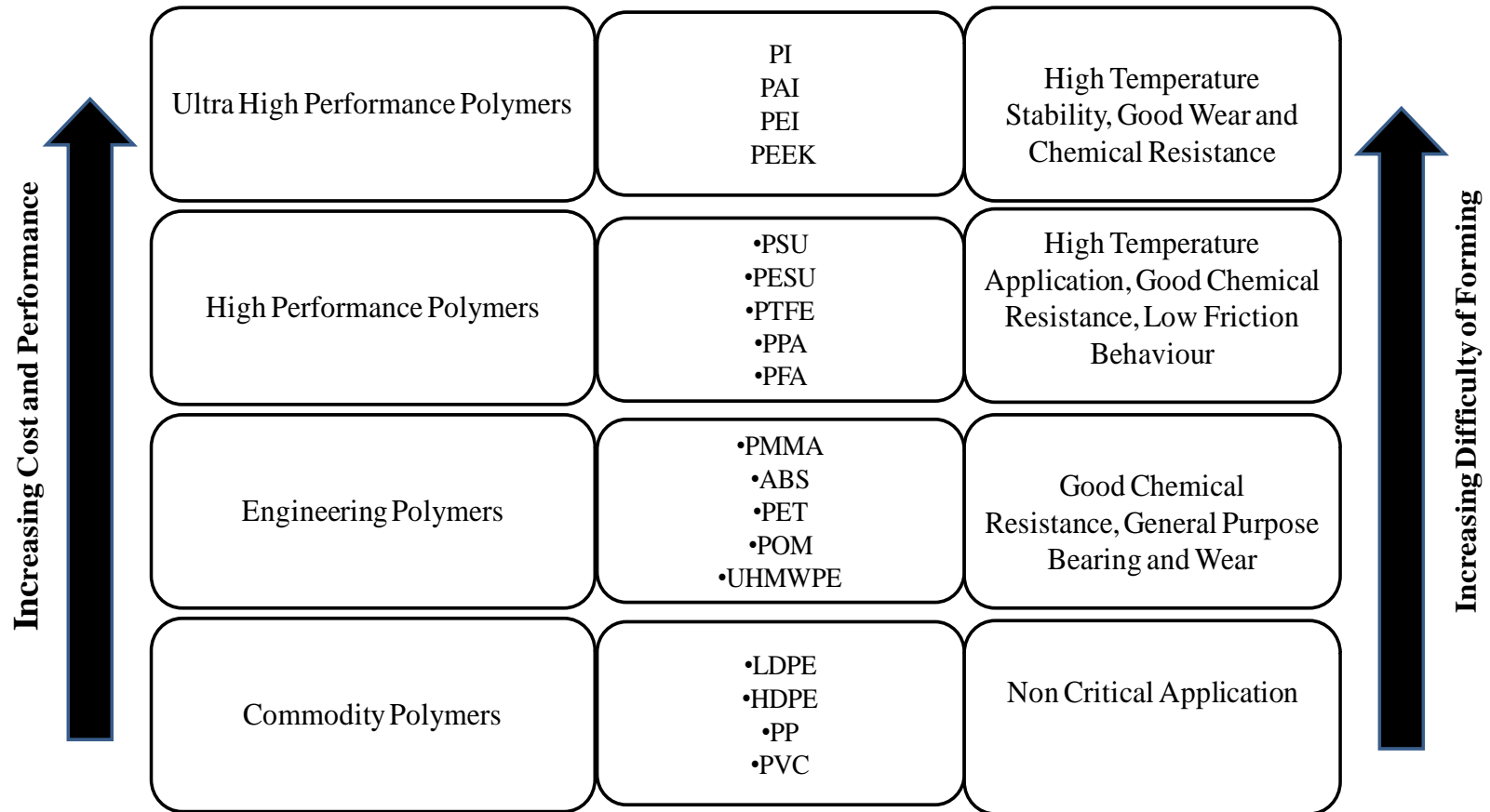


**Figure 2.14** Classification of polymers for wear applications (Friedrich 2018)



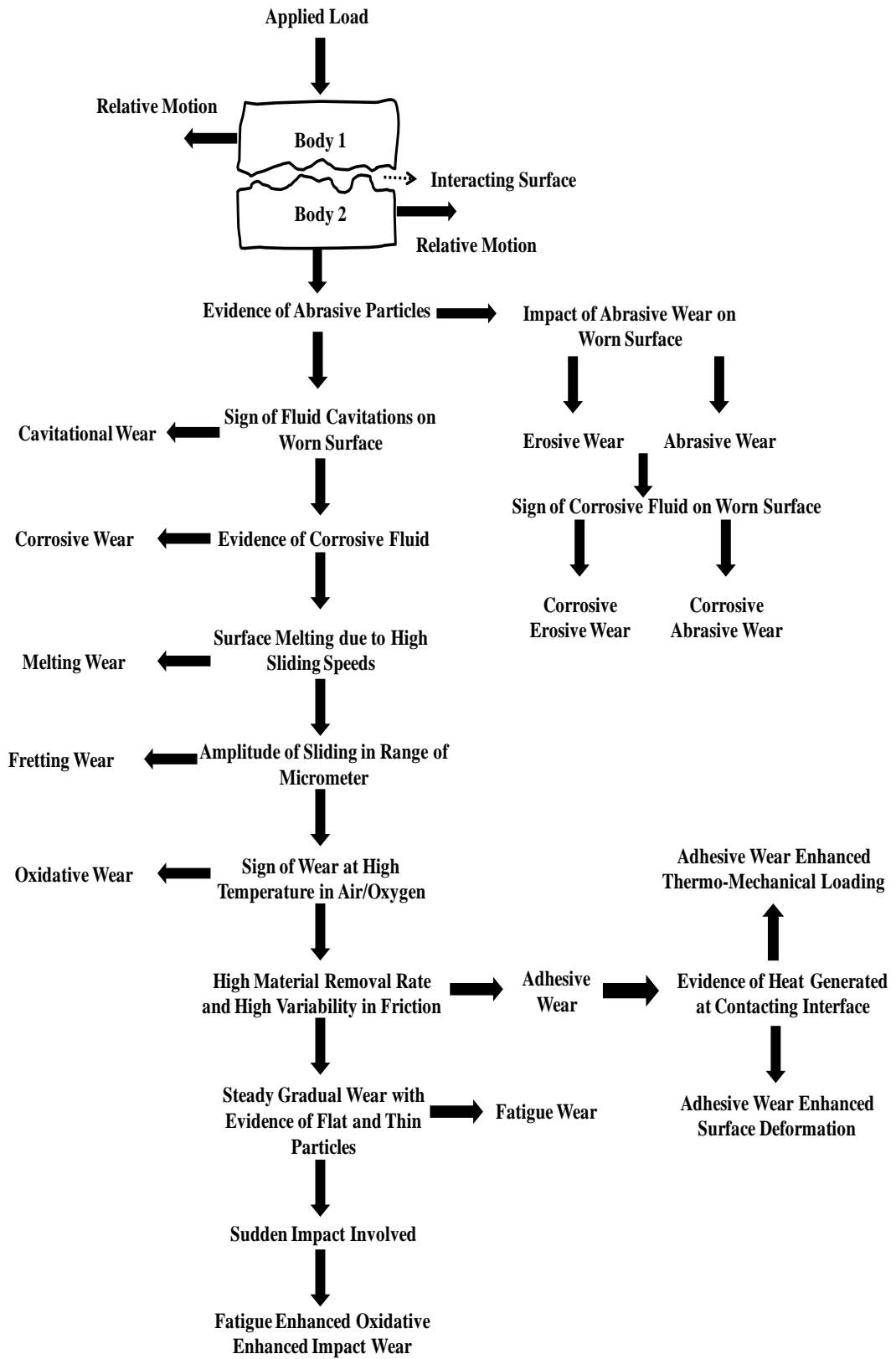


**Figure 2.15** Sequence of wear classification (Stachowiak and Batchelor 2011)

The wear sequence as shown in Figure 2.15 is usually helpful in determining the wear mechanism the PMC has undergone (Stachowiak and Batchelor 2011). With the replacement of metals, alloys with composites, the study of the erosive behaviour of composites under slurry environment is essential (Joshi et al. 2014). The slurry erosive study carried on Fe-TiC composite showed that addition of TiC in Fe matrix results in enhanced slurry erosive resistance of Fe-TiC composite (Manoj et al. 2008). The comparative study on erosive behaviour of fly ash reinforced Al-Cu alloy and unreinforced alloy showed that addition of fly ash enhances the erosion resistance (Mahendra and Radhakrishna 2007). The erosive behaviour of Al-SiC composite was studied and concluded that increase in the SiC resulted in enhanced resistance to erosion (Ramachandra and Radhakrishna 2006). The influence of erodent characteristics on erosion resistance of titanium was studied (Lindgren and Perolainen 2014). The slurry erosive behaviour of metal matrix coatings was also studied (Farahmand et al. 2015). The slurry erosive wear behaviour of SiC ceramic foam/epoxy co-continuous phase composite was studied (Ren et al. 2015). Slurry erosive behaviour of basalt reinforced low density polyethylene was studied (Akinci et al. 2011). The behaviour of metal matrix composite under slurry environment was studied (Kumar et al. 2018b; a). Slurry erosion resistance of polyethylene under conditions relevant for mineral processing was studied (Koskela et al. 2017).

Many researchers have studied the slurry erosive wear behaviour of metals, alloys and in the field of composites, metal matrix composites are concentrated. Since nowadays, the polymer matrix composites are replacing the metals, alloys and metal matrix composites owing to various advantages like cost and weight, the study of erosive behaviour of polymer matrix composites under slurry environment is essential (Joshi et al. 2014). Elastomers provide cutting edge advantage over other wear resistant materials in terms of resilience, ease of fabrication, corrosion resistance, toughness, vibration damping capability and so on. Natural rubbers have excellent resistance to erosion and abrasion when hydrocarbon and weathering resistance are not essential. Elastomers find their application in hoses, pipe linings, hose bends, side liners and pump casing (Xie et al. 2015).

There are various parameters that affect erosion rate during slurry pot testing like particle velocity, abrasive concentration, particle size and property of material (Levy and Crook 1991; Rao et al. 2016). There is no literature available on the slurry erosive wear behaviour of polymer matrix composites and especially flexible composites. The motion between two contacting surfaces results in damage and loss of material which is termed as wear. Adhesion, abrasion, erosion, fatigue and fretting are different types of wear observed in engineering applications and among them, abrasive wear is found to be most important (*ASM Handbook* 1992). Abrasive wear is brought about by the hard protuberances which move against the strong surface and constrained against it (Hutchings 1992). In case of two body wear, hard projections caused wear on only one surface. Neat polymeric materials are rarely used in wear applications (P.K. Mallik 2008). Flexible composites are found to exhibit wide range of tribological properties and are useful in applications such as material handling, transportation and secondary structural applications like claddings and thus, wear studies in these areas are acquiring more importance (Friedrich et al. 1995). Two body abrasion test of flexible composites are carried out according to ASTM D5963/ ISO4649 standards. Bidirectional fabrics have developed as an answer for satisfying the interest for more current materials having better execution and handling. Bidirectional fabrics have emerged as a solution for fulfilling the demand for newer materials having better execution and processing (Vishwanath et al. 1993). Matrix material used in the composite influences the wear resistance of the material to greater extent. Various engineering issues can be addressed by looking into the materials that the nature has provided us. For instance, for grinding and tearing purpose nature has provided us with teeth and nails. Similarly, to reduce the wear and tear during walking, the feet are provided with soft pads. Following the concept of nature, exploring the usage of flexible materials such as elastomers in wear resistant materials seems to be an interesting approach. However, elastomers exhibit small range of operating temperature at which they are suitable to be used for wear resistant applications. The ranges of some of the elastomers are provided in Table 2.13 (Sare et al. 2001). Figure 2.16 (Sare et al. 2001) justifies why flexible materials are preferred over stiffer ones by nature for wear resistance.

**Table 2.13** Temperature range and abrasion resistance of various elastomers

<b>Elastomer (Nomenclature)</b>	<b>Operating temperature (°C)</b>	<b>Glass transition temperature (°C)</b>	<b>Abrasion resistance</b>
Polyurethane (PUR)	Up to 75	-40 to -20 and 50 to 80	Excellent
Styrene butadiene rubber (SBR)	Up to 110	-60 to -50	Excellent
Natural rubber (NR)	-50 to 105	-52	Good/Excellent
Nitrile butadiene rubber (NBR)	-50 to 120	-55 to -20	Excellent
Chloroprene (CR)	-45 to 120	-45	Fair
Ethylene Propylene Diene Monomer (EPDM)	-50 to 125	-50 to -40	Fair

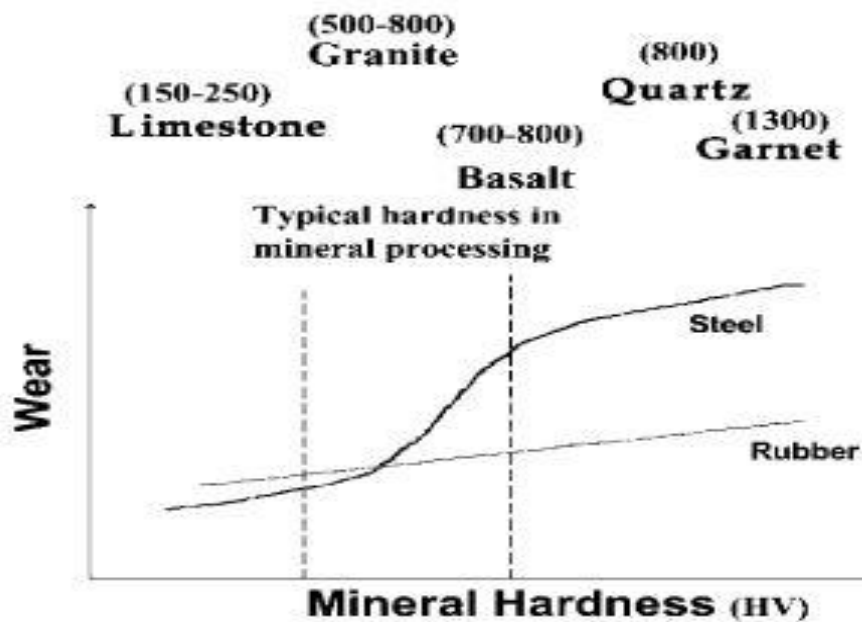


**Figure 2.16** Variation of wear rate for steel and rubber for different erodent (Sare et al. 2001)

The wear rate can be reduced by replacing steel with rubber or by having a rubber coating on the steel (Sare et al. 2001). Natural rubber which is abundantly available in nature offers excellent resistance to wear, tear and impact (Xie et al. 2015). Various researchers (Briggs, GAD; Briscoe 1976; D.H. Champ, E. Southern 1974; Grosch, KA and Schallamach 1965; Grosch 1990; Pulford 1983; Schallamach 1952, 1963) have proposed different wear mechanisms related to rubber.

## 2.6 Material selection approaches

Decision making is one of the critical tasks of a designer. In general, there are eight steps involved in decision making process as shown in Figure 2.17 (Bhushan 2004; Jackson and Pascual 2008).

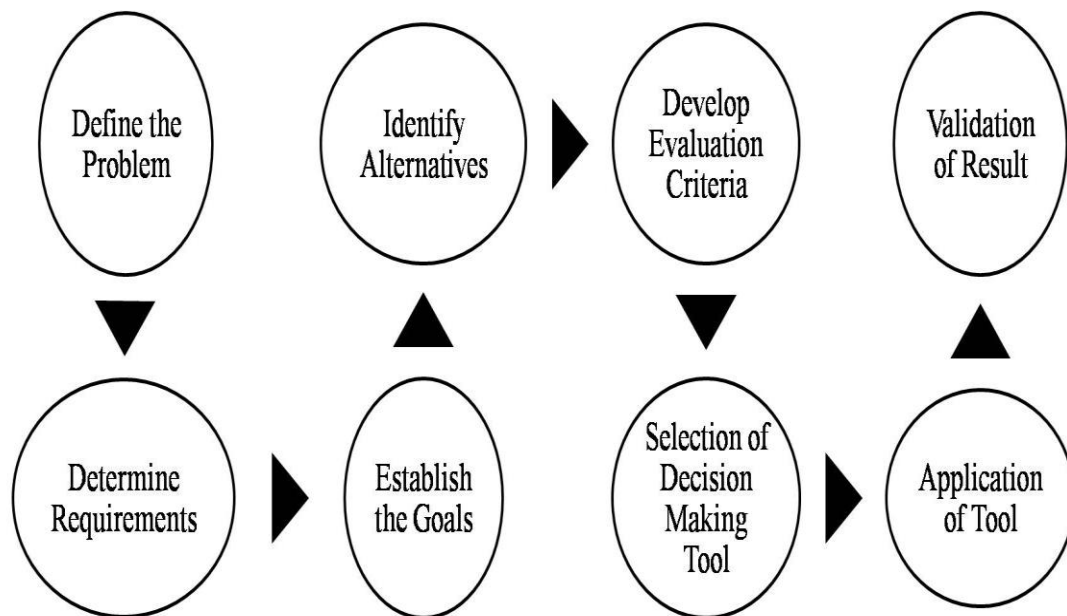


**Figure 2.17** Steps involved in decision making (Bhushan 2004; Jackson and Pascual 2008)

The most important thing in decision making is selection of an appropriate decision making tools to realise the required goals and objectives (Belton 1986), which is the first stage of decision making. Further, technical ground or expert judgement should be established to justify the obtained result.

Once the problem is defined, the requirements to realise the result should be established. Further, it is essential to establish the goals positively (Baker et al. 2002). Once the goal is established the designer/ engineer should list out the various alternatives available for selection. Usually, in the initial stage it will be impossible for the designer/ engineer to decide which alternative exactly fits the goals. Thus, multiple evaluation criteria are selected by the designer which forms the basis for comparison among the alternatives (Mateo 2011).

Now the designer should carefully select the appropriate decision making tool and apply it to get the result, which is nothing but the selection of appropriate option among the alternative that meets the goals exactly or nearly exact. Pertaining to material selection, one of the most challenging task for any engineer is to select an appropriate constituent, volume fraction of the selected constituent, stacking sequences of the composite (Sanjay et al. 2019) which finally affects the performance of the end product (Jahan et al. 2010; Rao 2006; Sapuan 2001).

It is to be born in mind that there is no hard and fast rule that the engineers are bound to follow as a reference. This makes their task even more complicated. The selection of the various parameters of the composite is totally dependent on the final task the product is intended to perform. There can be various criteria that has to be considered for selection of the material for a particular application and these criteria may be conflicting. Thus, the role of engineers in material selection is very crucial. There are various ranking methods available for material selection as shown in Figure 2.18.

In order to make the life of engineers easy, a tool called Multiple criteria decision making (MCDM) is available for problems such as material selection (Shanian and Savadogo 2006). MCDM can be further sub classified into multiple attribute decision making (MADM) approaches and multiple objective decision making (MODM)(Jahan et al. 2010). Whenever an engineer is facing a task to selecting a material with multiple selection criteria involved, MADM can be efficiently employed to arrive at conclusion (Rao 2008).

There are various approaches that the researchers have adopted for material selection problems namely Elimination Et Choix Traduisant la REalite meaning Elimination and Choice Expressing REality (ELECTRE) (Shanian and Savadogo 2006), Technique for Order Preference by Similarity to Ideal Solution (TOPSIS) (Rathod and Kanzaria 2011), Weighted Product Method (WPM) (Rathod and Kanzaria 2011), Simple Additive Weight (SAW) method (Chen 2012), Preference Selection Index (PSI) method (Maniya and Bhatt 2010), Analytic Hierarchy Process (AHP) (Jahan et al. 2010), Graph Theory and Matrix representation Approach (GTMA) (Chen 2012), Vise Kriterijumska Optimizacija Kompromisno Resenje (VIKOR) method (Jahan et al. 2010), TOPSIS-PSI approach (Yadav et al. 2019), combined DEMATEL-VIKOR (Chakraborty et al. 2018) and so on.

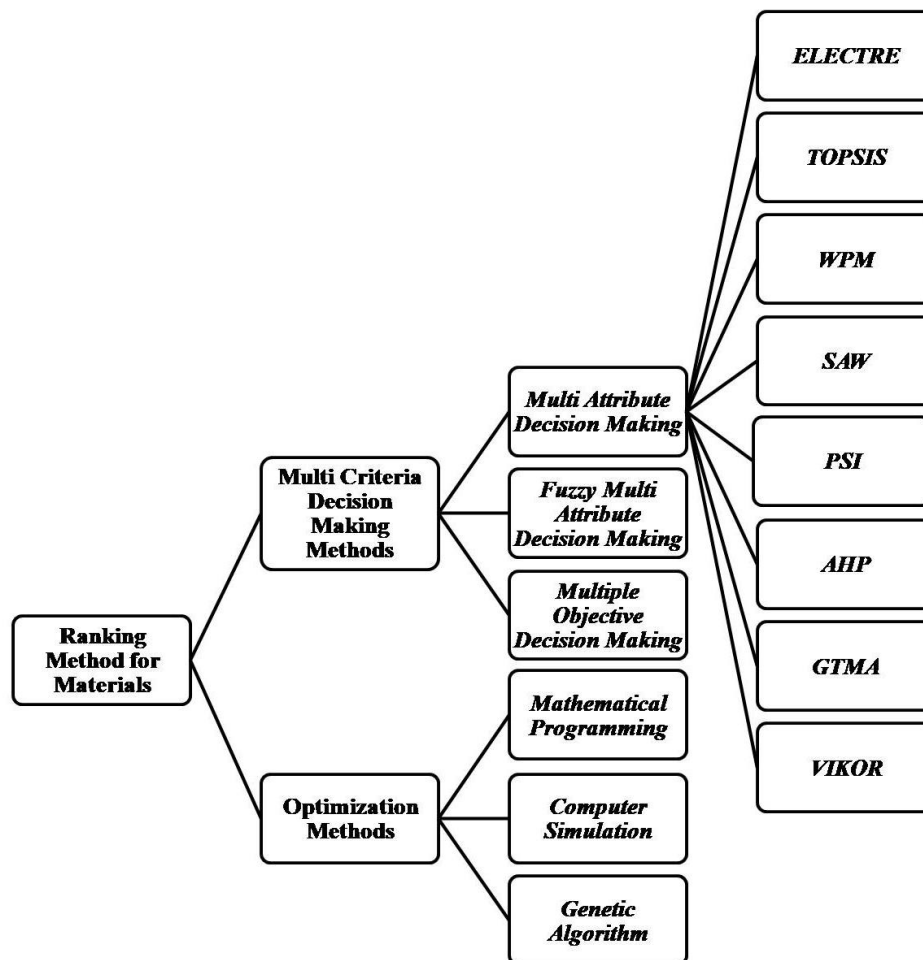


**Figure 2.18** Classification of ranking methods for material selection (Jahan et al. 2010)

Along with minimizing the engineer's effort in material selection, MADM also provides realistic results which have made it so popular. Out of all the possible approaches, TOPSIS is preferred by most of the engineers in the area of PMC as it considers both positive ideal solution and negative ideal solution while deciding the best material (Patel et al. 2018; Patel and Dhanola 2016; Patel and Rawat 2017; Sandeep Kumar, Patel V K, Mer KKS, Fekete Gusztav 2018). Along with TOPSIS, VIKOR method also proves to be promising method in material selection when there is a conflict among the criteria considered for material selection. In case of VIKOR, ranking to the materials is given based on the criteria that how close is the alternative to the ideal solution (Gangil and Pradhan 2018).

PSI is another simpler and easiest method that aids in material selection (Maniya and Bhatt 2010). It is said to be easiest method since this method does not warrant the assignment of weight to each of the criteria considered. In the field of material selection, many researchers have attempted the use of MCDM methodology for appropriate material selection. The details pertaining to the same are tabulated in Table 2.14.



**Table 2.14** Multi criteria decision making methods used for material selection

Type	Method Applied	Goal	Reference
MCDM	AHP	Selection of material in designing a product	(Desai et al. 2012)
	TOPSIS	Optimal material selection for roofing	(Rahman et al. 2012)
	TOPSIS	Impact optimization of composite	(Alemi-Ardakani et al. 2016)
	VIKOR	Material selection	(Chatterjee et al. 2009; Mahesh et al. 2019)
	PSI	Material selection	(Mahesh et al. 2019)
Hybrid MCDM	AHP and TOPSIS	Material selection in hydro power plants	(Kumar and Singal 2015)

<b>Type</b>	<b>Method Applied</b>	<b>Goal</b>	<b>Reference</b>
Hybrid MCDM	AHP and TOPSIS	Material selection	(Rao and Davim 2008)
	AHP and TOPSIS	Material selection in sugar industry	(Anojkumar et al. 2015)
	ANP and TOPSIS	Selection of material handling equipment	(Onut et al. 2009)
	TOPSIS and DOE	Robotics	(Tansel 2012)
	TOPSIS and VIKOR	Selection of cover material	(Huang et al. 2009)
	FEA and ELECTRE	Material selection for gas turbine components	(Shanian et al. 2012)
	M-BGV (MOBAC+BW+GRA+VIKOR)	Structural optimization problem for energy-absorbing structures in train collisions	(Zhang et al. 2019a)

<b>Type</b>	<b>Method Applied</b>	<b>Goal</b>	<b>Reference</b>
MCDM approaches with uncertain theories	Fuzzy TOPSIS	Abrasive material selection for grinding wheel	(Maity and Chakraborty 2013)
	Fuzzy VIKOR	Automotive material selection	(Jeya Girubha and Vinodh 2012)
	Fuzzy AHP and TOPSIS	Material selection for sugar industry	(Anojkumar et al. 2014)
	Fuzzy AHP and TOPSIS	Material selection	(Aly et al. 2013), (Rathod and Kanzaria 2011)
	Fuzzy AHP, VIKOR and TOPSIS	Material selection for sugar industry	(Anojkumar et al. 2015)
	Fuzzy ANP and PROMTHEE	Material handling equipment selection	(Tuzkaya et al. 2010)

From the available literature, it is well established that MADM method can be effectively used for material selection. However, from the review carried out it is found that merely 5.34% of literature are available on material selection which indicates the necessity of more exposure for the designers regarding the use of MADM approaches for material selection (Mardani et al. 2015).

## **2.7 Research gap and motivation for the work**

Though lot of research work has been carried out on impact behaviour of composites, much of them are concentrated on conventional PMC's concentrating on synthetic fiber reinforced composites and very little work was carried out on natural fiber reinforced composites. From the literature review, it was found that no emphasis was given on the impact study of green composites and especially flexible composites in particular. The available literature concentrates on developing the composite material for primary structural applications either for low velocity impact or ballistic impact and no emphasis was given for development of secondary structural/ sacrificial applications concentrating both the low velocity impact and lower ballistic impact. Also, the application of multi attribute decision making tool was found to be limited during selection of material for impact applications. Thus the present study is aimed at developing and assessing the mechanical, erosive wear, abrasive wear and impact (low velocity and lower ballistic) behaviour of green flexible composite fabricated using completely naturally available materials and selecting the best configuration of the proposed composite using multi attribute decision making method.

## **2.8 Objectives of proposed work**

From the literature survey, it is clear that there are limited or no reports available on the impact behavior of the flexible composites planned to be used as sacrificial structure. Thus a flexible composite is proposed for impact application.

1. To propose a flexible green composite material for impact applications.
2. To identify the different configurations of the proposed composite and study their impact properties using FE modelling.

3. To optimize the configuration of the proposed flexible composite for better impact performance and identify promising stacking sequence.
4. To experimentally evaluate the mechanical and tribological properties of composite coupon with optimized stacking sequence.
5. To evaluate the impact behaviour of the proposed flexible composite experimentally and study the nature of damage due to low velocity impact and lower ballistic impact.

## **2.9 Scope of proposed work**

1. Proposing jute as reinforcement and rubber matrix material for the flexible composite to study the impact response useful in armor cladding and ballistic applications.
2. To propose various possible configurations of flexible composite and study them for impact properties using commercially available FE software.
3. To select few best configurations of the flexible composite after optimization for experimental study.
4. Prepare the flexible composite coupons according to ASTM standard with optimized configuration and study its physical, mechanical, abrasion, erosion and impact behaviour.

The outcome of the proposed research work leads to a novel green flexible composite that aids in better energy absorption and helps to mitigate the failure when subjected to impact loading.

In this chapter, an extensive literature review has been carried out concentrating on the suitability of the naturally available materials as constituents for polymer matrix composites subjected to impact applications. The outcome of the literature review carried out reveals that there exists a gap in development of completely biodegradable flexible green composite intended for impact application. Though enormous amount of effort has been put by the researchers to assess the impact behavior of the composites experimentally, it is found that FE simulations have gained much importance during the initial feasible study in order to minimize the time and cost involved in experimentation. Also, FE simulation is found to be effectively used for

optimizing the composites. The introduction of simulation tools have resulted in major impact on the theoretical study of the composites. Vast experimental research carried out for impact studies reveals that though wide variety of composites are extensively used for impact application, the flexible green composites are found to be untouched. The next chapter deals with the materials, processing and methodologies adopted for carrying out the present work.

## CHAPTER 3

### 3 METHODOLOGY

The present work deals with the development and performance evaluation of flexible composites for impact applications. Assessing the mechanical properties of any material is most important prior using them in the intended application. Thus a methodology has been proposed as shown in Figure 3.1 to determine and evaluate the desired mechanical and tribological properties.

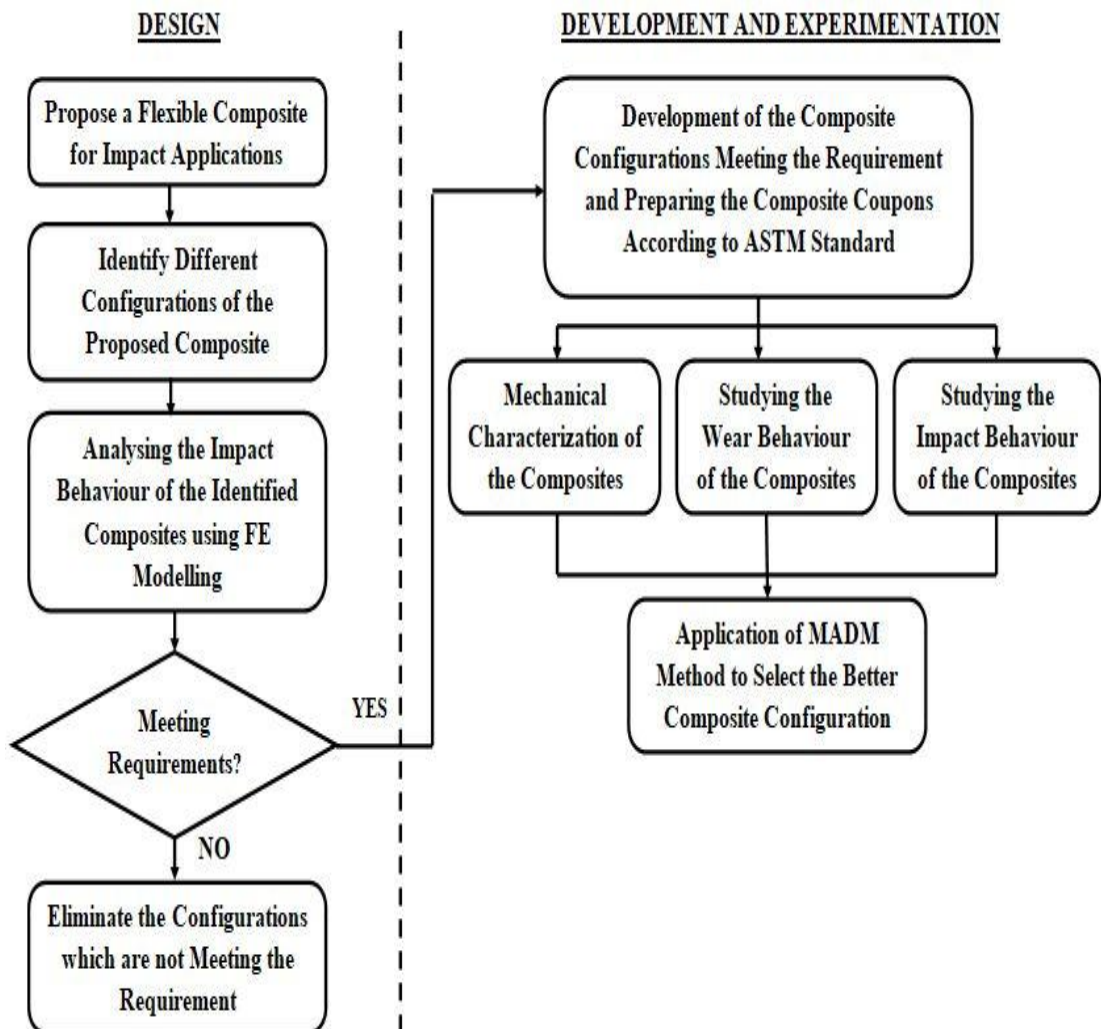


**Figure 3.1** Methodology of proposed work

### 3.1 Raw materials and processing methods

The proposed flexible composites are prepared using naturally available jute in the form of woven fabric; natural rubber and B stage cured natural rubber based pre peg.

#### 3.1.1 Reinforcement (Jute)



**Figure 3.2** Jute woven fabric

Jute is the most popularly used fiber among all the other natural fibers and the composites comprising of jute as reinforcement exhibits better impact strength with acceptable mechanical properties. Woven fabric of jute having density of  $1450 \text{ Kg/m}^3$  and GSM of 350 is shown in Figure 3.2. Properties of jute are shown in Table 3.1.

**Table 3.1** Properties of jute

Physical Property	Jute Fiber
Density ( $\text{g/cm}^3$ )	1.4-1.5
Elongation at break (%)	1.8
Cellulose content (%)	50-57
Hemicellulose (%)	13.6-20.4
Lignin content (%)	8-10
Ash (%)	0.5-2
Pectin (%)	0.2
Wax (%)	0.5
Moisture (%)	12.6



Tensile strength (MPa)	300-700
Youngs modulus (GPa)	10-30
Diameter ( $\mu\text{m}$ )	160-185
Lumen size ( $\mu\text{m}$ )	12

### 3.1.2 Natural rubber



**Figure 3.3** Natural rubber sheet

NR in the form of sheets is procured from Manjunath rubber, Baikampady, Mangaluru, India and is shown in Figure 3.3. The properties of the Natural rubber sheets determined experimentally are shown in Table 3.2

**Table 3.2** Properties of natural rubber sheet

<b>Test</b>	<b>Tensile Strength (MPa)</b>	<b>Ultimate Strain (%)</b>	<b>Modulus (MPa)</b>	<b>Density (Kg/m<sup>3</sup>)</b>
Tensile Test	0.05	210	0.45	987.18
Tear Test	<b>Tear Strength (N/mm)</b>			
	7.64			
Shore A	<b>Hardness value</b>			
Hardness	24			

### 3.1.3 B stage cured pre peg



**Figure 3.4** B stage cured pre peg

B stage cured pre peg is used to bind the jute fabric and the natural rubber sheet together firmly and acts as a matrix and is shown in Figure 3.4. Apart from acting as a matrix, it protects the natural rubber and jute from being affected by environmental conditions. The properties on NR based B stage cured pre peg are provided in Table 3.3.

**Table 3.3** Properties of NR based B stage cured pre peg

<b>Tensile Strength (MPa)</b>	<b>Modulus (300%) (MPa)</b>	<b>Elongation (%)</b>	<b>Shore A Hardness</b>
15.69-16.67	7.35-8.33	475-575	56-60

### 3.1.4 Processing techniques

Compression moulding method is used to prepare the proposed flexible composites. The processing is carried out at a temperature of 138<sup>0</sup>c for 7 minutes. The jute fabric and the rubber sheets are cut to desired size and arranged according to the desired configuration (stacking sequence). NR based B stage cured pre peg is placed in between each layer so as to bond the layers perfectly. The entire arrangement is placed in between the aluminium plates and kept in a compression molding machine where heat and pressure are applied. Figure 3.5 shows the steps involved in processing of flexible composite laminates. After curing, the specimens are cut for the different tests according to respective ASTM standards.

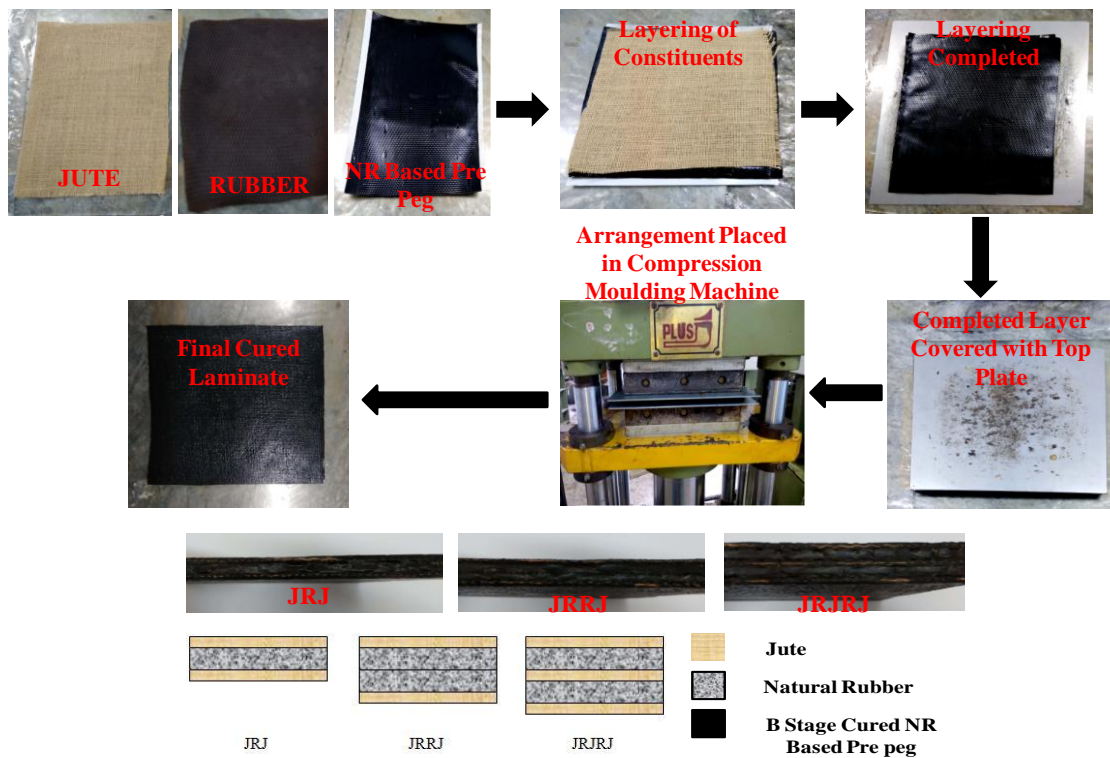


**Figure 3.5** Steps involved in processing of flexible composites

The steps involved in processing of the proposed flexible composite laminates are provided below:

A mould of 300 mm x 300 mm is used in the process. High vacuum silicone releasing agent is used for easy withdrawal of composite laminate. The steps used in fabrication of composite are given below:

Step 1: Jute fabric, rubber sheets and Nr based pre pegs are cut to required size and arranged according to required stacking sequence. The entire arrangement is placed between moulds and the mould is placed in the compression moulding machine.

Step 2: The temperature is set to 138<sup>0</sup>c in the compression moulding machine.

Step 3: Once the set temperature of 138<sup>0</sup>c is reached, the laminates are subjected to heat for 7 minutes.

Step 4: After 7 minutes, the temperature was turned off and the pressure was maintained for another 2 hours.

Step 5: The mould was removed from the compression moulding machine and then the composite was removed from the moulds.

### 3.2 Analytical approach

Analytical approach based on law of conservation of energy is proposed to assess the lower ballistic impact behaviour of the flexible composites.

#### 3.2.1 Analytical approach for lower ballistic impact

In order to predict the energy absorbed, residual velocity and ballistic limit of the proposed flexible composites, an analytical model based on the law of conservation of energy is proposed. The damage mechanisms occurring in the composites are identified and based on that, the analytical formulation is developed in order to predict the energy absorbed. The residual velocity of the projectile is determined based on the concept of the total energy absorbed by the damaged plate is equal to the reduction in kinetic energy of the projectile. The ballistic limit of the composite is obtained when total energy absorbed by the damaged plate equals the projectile's initial kinetic energy.

The fibers below the projectile are known as primary yarns and those away from the projectile as known as secondary yarns. Cone is formed on the back face of the composite as shown in Figure 3.6.

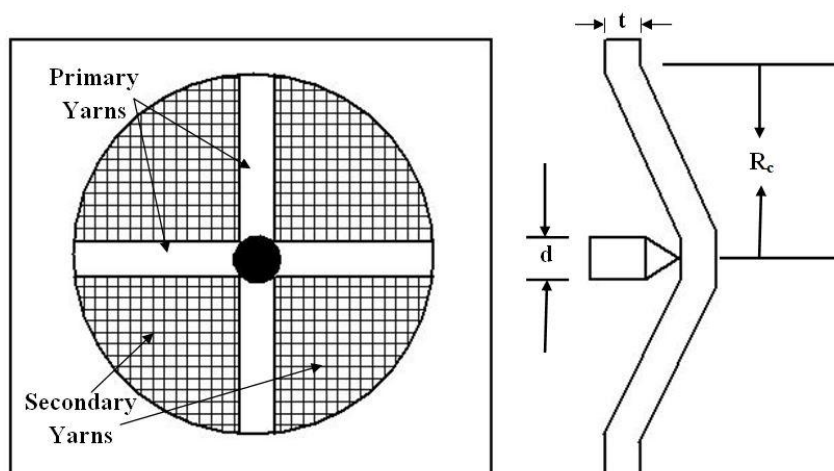


**Figure 3.6** Cone formation at the back face of the target

Following assumptions are made for the development of the analytical model:

1. Compared to total energy absorbed, the energy absorbed due to deformation of the projectile is negligible.
2. The loss of energy due to the result of friction between projectile and plate is negligible.
3. The material properties of the constituents used remain the same throughout.
4. Strain rate remains the same during perforation.
5. The motion of the projectile remains uniform during penetration.

At the start of an impact event, the initial kinetic energy of the projectile is represented by Eq. 1

$$E_i = \frac{1}{2} m_p v_i^2 \quad (1)$$

Where,  $m_p$  is the mass of the projectile and  $v_i$  is the initial velocity. The kinetic energy of the projectile will be absorbed by the composite laminate as it undergoes failure by different modes and thus the velocity of the projectile reduces to  $v_r$ . Thus, according to the law of conservation of energy, we get Eq. 2.

$$\frac{1}{2} m_p v_i^2 = E_a + \frac{1}{2} m_p v_r^2 \quad (2)$$

Where,  $E_a$  is the total energy absorbed by various failure modes and kinetic energy of moving cone.

During an impact event, the elastic and plastic waves propagate outwards from the point of impact and the velocity of elastic ( $C_e$ ) and plastic wave ( $C_p$ ) propagation is given by Eq. 3 and Eq. 4 respectively.

$$C_e = \sqrt{\frac{1}{\rho} \left( \frac{d\sigma}{d\varepsilon} \right)_{\varepsilon=0}} \quad (3)$$

$$C_p = \sqrt{\frac{1}{\rho} \left( \frac{d\sigma}{d\varepsilon} \right)_{\varepsilon=\varepsilon_p}} \quad (4)$$

As the wavelets of strain pass through a particular point of the yarn, there is an inward flow of the material towards the point of impact and transverse waves are developed whose velocity is given by Eq. 5

$$C_t = (1 + \varepsilon_p) \sqrt{\frac{\sigma_p}{\rho(1 + \varepsilon_p)}} - \int_0^{\varepsilon_p} C(\varepsilon) d\varepsilon = C_e \left( \sqrt{\varepsilon_p(1 + \varepsilon_p)} - \varepsilon_p \right) \quad (5)$$

The starting time of the impact to yarn breakage or stoppage of the projectile is given by Eq. 6 and radius of the cone depends on this time change ( $\Delta t$ )

$$\Delta t = \Delta\varepsilon / \dot{\varepsilon} \quad (6)$$

where,  $\dot{\varepsilon} = 2v_i/l$  and  $l$  is the length of laminate

As the projectile strikes the proposed flexible composite laminate during an impact event, the kinetic energy of the projectile is converted into energy absorption of the proposed flexible composite laminate by various damage mechanisms. In the proposed flexible composites laminates, the following damage mechanisms are identified:

- Tensile failure of primary yarns
- Elastic deformation of secondary yarns
- Matrix/Interleaved NR tearing

Consider a primary yarn under tensile loading. Strain at distance 'x' from the point of impact is given by  $\varepsilon(x)$ . The strain variation is given by Eq. 7.

$$\varepsilon(x) = \varepsilon_0 b^{x/a} \quad (7)$$

Where,  $\varepsilon_0$  is the strain at the point of impact;  $b$  is a magnitude less than 1;  $x$  is the distance and  $a$  is the yarn size. Energy absorbed can be represented by Eq. 8(Naik et al. 2006)

$$E_{TF} = Ax \int_0^\varepsilon \sigma dx \quad (8)$$

During an impact event, the fibers which come in direct contact with the projectile undergo elongation in tensile mode and then fail. The volume of such fibers is given by  $4R_c td$ . The area of the composite laminate beneath projectile fails completely due to the tensile mode and the energy absorbed due to this mode is given by  $3.14d^2t \frac{E_c}{4}$ . The remaining volume of the primary fibers given by  $4R_c td - \frac{3.14}{4}d^2t$  is under tension and experience plastic strain. Thus energy absorbed by these yarns is given by  $\left[4R_c td - \frac{3.14}{4}d^2t\right] E \varepsilon_p^2$ . Thus, the energy absorption during tensile failure of primary yarns ( $E_{TF}$ ) is given by Eq. 9 (Sikarwar et al. 2014)

$$E_{TF} = 3.14d^2t \frac{E_c}{4} + \left[4R_c td - \frac{3.14}{4}d^2t\right] E \varepsilon_p^2 \quad (9)$$

Where  $d$ : projectile diameter;  $t$ : laminate thickness;  $E_c$ : energy absorbed up to failure i.e. area under the stress-strain curve of the composite;  $R_c$ : Radius of cone-formed at back face of laminate;  $E$ : Young's modulus of composite;  $\varepsilon_p$ : Plastic strain is given by Eq. 10 obtained on simplification of Eq. 11 (Smith et al. 1958).

$$\varepsilon_p = v_i^2 / C^2 \quad (10)$$

$$v_i = C \left[ \sqrt{(1 + \varepsilon_p)\varepsilon_p - \left\{ \sqrt{(1 + \varepsilon_p)\varepsilon_p - \varepsilon_p} \right\}^2} \right] \quad (11)$$

Where,  $v_i$  is impact velocity;  $C$  is the velocity of waves in the composite given by Eq. 12.

$$C = \sqrt{\frac{E}{\rho}} \quad (12)$$

Where  $\rho$  is the density of composite laminate.

All the other yarns except primary yarns are known as secondary yarns which do not directly come under the projectile. Such yarns undergo some elastic deformation and thereby absorbing some kinetic energy of the projectile. Assuming that within the

secondary yarns, there is a linear variation of strain from plastic to zero, boundary conditions as in Eq. 13 are imposed.

$$\begin{aligned}\varepsilon &= \varepsilon_f \text{ at } r = d/\sqrt{2} \\ &\text{and} \\ \varepsilon &= 0 \text{ at } r = R_c\end{aligned}\tag{13}$$

Where,  $\varepsilon_f$  is the failure strain of the composite. The variation of the strain can be expressed by Eq. 14.

$$\varepsilon = \varepsilon_f \frac{\sqrt{2}(R_c - r)}{\sqrt{2}R_c - d}\tag{14}$$

The energy absorbed by the secondary yarns per unit volume is given by Eq. 15.

$$E_{eds}^v = \int_0^\varepsilon \sigma_{sy} d\varepsilon\tag{15}$$

The total energy absorption by elastic deformation of secondary yarns ( $E_{eds}$ ) is given by Eq. 16 (Sikarwar et al. 2014).

$$E_{eds} = 3.14E\varepsilon_p^2 \int_d^{R_c} r h dr = \frac{3.14Et\varepsilon_p^2}{2} (R_c^2 - d^2)\tag{16}$$

The energy absorption by Matrix/Interleaved NR tearing mechanism ( $E_t$ ) is given by Eq. 17 (Zhang et al. 2019b).

$$E_t = 3.21\left(\frac{t}{\lambda}\right)^{0.6} \sigma_0 v_t\tag{17}$$

Where  $\lambda$ : critical tearing length where the steady tearing state has been reached. In most practical cases,  $\lambda$  can be taken as a width of tearing object or damage width. If steady-state is not reached,  $\lambda$  is equal to tearing length;  $\sigma_0$ : flow stress of material given by Eq. 18 and  $v_t$ : is the volume of torn material.

$$\sigma_0 = 0.5[\sigma_y + \sigma_u]\tag{18}$$

Where,  $\sigma_y$ : yield stress and  $\sigma_u$ : is the ultimate tensile stress.

The total energy absorbed by the flexible composite laminate is the sum of energy absorption during tensile failure of primary yarns ( $E_{TF}$ ), energy absorption by elastic deformation of secondary yarns ( $E_{eds}$ ) and energy absorption by Matrix/Interleaved NR tearing mechanism ( $E_t$ ). Thus, mathematically, it is represented as in Eq. 19.



$$E_a = E_{TF} + E_{eds} + E_t + E_{KE} \quad (19)$$

Where,  $E_{KE}$  is the kinetic energy of moving cone given by Eq. 20

$$E_{KE} = \frac{1}{16} m_c v_i^2 = \frac{3.14}{16} R_c^2 t v_i^2 \rho \quad (20)$$

Where,  $m_c$ : the mass of moving cone during perforation given by Eq. 21 obtained after simplification of Eq. 20;  $v_i$  is the impact velocity.

$$m_c = 3.14 R_c^2 t \rho \quad (21)$$

According to the law of conservation of energy, the energy balance can be represented by Eq. 2. On simplification of Eq. 2, the residual velocity is given by Eq. 22.

$$v_r = \sqrt{v_i^2 - \frac{2E_a}{m_p}} \quad (22)$$

For the ballistic limit, the residual velocity of the projectile is zero. Thus, from Eq. 22, the equation for the ballistic limit is derived and presented as Eq. 23.

$$v_{bl} = \sqrt{2E_a/m_p} \quad (23)$$

The areal density of the proposed flexible composites is calculated using Eq. 24. The SEA of the proposed flexible composites is calculated using Eq. 25.

$$\rho_a = \rho \times t \quad (24)$$

Where,  $\rho$  is the density of the composite in Kg/m<sup>3</sup> and  $t$  is the thickness of composite in m.

$$\text{At ballistic limit, } SEA = E_a^{bl} / \rho_a \quad (25)$$

$$\text{At impact velocity other than ballistic limit, } SEA = E_a / \rho_a$$

Where,  $E_a$  is energy absorbed in J and  $\rho_a$  is the areal density in Kg/m<sup>2</sup>.

### 3.3 Finite element analysis

The finite element analysis is carried out to study the impact behaviour of JE and JE-R-JE composite and assess the role of introducing rubber as core material. Also, the FE approach is adopted to analyze the impact behaviour of flexible composites with

different stacking sequences and optimize the stacking sequence. Lower ballistic impact behaviour of the optimized stacking sequences of flexible composites are also studied.

### 3.3.1 Comparative study of impact behaviour of jute-epoxy composite laminate and jute-epoxy-rubber sandwich composite

Selecting the constituents of the composites for any particular application is an important stage. Thus, as a part of initial feasible study, the structural performance of composite plate under low velocity impact is studied using commercial finite element package. Two types of layup sequence namely jute-epoxy laminate (JE) and jute-epoxy-rubber sandwich (JE-R-JE) are considered for evaluation.

Study of low velocity impact behavior and stress analysis of both the laminate and sandwich structure is carried out and comparison is made to discuss the effect of introducing rubber as a core material. The numerical simulation of the present study is carried out commercially available software. The procedure adopted in the study of current modelling has been validated with the results obtained in the literature (Karas 1939) for normal impact loading and the results of oblique impact loading has been compared with normal impact loading as followed earlier (Meybodi et al. 2016).

The schematic representation for the normal and oblique impact of the JE laminate and JE-R-JE sandwich model considered for the present study are shown in Figure 3.7 and Figure 3.8 respectively, where all the dimensions represented are in mm. The dimensions of Laminate and sandwich are chosen according to ASTM D7136/D7136M standard. The thickness of the laminate is considered as 12 mm, face sheets as 3 mm each and core as 6 mm in the sandwich. The oblique angle is defined as the angle between axis of the impactor and normal to the plate.

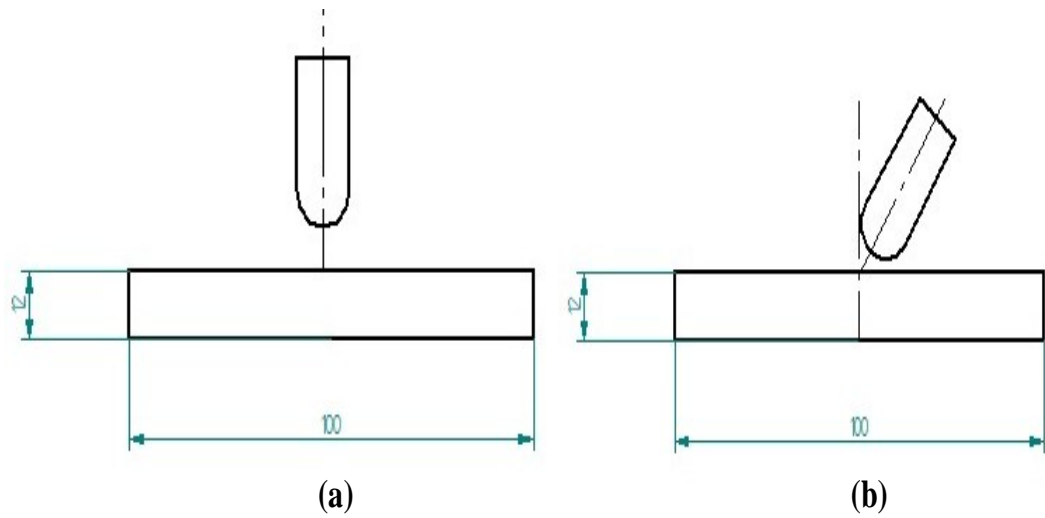


**Figure 3.7** Schematic representation of (a) normal and (b) oblique impact of jute epoxy composite

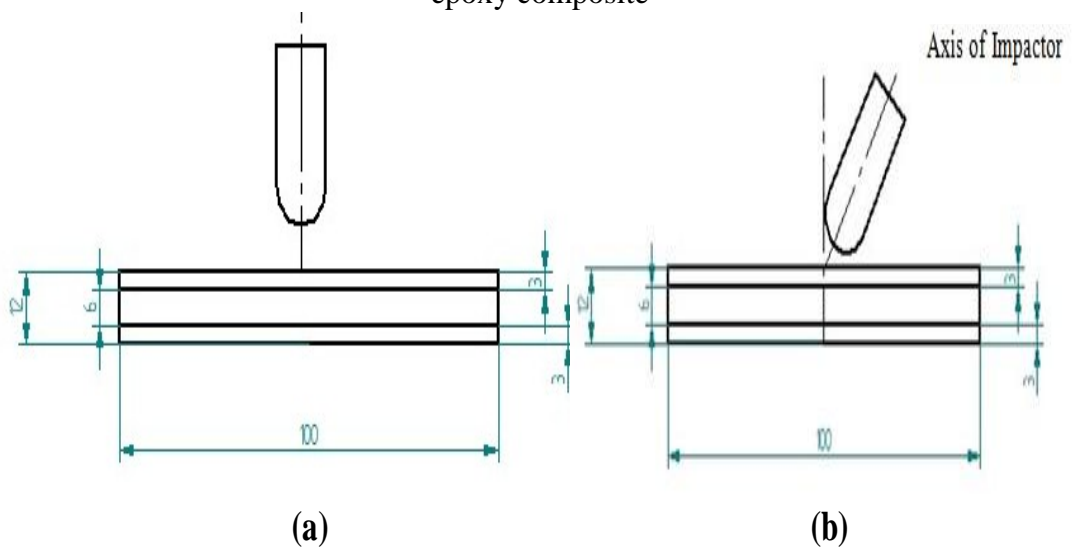


**Figure 3.8** Schematic representation of (a) normal and (b) oblique impact of jute epoxy-rubber-jute epoxy sandwich composite

### 3.3.1.1 Finite element model

The modelling and meshing of the JE and JE-R-JE composites are shown in Figure 3.9 and Figure 3.10 respectively. The boundary condition applied to the laminate and sandwich structure is fixed support on the edges of the sandwich structure as well as on the four side faces and the impactor is given a velocity of 10 m/s as shown in Figure 3.11. The model is meshed using shell type element. It was assumed that there is a perfect bonding between face sheet and core and surface to surface contact

relations were defined at the face sheet core interface using contact conditions with friction between impactor and composite being neglected. The impactor was modelled as a rigid body and its motion was governed by the rigid body reference node. The material properties of structural steel used for the impactor and rubber used for core are predefined in commercially available software and is given in Table 3.4. The initial velocity of the impactor is 10 m/s and it is constrained only to move in Z direction. Explicit dynamic analysis type is selected to perform the low velocity impact test on laminate and sandwich structure. The laminate and sandwich structure is defined as flexible material and impactor as rigid material. Based on the available literature (Balasubramani et al. 2013; Hossain et al. 2013; Mir et al. 2014; Sangamesh et al. 2018; Stuart 1992), the material properties of jute-epoxy used for analysis are derived and tabulated in Table 3.5.

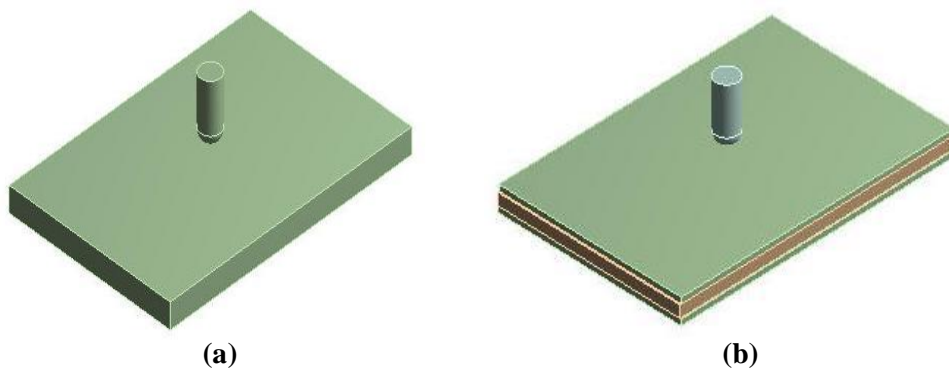


**Figure 3.9** Modeling of (a) jute epoxy and (b) jute epoxy-rubber-jute epoxy composite

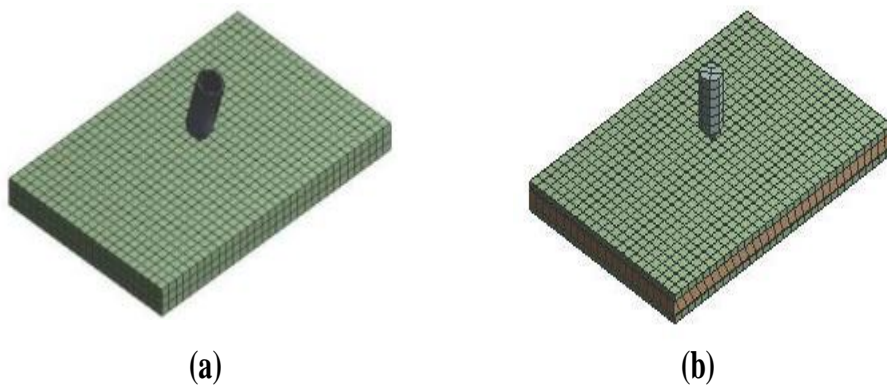


**Figure 3.10** Meshing of (a) jute epoxy and (b) jute epoxy-rubber-jute epoxy composite

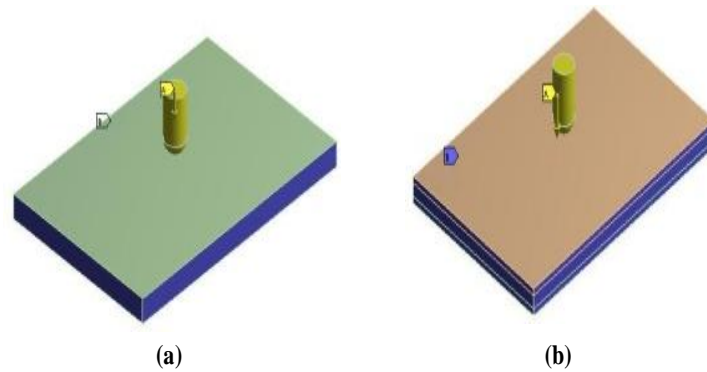


**Figure 3.11** Boundary conditions applied to (a) jute epoxy and (b) jute epoxy-rubber-jute epoxy composite

**Table 3.4** Material properties of structural steel and rubber

Properties	Structural Steel (Impactor)	Rubber (Core)
Density (Kg/m <sup>3</sup> )	7,850	1,000
Modulus of Elasticity (MPa)	2,00,000	1
Poisson's Ratio	0.3	0.5
Bulk Modulus (MPa)	1,66,600	0
Shear Modulus (MPa)	76,900	0.3
Equation of State	Linear	Linear

**Table 3.5** Material properties of jute epoxy

Density (Kg/m <sup>3</sup> )	Modulus of Elasticity (GPa)	Tensile strength (GPa)	Poisson's Ratio	Shear Modulus (GPa)
1337.5	12.57	0.056	0.34	2.45

The details pertaining to element and mesh are provided in Table 3.6.

**Table 3.6** Element and mesh details used in finite element analysis

Target	Element type	Number of elements	Mesh type
JE and JE-R-JE	Shell element	61,056	Quad
Impactor	Solid	1560	Tetrahedral

### 3.3.2 Comparative study on stiff and flexible composites

The comparative study on impact behaviour of stiff composite and flexible composite is carried out to understand their impact behaviour. JE is chosen as the stiff composite and jute-rubber-jute (JRJ) is chosen as the flexible composite for the purpose of study. The analysis for the low velocity impact behaviour of the chosen composites is carried out using commercially available software. The target is modelled according to ASTM D7136/D7136M standard. The thickness of JE is chosen as 0.21 cm and in case of JRJ, each layer of jute skin is of thickness 0.005 cm and rubber core is 0.2 cm. The impactor is considered to be made up of steel and of hemispherical shape whose radius is 6.5 mm with a mass of 1.5 Kg.

The assembled view of JE and JRJ composites along with their boundary conditions, meshing and exploded views are shown in Figure 3.12. The boundary conditions are applied to the plate such that its edges are fixed in all the direction and the impactor movement is restricted only in Z direction with an impact velocity of 10 m/s. For the JRJ sandwich, interaction properties are defined for each layer.

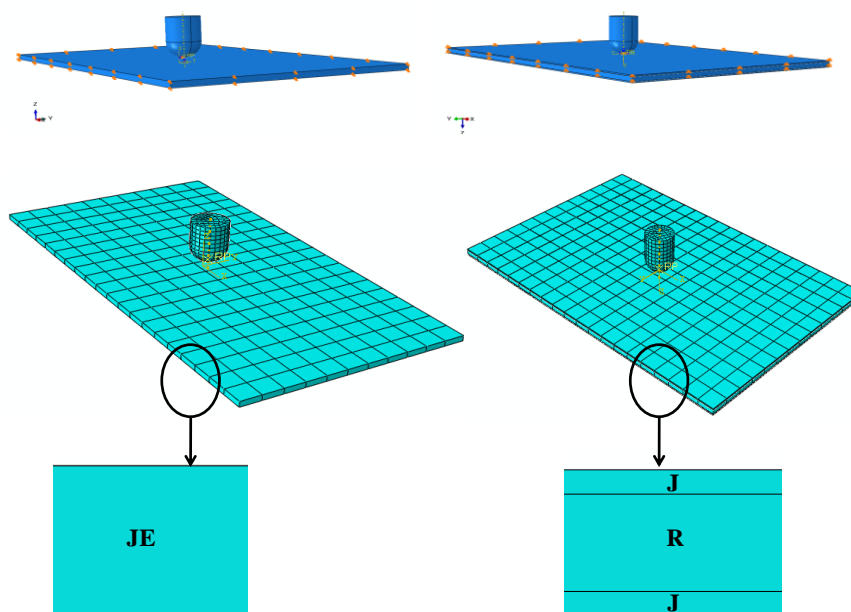


**Figure 3.12** Assembled view of jute epoxy laminate and jute/rubber/jute sandwich along with boundary condition and meshing

The material properties of jute and B stage cured prepeg and rubber are experimentally determined and the properties of JE are taken from available literature (Balasubramani et al. 2013; Hossain et al. 2013; Mir et al. 2014; Sangamesh et al. 2018; Stuart 1992) and provided in Table 3.7. Mesh details are provided in Table 3.8.

**Table 3.7** Material properties used for jute epoxy and jute/rubber/jute composite

<b>Material</b>	<b>Density (Kg/m<sup>3</sup>)</b>	<b>Tensile strength (GPa)</b>	<b>Modulus of Elasticity (GPa)</b>	<b>Poisson' s Ratio</b>	<b>Shear Modulus (GPa)</b>
Jute+B stage cured pre peg	1548	0.022	0.014	0.4	0.0072
Rubber	987.18	5E-5	0.00045	0.49	0.3
JE	1337.5	0.056	12.57	0.34	2.45

**Table 3.8** Details of element type used in finite element analysis

<b>Target</b>	<b>Element type</b>	<b>Number of elements</b>
JE	C3D8R	1260
JRJ	C3D8R	1260
Impactor	R3D4	299

### 3.3.3 Identification of different stacking sequences of flexible composite

Once the rubber is identified as the potential material to be used in LVI applications, the behaviour of natural rubber with other engineering materials for normal and oblique impact is studied. Suitability study of jute-epoxy composite for low and high velocity impact applications, Comparative study on energy absorbing behavior of stiff and flexible composites under low velocity impact were also studied before finalizing the flexible composite as the material of present study. Six different configurations of the jute/natural rubber based flexible composites which are considered for further study are tabulated in Table 3.9.

**Table 3.9** Configurations of composite considered

Sl.No.	Configuration	Representation
1	Jute-Rubber-Jute	JRJ
2	Jute-Rubber-Rubber-Jute	JRRJ
3	Jute-Rubber-Jute-Rubber-Jute	JRJRJ
4	Rubber-Jute-Rubber	RJR
5	Rubber-Jute- Rubber-Jute	RJRJ
6	Rubber-Jute- Rubber-Jute-Rubber	RJRJR

### 3.3.4 Determining optimum configuration of flexible composite

Out of the six different configurations proposed, in order to select the optimum configuration, FE analysis is carried out using commercially available FE software to analyze the behaviour of the configurations subjected to low velocity impact. The rank is assigned to the configurations based on the criteria that the configuration with maximum contact force is assigned rank 1 since larger contact force implies highest resistance to damage. The laminates are modeled according to ASTM D7136 standard using commercially available software as a 3D deformable bodies and the impactor is modeled as hemispherical shaped rigid impactor with mass  $m$  as 1.5 kgs. The jute and rubber layers are modeled and assembled according to the configuration required. The laminate is provided with a boundary condition of Encastre ( $U_1=U_2=U_3=UR_1=UR_2=UR_3=0$ ) on all the four sides and the movement of the impactor is restricted only in Z direction with a velocity  $v$  of 10 m/s. The assembled view for one of the configuration JRJ and the boundary condition applied is shown in Figure 3.13 and the meshing is shown in Figure 3.14. The same is repeated for all the configurations under consideration.



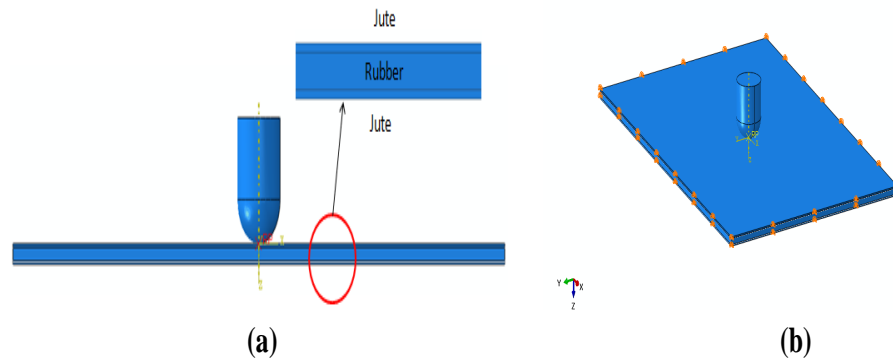


**Figure 3.13** Assembled view of jute/rubber/jute configuration and boundary condition applied

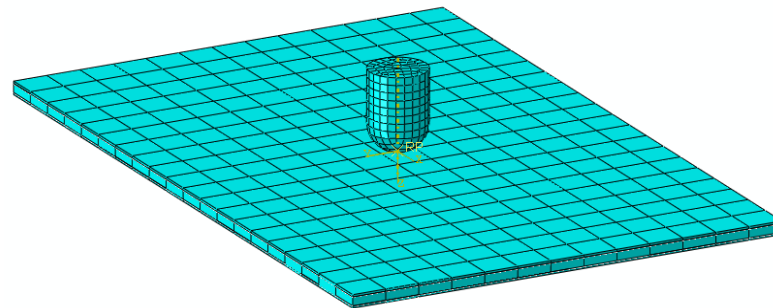


**Figure 3.14** Meshing of jute/rubber/jute composite and impactor

The material properties of jute along with B stage cured pre peg and that of rubber used in the analysis are presented in Table 3.7.

### 3.3.5 Finite element analysis of lower ballistic impact

The FE simulation is carried out using commercially available FE software. The flexible composites of different proposed configurations and the projectile are modelled and analyzed according to experimental conditions. The proposed flexible composite is modelled as flexible material, projectile as a rigid material. Corresponding material properties are assigned to the composite plates and mass is assigned to the projectile. The dimensions of the laminates and the projectile are maintained the same as used in experimental conditions. Jute and rubber plates are modelled separately and then assembled together. To maintain the proper interaction among the jute and rubber plates, the surface to surface contact is defined. The boundary condition is applied such that all the four sides of the laminate are restricted

for their linear and rotational movement and the projectile movement is allowed in only one direction. The reference point is defined for the projectile at which the velocity is provided. The free mesh is applied for both the laminates and the projectile. Before the actual FE study is carried out, a mesh convergence study is performed on the similar grounds available in literature (Ansari and Chakrabarti 2016a; b; Husain et al. 2017) for ballistic impact studies. The model modelled using the FE method is shown in Figure 3.15. The number of elements used and the element types used are presented in Table 3.10.

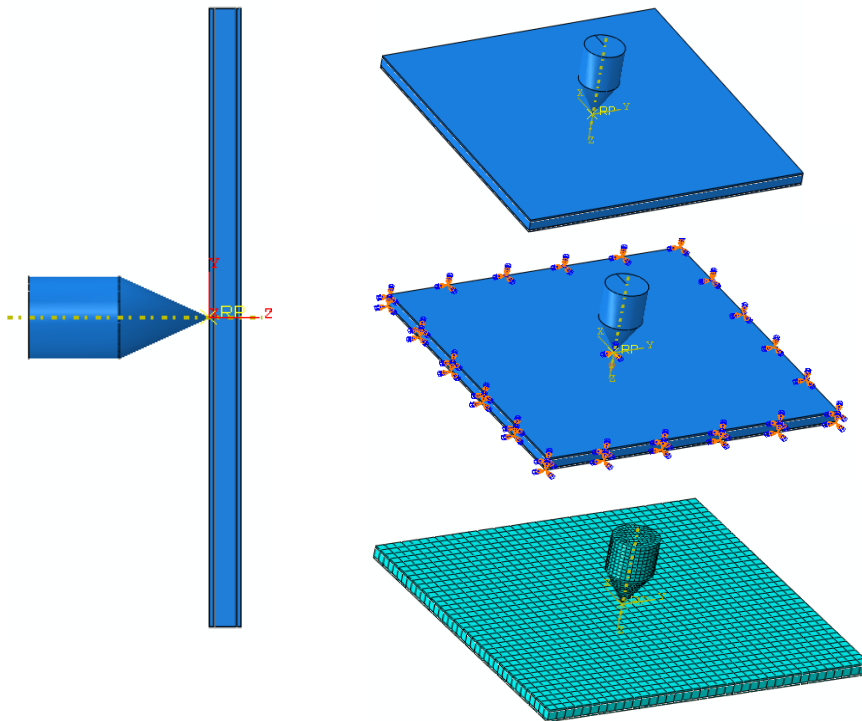


**Figure 3.15** Modeling of proposed flexible composite laminates and projectile

**Table 3.10** Type of elements and number of elements used in composite plate and projectile

Part	Type of element	Number of elements
Plate	SC8R (Continuum Shell	JRJ:160000
	Element)	JRRJ:192000
		JRJRJ:208000
Projectile	C3D8R (Brick element)	1145

The properties of the constituent materials are determined experimentally and used for FE analysis is presented in Table 3.11.

**Table 3.11** Material properties used in finite element analysis

<b>Properties</b>	<b>Jute+NR based B stage cured pre peg</b>	<b>Natural rubber</b>
Density (Kg/m <sup>3</sup> )	1548	987.18
Youngs modulus (GPa)	0.014	0.00045
Poisson's ratio	0.4	0.49
Tensile strength (GPa)	0.022	0.00005

### 3.4 Testing

Testing of the constituents and the proposed flexible composites are carried out to determine the curing characteristics of the matrix, peel strength of the constituents, physical, mechanical properties, erosive and abrasive behaviour and impact behaviour

#### 3.4.1 Curing characteristics of natural rubber based pre peg

The rubber based matrix was subjected to compound development and kinetic studies using an oscillating disk rheometer (ODR) according to ASTM 5289-95. About 5 gms of the rubber based matrix was placed in between the disks of rheometer. The minimum torque ( $M_L$ ), Maximum torque ( $M_H$ ), scorch time ( $t_{S2}$ ), 90% of cure time ( $t_{C90}$ ), thermo plasticity (TP) were observed. The optimal curing time and temperature was found through this study.

#### 3.4.2 Determining the peel strength of the constituents

Peel test using a T-peel specimens are carried out to determine the bonding between two interfaces such as jute and B stage cured pre peg; NR and B stage cured pre peg. The jute/rubber is cut and in between the jute/ rubber and rubber gum, a separator is placed to get the required opening. The entire arrangement is placed in a compression molding machine under required temperature and pressure. The separator is smeared with silicone releasing agent so that the rubber gum does not bond with the separator.

Later, the T-peel specimens are cut to the required dimension (160mm x 25 mm) as shown in Figure 3.16. The initial crack obtained is shown in Figure 3.17.

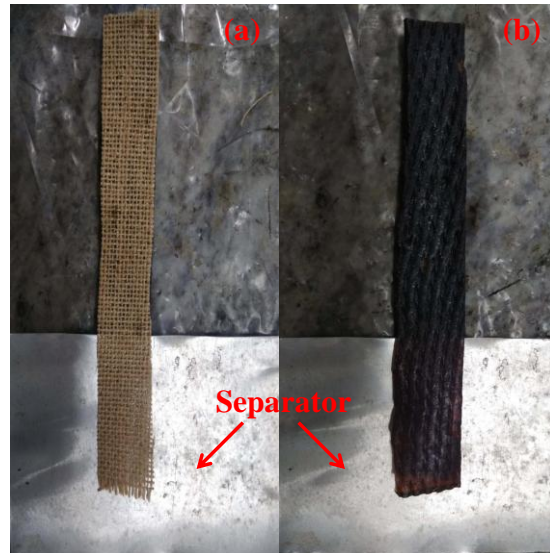


**Figure 3.16** T-Peel specimens of (a) Jute-Rubber gum and (b) Rubber-Rubber gum

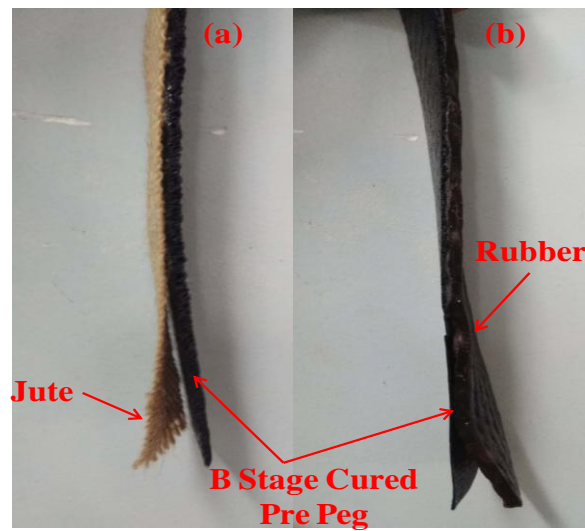


**Figure 3.17** Initial separation obtained in T-Peel specimens

The prepared T- Peel specimens are mounted on the universal testing machine (UTM) with each free end being connected to the fixtures as shown in Figure 3.18. The peel test is carried out at cross head speed of 500 mm/min to measure the peel strength of the jute fabric and rubber gum; rubber and rubber gum.

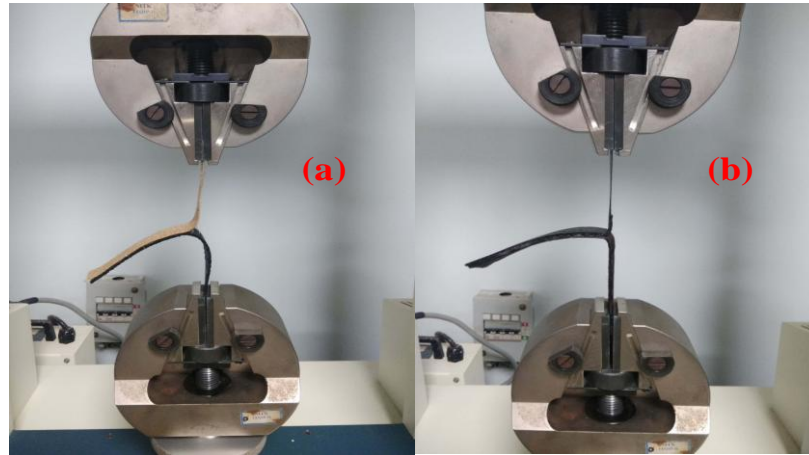


**Figure 3.18** Peel specimen mounted on universal testing machine

The force against displacement graph is obtained from the UTM and the peel strength is calculated using Eq. 26

$$P_s = \frac{2F}{w} \quad (26)$$

Where,  $P_s$  is the peel strength in N/mm,  $F$  is the maximum peel force in N and  $w$  is the width of the specimen in mm.

### 3.4.3 Physical and mechanical characterization

For the purpose of carrying out physical and mechanical characterization, following tests are carried out on the jute/natural rubber based flexible composites with configurations as shown in Table 3.12.

**Table 3.12** Stacking sequences and fiber weight percentage

Stacking Sequence	Representation	Fiber Weight Fraction (%)
Jute-Rubber-Jute	JRJ	12
Jute-Rubber- Rubber-Jute	JRRJ	7
Jute-Rubber-Jute-Rubber-Jute	JRJRJ	10

#### 3.4.3.1 Void content

Density is one of the critical parameter in deciding a material for a particular engineering application. The theoretical density of composite is calculated using rule

of mixtures and the experimental density of composite is calculated using standard water displacement method. At the time of incorporating the fibers into the matrix or during the process of manufacturing the composite laminates, air or other volatiles may be entrapped into the material. These air or entrapped volatiles lead to voids in the composite, which may affect some properties of composites significantly. The void content of the composite is calculated using the Eq. 27

$$\text{Void content (\%)} = \left( \frac{\rho_t - \rho_e}{\rho_t} \right) \times 100 \quad (27)$$

Where,  $\rho_t$  is the theoretical density and  $\rho_e$  is the experimental density.

#### 3.4.3.2 Water absorption

ASTM D 570-98 standard is used to determine the water absorption behaviour of the composite. The water absorption in percentage is calculated using Eq. 28.

$$\text{Water absorption (\%)} = \left( \frac{w_f - w_i}{w_i} \right) \times 100 \quad (28)$$

Where  $w_f$  is the final weight of sample after test and  $w_i$  is the initial weight of sample before test. The samples of dimension 76x25 mm are weighed initially using precision electronic weighing machine before immersing them in water. Later they are immersed in water and their weights are checked using the same precision electronic weighing machine at 2 hrs, 6 hrs, 12 hrs, 24 hrs, 48 hrs and 72 hrs. Each time they were taken out, they were gently blotted with filter paper to remove excess water from surface and were weighed.

#### 3.4.3.3 Tensile test

Tensile testing is carried out according to ASTM D412 standard with five specimens in each of the configurations and later the average values are considered. The test is carried out with cross head speed of 500 mm/min. The specimens used for carrying out the tensile test are shown in Figure 3.19.

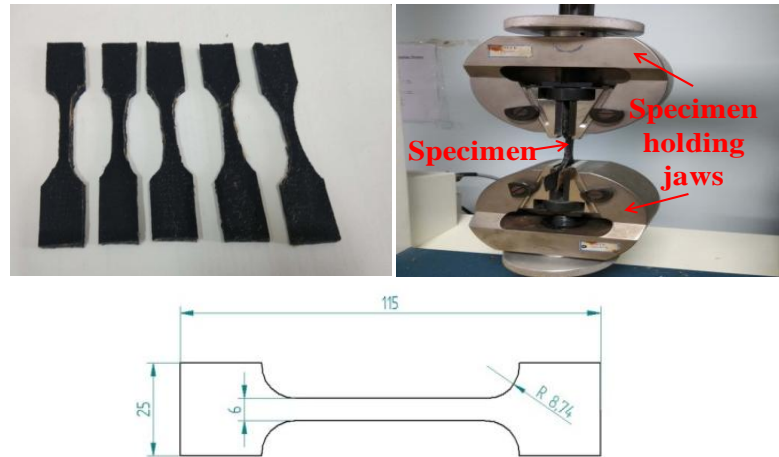


**Figure 3.19** Tensile test specimen

#### 3.4.3.4 Tear test

Tear test is carried out according to ASTM D 624 standard and type C specimen. The tear test gives the tear strength of the proposed composite. Figure 3.20 shows the specimen used for tear test. The tear strength is calculated using the Eq. 29.

$$T_s = \frac{F_{max}}{t} \quad (29)$$

Where,  $T_s$  is the tear strength,  $F_{max}$  is the maximum force in Newtons and  $t$  is the thickness of specimen

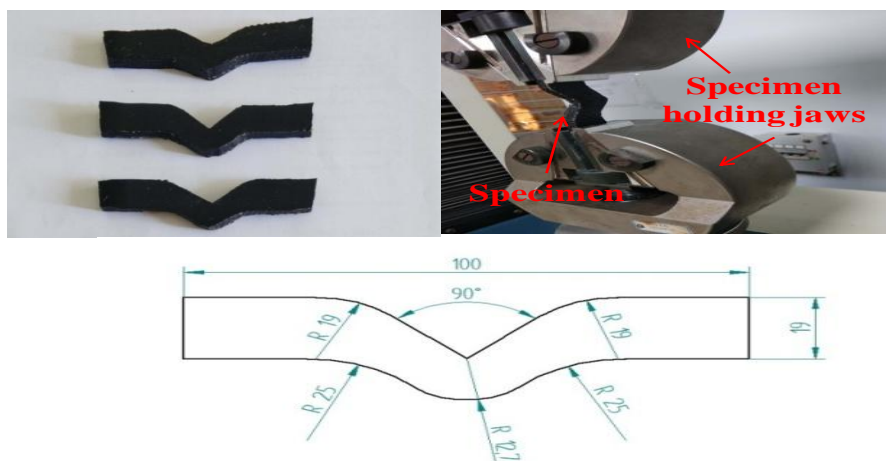


**Figure 3.20** Tear test specimen

### 3.4.3.5 Interlaminar shear strength (ILSS) characterization

The ILSS of the proposed flexible composites was measured using an INSTRON-3366 universal testing machine with loading capacity of 10 kN at cross head speed of 1 mm/min according to ASTM D2344 standard. Loading nose diameter was 6mm and supporting rollers were 3 mm each. The span length was maintained at four times the thickness of the specimen being tested. The load against displacement data was recorded from the data acquisition system and the ILSS was calculated using Eq. 30

$$F_{sbs} = 0.75 \times \left( \frac{P_m}{b \times h} \right) \quad (30)$$

Where,  $F_{sbs}$  is the short beam strength in MPa,  $P_m$  is the maximum load observed during the test in N,  $b$  is the measured specimen width in mm and  $h$  measured specimen thickness in mm. The specimens used for ILSS testing and its loading in UTM are shown in Figure 3.21.

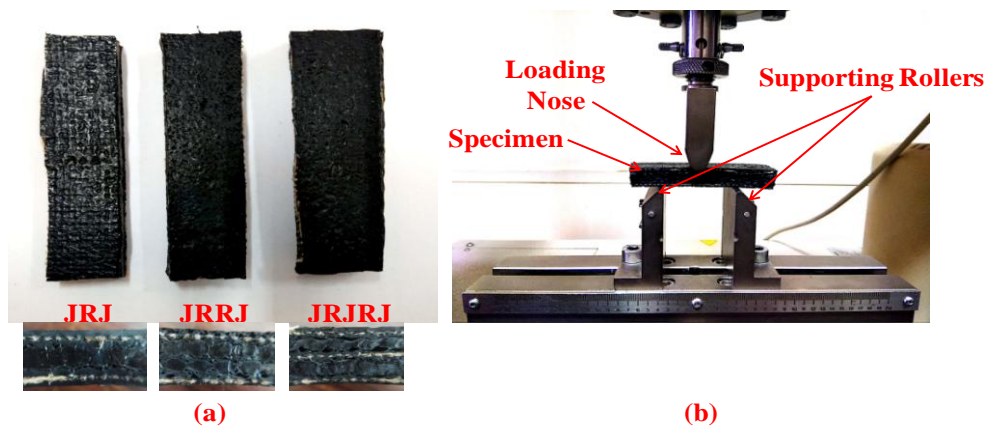


**Figure 3.21** Specimens used for interlaminar shear strength testing along with its cross section and (b) its loading in universal testing machine

### 3.4.4 Erosion and abrasion testing

The slurry erosive behavior of the three configurations JRJ, JRRJ and JRJRJ are studied by subjecting the flexible composites to slurry erosion test using a Ducom slurry erosion tester. The slurry is prepared by adding 50, 75 and 100 gms of sand to 1 liter of water based on the requirement and the mixture is stirred well. The test was



conducted at room temperature. The pre weighed samples were fixed into the specimen holder. The slurry pot is fixed in its position and the specimen was rotated inside the slurry at a speed of 500, 1000 and 1500 rpm based on the requirement. Three such specimens were subjected to testing and each time new slurry concentration is prepared. The wear of the samples were measured as a function of weight loss. The samples after test were dried and cleaned using acetone. Since the composite is made of only jute and rubber, it has a tendency to absorb water. Hence, the specimen after test was dried and then weighed using electronic weighing machine. The slurry erosion test is carried out at three different speeds and three different sand concentrations for all the three stacking sequences using Taguchi's L9 orthogonal array using silica sand as the abrasive medium. The initial and final weight of the specimen is calculated and the weight loss is determined using Eq. 31.

$$\text{Weight loss} = \text{Initial weight} - \text{Final weight} \quad (31)$$

Taguchi's DOE is carried out to determine the effect of various factors on the erosive behaviour of the proposed flexible composites. The factors and levels used in Taguchi's L9 orthogonal array are provided in Table 3.13.

**Table 3.13** Factors and levels used

<b>Factors</b>	<b>Level 1</b>	<b>Level 2</b>	<b>Level 3</b>
Stacking sequence	JRJ	JRRJ	JRJRJ
Rotation speed (rpm)	500	1000	1500
Sand concentration (g/L)	50	75	100

The specimen with dimension 76 mm x 25 mm needed to carry out the slurry erosion test is cut from the laminated prepared as shown in Figure 3.22 and the slurry erosion setup is shown in Figure 3.23. Silica sand used as the abrasive medium and its microstructure is shown in Figure 3.24.

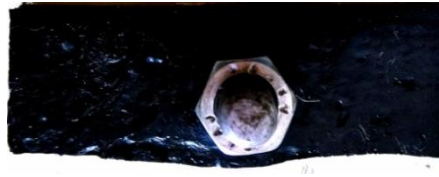


**Figure 3.22** Specimen used for slurry erosion test



**Figure 3.23** Slurry erosion setup



**Figure 3.24** Sand used as abrasive medium

Since lower weight loss of the composite is desired, S/N ratios are calculated for minimum weight loss with “smaller is better” criteria as logarithmic transformation of the loss function given by Eq. 32.

$$S/N = -10 \log_{10} \left( (\Sigma y^2) / n \right) \quad (32)$$

where 'y' is the responses for the given factor level combination and 'n' is the number of responses in the factor level combination. The present study makes use of commercially available statistical tool MINITAB 17 for the computational purpose. The response 'Weight loss' of the composite was analysed and the effect of the factors on the response were studied.

The statistical way of finding the significant factors can be accomplished by ANOVA as it indicates to what extent the process parameter influences the response and significance level of the factor considered. The significance of the control factors are studied by Fischer value (F value) obtained by ANOVA. The higher values of F indicate that the particular factor is highly significant in terms of affecting the response of the process. The percentage contribution is calculated using Eq. 33.

$$\% \text{ contribution} = \left( \frac{SS_f}{SS_t} \right) \times 100 \quad (33)$$

Where  $SS_f$  is the sum of squares of factor and  $SS_t$  is the total sum of squares. Finally, the regression model is developed. The R-sq value indicates the coefficient of determination. R-sq values more than 95 % indicates that the model developed gives good results and helps to predict the weight loss values within experimental conditions. In order to validate the model developed, the experimental results are compared with the predicted results.

Two body abrasion tests according to ASTM D5963/ ISO4649 is the most commonly used method to find the abrasive properties of elastomers and compounds containing elastomers. This method consists of a rotating drum which is wrapped with abrasive paper (Grit size = 60 and length of paper = 400 mm) as the abrasive medium over which the specimen to be tested is moved. The samples and DIN abrader used to perform the test are shown in Figure 3.25.



**Figure 3.25** Samples, schematic and DIN abrader

Hollow drills are used to obtain the sample, which is later positioned in the sample holding location of DIN abrader. The drum is set to rotation motion and at the same time, the sample moves laterally. The diameter and the length of the cylindrical drum are 150 mm and 500 mm respectively. The rotational frequency of the abrader is 40 rpm. Method B of ASTM D5963 is used to carry out the test. Precision weighing balance is made use of to measure the weight of the sample before and after the test.

Mass and volume losses are found out using Eq. 31 and Eq. 34 respectively. Three different loads of 9.81 N, 12.26 N and 14.71 N along with three different abrading distances of 0.4 m, 0.8 m and 1.2 m are used to carry out the experiment. The densities of the composites are determined by standard water displacement method.

$$V_l = \frac{M_l}{\rho} \quad (34)$$

where  $M_l$  is the loss of mass (gms) and the density of the composite is represented by  $\rho$  ( $\text{g}/\text{m}^3$ ). The specific wear rate ( $K_s$ ) in  $\text{m}^3/\text{Nm}$  is calculated using Eq. 35.

$$K_s = \frac{V_l}{L \times D} \quad (35)$$

where  $V_l$  is volume loss ( $\text{m}^3$ ), the load applied is represented by  $L$  (N) and sliding distance  $D$  (m). The factors and their levels used in the present study are presented in Table 3.14.

**Table 3.14** Factors and levels for two body wear

<b>Factors (Designation)</b>	<b>Level 1</b>	<b>Level 2</b>	<b>Level 3</b>
Composite configuration (A)	JRJ	JRRJ	JRJRJ
Abrading distance (B)	0.4 m	0.8 m	1.2 m
Load (C)	9.81 N	12.26 N	14.71N

Since lower weight loss of the composite is desired, S/N ratios are calculated for minimum weight loss with “smaller is better” criteria as logarithmic transformation of the loss function according to Eq. 32. The significance of the control factors are studied by Fischer value (F value) obtained by ANOVA. The higher values of F indicate that the particular factor is highly significant in terms of affecting the response of the process. The percentage contribution is calculated using Eq. 32 and finally a regression model is developed which is validated by comparing the experimental and predicted results.

#### 3.4.5 Impact testing

In the present study, energy absorption, peak force, coefficient of restitution, energy loss percentage and damage behavior due to LVI loading of jute/rubber based flexible composite is investigated. To accomplish this, LVI tests is carried out using a drop weight impact tester with conical impactor at three different impact energies and three different stacking sequences of the flexible composite. The energy absorption and damage resistance capability of the proposed flexible composites are studied. In order to evaluate the low velocity impact behaviour of the proposed flexible composites, the composites are subjected to low velocity impact test using a drop weight impact machine as shown in Figure 3.26. The impactor has a conically shaped nose with the total impactor assembly mass of 3.5 Kgs. The positioning of the specimen is done in the specimen holder and the impactor was then raised to the desired height from which it is made to fall on the specimen. Three different heights are chosen in the present study (300mm, 700 mm and 1100mm) so that an impact velocity of 2.42 m/s, 3.70 m/s and 4.64 m/s is achieved. This provides the impact energy of 10.24 J, 23.95 J, and 37.67 J respectively. The test is performed at room temperature. The different energies of impact are obtained by varying the drop height of the impactor. The

potential energy of the impactor increases with an increase in the height of the drop. Once the impactor assembly is released from a certain height, the potential energy is converted to kinetic energy of the impactor. Table 3.15 gives details of the test conditions. All the three stacking sequences of the flexible composites are tested for the test conditions mentioned in Table 3.15.

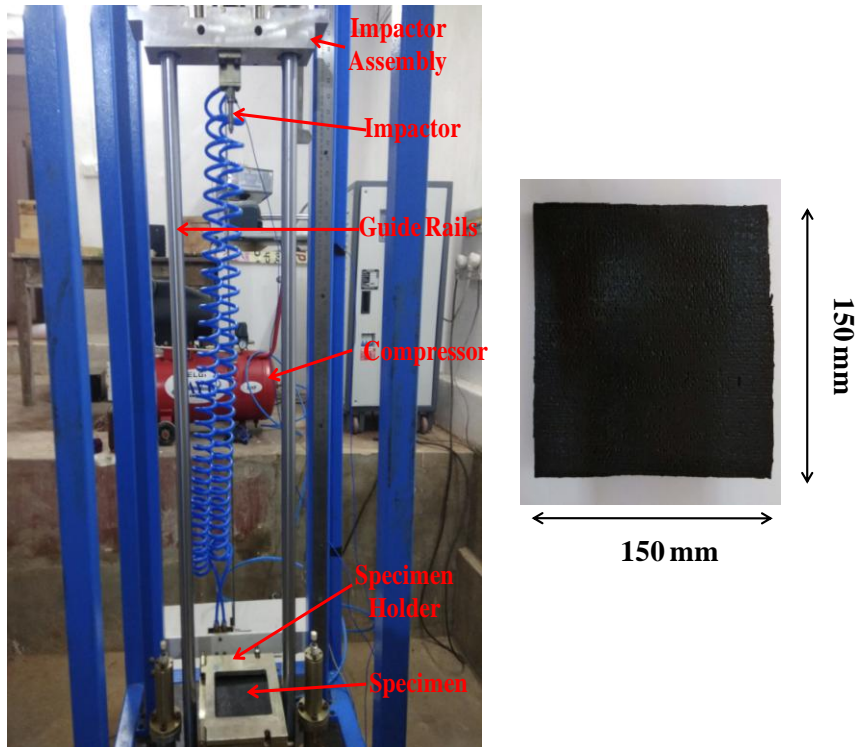


**Figure 3.26** Drop weight impact set up and specimen used

**Table 3.15** Impact test conditions

Drop height (mm)	Impact velocity (m/s)	Impact energy (J)
300	2.42	10.24
700	3.70	23.95
1100	4.64	37.67

The energy time history and force time history curves are obtained for each case. The absorbed energy and elastic energy for each of the cases are obtained from their respective energy time curve and the data pertaining to point of first damage and peak load are obtained from the force time history. The energy absorption ratio, coefficient

of restitution (CoR) and energy loss percentage (ELP) are calculated according to Eq.36, Eq. 37 and Eq. 38 respectively.

$$\text{Energy absorption ratio} = \left( E_a / E_i \right) \times 100 \quad (36)$$

$$CoR = \frac{v_r}{v_i} \quad (37)$$

$$ELP = (1 - CoR^2) \times 100 \quad (38)$$

Where,  $E_a$  is the absorbed energy (J) given by Eq. 39,  $E_i$  is the impact energy (J) given by Eq. 40,  $v_r$  is the residual velocity (m/s),  $v_i$  is the impact velocity (m/s).

$$E_a = \frac{1}{2} m (v_i^2 - v_r^2) \quad (39)$$

$$E_i = \frac{1}{2} m v_i^2 \quad (40)$$

Where,  $m$  is the mass of the drop weight in Kgs.

The global impact damage is assessed by finding the depth of the damage created due to the impact. A rod is inserted into the damage created up to the undamaged layer. Then, the length of rod that was inserted into the damaged portion is measured using a calliper. Scanning electron microscope (SEM) analysis is used to study the internal damage mechanism of the flexible composites. Before carrying out the SEM analysis, the damaged specimen is cut and the damaged area which is to be studied is sputtered with gold.

Lower ballistic impact tests were carried out using a gas gun apparatus in the velocity range of 50-120 m/s. The impact velocity of the projectile was measured by means of light emitting diodes (LED) placed at the point where the projectile leaves the barrel and the residual velocity was measured by means of a chronograph placed immediately after the target. The specimen of size 300 mm x 300 mm was clamped firmly to the fixture and the conical shaped projectile with diameter of 12 mm, conical nose angle of 34 degrees, length of 40 mm and mass of 10 gms was used to impact the

target. Figure 3.27 shows the gas gun arrangement and Figure 3.28 shows the specimen clamped to the fixture and the projectile used to carry out high velocity impact test.

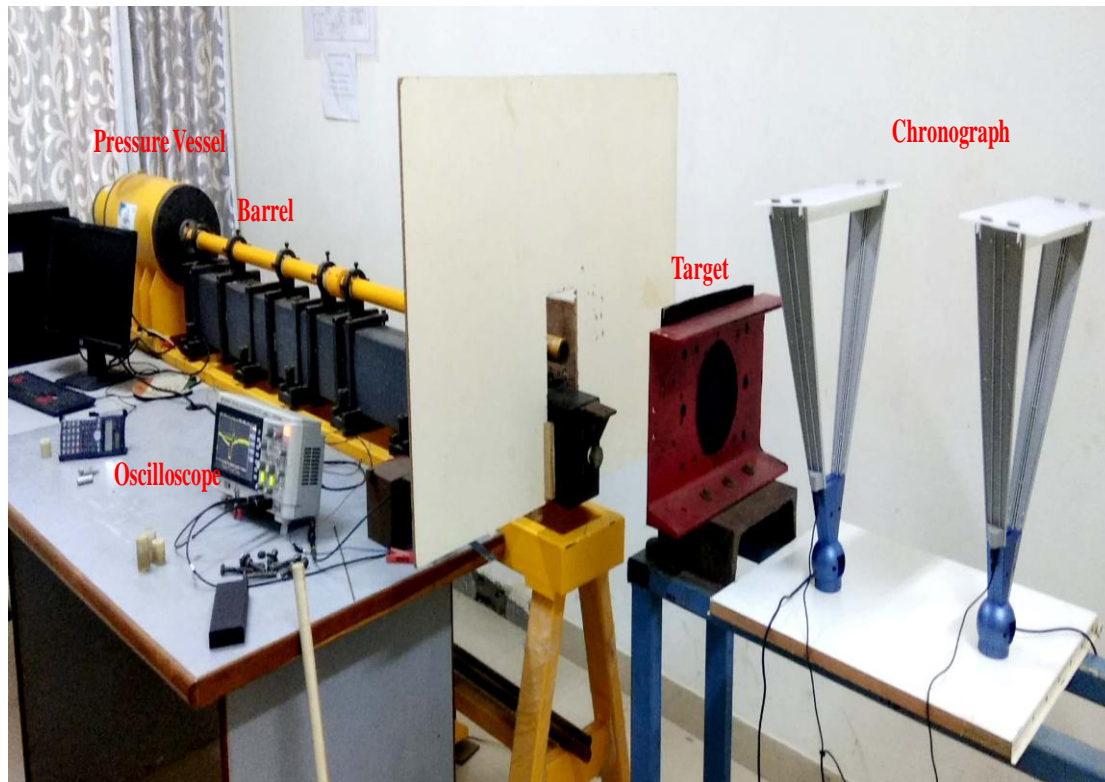


**Figure 3.27** Gas gun arrangement used to carry out high velocity impact test

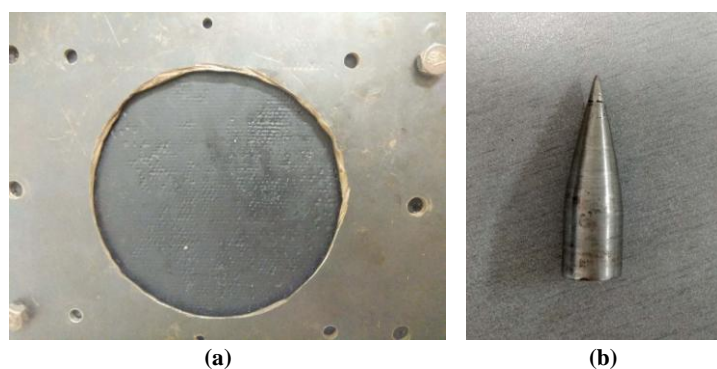


**Figure 3.28** (a) Specimen clamped in fixture and (b) projectile used

The ballistic limit of the proposed flexible composites (JRJ, JRRJ and JRJRJ) are determined experimentally based on the definition of ballistic limit which states



“Ballistic limit is the average number of maximum partial penetration velocities and minimum complete penetration velocities of a projectile and target combination”. The energy absorbed by the target is calculated using Eq. 41

$$E_a = \frac{1}{2} m_p (v_i^2 - v_r^2) \quad (41)$$

Where,  $E_a$  is the energy absorbed by the target in J,  $m_p$  is the mass of the projectile in Kgs,  $v_i$  and  $v_r$  are the impact and residual velocities in m/s. At the ballistic limit, energy absorption is calculated using Eq. 42. Further, the energy absorption percentage ( $E_{\%}$ ) is calculated using Eq. 43.

$$E_a^{bl} = \frac{1}{2} m_p v_{bl}^2 \quad (42)$$

Where,  $E_a^{bl}$  is the energy absorption at the ballistic limit,  $v_{bl}$  is the ballistic limit velocity.

$$\text{At ballistic limit, } E_{\%} = \left( \frac{E_a^{bl}}{E_i} \right) \times 100 \quad (43)$$

$$\text{At other than ballistic limit, } E_{\%} = \left( \frac{E_a}{E_i} \right) \times 100$$

Where,  $E_i$  is the impact energy given by Eq. 44

$$E_i = \frac{1}{2} m_p v_i^2 \quad (44)$$

### 3.5 Optimization using multi attribute decision making approach

MADM approach namely VIKOR and PSI methods are used to determine the optimal stacking sequence of the proposed flexible composites with tensile strength, tear strength, ILSS, specific energy absorption (SEA) of proposed flexible composites at low velocity and lower ballistic impact and specific wear rate which are determined experimentally as the attributes. The methodology adopted for the same is shown in Figure 3.29.

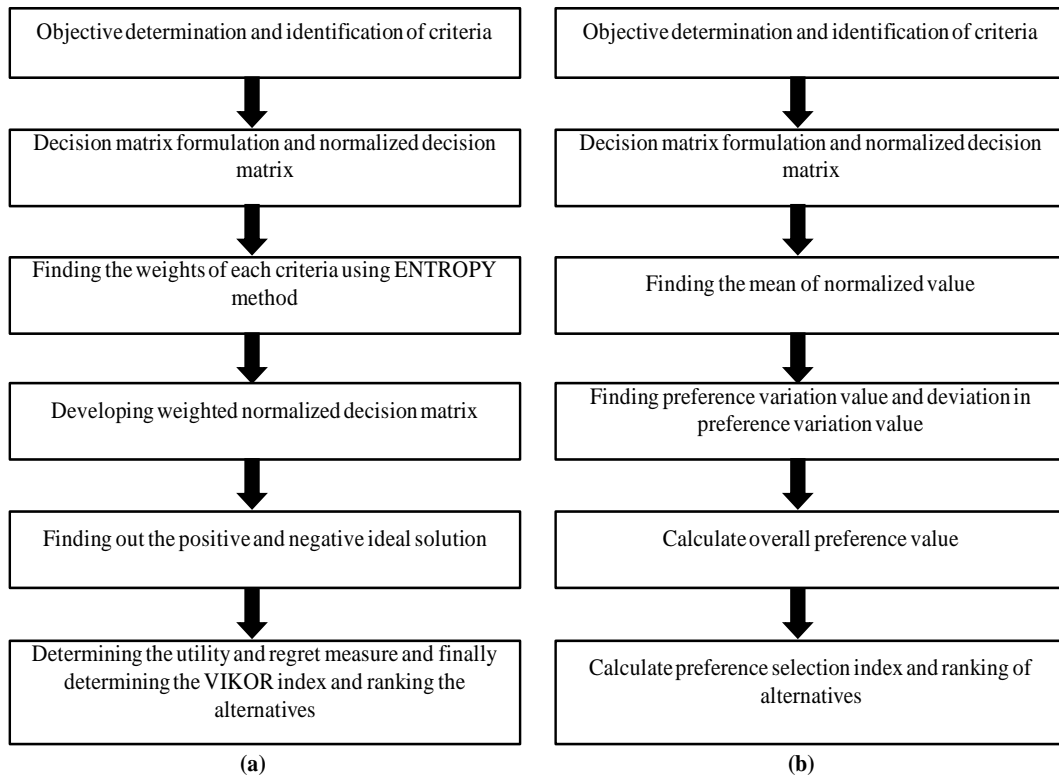


**Figure 3.29** Flowchart of the proposed (a)VIKOR and (b)PSI methods

The procedure used in case of VIKOR and PSI methods is as follows:

### 3.5.1 VIKOR method

The VIKOR method is used for the purpose of optimization of complex problems with multiple criteria and has been proposed by many researchers to solve MADM problems with contradicting criteria and the criteria which are not measurable by the same standard. This method aims at obtaining a compromise solution for a problem having contradicting criteria by comparing the measure of closeness to the ideal alternative and thus ranking the alternatives. The weights initially assigned to each criterion. In order to calculate the weights of the different criteria for using in the VIKOR method, the entropy method is used.

$$D = \begin{bmatrix} x_{11} & x_{12} & x_{13} & x_{14} & x_{15} & x_{16} \\ x_{21} & x_{22} & x_{23} & x_{24} & x_{25} & x_{26} \\ x_{31} & x_{32} & x_{33} & x_{34} & x_{35} & x_{36} \end{bmatrix} \quad (45)$$

Eq. 45 shows decision matrix ‘D’ of the present multi-criteria problem with 3 alternatives (JRJ, JRRJ, and JRJRJ) and 6 criteria (tensile strength, tear strength, ILSS, SEA of LVI, SEA of Lower ballistic impact and specific wear rate). The decision matrix is normalized by initially finding the normalized vector “ $r_{ij}$ ” using Eq. 46 and then building a normalized matrix using the normalized vector. Normalization is carried out in order to obtain dimensionless values of different criteria for the purpose of comparing them.

$$r_{ij} = \frac{x_{ij}}{\sqrt{\sum_{i=1}^m x_{ij}^2}} \quad (46)$$

Where,  $i = 1, 2, \dots, m$  and  $j = 1, 2, \dots, n$

The weights used for developing the weighted normalized matrix is found using “Entropy method”. The proportion “ $P_{ij}$ ” of the index is calculated using Eq. 47 and entropy  $E_j$  of index  $j$  is calculated using Eq. 48.

$$P_{ij} = \frac{x_{ij}}{\sum_{i=1}^m x_{ij}} \quad (47)$$

$$E_j = -k \sum_{i=1}^m P_{ij} \ln P_{ij} \quad (48)$$

Where  $k$  is calculated using Eq. 49

$$k = 1/\ln m \quad (49)$$

Where  $m$  is the number of alternatives ( $m=3$  in the present study)

The entropy weight “ $w_j$ ” of index “ $j$ ” is calculated using Eq. 50

$$w_j = \frac{[1 - E_j]}{\sum_{j=1}^n [1 - E_j]} \quad (50)$$

The standardized value of weight “ $v_{ij}$ ” is calculated using Eq.51 and the standardized weighted normalized matrix is built.

$$v_{ij} = w_j r_{ij} \quad (51)$$

Where,  $i = 1, 2, \dots, m$  and  $j = 1, 2, \dots, n$

The positive and negative ideal solution is determined using Eq. 52 and Eq. 53 respectively.

$$A^+ = \{\max v_{ij}\} = v_1^+, v_2^+, v_3^+, \dots v_n^+ \text{ for maximization problems} \quad (52)$$

$$A^+ = \{\min v_{ij}\} = v_1^+, v_2^+, v_3^+, \dots v_n^+ \text{ for minimization problems}$$

$$A^- = \{\min v_{ij}\} = v_1^-, v_2^-, v_3^-, \dots v_n^- \text{ for maximization problems} \quad (53)$$

$$A^- = \{\max v_{ij}\} = v_1^-, v_2^-, v_3^-, \dots v_n^- \text{ for minimization problems}$$

The utility and regret measures for each non dominated solution are calculated according to Eq. 54 and Eq. 55 respectively.

$$S_i = \sum_{j=1}^n w_j (v_j^+ - v_{ij}) / (v_j^+ - v_j^-) \quad (54)$$

$$R_i = \max [w_j (v_j^+ - v_{ij}) / (v_j^+ - v_j^-)] \quad (55)$$

Where,  $S_i, R_i \in [0,1]$ , 0 denotes the best and 1 denotes the worst situations. VIKOR index is calculated using Eq. 56 and ranking is done with the alternative having smaller VIKOR index as the best one

$$Q_i = \alpha \left[ \frac{S_i - S^-}{S^+ - S^-} \right] + (1 - \alpha) \left[ \frac{R_i - R^-}{R^+ - R^-} \right] \quad (56)$$

Where  $\alpha$  is a weighing factor ranging from 0 to 1. Usually,  $\alpha$  is selected to be 0.5

### 3.5.2 PSI method

PSI method is an approach to solve MADM problems that were developed by (Maniya and Bhatt 2010). This is a simple approach to select the best alternative as there is no necessity to assign relative importance between the attributes and also there is no need to find and assign the weights for the attributes. The steps involved in PSI method are as follows:

Step 1. Problem definition: In this step, the objectives are determined; attributes and alternatives involved in decision making are identified.

Step 2. Decision matrix formulation: The decision matrix is formulated based on the attributes and alternatives. Each row of the decision matrix represents the attributes of each alternative and each column is dedicated to one attribute. Hence, in an element  $x_{ij}$  of the decision matrix represents  $x$  value of  $j^{\text{th}}$  attribute in real values which is non-normalized for  $i^{\text{th}}$  alternative. Hence, if there are  $m$  alternatives with  $n$  attributes for decision making, the matrix will be of the order  $m \times n$  and represented as in Eq. 57

$$x_{ij} = \begin{bmatrix} x_{11} & x_{12} & x_{13} & \dots & x_{1m} \\ x_{21} & x_{22} & x_{23} & \dots & x_{2m} \\ \dots & \dots & \dots & \dots & \dots \\ x_{n1} & x_{n2} & x_{n3} & \dots & x_{nm} \end{bmatrix} \quad (57)$$

Step 3. Normalization: It is essential to make the values of the attributes dimensionless in MADM approaches. This is carried out by converting the attribute values to a value between 0 and 1. For the beneficial kind of attributes, the larger values are desired. Hence, normalization is carried out using Eq. 58 and for nonbeneficial kind of attributes, smaller values are desired and thus normalization is carried out using Eq. 59.

$$n_{ij} = x_{ij} / x_j^{\max} \quad (58)$$

$$n_{ij} = x_j^{\min} / x_{ij} \quad (59)$$

Where,  $x_{ij}$  is the measure of attribute ( $i = 1, 2, 3, \dots, m$  and  $j = 1, 2, 3, \dots, n$ )

Step 4. Finding the mean of normalized value: For every attribute, the mean value of the normalized data is calculated using Eq. 60.

$$M = \frac{1}{m} \sum_{i=1}^m n_{ij} \quad (60)$$

Step 5. Finding preference variation value: For every attribute, the preference variation value is calculated using Eq. 61.

$$\varphi_j = \sum_{i=1}^m [n_{ij} - M]^2 \quad (61)$$

Step 6. Finding the deviation in preference value: Here, for each of the attribute, the deviation in the preference value is calculated using Eq. 62.

$$\Delta_j = [1 - \varphi_j] \quad (62)$$

Step 7. Calculate overall preference value: For each of the attribute, the overall preference value is calculated using Eq. 63. The total value of  $\sum_{j=1}^K \Delta_j$  should be equal to 1.

$$\epsilon_j = \frac{\Delta_j}{\sum_{j=1}^n \Delta_j} \quad (63)$$

Step 8. Calculate preference selection index: For each of the alternative, preference selection index (PSI) is calculated using Eq. 64.

$$PSI_i = \sum_{j=1}^n x_{ij} \epsilon_j \quad (64)$$

Step 9. Ranking and selection of suitable alternative: The alternative with the highest PSI will be ranked 1 and so on.

In this chapter, details about the analytical, FE and experimental methodology adopted for the present work has been discussed in detail. The next chapter deals with the results obtained after adopting the above said methodologies followed by discussions on the same

## **CHAPTER 4**

### **4 RESULTS AND DISCUSSIONS**

This chapter presents the results and discussion pertaining to the comparative study of impact behaviour of JE and JE-R-JE composite, impact behaviour of various configurations of the flexible composites through FE method; physical, mechanical, wear and impact characterization of the flexible composites. Finally, the results obtained through application of MADM approach for selecting the best configuration is discussed.

#### **4.1 Analytical approach**

The results obtained through analytical method based on law of conservation of energy matches well with the experimental approach adopted and the results and discussion are presented along with experimental results under testing section for the purpose of comparison and validation.

#### **4.2 Finite element analysis**

This section presents the results and discussions pertaining to FE methodology adopted in the present study for studying the impact response of stiff JE composite and JE-R-JE sandwich composite. Also, the results pertaining to impact behaviour of the flexible composites with different configurations are presented in this section. However, the FE results pertaining to the lower ballistic impact behaviour of the proposed flexible composites with optimized stacking sequence are presented along with experimental and analytical results in testing section for the purpose of comparison and validation.

##### **4.2.1 Results of comparative study on impact behaviour of jute-epoxy composite laminate and jute-epoxy-rubber sandwich composite**

In order to validate the FE model used in the analysis, the methodology adopted for low velocity impact analysis in the literature (Karas 1939) is taken as a reference in

the present study. The same methodology was employed to validate the study on graphite-epoxy composite (Park 2017).

#### 4.2.1.1 Contact force developed for jute epoxy and jute epoxy-rubber-jute epoxy composite during impact

Peak contact force is of great importance in impact loading as it can control damage initiation. The higher the peak load, the damage initiation is earlier. For all the tested angles ( $0^\circ$ ,  $5^\circ$ ,  $10^\circ$ ,  $15^\circ$ , and  $20^\circ$ ) on JE and JE-R-JE composite the graph of contact force as a function of time is presented in Figure 4.1.

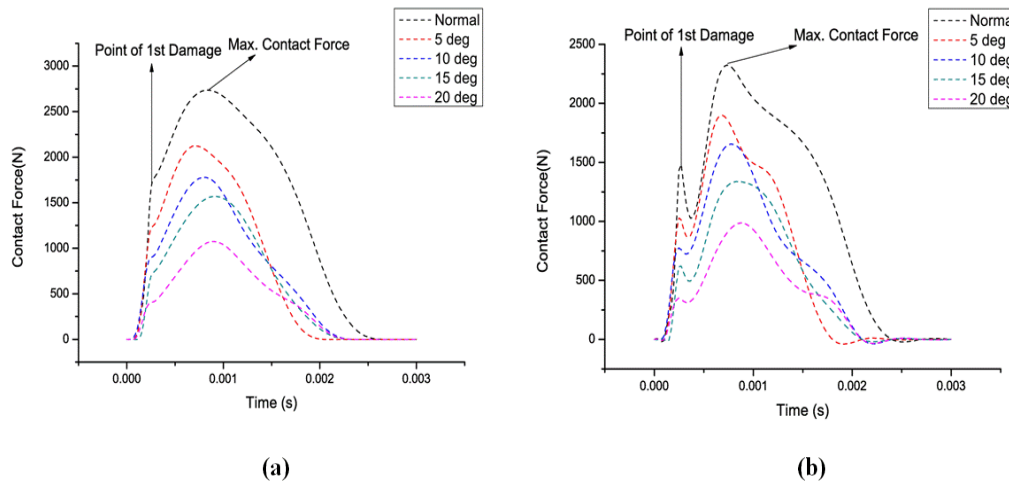


**Figure 4.1** Variation of contact force with time for (a) jute epoxy and (b) jute epoxy-rubber-jute epoxy composite

All the curves show same trends where the loading and unloading parts of curve are smooth. The duration for which the impactor is in contact with a sandwich is studied from the graph. Till the point of initiation of damage or peak load, the variation of force with time is linear. The point where the failure is just initiated on the graph is referred to as the maximum load carrying ability. This point was called as incipient point of damage (Siow and Shim 1998) which is usually a matrix failure. The extent of damage is very little or no visible damage. This results in drop in the magnitude of force showing reduction in stiffness of the material. Penetration and perforation damages are the results of a combination of such failures. The peak load for JE laminate and JE-R-JE sandwich is tabulated in the Table 4.1.



**Table 4.1** Contact force variation at various loading conditions

Type of Loading	JE Laminate		JE-R-JE Sandwich	
	Max. Contact Force at Incipient Point of Damage (N)	Peak Contact Force (N)	Max. Contact Force at Incipient Point of Damage (N)	Peak Contact Force (N)
Normal	1865.36	2805.31	1434.9	2157.9
5°	1307.01	2281.80	1029.1	1796.7
10°	929.55	1885.74	774.6	1571.4
15°	770	1664.82	616	1331.9
20°	424	1192.09	350.4	985.2

The tabulated results show that the peak load will be more in laminate when compared to sandwich structure for any given case of loading, indicating earlier damage initiation in laminate compared to the sandwich. The contact force histories also conclude that with increasing in angle of impact, there is a reduction in peak contact force. The descending part of the unloading is due to continuous loading beyond the peak point where there is a continuous progression of damage to the structure and thus a reduction in the contact force. Therefore the major mode of failure for this impact loading scenario is due to bending stress at the edges coupled with shear and crushing at the point of impact.

#### 4.2.1.2 Energy absorption of jute epoxy and jute epoxy-rubber-jute epoxy composite

Gathering knowledge about ability of composite to absorb energy under impact loading is very important and it is the critical parameter studied by most of the researchers. The energy absorbed by the composite is obtained by the difference between initial and final kinetic energy of impactor. The variation of kinetic energy with respect to time for various loading conditions on JE laminate and JE-R-JE sandwich is as shown in Figure 4.2.

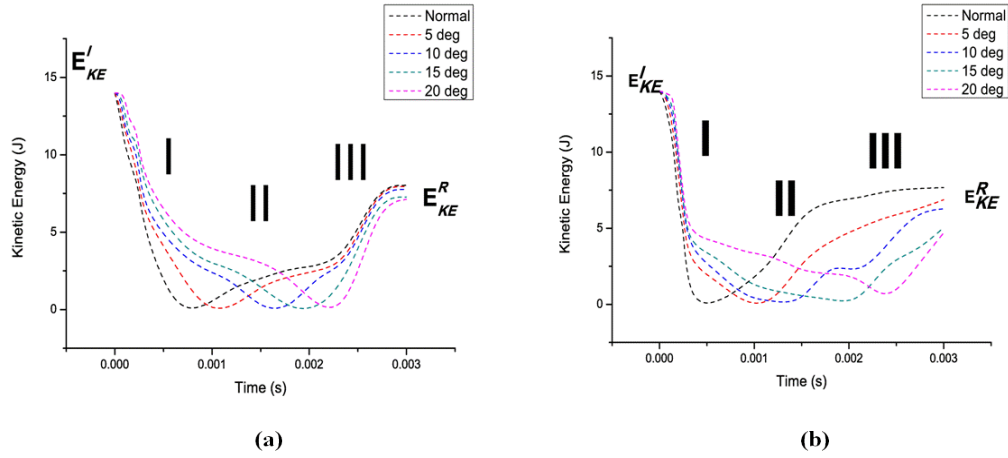


**Figure 4.2** Variation of kinetic energy with time for (a) jute epoxy and (b) jute epoxy-rubber-jute epoxy composite

For illustrating the variation of kinetic energy against time during an impact event, the case of normal impact in a laminate is considered. It can be noted that for all types of loading conditions the kinetic energy of impactor reaches zero at some point of time and after that the kinetic energy increases. With the increase in impact angle, the time at which the kinetic energy becomes zero increases and also the residual kinetic energy decreases and hence the residual velocity also decreases. For illustrative purpose, the normal impact loading case in JE laminate is considered. In stage I, kinetic energy (KE) of the impactor is dropping rapidly after contact with laminate, which is transformed into internal energy of the laminate. At stage II, Kinetic energy of the impactor becomes zero at the lowest position. At the same time, internal energy (IE) of the laminate becomes the largest. As impact continues, kinetic energy of the impactor increases again with rebound of the impactor, which is stage (III). At the end of the impact event, the impactor is separate from the laminate with a constant rebound kinetic energy or residual kinetic energy  $E_{KE}^R$ . The same concept applies to all the loading conditions in laminate as well as sandwich. The volume of the impactor is found to be  $3.62 \times 10^{-5} \text{ m}^3$  from the modelling software and using the volume, the mass of the impactor is calculated as 0.28 Kg using Eq. 65.

$$m = \rho \times v \quad (65)$$

Where,  $\rho$  is the density of the impactor material in  $\text{Kg/m}^3$  and  $v$  is the volume of the impactor in  $\text{m}^3$ .

It can be seen from the energy history curve with respect to time that as the impact angle increases, the final energy of impactor i.e. residual kinetic energy decreases. This means that the growth of impact angle leads to increase in energy absorption. The initial kinetic energy, residual kinetic energy, residual velocity of the impactor and the energy absorbed by the composites are tabulated in Table 4.2.

**Table 4.2** Kinetic energy and internal energy for jute epoxy laminate and jute epoxy-rubber-jute epoxy sandwich

Type of Loading on Laminate	Initial Kinetic Energy (J)	Residual Kinetic Energy(J)		Energy Absorbed (J)		Residual Velocity (m/s)	
		JE	JE-R-JE	JE	JE-R-JE	JE	JE-R-JE
Normal ( $0^\circ$ )		8.03	7.66	5.97	6.34	7.57	7.40
$5^\circ$	14	7.95	6.86	6.05	7.14	7.53	7.00
$10^\circ$		7.76	6.28	6.24	7.72	7.44	6.70
$15^\circ$		7.27	5.04	6.73	8.96	7.20	6.00
$20^\circ$		7.12	4.70	6.88	9.30	7.13	5.80

As the angle of impact increases, the residual kinetic energy and residual velocity of impactor decreases and the energy absorbed by JE and JE-R-JE increases. Thus, it can be concluded that as the impact angle increases the energy absorption increases and also JE-R-JE sandwich absorbs more energy compared to JE laminate which can be due to the presence of rubber core which makes the sandwich less brittle compared to laminate.

#### 4.2.1.3 Deflection of jute epoxy and jute epoxy-rubber-jute epoxy composite

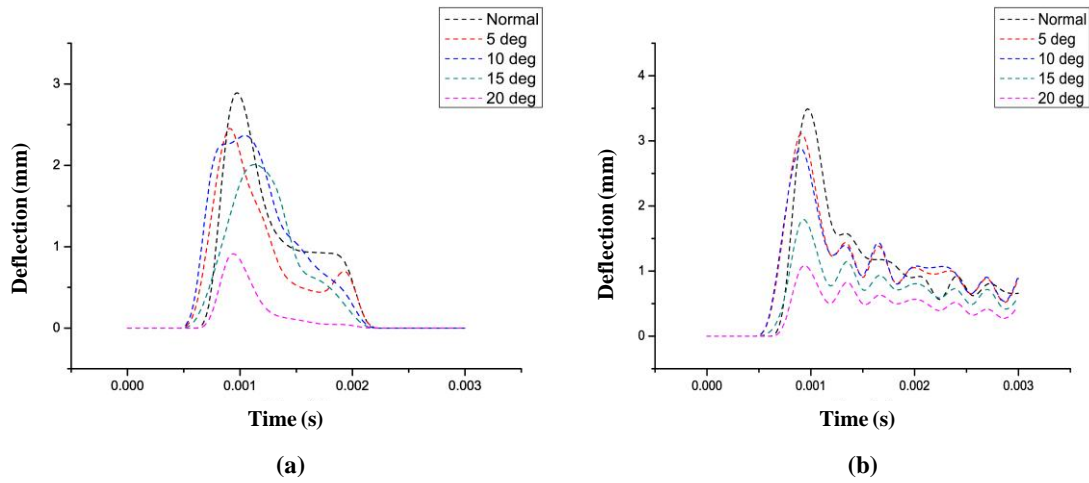


**Figure 4.3** Variation of deflection with time for (a) jute epoxy and (b) jute epoxy-rubber-jute epoxy composite

Figure 4.3 shows the deflection against time for JE laminate and JE-R-JE sandwich. Due to the impact at the velocity 10 m/s, the maximum deflection obtained in JE laminate are 3.15 mm, 2.89 mm, 2.47 mm, 2.06 mm and 1.11 mm respectively, for normal impact and oblique impact with 5°, 10°, 15° and 20° loading and for the JE-R-JE sandwich the same is found to be 3.81 mm, 3.66 mm, 3.35 mm, 2.18 mm and 1.32 mm respectively. The maximum deflection is noticed at the centre of JE laminate and at the centre of the top face sheet and minimum deflection at the edges as the four side faces of the sandwich are constrained in all the cases. The maximum deflections of sandwich occur when the impact force becomes equal to zero. During the impact event, the travelling of the impacted surface is indicated by the displacement. Since, drop height of the impactor is same in all the cases, the amount of energy it delivered on the laminate and sandwich will be same according to (Remennikov et al. 2011). The laminate or sandwich which can resist maximum load will undergo least displacement as load and displacement depends on the amount of energy dissipated by sandwich.

**Table 4.3** Deflection for jute epoxy laminate and jute epoxy-rubber-jute epoxy sandwich

Deflection in mm	Normal (0°)	5°	10°	15°	20°
JE Laminate (mm)	3.15	2.89	2.47	2.06	1.11
JE-R-JE Sandwich (mm)	3.81	3.66	3.35	2.18	1.32

It can be concluded from the Table 4.3 that as the oblique angle under consideration increases, the deflection reduces. Sandwich and laminate with 20° loading condition can take more loads compared to normal loading condition.

4.2.1.4 Analysis of damage through stress pattern in jute epoxy and jute epoxy-rubber-jute epoxy composite

The stress profiles leading to damage in both JE laminate and JE-R-JE sandwich subjected to normal and various oblique impact loading conditions are shown in Figure 4.4.

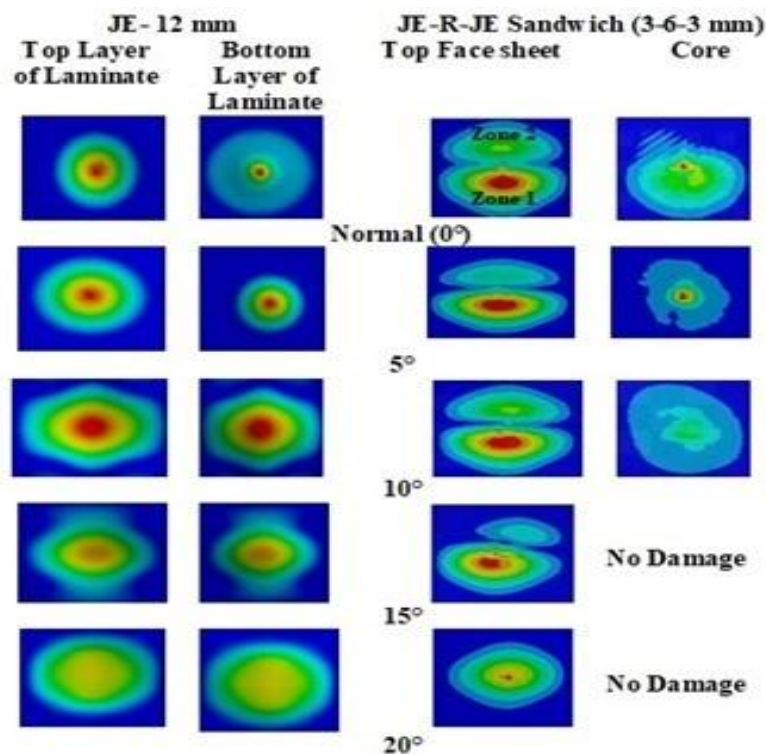


**Figure 4.4** Von Mises stress patterns in jute epoxy laminate and jute epoxy-rubber-jute epoxy sandwich

In case of JE laminate the occurrence of damage is observed in both top and bottom faces. It can also be seen that as the angle of incidence with respect to normal increases, the bands of damage get reduced, indicating that the intensity of damage is being reduced and damage is passed to the bottom surface of laminate due to the brittleness of the JE laminate. This is schematically represented in Figure 4.5 (a).

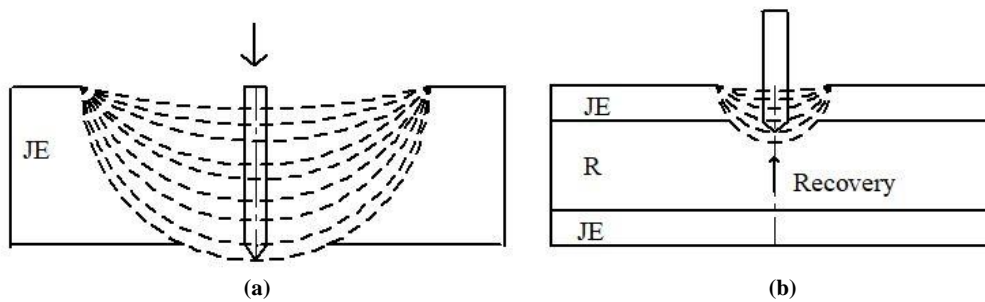


**Figure 4.5** Schematic representation of damage progression in (a) jute epoxy and (b) jute epoxy-rubber-jute epoxy composite

By comparing the stress pattern under different loading condition, it is conclusive that there is no much difference in the nature of damage from normal impact and oblique impact with  $5^\circ$  impact angle. With further increase in the oblique angle, it can be seen that the damage zone 2 caused due to the effect of zone 1 gradually reduces and moves away from zone 1. The size of damage zone 2 gradually becomes smaller with an increase in oblique angle due to the reduced intensity of the load. For oblique impact at  $20^\circ$ , it can be seen that the zone 2 has been completely vanished and only zone 1 exists.

In case of JE-R-JE sandwich, the top face sheet is damaged under all types of impact loading. The damage on the top surface of the core was observed only for normal,  $5^\circ$  and  $10^\circ$  degree impact loading conditions, whereas the bottom face sheet is unaffected in all the cases. This can be due to the presence of rubber core. The elastic recovery nature of rubber arrests the strain energy resulting in prevention of damage to proceed further. This is schematically represented in Figure 4.5 (b). Also in JE-R-JE sandwich the two zones of damage are observed, Zone 1 which is the primary zone of damage and zone 2 which is the secondary zone of damage. The secondary zone of damage gradually reduces as the angle of incidence of impact increases. Also the intensity of

damage reduces. When the damage pattern in JE laminate is compared with JE-R-JE sandwich, it is conclusive that the damage in the sandwich is less compared to the laminate of the same thickness. The presence of rubber as a core material which is elastic in nature is the cause for the same.

#### 4.2.2 Results of comparative study on stiff flexible composite

The results obtained from the comparative study of stiff and flexible composites for their impact behaviour are presented in Table 4.4.

**Table 4.4** Energy absorption of jute epoxy and jute epoxy/rubber/jute epoxy composite

<b>Material</b>	<b>Impact Velocity (m/s)</b>	<b>Residual Velocity (m/s)</b>	<b>Energy Absorbed (J)</b>	<b>Velocity Drop (m/s)</b>	<b>Energy Absorption Ratio (%)</b>
JE	10 m/s	7.58	31.87	2.42	42.49
JRJ		5.59	51.56	4.41	68.74

It can be observed that, JRJ composite absorbs 61.78% more energy compared to JE composite laminate. This is due to the addition of rubber as a core material in JRJ. Rubber has higher energy absorption capability and also JRJ is not brittle as JE laminate.

#### 4.2.3 Results of identification of different configurations of flexible composite

Based on the constituents selected for the proposed flexible composite and realising that flexible composites are better energy absorbers compared to stiff composites, six different configurations which are tabulated in Table 4.5 are initially considered for the present study.

**Table 4.5** Configurations of composite considered in the present study

<b>Sl.No.</b>	<b>Configuration</b>	<b>Representation</b>
1	Jute-Rubber-Jute	JRJ
2	Jute-Rubber-Rubber-Jute	JRRJ

Sl.No.	Configuration	Representation
3	Jute-Rubber-Jute-Rubber-Jute	JRJRJ
4	Rubber-Jute-Rubber	RJR
5	Rubber-Jute- Rubber-Jute	RJRJ
6	Rubber-Jute- Rubber-Jute-Rubber	RJRJR

#### 4.2.4 Results of determining optimum configuration of flexible composite

The FE analysis of LVI is carried out on the six configurations selected in order to determine the optimum configuration suitable for the proposed applications. The results of this FE study is summarized in Table 4.6 which gives the energy absorbed, specific energy absorbed and contact force for each of the configuration considered in the present study. The rank is assigned to the configurations based on the criteria that the configuration with maximum contact force is assigned rank 1 since larger the contact force larger is the resistance to impact force leading to minimal damage. JRJRJ configuration provides maximum contact force followed by JRJ, JRRJ, RJRJR, RJRJ and RJR. The energy absorbed and contact force depends on the compliance of the material. More the compliance less will be the contact force. The addition of jute as reinforcement enhances the contact force. Figure 4.6 (a) shows the variation in kinetic energy for different configurations considered in the present study.

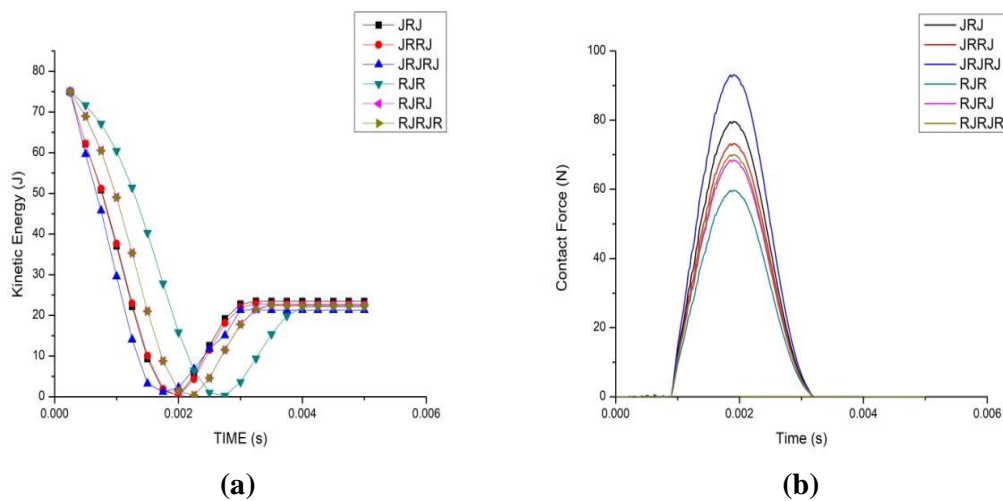


**Figure 4.6** Variation in (a) kinetic energy and (b) contact force for different configurations



The initial kinetic energy remains same for all the configurations since the impact velocity provided to the impactor is same in all the cases. The kinetic energy of the impactor reduces gradually after coming in contact with the laminate, during which the internal energy of the laminate starts increasing. The internal energy of the laminate becomes maximum when the kinetic energy of the impactor reaches its minimum. The kinetic energy of impactor after reaching its minimum, starts increasing again which is due to the rebound of the impactor from the laminate and becomes constant at certain stage. This constant energy is taken as the residual energy ( $KE^R$ ) of the impactor. The energy absorbed ( $E^a$ ) by the laminate is the difference between initial and residual kinetic energy. Figure 4.6 (b) shows the variation in contact force against time for all the six configurations considered. It can be seen that the JRJRJ has maximum contact force followed by JRJ, JRRJ, RJRJR, RJRJ and RJR. Figure 4.7 shows the comparison of the sp. energy absorbed and contact force for different configurations in the present study. It can be seen that though RJR absorbs maximum specific energy, the variation among the configurations is negligible and thus the variation in contact force of the different configurations is considered for ranking. Higher contact force indicates higher resistance to damage.

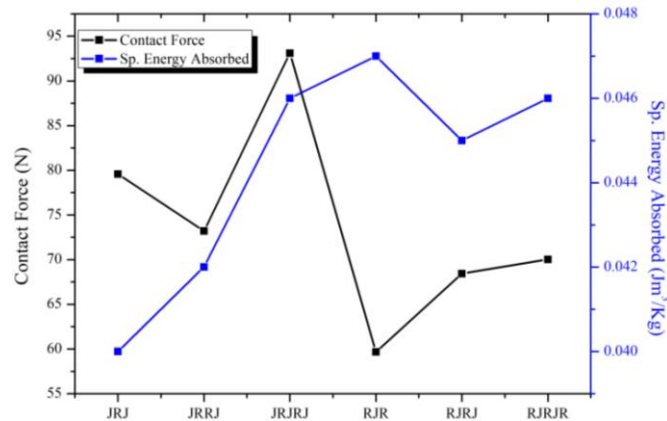


**Figure 4.7** Comparison of sp. energy absorption and contact force for different configurations

The damage analysis carried out as represented in Figure 4.8 shows that composites with rubber on the impact side (RJR, RJRJ and RJRJR) undergoes tearing type of damage, whereas for the composites with jute on the impact side (JRJ, JRRJ and JRJRJ), no damage of any kind is visible.

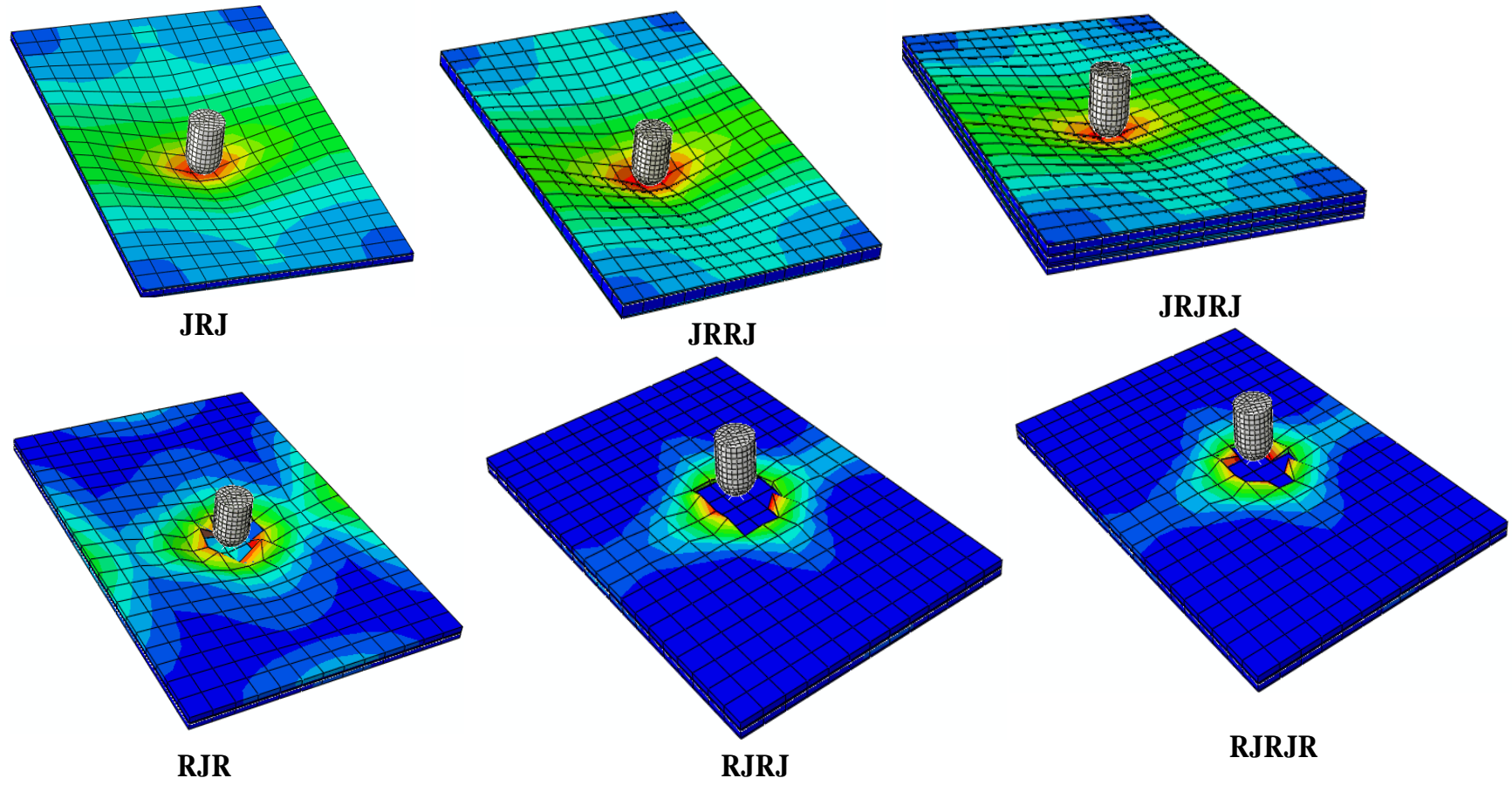


**Figure 4.8** Damage behavior of various configurations of flexible composite

**Table 4.6** Summary of energy absorbed and contact force during impact behaviour of different configurations of flexible composites through finite element approach

<b>Configuration</b>	<b>Initial Kinetic Energy (J)</b>	<b>Residual Kinetic Energy (J)</b>	<b>Energy Absorbed (J)</b>	<b>Density (Kg/m<sup>3</sup>)</b>	<b>Sp. Energy Absorbed (Jm<sup>3</sup>/Kg)</b>	<b>Contact Force (N)</b>	<b>Rank</b>
JRJ	75	23.44	51.55	1178.1	0.040	79.57	2
JRRJ	75	22.73	52.26	1138	0.042	73.21	3
JRJRJ	75	21.30	53.69	1165.02	0.046	93.10	1
RJR	75	22.10	52.89	1106.8	0.047	59.68	6
RJRJ	75	22.47	52.52	1138	0.045	68.43	5
RJRJR	75	22.31	52.68	1126.02	0.046	70.02	4

### 4.3 Testing

Testing of the constituents and the proposed flexible composites are carried out to determine the curing characteristics of the matrix, peel strength of the constituents, physical, mechanical properties, erosive and abrasive behaviour and impact behaviour. The outcomes of each testing are presented in further sections.

#### 4.3.1 Results of curing characteristics of natural rubber based pre peg

Various kinetic parameters like order of the cure reaction and rate of reaction were evaluated from the oscillating disk rheometer graph of Torque v/s Time as shown in Figure 4.9. Initially the compound gets heated up under the pressure resulting in viscosity drop and reducing the torque exerted on the rotor of rheometer. This lowest value of torque is referred to as minimum torque ( $M_L$ ) which is the measure of stiffness of uncured rubber compound at a given temperature. The phase up to this stage is referred to as induction and scorch phase. As the curing of the NR based B stage cure pre peg matrix begins, the torque increases and this phase is referred to as curing phase, at the end of which the NR based B stage cure pre peg matrix will be cured. After the curing phase, the curve attains a stabilized form representing phase that provides the physical properties of the NR based B stage cure pre peg matrix. Over curing in case of NR based B stage cure pre peg matrix may lead to 'reversion' resulting in deterioration of physical properties of the matrix.

The minimum torque ( $M_L$ ), Maximum torque ( $M_H$ ), scorch time ( $t_{S2}$ ), 90% of cure time ( $t_{C90}$ ), CRI and end temperature obtained for the NR based B stage cure pre peg matrix sample is provided in Table 4.7.

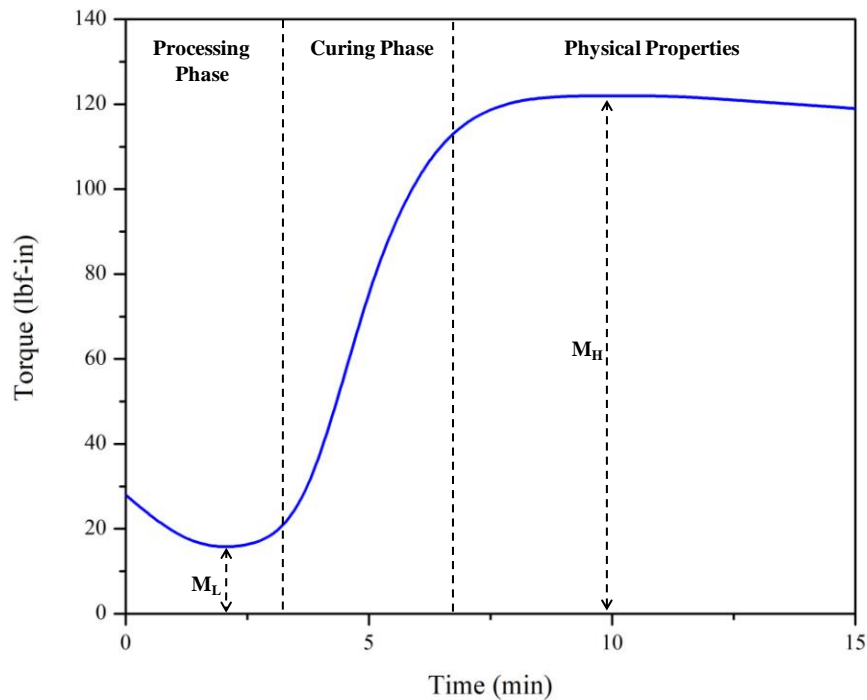


**Figure 4.9** Oscillating disk rheometer graph representing curing behaviour of natural rubber based B stage cure pre peg

**Table 4.7** Cure characteristics of natural rubber based B stage cure pre peg matrix

$M_L$ (lbf-in)	$M_H$ (lbf-in)	$t_{s2}$ (min)	$t_{c90}$ (min)	CRI ( $\text{min}^{-1}$ )	End temperature ( $^{\circ}\text{C}$ )
13.92	121.3	3.19	6.31	32.06	138.7

#### 4.3.2 Results of determining peel strength of constituents

The variation of the peel force against the displacement for jute bonded with rubber gum and rubber bonded with rubber gum is shown in Figure 4.10. It can be seen that the peel force required to separate the adherand is more in case of rubber bonded to rubber gum compared to jute bonded to rubber gum. This is because of the higher tackiness provided by the rubber which results in more amount of force being needed to separate the rubber from the rubber gum.

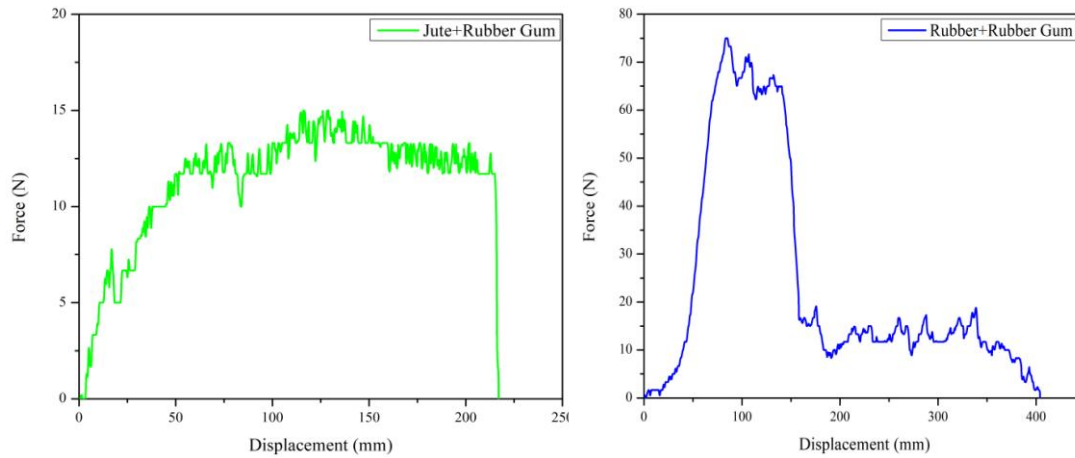


**Figure 4.10** Force vs displacement plot for jute and rubber

Table 4.8 summarizes the results obtained from the peel test. It is found that the peel strength and strain energy release rate of rubber is 5 times and 2.91 times more than jute when bonded with rubber gum.

**Table 4.8** Summary of peel strength of rubber and jute when bonded with natural rubber based B stage cured pre peg

Adherand	Max. Peel Force: F (N)	Width: b (mm)	Peel Strength: $P_s$ (N/mm) or (KJ/m <sup>2</sup> )
Rubber	75	25	6
Jute	15	25	1.2

### 4.3.3 Results of physical and mechanical characterization

Physio mechanical characterization of the proposed flexible composites are performed according to their respective standards and the overview of the results are tabulated in Table 4.9.

**Table 4.9** Summary of physical and mechanical characterization

Test	Material	Theoretical	Experimental Density						Void Content (%)					
		Density (Kg/m <sup>3</sup> )	Density (Kg/m <sup>3</sup> )						Density (Kg/m <sup>3</sup> )					
Void content	JRJ	1178.1	1159.64						1.56					
	JRRJ	1138	1121.57						1.44					
	JRJRJ	1165	1118.81						3.96					
	Material	Initial weight (gms)	Final weight (gms)						Water Absorption (%)					
			2 hrs	6 hrs	12 hrs	24 hrs	48 hrs	72 hrs	2 hrs	6 hrs	12 hrs	24 hrs	48 hrs	72 hrs
Water Absorption	JRJ	2.91	2.92	2.95	2.96	2.97	2.97	2.97	0.34	1.37	1.71	2.06	2.06	2.06
	JRRJ	4.44	4.46	4.49	4.55	4.56	4.56	4.56	0.45	1.12	2.47	2.7	2.7	2.7
	JRJRJ	5.01	5.04	5.11	5.15	5.17	5.17	5.17	0.59	2	2.79	3.19	3.19	3.19

	<b>Material</b>	<b>Ultimate Stress (Mpa)</b>	<b>Ultimate Strain (%)</b>	<b>Modulus (Mpa)</b>
Tensile Test	JRJ	2	160	30.6
	JRRJ	1.268	193	30.07
	JRJRJ	1.216	196	28.14
	<b>Material</b>	<b>Tear Strength Ts (N/mm)</b>		
Tear Test	JRJ	31.78		
	JRRJ	31.65		
	JRJRJ	31.04		



#### 4.3.3.1 Results of void content

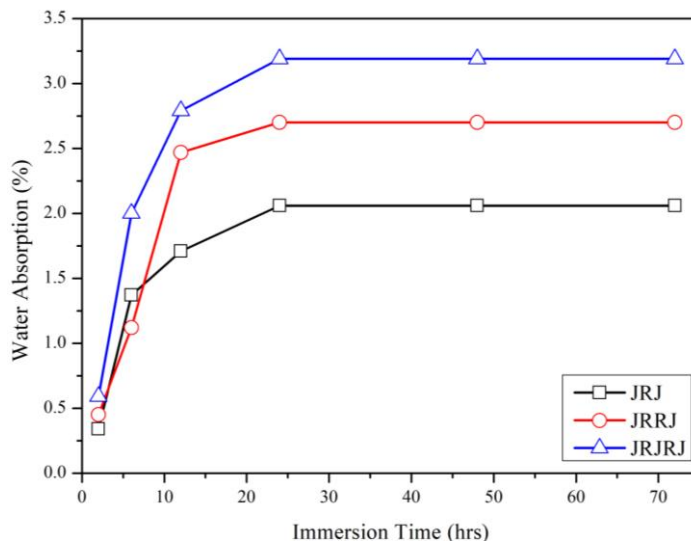
The density of the composite manufactured mainly depends on the void contents present in composite. Void content of the composite is calculated using Eq. 27. The density of the composite can be found to reduce as the number of plies increases, whereas the void content increases with increasing plies. The lumens present in the natural fiber acts at void and increases the void content in composite (Shuhimi et al. 2016). The void content is minimum in case of JRRJ and maximum with JRJRJ.

The composite with weight fraction of 12%, 7% and 10% fiber gives void content of 1.56%, 1.44% and 3.56% respectively. The void percentage reduces for JRRJ (7% weight fraction) stacking sequence because of the arrangement of the plies. Two rubber layers are successively in contact with each other and binds together leaving no room for voids. As the additional jute layer is introduced in between them (JRJRJ), the weight fraction of fiber increases to 10% and creates a room for introduction of voids and thus the void percentage increases drastically.

#### 4.3.3.2 Results of water absorption test

Moisture absorption is considered as one of the major drawback of natural fiber reinforced composites. Thus, it becomes essential to investigate the moisture absorption behaviour of such composites. The water absorption of the composites over the period of time is shown in Figure 4.11. The composites were immersed in water for a total of 72 hours and their weight was checked after 2 hrs, 6 hrs, 12 hrs, 25 hrs, 48 hrs and 72 hrs. It is clear from the Figure 4.11 that for all the composites, after 24 hours of immersion, the water absorption is saturated and remains constant. JRJ absorb less water compared to JRRJ and JRJRJ. This is due to the minimum amount of fiber used in JRJ composite. Water absorption of JRRJ is higher than that of JRJ which indicates that the rubber also contributes to water absorption. The higher water absorption ability lies with JRJRJ as it has maximum amount of fiber in it compared

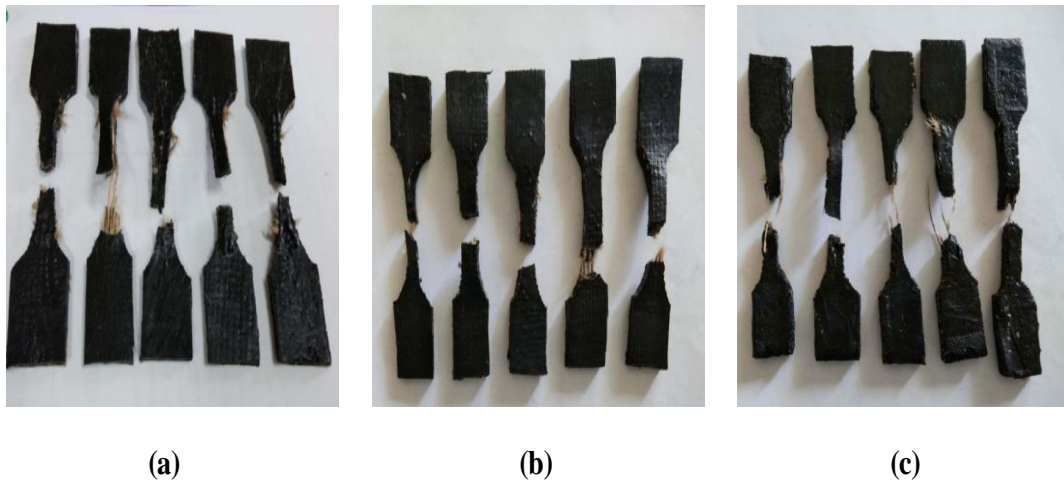
to JRJ and JRRJ. The water absorption increases with increasing plies in composite. The rubber as well as jute both contributes to the water absorption in the composite with natural fiber being the major constituent contributing to water absorption due to its hydrophilic nature as opposed to rubber which is hydrophobic. Natural fibers have a tendency to swell when exposed to water which is due to the hydrophilic nature of natural fibers. Also, as the number of plies increases, the interfacial area between fiber and matrix is greater leading to more water absorption. The water absorption of stacking sequence increases in the order JRJ < JRRJ < JRJRJ. It is to be noted here that both the jute and rubber contributes to the water absorption of composite and thus number of plies (both rubber and jute together) are the deciding factor in water absorption rather than weight percentage of fiber alone.



**Figure 4.11** Water absorption of the composites over a period of time

#### 4.3.3.3 Results of tensile test

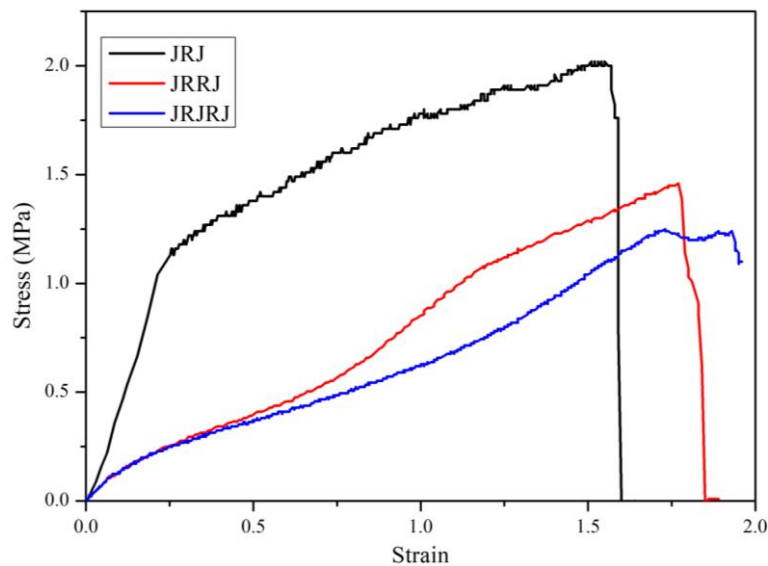
The tensile specimens after fracture are shown in Figure 4.12. The type of failure observed during the tensile testing of the composite is fiber pull out and matrix tearing. The similar mode of failure is observed in JRJ, JRRJ and JRJRJ stacking sequences.



**Figure 4.12** Tensile specimens of (a) jute/rubber/jute (b) jute/rubber/rubber/jute and (c) jute/rubber/jute/rubber/jute after fracture

Figure 4.13 shows the stress v/s strain plot for each of the specimen tested for all types of configurations. It can be concluded from the tensile results that the tensile properties of the composite lie in between that of jute and natural rubber sheet. The ultimate strength of JRJ is higher followed by JRRJ and JRJRJ. The tensile strength of JRJ (12% weight fraction) is found to be better followed by JRRJ (7% weight fraction) and JRJRJ (10% weight fraction). The drop in tensile strength of JRRJ is due to addition of rubber which is a compliant and elastic material having less tensile strength. However, addition of jute in case of JRJRJ resulting in 10% weight fraction of fiber further reduces the tensile strength but not so drastically as compared to reduction of tensile strength from JRJ to JRRJ. This can be due to absence of sufficient rubber matrix to hold the fibers together. Also, it can be said that the drastic reduction of tensile strength from JRJ to JRRJ is due to reduction in weight fraction of fiber and this trend of drastic reduction in tensile strength is avoided from JRRJ to JRJRJ due to addition of jute fiber. Though increasing the fiber weight fraction from 7% to 10% does not enhance the tensile strength of composite, it helps in eliminating the drastic reduction in tensile strength of composite and is an evidence of effect fiber

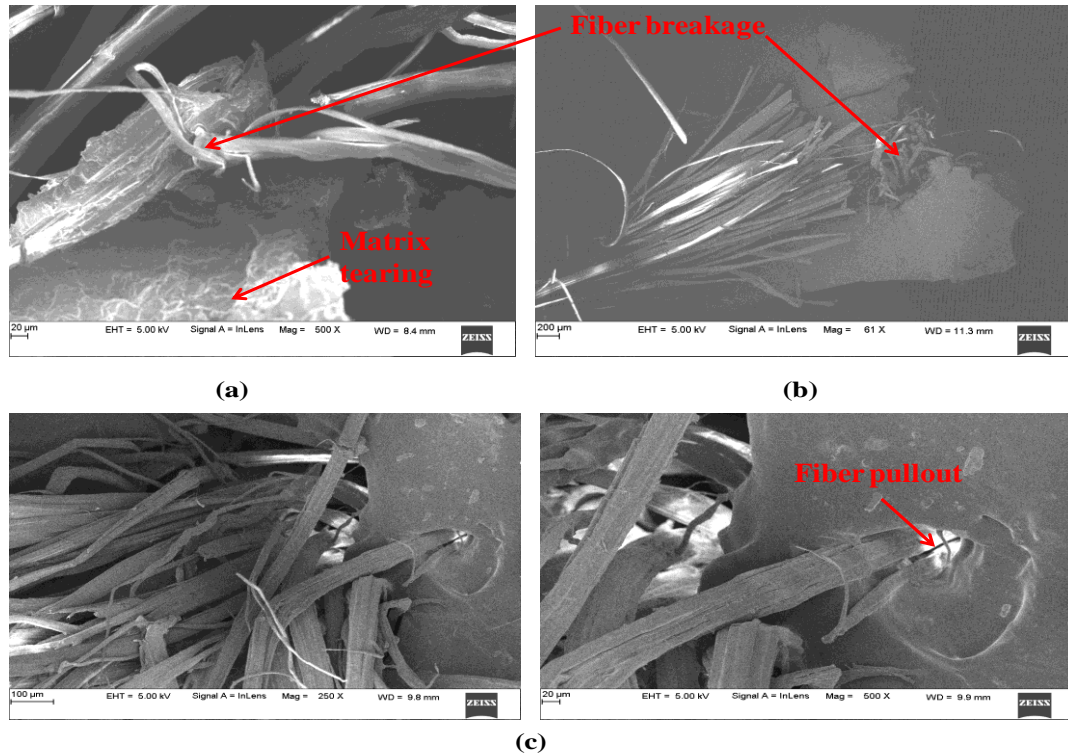
on the tensile strength of composite. There is no much variation in the modulus of all the three configurations considered with JRJRJ giving higher ultimate strain followed by JRRJ and JRJ and JRJ being lighter in weight followed by JRJRJ and JRRJ. The tensile strength of JRJ, JRRJ and JRJRJ are enhanced by 40, 25.36 and 24.32 times and modulus is enhanced by 68.1, 66.82 and 62.53 times compared to natural rubber sheet. Comparing the tensile strength of JRJ, JRRJ and JRJRJ, it is found that the tensile strength of JRJ is highest followed by JRRJ and JRJRJ. The tensile strength of JRJ is 57.7% and 64.47% higher compared to JRRJ and JRJRJ respectively.



**Figure 4.13** Stress v/s strain plots of proposed flexible composites

The fractography analysis of the samples subjected to tensile test is presented in Figure 4.14. The SEM images show the failure of the composite due to fiber fracture, fiber pull out, tearing of matrix and voids at the fracture surface of the composites. Unlike the conventional stiff composites, where matrix cracking is most commonly found, the present flexible composites are free from failure due to matrix cracking. Instead, matrix tearing phenomenon is observed in the flexible composites. Matrix deformation can be observed and inhibition of propagating fracture path by reinforced fibers is found. It is concluded from the SEM images that, the fiber extrusion took

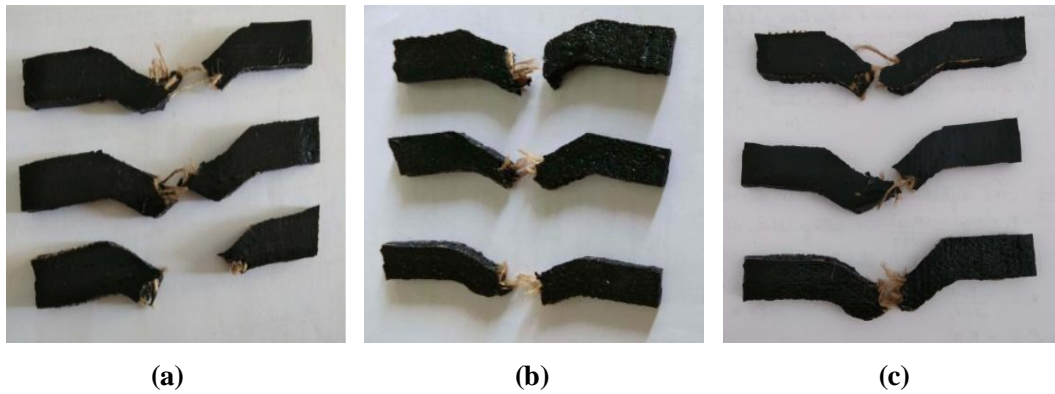
place due to fiber pull out which resulted in matrix tearing, fiber breakage and creation of voids.



**Figure 4.14** Fractography of (a) jute/rubber/jute (b) jute/rubber/rubber/jute and (c) jute/rubber/jute/rubber/jute after tensile test

#### 4.3.3.4 Results of tear test

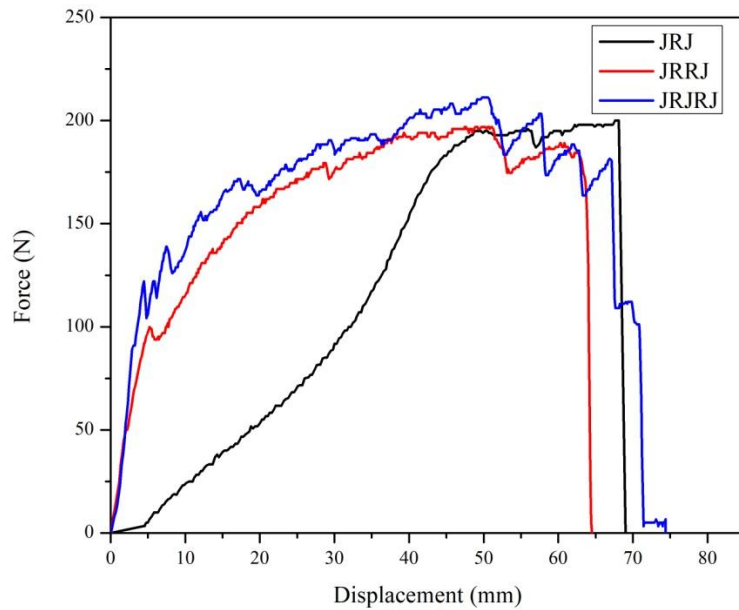
Three specimens in each configuration is tested for tear strength and since the variation tear strength of all three specimens in each configuration is with 20%, according to ASTM standard, the average of three specimens are taken as tear strength of the composite. The most expected type of failure in flexible composite involving elastomer is tearing at the area of higher stress concentration. Specimens are tested for tear strength using the same UTM used for tensile test with cross head speed of 500 mm/min. The results obtained are tabulated in Table 4.9 and the fractured specimens are shown in Figure 4.15.



**Figure 4.15** Fractured specimens of (a) jute/rubber/jute (b) jute/rubber/rubber/jute and (c) jute/rubber/jute/rubber/jute after tear test

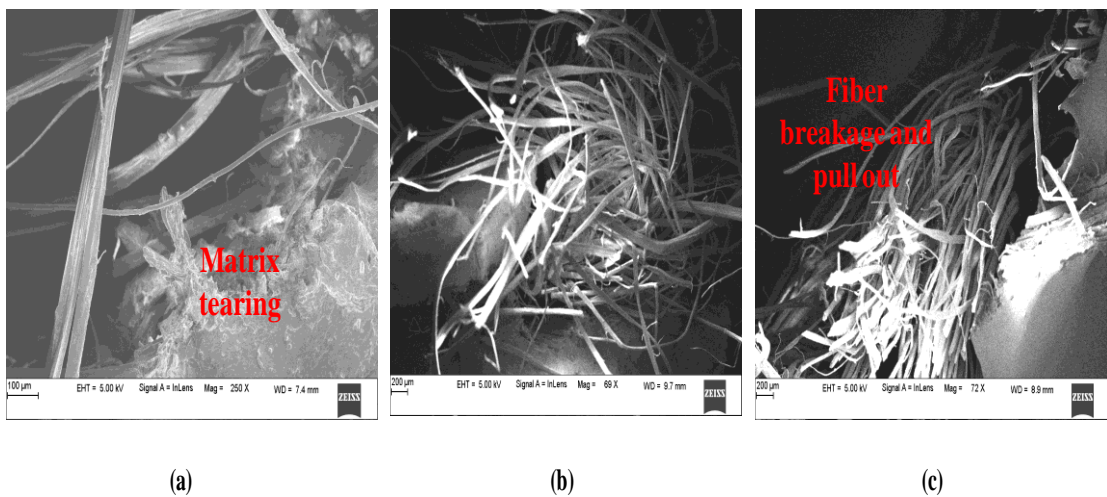
It was found that the tearing of rubber and fiber pull out contributes to the failure of the specimen in all the three stacking sequences considered in the present study. It is found that there is no much variation of tear strength of all the stacking sequences of the composites considered and is evident that fiber weight fraction has negligible effect on the tear strength of the composite. Since the proposed composites are flexible composite which are elastomer dominated, tear strength being the dominant property of elastomeric materials could be the reason behind this behaviour. However, the addition of fiber enhances the tear strength of composite which is conclusive looking into the tear strength of the natural rubber sheet provided in Table 3.2.

Figure 4.16 shows the graph of force against position obtained during tear test of JRJ, JRRJ and JRJRJ. It can be seen that JRJ has highest tear strength followed by JRRJ and JRJRJ. The tear strength of JRJ is 0.41% and 2.38 % more than that of JRRJ and JRJRJ. The force required to cause tearing damage in JRJ is more compared to other two configurations.



**Figure 4.16** Force v/s displacement plots of proposed flexible composites

The fractography analysis of samples subjected to tear test is presented in Figure 4.17. It is evident that matrix tearing followed by fiber pullout and breakage are the predominant failure mechanisms observed.



**Figure 4.17** Fractography of (a) jute/rubber/jute (b) jute/rubber/rubber/jute and (c) jute/rubber/jute/rubber/jute after tear test

#### 4.3.3.5 Results of interlaminar shear strength

In order to facilitate the comparison of ILSS of the proposed flexible composites, the loads on the specimen are converted to ILSS using Eq. 30 and the normalized deformation by displacement/ thickness was adopted to represent the deformation of each type of sample (Wang et al. 2016c). Figure 4.18 shows the load v/s displacement graphs and the normalized ILSS graph for three different stacking sequences of flexible composites. The normalization values goes beyond 1 due to the fact that the flexible composites deform almost twice their thickness owing to its flexibility.

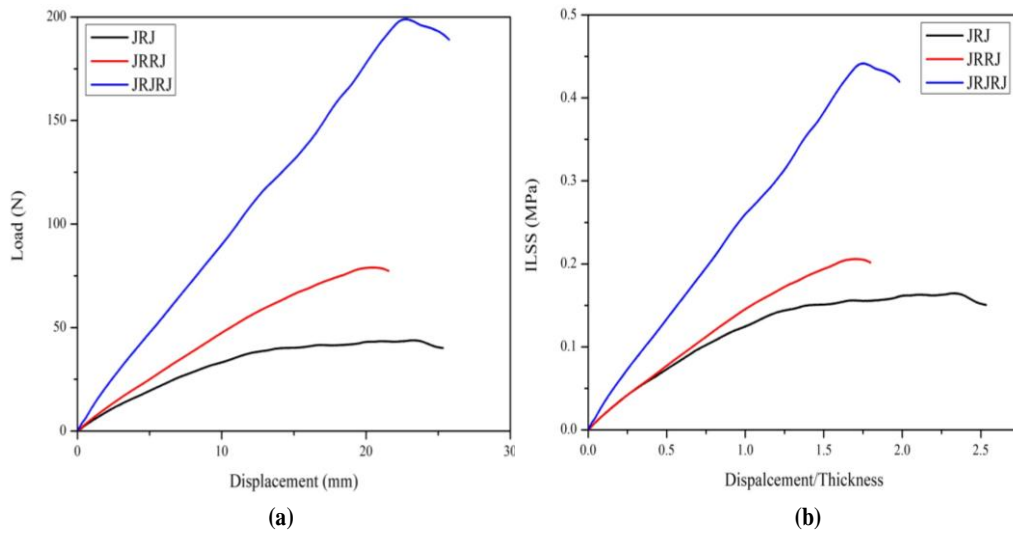


**Figure 4.18** (a) Load-displacement graphs and (b) normalized interlaminar shear strength graph for flexible composites

Table 4.10 provides the average results obtained from the ILSS testing of proposed flexible composites.



**Table 4.10** Average experimental interlaminar shear strength values of flexible composites

<b>Stacking Sequence</b>	<b>Flexural Load (N)</b>	<b>Short Beam Strength: ILSS (Mpa)</b>	<b>Failure Mode</b>
JRJ	43.89	0.16	Interlaminar
JRRJ	79.04	0.21	Delamination
JRJRJ	199	0.44	

Short beam strength (SBS) test is used to measure the ILSS of proposed flexible composites. It is not necessary that in SBS the specimen will fail by pure shear (Abali et al. 2003; Daniels et al. 1971; Rosselli and Santare 1997). Figure 4.19 shows the calculated ILSS for the proposed flexible composites variants (JRJ, JRRJ and JRJRJ) considered in the present study. Comparing the load carrying capability, it can be seen that the flexible composite variants have a load carrying capacity in the order JRJRJ > JRRJ > JRJ. This is due to the fact that in case of JRJRJ there are three layers of reinforcement used as opposed to JRJ and JRRJ which enables it to withstand more load compared to JRJ and JRRJ. Also, considering the void percentage in the composites, it can be said that there is no much variation in the void percentage and the combination of void content, fiber weight percentage along with thickness determine the load carrying capability of the composites.

In case of flexible composites, unlike stiff composites the presence of voids does not lead to matrix cracking and thus void content is not that significant in determining the strength of the flexible composites. The load carrying capacity of JRRJ compared to JRJ is better due to the interleaving of two layers of natural rubber sheet as compared to one in case of JRJ. It is observed that the ILSS of the proposed flexible composites ranges from 0.16 Mpa to 0.44 Mpa. The maximum ILSS of composite is obtained for stacking sequence of JRJRJ with increase in 2.75 and 2.09 times compared to JRJ and

JRRJ. This result indicates that ILSS of flexible composites depends mainly on thickness apart from fiber and void content. The plots of load v/s displacement for all the three flexible composites make it clear that the flexible composites are subjected to ‘homogeneous shear’(Daniels et al. 1971).

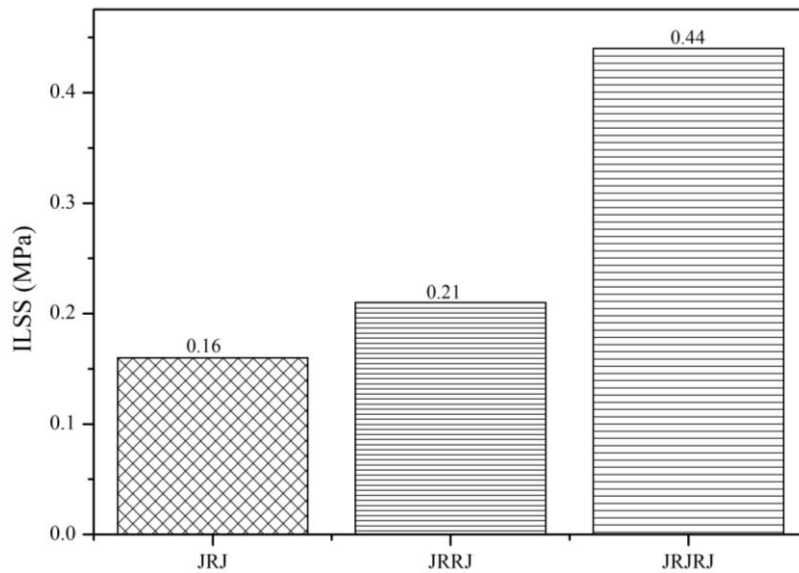


**Figure 4.19** Variation of interlaminar shear strength for flexible composites

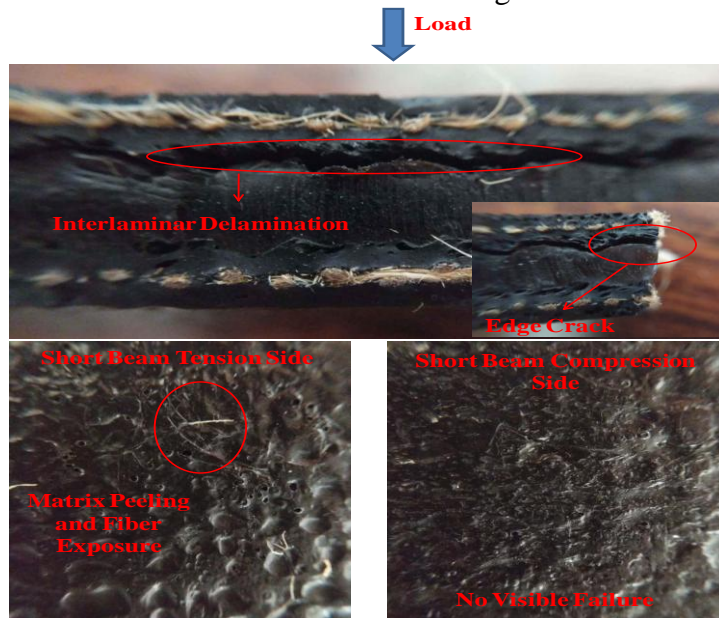


**Figure 4.20** Short beam failure pattern of jute/rubber/jute

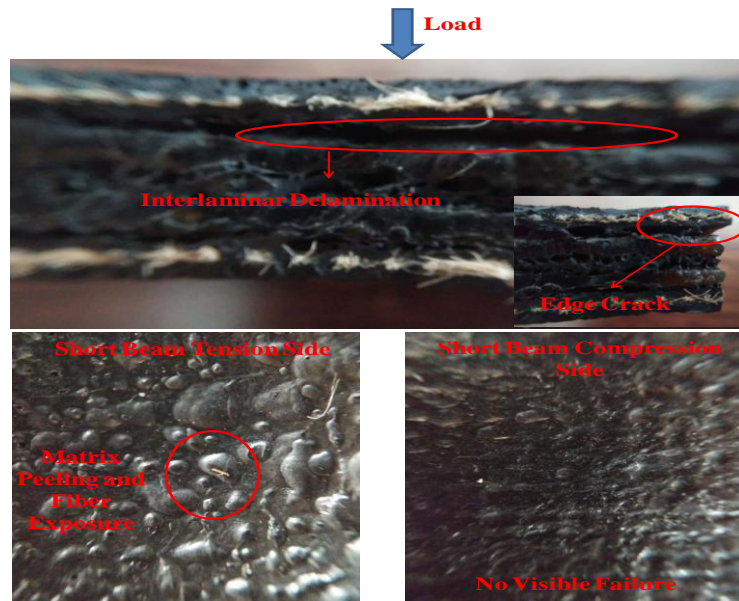


**Figure 4.21** Short beam failure pattern of jute/rubber/rubber/jute

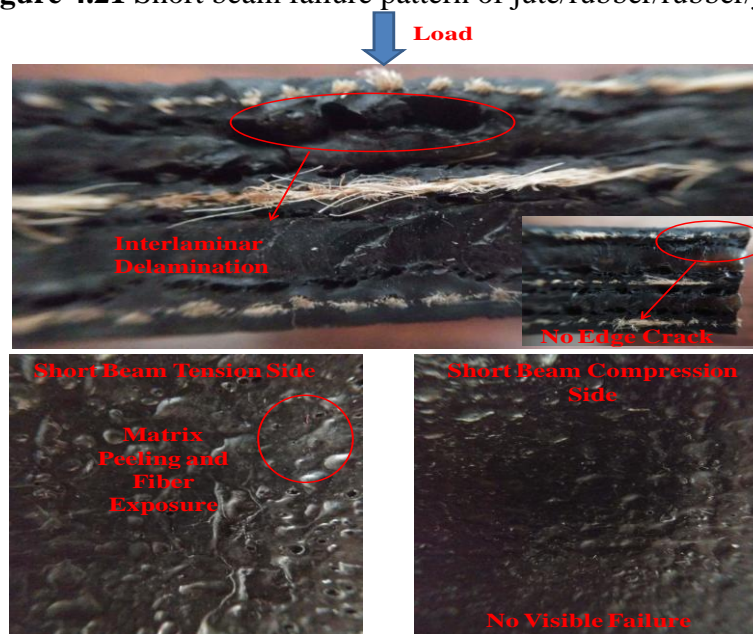


**Figure 4.22** Short beam failure pattern of jute/rubber/jute/rubber/jute

The nature/ pattern of damage and the areas of damage for each variant of flexible composites are shown in Figure 4.20, Figure 4.21 and Figure 4.22 for JRJ, JRRJ and JRJRJ respectively. It was found that the tension side of short beam sample undergoes

outward lateral deformation with matrix peeling leading to minimal fiber exposure. However, for the compression side of short beam samples, no visible macro damage was observed on the surface of the structure. In flexible composite with JRJ and JRJRJ stacking sequences separation of the layers leading to delamination can be observed due to shear loading and since the neutral axis passes along the natural rubber sheet in case of JRJ and along jute layer in JRJRJ, there is no shear failure observed along the neutral axis for both the stacking sequences. However, in case of the flexible composite with stacking sequence JRRJ along with the separation of the layers failure at neutral axis is also found. Also it is found that the crack at the edges is found only in JRJ and JRRJ stacking sequences and no edge cracking is found in JRJRJ. This may be possibly due to the thickness of the stacking sequence and insertion of second jute layer in between, which helps in resisting the shear by taking more load and thereby avoiding edge cracking. It can be seen from the figure that there is no complete separation of the samples into two pieces and they exhibit resistance to shear loading due to flexible nature of the composites and due to better and stronger interlaminar bonding produced during curing. The void content, position and size of voids in the composites affects the interlaminar and flexural properties of the composites. In the proposed flexible composites, the voids were concentrated near the interfaces between the laminates resulting in failure of load transfer across the thickness of the composite and hence resulted in delamination of the composites at weaker interlaminar interfaces.

The fractography analysis of flexible composites subjected to short beam shear test is shown in Figure 4.23. It is clear from the SEM analysis that shear forces lead to interlaminar delamination between the laminates. It was also found that the bonding between jute fibers and the rubber based resin is very strong as most of the fibers are impregnated into rubber surface without being separated from one another, although very little amount of fiber pullout is evident. The reason behind this better adherence

could be diffusion of rubber based resin to jute surface and interleaved rubber sheets, creating mechanical locks.

No evidence of matrix cracking as found in conventional stiff composites is found in the proposed flexible composites; instead the delamination occurs due to debonding of the layers at the interlaminar region. This is the different mechanism observed in flexible composites where a delamination happens without matrix cracking or fiber breakage and possibly due to transfer to shear load to the interlaminar region.

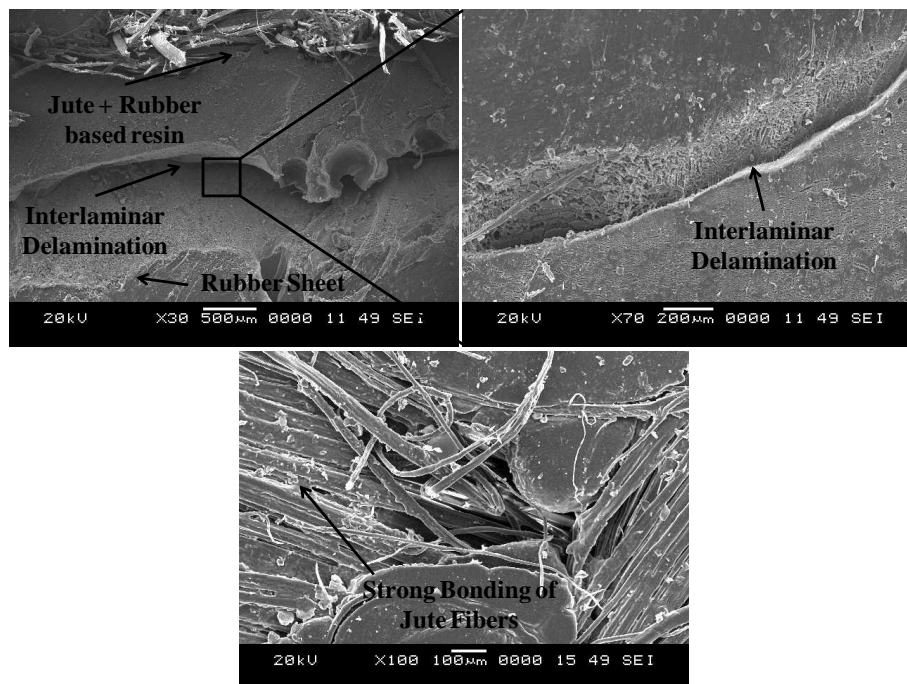


**Figure 4.23** Fractography analysis of flexible composite

#### 4.3.4 Results of erosion and abrasive study

The experimentation is carried out according to Taguchi's L9 orthogonal design. Weight loss, SN ratio and mean are tabulated in Table 4.11. Since lower weight loss of the composite is desired, S/N ratios are calculated for minimum weight loss with "smaller is better" criteria as logarithmic transformation of the loss function. The

present study makes use of commercially available statistical tool MINITAB 17 for the computational purpose. The response ‘Weight loss’ of the composite was analysed and the effect of the factors on the response were studied. The responses for SN ratios are tabulated in Table 4.12.

**Table 4.11** Response, signal to noise ratio and mean for various combinations of control factors for different stacking sequence for slurry erosion study

<b>Stacking sequence</b>	<b>Rotation speed (rpm)</b>	<b>Sand concentration (g/L)</b>	<b>Weight loss (gms)</b>	<b>SN ratio (dB)</b>	<b>Mean</b>
JRJ	500	50	0.091	20.74	0.088
JRJ	1000	75	0.179	15.30	0.173
JRJ	1500	100	0.221	12.83	0.229
JRRJ	500	75	0.166	15.31	0.174
JRRJ	1000	100	0.224	12.91	0.221
JRRJ	1500	50	0.118	18.92	0.112
JRJRJ	500	100	0.247	12.50	0.241
JRJRJ	1000	50	0.114	18.58	0.122
JRJRJ	1500	75	0.220	13.07	0.217

**Table 4.12** Response table for signal to noise ratio of all three stacking sequences for slurry erosion study

<b>Level</b>	<b>Stacking sequence</b>	<b>Rotation Speed (rpm)</b>	<b>Sand Concentration (g/L)</b>
1	36.29	36.19	39.41
2	35.72	35.60	34.56
3	34.72	34.94	32.75
Delta	1.57	1.25	6.66
Rank	2	3	1

Analysing the results in Table 4.12, it can be concluded that the influence of sand concentration on weight loss is more followed by stacking sequence and rotation speed.

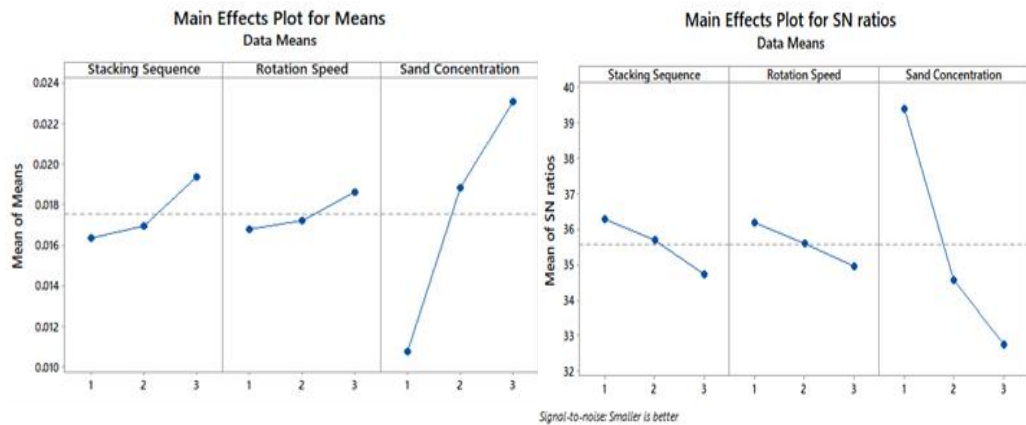


**Figure 4.24** Main effect plot for means and signal to noise ratio for slurry erosion study

The main effect plots for means and SN ratio are shown in Figure 4.24. Analysing the main effect plots for means, it can be concluded that with increase in the number of plies, rotation speed and sand concentration, the weight loss of the composite increases, but increase in weight loss is more drastic when sand concentration is increased compared to rotation speed and number of plies. Thus sand concentration is the most significant factor affecting weight loss. The main effect plot for SN ratio supports this argument. Analysing the SN ratio plot, it can be concluded that stacking sequence, rotation speed and sand concentration of level 1 is preferred since they have highest value of SN ratio. Interpreting the interaction plot for weight loss as shown in Figure 4.25, it can be said since there are no parallel lines; there exists an interaction among all the factors considered on the weight loss of the composite. Hence it can be concluded that stacking sequence, rotation speed and sand concentration affects the erosion of composite with sand concentration being the more significant factor.

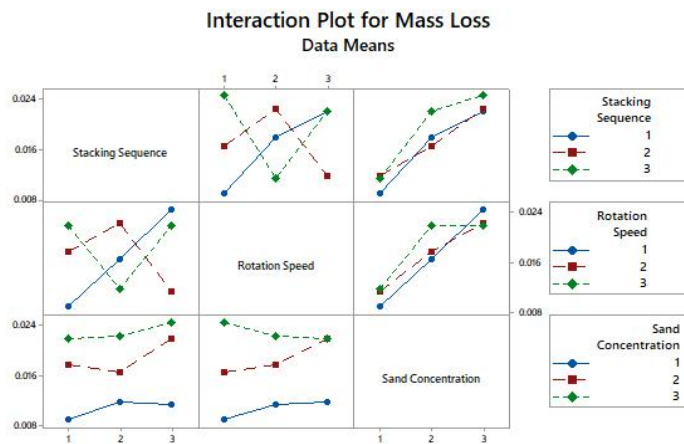


**Figure 4.25** Interaction effect plot for weight loss during slurry erosion study

The statistical way of finding the significant factors can be accomplished by ANOVA as it indicates to what extent the process parameter influences the response and significance level of the factor considered. The ANOVA values for weight loss are presented in Table 4.13.

**Table 4.13** Analysis of variance for weight loss during slurry erosion study

Source	DF	SS	MS	F value	P Value	Percentage Contribution
Stacking sequence	2	0.000015	0.000008	4.45	0.185	5.81
Rotation Speed	2	0.000006	0.000003	1.61	0.384	2.32
Sand Concentration	2	0.000234	0.000117	68.33	0.014	90.69
Error	2	0.000003	0.000002			1.16
Total	8	0.000258				100

S= 0.0013094, R-sq = 98.67 %, R-sq (adj) = 94.69 %



It can be concluded from the ANOVA that among the control factors, ‘sand concentration’ has highest F value followed by ‘stacking sequence’ and ‘rotation speed’. Also the percentage contribution is highest for sand concentration which indicates that sand concentration has significant effect on the weight loss of composite due to erosion. The R-sq value indicates the coefficient of determination of the respective equation. The R-sq values is more than 95% which indicates that the model developed gives good results and helps to predict the weight loss values within experimental conditions. Regression models are developed for the output responses and the regression equation developed is shown in Eq. 66.

$$\text{Weight Loss} = 0.00042 + 0.0015 \text{ Stacking sequence} + 0.000917 \text{ Rotation speed} + 0.00615 \text{ Sand concentration} \quad (66)$$

The coefficient associated with the control factors indicates that increase in stacking sequence, rotation speed and sand concentration results in increase of weight loss. Further, sand concentration has highest coefficient indicating the influence of sand concentration on weight loss is significant compared to other two factors.

In order to validate the model developed, the experimental results are compared with the predicted results as shown in Table 4.14. It was found that the error percentage is within 15% indicating that the developed models are adequate and feasible to predict the weight loss due to slurry erosion within the range of experimental conditions. Figure 4.26 shows the comparison of experimental and predicted weight loss.

**Table 4.14** Comparison on experimental and calculated weight loss for slurry erosion study

<b>Stacking sequence</b>	<b>Rotation speed (rpm)</b>	<b>Sand concentration (g/L)</b>	<b>Experimental Weight loss (gms)</b>	<b>Predicted Weight loss (gms)</b>	<b>Percentage Error</b>
JRJ	500	50	0.009	0.009	2.20

Stacking sequence	Rotation speed (rpm)	Sand concentration (g/L)	Experimental Weight loss (gms)	Predicted Weight loss (gms)	Percentage Error
JRJ	1000	75	0.017	0.016	10.61
JRJ	1500	100	0.022	0.023	-4.52
JRRJ	500	75	0.016	0.016	0.00
JRRJ	1000	100	0.022	0.023	-5.80
JRRJ	1500	50	0.011	0.012	-4.24
JRJRJ	500	100	0.024	0.024	2.02
JRJRJ	1000	50	0.011	0.012	-13.16
JRJRJ	1500	75	0.022	0.019	9.55

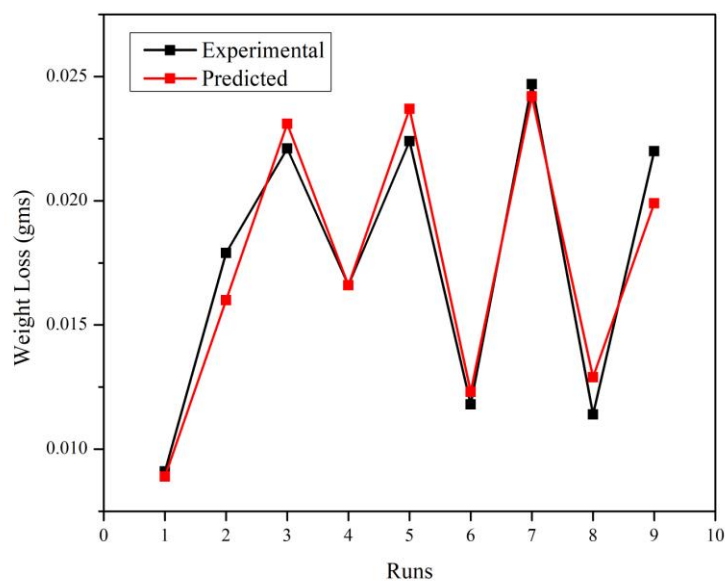


**Figure 4.26** Comparison of experimental and calculated weight loss for slurry erosion study

In order to determine the factor influencing two body abrasive behaviour of the proposed flexible composite, the experimentation plan is charted according to Taguchi's L9 orthogonal array. The specific wear rate is chosen to be the response of

each trial. Since the wear rate has to be minimized, the SN ratio is calculated using “smaller the better” criteria. Table 4.15 provides the responses and the SN ratio for all the trials considered and Table 4.16 provides the responses for SN ratio.

**Table 4.15** Response and signal to noise ratio for the trials during two body abrasion study

<b>Composite configuration: A</b>	<b>Abrading distance in m: B</b>	<b>Load in N: C</b>	<b>Specific wear rate x <math>10^{-7}</math> in <math>m^3/Nm</math>: D</b>	<b>SN ratio</b>
JRJ	0.4	9.81	0.56	4.92
JRJ	0.8	12.26	0.42	8.10
JRJ	1.2	14.71	0.29	10.28
JRRJ	0.4	12.26	0.56	4.57
JRRJ	0.8	14.71	0.44	7.02
JRRJ	1.2	9.81	0.29	11.32
JRJRJ	0.4	14.71	0.82	2.29
JRJRJ	0.8	9.81	0.43	6.86
JRJRJ	1.2	12.23	0.32	9.78

**Table 4.16** Response table for signal to noise ratio for two body abrasion study

<b>Level</b>	<b>Composite configuration: A</b>	<b>Abrading distance: B</b>	<b>Load: C</b>
1	7.77	3.93	7.70
2	7.64	7.33	7.48
3	6.31	10.46	6.53
Delta	1.45	6.53	1.17
Rank	2	1	3

It is conclusive from the responses of SN ratio that, abrading distance influences the specific wear rate followed by composite configuration and load. Figure 4.27 shows

the main effect plots for means and SN ratio and Figure 4.28 shows the interaction plots among the factors considered.

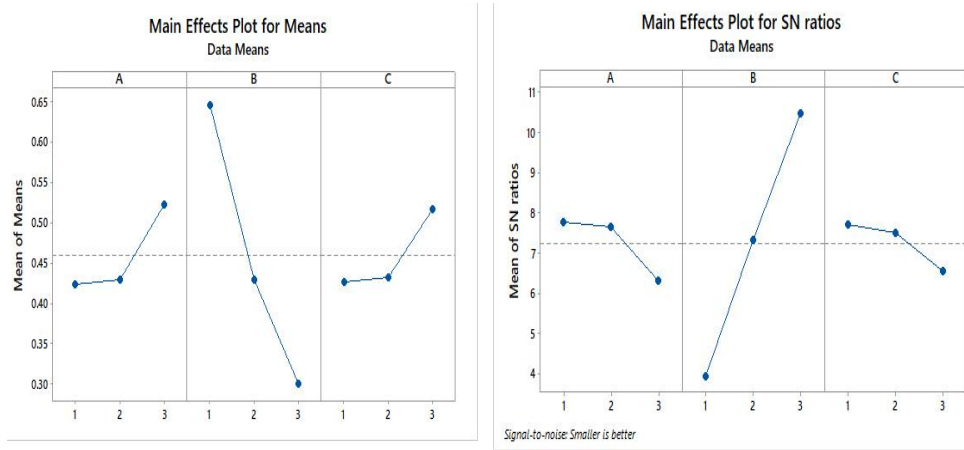


**Figure 4.27** Main effect plots for means and signal to noise ratios (Two body wear)

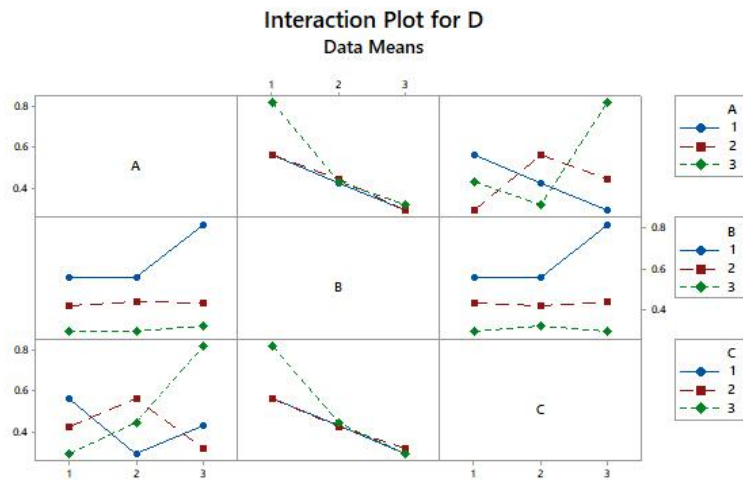


**Figure 4.28** Interaction plots for means and signal to noise ratios for two body abrasion study

From, the main effect plots, it can be said that as the factor A (Composite configuration) with level 1 (JRJ) yields lower wear rate, followed by level 2 (JRRJ) and level 3 (JRJRJ). At the same time, the wear rate is found to be minimum at level 3

(1.2 m) of factor B (Abrading distance) and level 1 (9.81 N) of factor C (Load). This is attributed to the fact that at an abrading distance of 1.2 m, rubber is exposed to abrasive medium and rubber being high wear resistant material results in lower weight loss and thus lower specific wear rate. For better resistance of wear, the composite with stacking sequence JRJ configuration has to be selected with the highest sliding distance (1.2 m) and minimal load (9.81 N). From the interaction plot, it is evident that there exists an interaction between the factors since the lines are not parallel to each other. ANOVA is used to statistically determine the significant factors as it indicates to what extent the process parameter influences the response. Table 4.17 shows the ANOVA for weight loss of the proposed flexible composites under two body abrasion. Higher value of F in the table indicates that the particular factor influences the response to a greater extent.

**Table 4.17** Analysis of variance for weight loss during two body abrasion study

Source	DF	SS	MS	F value	P Value	Percentage Contribution.
A	2	0.015	0.015	3.34	0.127	7.15
B	2	0.180	0.180	40.11	0.001	<b>85.98</b>
C	2	0.012	0.012	2.70	0.161	5.79
Error	6	0.002	0.004			1.06
Total	12	0.209				100

---

S= 0.0670406, R-sq = 90.22 %, R-sq (adj) = 84.36 %

---

Accordingly, the factor B (abrading distance) has the highest F value of 40.11 indicating that the parameter affecting the wear in the composite is sliding distance followed by composite configuration and load. This is also supported by the percentage contribution value with factor B contributing 85.98% for the specific wear rate as compared to factor A and C which contributes only 7.15% and 5.79% respectively. The R-sq values is more than 90% which indicates that the model

developed gives good results and helps to predict the weight loss values within experimental conditions. Regression analysis is carried out for the present model and the regression equation is developed which is provided in Eq. 67.

$$\text{Specific wear rate} = 0.6156 + 0.0500 \text{ Composite configuration} - 0.1733 \text{ Abrading distance} + 0.0450 \text{ Load} \quad (67)$$

In order to validate the regression model developed, the experimental results are compared with the predicted results as shown in Table 4.18. Figure 4.29 provides a comparison of experimental and predicted specific wear rate.

**Table 4.18** Comparison of experimental and predicted values of specific wear rate for two body abrasive study

Composite config.	Abrading distance (m)	Load (N)	Specific Wear rate x 10 <sup>-7</sup> (m <sup>3</sup> /Nm)		Percentage error
			Experiment	Predicted	
JRJ	0.4	9.81	0.56	0.54	4.05
JRJ	0.8	12.26	0.42	0.41	2.61
JRJ	1.2	14.71	0.29	0.28	3.20
JRRJ	0.4	12.26	0.56	0.63	-12.91
JRRJ	0.8	14.71	0.44	0.50	-14.54
JRRJ	1.2	9.81	0.29	0.24	17
JRJRJ	0.4	14.71	0.82	0.73	11.30
JRJRJ	0.8	9.81	0.43	0.46	-7.90
JRJRJ	1.2	12.26	0.32	0.34	-4.90

It is found from the comparison of experimental and predicted wear rate that the error percentage is within 15% which indicates that the developed regression model is acceptable and feasible to predict the wear rate within range of experimental conditions.

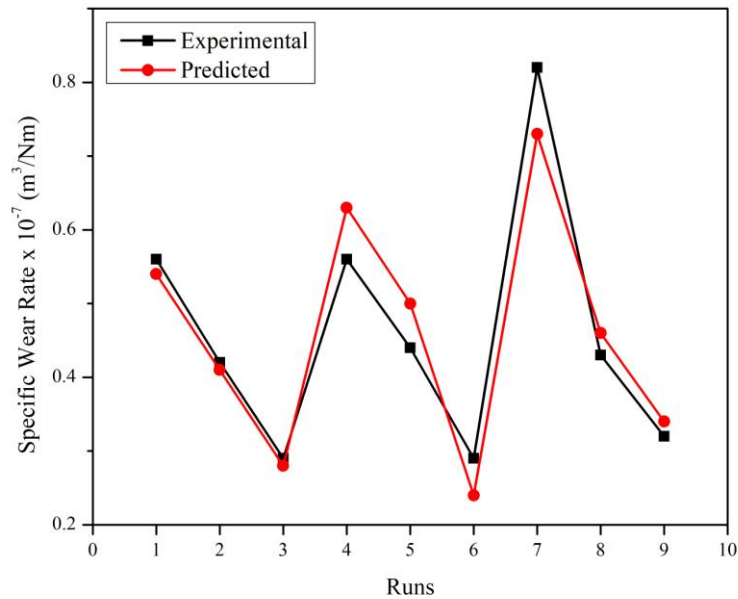


**Figure 4.29** Comparison of experimental and predicted specific wear rate for two body abrasion study

The different wear mechanisms involved in two body abrasive wear are presented in Figure 4.30. From, Figure 4.30 (a), it can be seen that when rubber is exposed to abrasive medium, the composite exhibits a characteristic of wave like pattern. The sharp and pointy emery paper attaches to an asperity of the rubber and stretches it. By applying more force, a crack develops into the material starting from the bottom of the asperity. The wavelike pattern, which can be seen in Figure 4.30 (a), develops because of this mechanism, where the waves represent the stressed asperities. The stretching of the asperities continues with the test until the uppermost part, the “tongue”, ruptures, what ultimately transposes to material loss. With progress in wear of the material, the waviness reduces (Figure 4.30 (b) and Figure 4.30 (c)) as rubber material in the composite is lost and jute starts to expose to the abrasive medium. Once the jute is exposed to abrasive medium, the mechanism of wear changes and the jute surface is abraded through fiber breakage as show in Figure 4.30 (d).

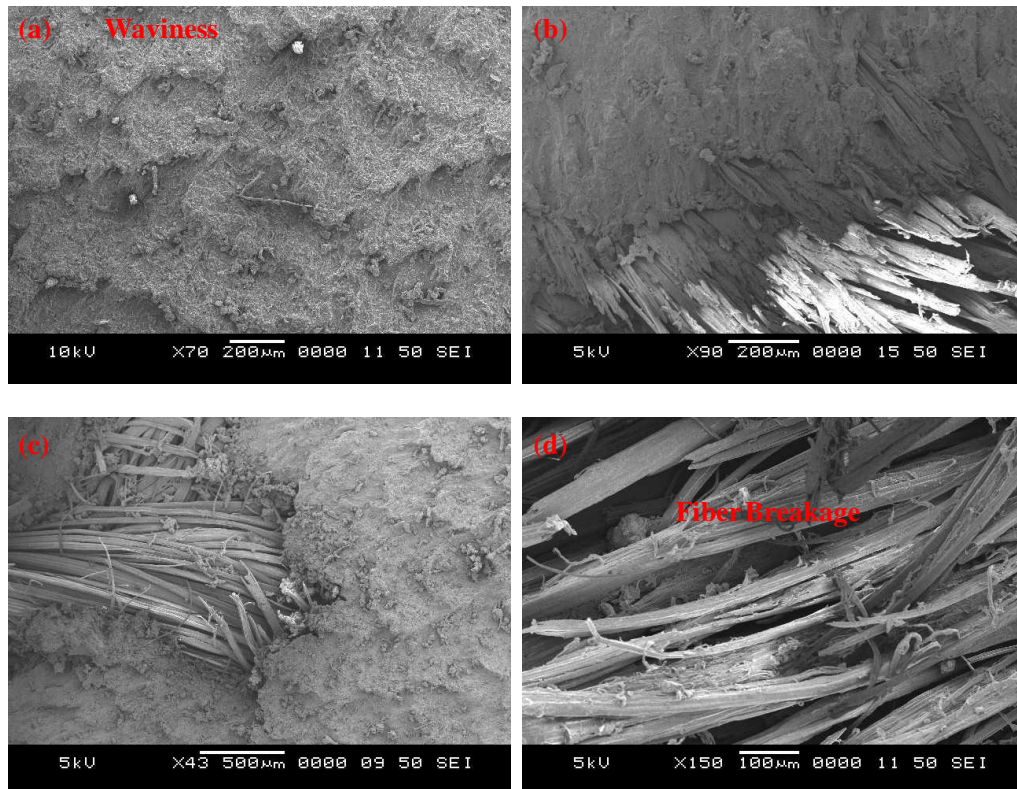


**Figure 4.30** Surface morphology of composite at different stages of wear

#### 4.3.5 Results of impact testing

The proposed flexible composite specimens were subjected to LVI at different impact velocities of 2.42 m/s, 3.7 m/s and 4.64 m/s with corresponding impact energies of 10.24 J, 23.95 J and 37.67 J. The summary of the impact properties obtained are tabulated in Table 4.19.



**Table 4.19** Summary of energy absorption, impact damage initiation and peak force during low velocity impact

Proposed flexible composite configuration	Height of fall (mm)	Energy (J)			Impact Damage Initiation Force (N)	Peak Force (N)	Energy Absorption Ratio ( $E_a/E_i$ ) in %
		Impact	Elastic	Absorbed			
JRJ	300	10.24	4.12	6.12	986.43	1295.66	59.77
	700	23.95	8.58	15.37	2105.46	2598.32	64.18
	1100	37.67	6.95	30.72	3298.75	3873.69	81.55
JRRJ	300	10.24	4.27	5.97	1221.06	1373.4	58.30
	700	23.95	9.44	14.51	2168.65	2762.58	60.58
	1100	37.67	8.91	28.76	3384.87	4039.41	76.35
JRJRJ	300	10.24	4.6	5.64	1282.28	1471.5	55.08
	700	23.95	10.51	13.44	2441.71	2878.38	56.12
	1100	37.67	11.6	26.07	3502.35	4196.5	69.21

#### 4.3.5.1 Energy-time history of flexible composites subjected to low velocity impact

The energy absorbed by the proposed flexible composites at various energy levels are derived from the energy-time history as shown in Figure 4.31 and the variation of energy absorption ratio is shown in Figure 4.32.

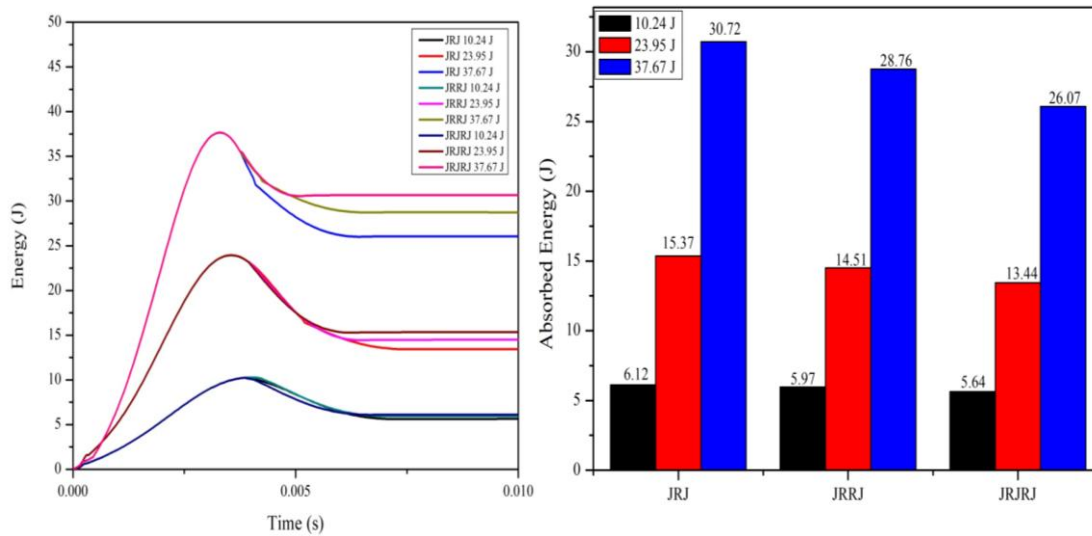


**Figure 4.31** Energy absorbed by proposed flexible composite at various energy levels

An examination of energy-time traces is presented in Figure 4.31 from which the absorbed and elastic energies are derived. During an impact event, out of the total energy of impact, some amount of energy gets dissipated by the specimen in the form of damage formation. This is referred to as the absorbed energy. From the moment of contact ( $t=0s$ ), the impactor delivers its kinetic energy to the specimen, out of which some amount of energy is stored within the specimen in the form of elastic deformation and the remaining is dissipated mainly by development of damage and negligible amount of energy is dissipated through friction, sound, and heat.

Once the impactor completely transfers its kinetic energy to the specimen, the entire kinetic energy of the impactor is converted into elastic strain energy and stored in the specimen. The curve then shows a declining trend during which the stored elastic

energy is returned back to the impactor until separation. The final energy values correspond to the energy absorbed by the specimen (Tan et al. 2010). In case of the stacking sequences, JRJ and JRRJ, the residual kinetic energy increases to 8.58 J and 9.44 J respectively up to impact energy of 23.95 J, later which it starts to decline dramatically in case of JRJ compared to JRRJ. This is due to the reason that JRJ absorbs more energy during an impact event, thereby returning less amount of energy back to the impactor as compared to JRRJ and JRJRJ. Whereas in case of JRJRJ the residual kinetic energy of the impactor continues to increase as the impact energy increases, with the increase being more drastic up to impact energy of 23.95 J and the rate of increase in the residual kinetic energy is less from 23.95 J to 37.67 J compared to the increase from 10.24 J to 23.95 J. In order to compare the proposed composites in terms of energy absorption, the SEA of the composites at different impact energies are calculated and presented in Table 4.20. Analyzing the SEA of the proposed flexible composites, it is found that there is no appreciable variation in energy absorbing capability of the proposed flexible composite in the low velocity impact regime.

**Table 4.20** Specific energy absorption of proposed flexible composites subjected to low velocity impact

<b>Proposed flexible composite configuration</b>	<b>Impact energy (J)</b>	<b>SEA (Jm<sup>3</sup>/Kg)</b>
JRJ	10.24	0.005
	23.95	0.013
	37.67	0.026
JRRJ	10.24	0.005
	23.95	0.013
	37.67	0.026
JRJRJ	10.24	0.005
	23.95	0.012
	37.67	0.024

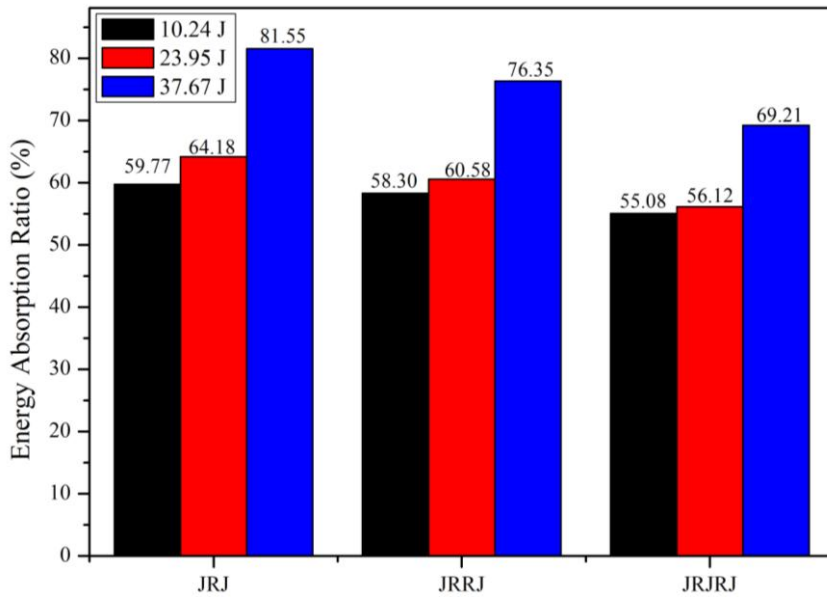


**Figure 4.32** Variation of energy absorption ratio of flexible composites at different impact energies

The variation of the absorption ratio for the different stacking sequences of the flexible composites subjected to impact at different impact energies are presented in Figure 4.32. The ratio of energy absorption increases with increasing impact energy. The energy absorption ratio ranges from 55.08% to 59.77%, 56.12% to 64.18% and 55.08% to 81.55% for impact energies of 10.24J, 23.95J and 37.67J respectively.

It is found that, as the impact energy increases, the absorption ratio increases irrespective of the stacking sequence with JRJ having highest absorption ratio at all the three impact energies considered. This means that maximum of the impact energy is absorbed at higher impact energy with JRJ absorbing more energy compared to JRRJ and JRJRJ. This behavior is due to the extent of damage that JRJ has undergone compared to JRRJ and JRJRJ resulting in more amount of energy being absorbed.

#### 4.3.5.2 Force-time history of flexible composites subjected to low velocity impact

The force-time history for the proposed flexible composites at impact energy of 10.24 J is presented in Figure 4.33. The trends for all proposed flexible composite under different energy levels remains the same with variation in peak load as shown in Figure 4.33.

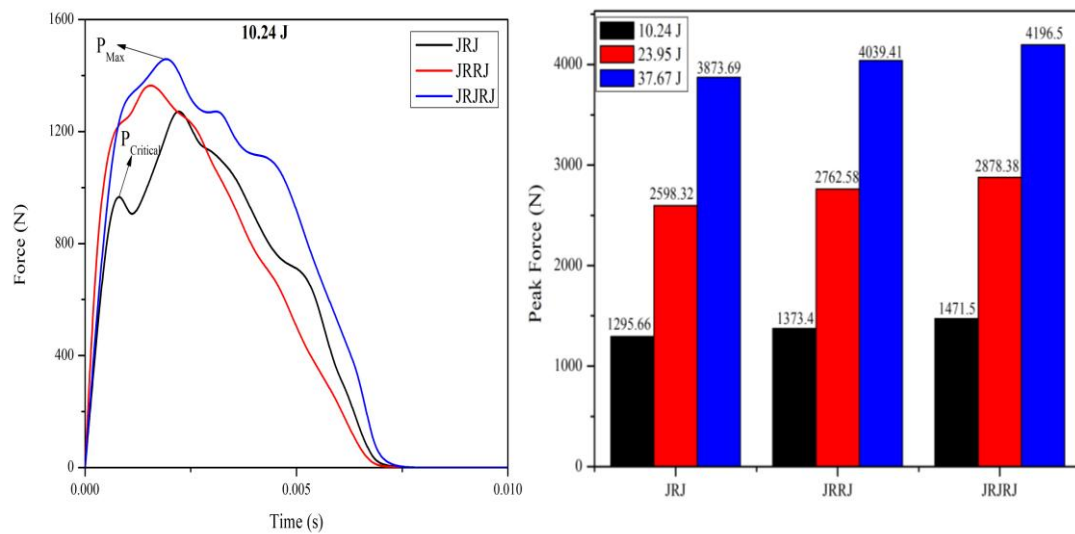


**Figure 4.33** Force-Time history of proposed flexible composites at impact energy of 10.24 J and variation of peak force at different impact energies

The force gradually increases initially and drops down at a particular point which can be due to the first layer failure. The curve again tends to increase up to the peak force and after which it starts to reduce. In the force-time curve, a smoothing process has been carried out to remove the fluctuations. A linear increase in the impact force is found out until a point where a drop in force value is observed. This drop in force value indicates a stiffness change of the composite due to damage initiation and is known as critical force ( $P_{Critical}$ ). Thus, the ability of the composite to resist damage is measured by  $P_{Critical}$  (Caprino et al. 2015).

Beyond the critical force, the impact force behavior can be associated with the development of damage in the composite. It is observed that there is no force perturbation after impact damage initiation force. Instead, the force curve immediately raises up to the peak value. This can be related to the absence of delamination kind of damage within the proposed flexible composite. It is worth noting that delamination, which is a dominant mode of failure in conventional stiff composites (Tan et al. 2010), has been got rid off in the proposed flexible composites. Hence, the proposed flexible composite can be said to have higher delamination resistance. Peak force is an indication of load-bearing capacity of the material. The variation in the peak force of the flexible composites at different impact energies considered in the present study is shown in Figure 4.33.

It can be seen that the peak force of JRJRJ is high at any impact energy considered compared to JRRJ and JRJ indicating JRJRJ has the highest damage resistance compared to the other two stacking sequences. The continuous increase in the peak force of the flexible composites with an increase in impact energy is an indication that the saturation level of the peak force is yet to take place (Kim et al. 2013). Hence, the proposed flexible composites are capable of withstanding higher impact energies. It can be observed that the contact time of the impactor with the specimen is constant at all the three impact energy levels considered in the present study. This trend is in agreement with the finding reported in the literature (Feraboli and Kedward 2006) .

#### 4.3.5.3 Coefficient of restitution (CoR)

During an impact between two bodies, mere solving of linear momentum equation does not help in finding out the velocity of the body after impact which is mainly due to the plastic deformation associated with both the bodies. Hence, Coefficient of restitution (CoR) is introduced, which can be defined as the ratio between relative velocities of the bodies after and before impact. CoR lies between 0 and 1. When CoR=0, it indicates that the nature of impact is completely plastic. If CoR = 1, it is an

indication of a completely elastic impact. In practical applications, the value of CoR lies between 0 and 1 (Aryaei et al. 2010; Chatterjee 1997). Out of the two impacting bodies, if any one of the body is at rest, then CoR can be expressed as shown in Eq. 37. Now, consider the drop weight impact testing of composites for low velocity impact behaviour. When the impactor is made to fall on the composite laminate from height 'h', neglecting the air resistance as suggested in literature (Minamoto and Kawamura 2009; Weir and Tallon 2005; Wong et al. 2009), CoR is calculated using Eq. 37. Usually, during an impact event, there is a loss of energy involved and the energy loss percentage (ELP) is calculated using Eq. 38.

There are no tangential forces between the two impacting bodies in case of normal impact. Thus, friction has no significant role to play in normal impact (Vu-quoc et al. 2001; Vu-Quoc et al. 2016). Whereas, the effect of friction has to be considered in case of oblique impact due to the tangential forces between two impacting bodies. The present study deals with the normal impact loading condition and hence, frictional forces are neglected. The coefficient of restitution depends on many elements, such as the geometry of the bodies in contact, the approach velocity, the material properties, the duration of contact and, possibly, friction (Arya et al. 2016; Gilardi and Sharf 2002). In Newton's model, the coefficient of restitution is defined as the ratio of final to initial velocity. This model is based on a kinematic point of view and only the initial and final values for the relative normal velocity are taken into account. Meaningly, Newton presumed that the coefficient of restitution is a material property.

In this case, the impactor is dropped on to the proposed flexible composite from three different heights (300 mm, 700 mm and 1100 mm) and it impacts the target at an impact velocity  $v_i$ . The energy-time history is obtained from the data acquisition system from which the absorbed energy, elastic energy are found out. The CoR and ELP of the proposed flexible composites at different impact energies are tabulated in Table 4.21.

**Table 4.21** Coefficient of restitution and energy loss percentage of the flexible composites subjected to low velocity impact

<b>Proposed flexible composite configuration</b>	<b>Impact Energy (J)</b>	<b>CoR</b>	<b>ELP</b>
JRJ	10.24	0.63	60.31
	23.95	0.60	64
	37.67	0.43	81.51
JRRJ	10.24	0.65	57.75
	23.95	0.63	60.31
	37.67	0.49	75.99
JRJRJ	10.24	0.67	55.11
	23.95	0.66	56.44
	37.67	0.55	69.75

It is found that the CoR reduces with increase in impact energy. This indicates that, as the impact energy increases, the bouncing back of impactor is minimized as most of the energy is absorbed by the target as a result of damage initiation and propagation.

The CoR for different stacking sequences of the proposed flexible composite at any impact energy considered is in the order JRJRJ > JRRJ > JRJ. This indicates that impactor, when impacted to JRJRJ, bounces back more as the non dissipated energy during the impact event is more compared to JRRJ and JRJ. This result in JRJRJ absorbing less energy and providing more damage resistance compared to JRRJ and JRJ. On the same lines, JRJ limits the bouncing back of impactor to a better extent and thus it has better energy absorbing ability and least damage resistance compared to the other two stacking sequences. This argument is supported by the energy absorbing and peak force results presented in Table 4.19. ELP increases with increased impact energy for any stacking sequence considered in the order JRJ > JRRJ > JRJRJ, indicating that the kinetic energy of the impactor is lost to a larger extent when it is impacted to JRJ compared to JRRJ and JRJRJ as most of the kinetic



energy of the impactor is converted to absorbed energy in case of JRJ. Thus, analysis of ELP indicates that JRJ absorbs more energy compared to JRRJ and JRJRJ.

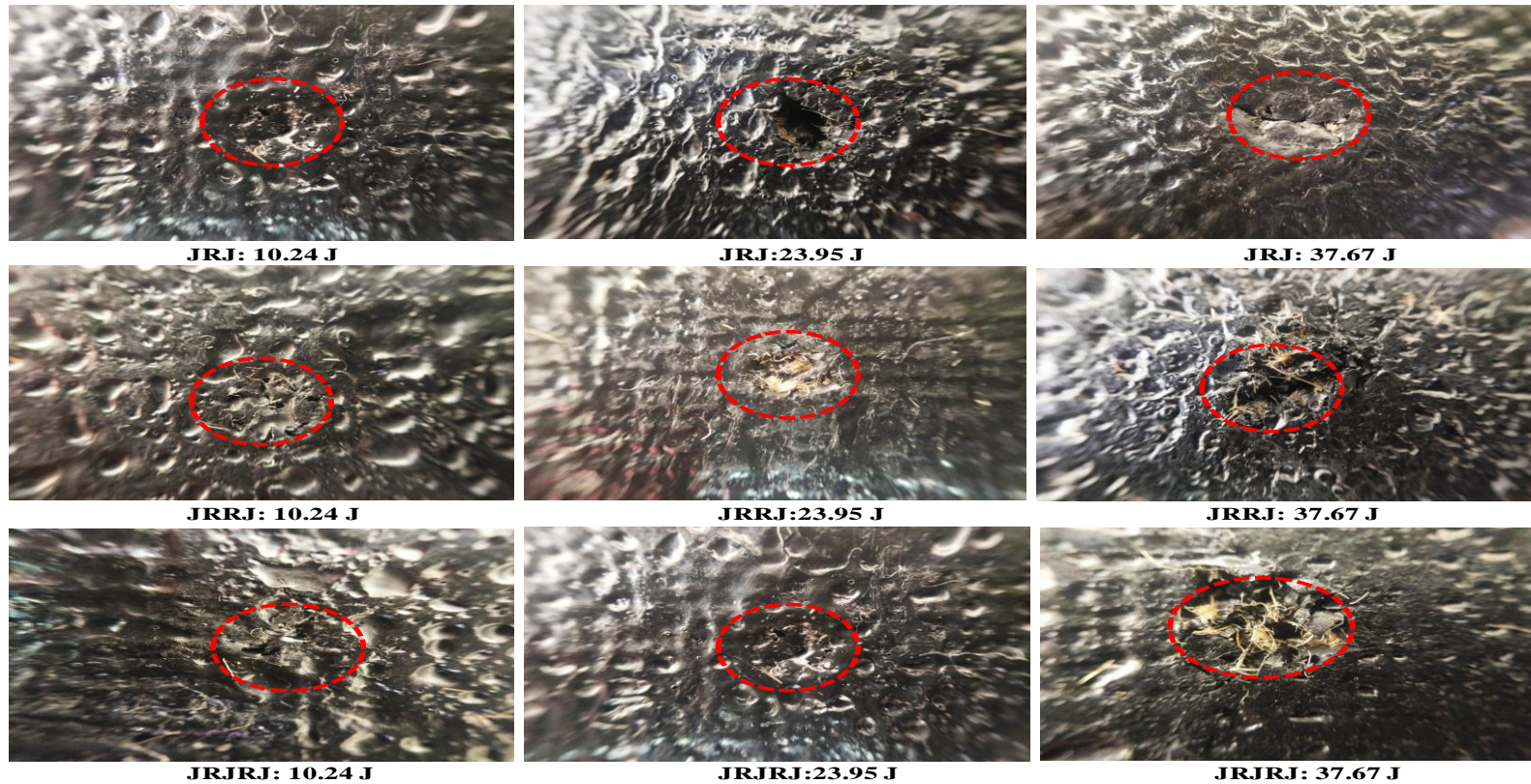
#### 4.3.5.4 Damage analysis and fractography of flexible composites subjected to low velocity impact

Table 4.22 shows the depth of damage of the proposed flexible composite at different energy levels. The depth of damage is determined by inserting a rod into the damage created due to impact up to the undamaged layer and then measuring the length of rod that was inserted into the damaged portion.

**Table 4.22** Depth of damage of the proposed flexible composite

Proposed flexible composites configuration	Height of fall (mm)	Energy (J)			Depth of Damage (mm)
		Impact	Elastic	Absorbed	
JRJ	300	10.24	4.12	6.12	8
	700	23.95	8.58	15.37	9.4
	1100	37.67	6.95	30.72	9.7
JRRJ	300	10.24	4.27	5.97	4.2
	700	23.95	9.44	14.51	5.1
	1100	37.67	8.91	28.76	5.3
JRJRJ	300	10.24	4.6	5.64	4
	700	23.95	10.51	13.44	4.9
	1100	37.67	11.6	26.07	5.2

The enlarged view of damages on the front face of the proposed flexible composite is shown in Figure 4.34. The damage in the proposed flexible composite is dominated by puncture type of damage caused due to the tearing mechanism.



**Figure 4.34** Enlarged View of the damages on the front face of the flexible composites subjected to low velocity impact at different energy levels

JRJ clearly absorbs more energy compared to JRRJ and JRJRJ at the same impact energy level, which is an indication that JRJ exhibits more severe damage than JRRJ and JRJRJ. This is supported by the depth of damage of the proposed flexible composites found out at different impact energy levels. For a low energy level, with impact velocity ranging from 2.42 m/s to 4.64 m/s, the proposed composites show excellent damage resistance as no much significant damage was found in any stacking sequence of the proposed flexible composite at any of the impact energy levels since it was found that the rear face of the proposed flexible composites remained undamaged at all the three impact energies considered. However, among the three stacking sequences considered, JRJRJ is found to have excellent damage resistance compared to JRRJ and JRJ. Most of the stiff composites studied by researchers (Dhakal et al. 2012; Majid et al. 2018; Mathivanan and Jerald 2010; Ude et al. 2013) exhibit a catastrophic failure within the chosen range of impact velocity. But, in the same range of impact velocity, the flexible composites proposed in the present study do not exhibit a catastrophic failure.

The relation of the depth of damage with energy absorption ratio and CoR is analyzed from the Figure 4.35. It can be clearly seen that the depth of damage increases with an increase in impact energy which means that more damage is caused to the flexible composite at higher impact energy. At higher impact energy, the composite absorbs more energy compared to lower impact energies. When all the three stacking sequences are considered, it is evident from the graph that at any impact energy considered in the present study, JRJ has higher energy absorption ratio and larger depth of damage compared to remaining two stacking sequences. This means that JRJ undergoes a larger amount of damage and thereby absorbs more amount of energy returning only a smaller amount of elastic energy back to the impactor.

On the other hand, when CoR is considered, it can be clearly seen that with an increase in the depth of damage, CoR reduces. At any impact energy considered, the CoR of JRJRJ is highest followed by JRRJ and JRJ indicating that when the impactor

impacts JRJRJ, more amount of resistance is provided by this stacking sequence against damage and thereby providing more amount of residual/rebound velocity to the impactor resulting in higher CoR.

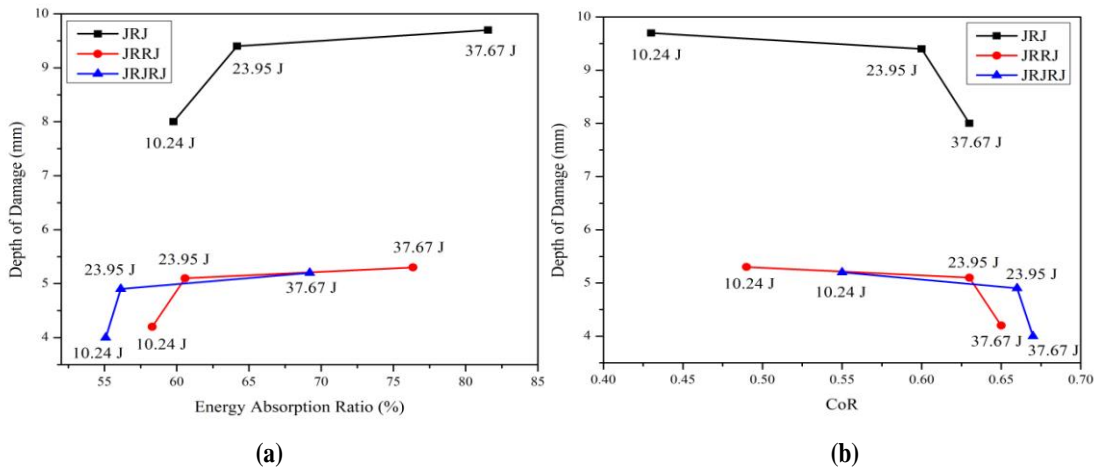


**Figure 4.35** Variation of depth of damage against (a) energy absorption ratio and (b) coefficient of restitution

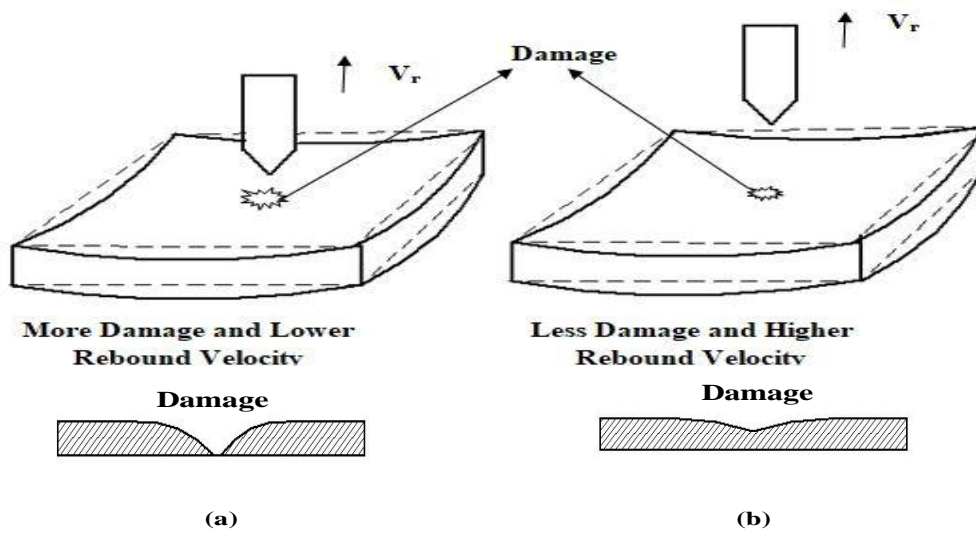


**Figure 4.36** Schematic representing the relation between rebound velocity and extent of damage for (a) jute/rubber/jute and (b) jute/rubber/jute/rubber/jute in case of low velocity impact

The schematic representation of the relation between rebound velocity and extent of damage during an impact event of the flexible composite is shown in Figure 4.36. In case of the flexible composite having higher energy absorption ability (JRJ), the impactor penetrates deeper into the laminate causing more damage. Thus more amount of energy will be absorbed by the laminate resulting in a lesser amount of elastic energy being returned to the impactor due to which the rebound or residual velocity  $V_r$  of the impactor will be less. However, the opposite phenomenon can be observed during an impact event of JRJRJ flexible composite. The penetration of impactor into the JRJRJ laminate is less compared to JRJ leading to the lesser amount of damage and more residual velocity of the impactor. From these mechanisms, it is clear that JRJ undergoes maximum damage thereby absorbing maximum energy whereas, JRJRJ has excellent resistance to damage but leads to bouncing of the impactor.

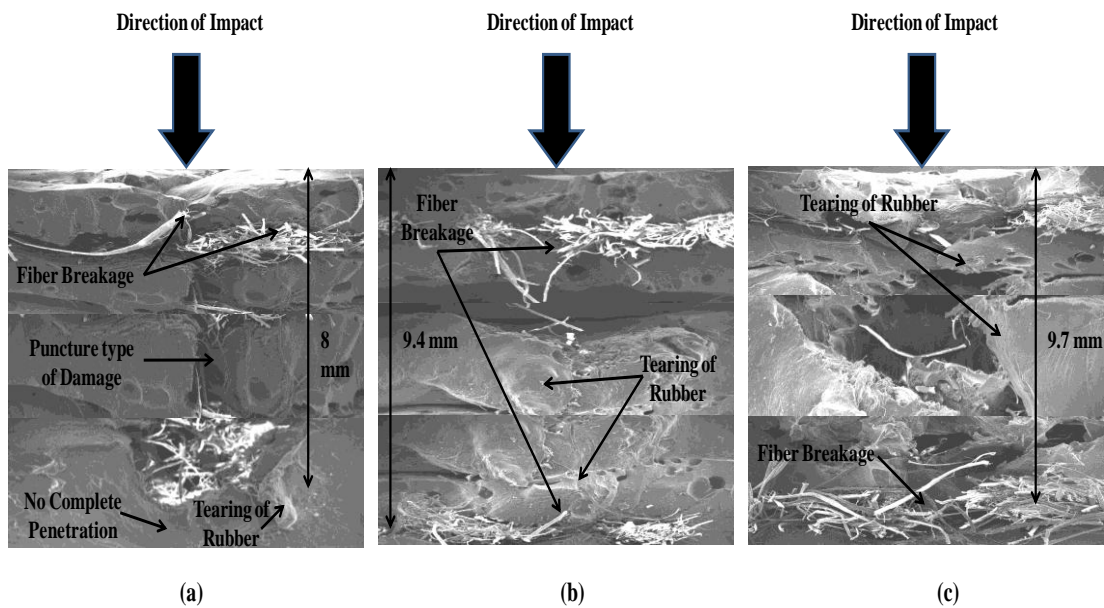


**Figure 4.37** Internal damage mechanism in jute/rubber/jute flexible composite subjected to low velocity impact at (a) 10.24 J (b) 23.95 J and (c) 37.67 J

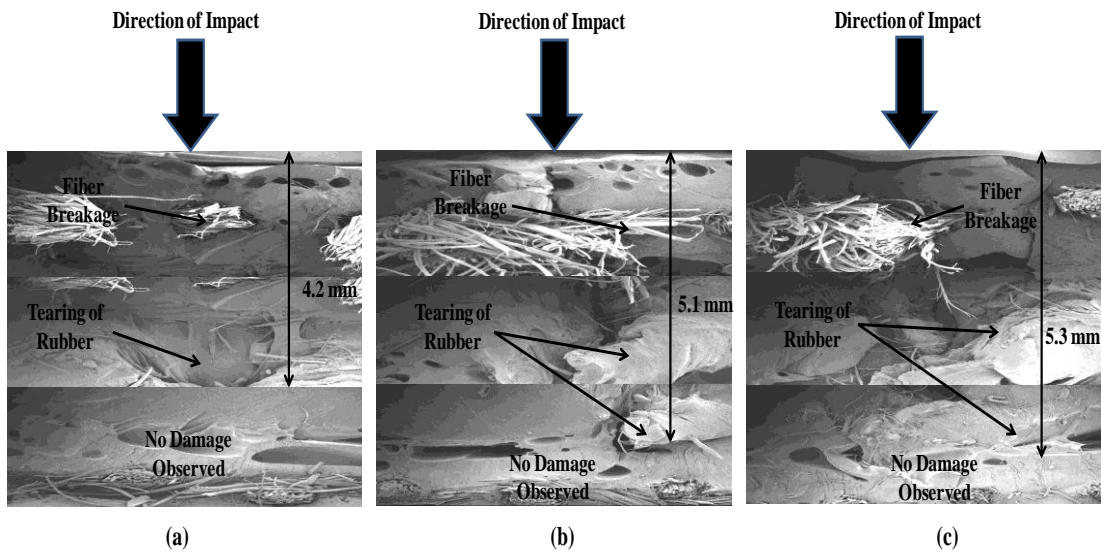


**Figure 4.38** Internal damage mechanism in jute/rubber/rubber/jute flexible composite subjected to low velocity impact at (a) 10.24 J (b) 23.95 J and (c) 37.67 J

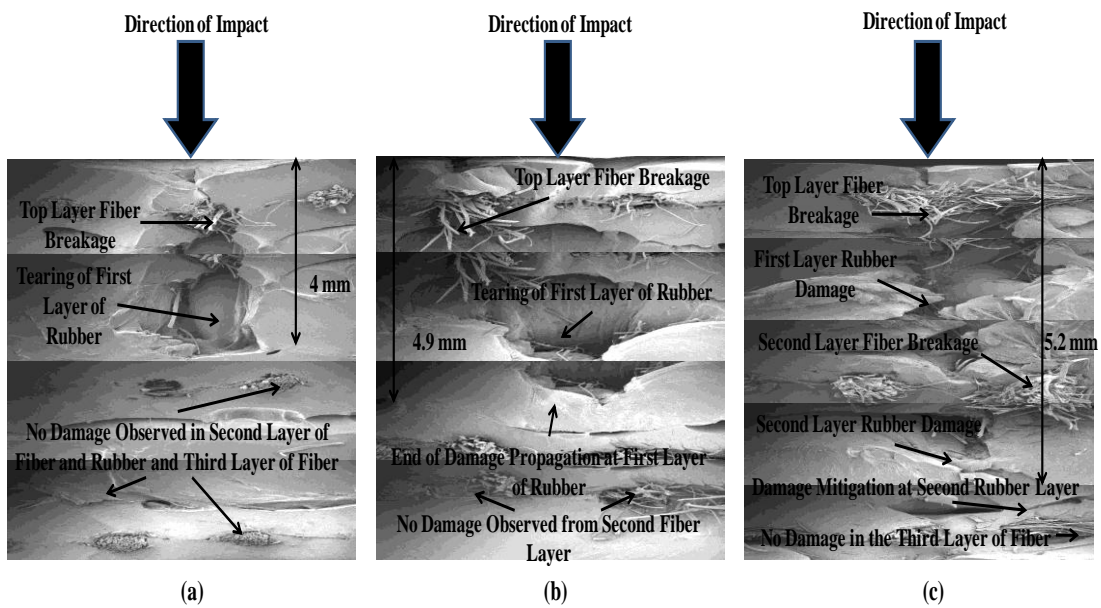


**Figure 4.39** Internal damage mechanism in jute/rubber/jute/rubber/jute flexible composite subjected to low velocity impact composite at (a) 10.24 J (b) 23.95 J and (c) 37.67 J

The damage mechanisms involved during the impact of different stacking sequence of flexible composites at different impact energies are presented in Figure. 4.37 to Figure 4.39. It is found from the SEM analysis of the cut section of the damaged portion of the flexible composites that the major mechanism through which the damages occur are fiber breakage for reinforcement and tearing in case of a matrix. It is also evident that there is no indication of delamination in any of the stacking sequences which was strongly argued while analyzing the force-time histories of the composites. From Figure 4.37, it can be seen that for JRJ stacking sequence, no complete penetration of the impactor happens at impact energy of 10.24 J with the last layer of jute not suffering from fiber breakage and is intact. Whereas, at the remaining two energy levels (23.95 J and 37.67 J), the fiber breakage leads to failure of the last layer of jute and still the no complete penetration of laminate is observed due to the flexible matrix used, though the damage mitigates till the end of the laminate. From Figure 4.38 which represents the stacking sequence JRRJ, it is seen that introduction of an additional layer of rubber compared to JRJ helps in resisting the damage mitigation and no complete penetration is observed at any of the impact energies, though, the damage mechanism remain same. From Figure 4.39 representing JRJRJ stacking sequence, it is found that at an impact energy of 10.24 J, only the top layer of fiber and rubber gets damaged and no evidence of damage mitigating to either next layers of fiber or rubber is found. At impact energy of 23.95 J, the extent of the damage remains the same with the damage being propagated till the end point of the first layer of rubber. At the impact energy of 37.67 J, it was found that the damage propagates till the second layer of rubber beyond which no damage is evident. However, at all the three impact energies, no complete penetration of the impactor is observed.

#### 4.3.5.5 Ballistic limit of the proposed flexible composites

In order to determine the ballistic limit velocities of the proposed flexible composites a minimum of three highest partial penetration velocities and three minimum

complete penetration velocities are used and their average provides the ballistic limit velocity of the particular target and projectile combination (Pandya et al. 2012). This approach followed to determine the ballistic limit velocities experimentally and FE approach is in line with the approach available in literature (Khodadadi et al. 2019b). Analytically, the ballistic limits are calculated using Eq. 23. Thus obtained ballistic limit values are presented in Table 4.23.

**Table 4.23** Ballistic limits of proposed flexible composites determined analytically, through FE approach and experimentally

Flexible Composite Configuration	Ballistic Limit (m/s)		
	Analytical	FE	Experimental
JRJ	65	61	63
JRRJ	86	82	83
JRJRJ	92	85	88

The ballistic limit velocities of the flexible composites with stacking sequences JRJ, JRRJ and JRJRJ found experimentally as 63 m/s, 83 m/s and 88 m/s respectively. It can be seen that the inclusion of an additional layer of rubber (JRJ to JRRJ) enhances the ballistic limit by 32 % and the inclusion of an additional layer of jute (JRRJ to JRJRJ) enhances the ballistic limit by 6 %. This shows that the rubber layer can significantly enhance the ballistic limit of the flexible composite compared to the jute layer.

The same trend is found in the case of the FE approach with ballistic limit velocities of 61 m/s, 82 m/s and 85 m/s for JRJ, JRRJ and JRJRJ respectively. In the case of the analytical approach, the ballistic limits of proposed flexible composites are found to be 65 m/s, 86 m/s and 92 m/s for JRJ, JRRJ and JRJRJ respectively which agrees well with the experimental and FE approach.



#### 4.3.5.6 Residual velocity of the proposed flexible composites at different lower ballistic impact velocities

The residual velocity of the projectile after impacting flexible composites of different stacking sequences (JRJ, JRRJ, and JRJRJ) are obtained from chronograph placed immediately after the target in case of an experimental approach. In case of an analytical approach, Eq. 22 is made use of to determine the residual velocities. The residual velocities obtained for different stacking sequences at different impact velocities in all three approaches are tabulated in Table 4.24.

**Table 4.24** Residual velocities of the proposed flexible composites at different lower ballistic impact velocities

Flexible Composite Configuration	Impact Velocity (m/s)	Residual Velocity (m/s)		
		Analytical	FE	Experimental
JRJ	80	45.27	38	42
	100	69.28	63	71
	120	89.09	82	92
JRRJ	80	6.32	0	0
	100	44.15	40	48
	120	66.27	65	69
JRJRJ	80	4.47	0	0
	100	33.45	32	35
	120	53.52	59	62

It is evident from Table 4.24 that JRJRJ exhibits better lower ballistic impact performance followed by JRRJ and JRJ. It can be seen that at all the impact velocities considered in the present study, the residual velocity of JRJ is more compared to JRRJ and JRJRJ indicating that JRJ offers the least resistance to damage compared to JRRJ and JRJRJ. The viscous damping characteristics of rubber enable the flexible

composites to absorb larger energy leading to a reduction in the projectile velocity. JRRJ and JRJRJ having two layers of rubber that provides better energy absorption and damage resistance behaviour. Rubber being compliant material stretches to a larger extent resisting the projectile penetration. The variation in the residual velocity of the projectiles in experimental, FE and analytical studies are in agreement with each other.

#### 4.3.5.7 Energy absorption of the proposed flexible composites when subjected to lower ballistic impact velocity

The energy absorption of the proposed flexible composites at ballistic limit velocities is calculated using Eq. 42 for all the approaches considering their respective ballistic limits and at other impact velocities, the energy absorbed is determined using Eq. 41 for experimental and FE approach; and Eq<sup>s</sup> (1-21) for an analytical approach. The energy absorbed by the proposed flexible composites at their ballistic limits is tabulated in Table 4.25. Table 4.26 provides the energy absorption of the proposed flexible composites at impact velocities other than ballistic limit velocity.

**Table 4.25** Energy absorption of the proposed flexible composites at the ballistic limit

Flexible Composite Configuration	Energy Absorbed (J)		
	Analytical	FE	Experimental
JRJ	21.12	18.6	19.84
JRRJ	36.98	33.62	34.44
JRJRJ	42.32	36.12	38.72

It is found that the energy absorption by the flexible composites JRJ, JRRJ and JRJRJ at their respective ballistic limits in case of experimental study is found to be 19.84 J, 34.44 J and 38.72 J respectively. The energy absorption of JRJRJ is more compared to JRJ and JRRJ by 95.16% and 12.42% respectively.

The energy absorption of JRRJ is enhanced by 73.58% compared to JRJ. Further, in the case of FE and analytical study, a similar trend is observed and the results agree well with each other. This shows that an additional layer of rubber enhances the energy absorption of the flexible composite significantly compared to an additional layer of jute.

**Table 4.26** Energy absorption at lower ballistic impact velocity of 80m/s, 100m/s and 120m/s

Flexible Composite Configuration	Impact Velocity (m/s)	Energy Absorbed (J)		
		Analytical	FE	Experimental
JRJ	80	21.75	24.78	23.18
	100	26.00	30.16	24.80
	120	32.31	38.38	29.68
JRRJ	80	31.80	32.00	32.00
	100	40.25	42.00	38.48
	120	50.04	50.88	48.20
JRJRJ	80	31.90	32.00	32.00
	100	44.41	44.88	43.88
	120	57.68	54.60	52.78

Further, the energy absorbed by the flexible composites is calculated for impact velocities of 80m/s, 100 m/s and 120 m/s considering the ballistic limits of the flexible composites to assess the behaviour of the composites at enhanced velocities. The majority of the kinetic energy of the projectile during an impact event is absorbed by the primary yarns when the projectile strikes the fabric. Further, the secondary yarns are pulled by the transverse deflection of the primary yarns thereby assisting in the dissipation of the projectile's kinetic energy. Primary yarns are pulled out significantly as they were directly impacted by the projectile.

In the proposed flexible composites, the elastic nature of rubber aids in better transfer of impact load from primary to secondary yarns which further enables the fabric in resisting and absorbing the kinetic energy of the projectile. Better and consistent fabric arrangement with an integrated and uniform coating of the fabric can be achieved by the rubber matrix. Rubberized matrix also eliminates sliding, extracting, windowing under impact loading. In addition, rubber being a material with good damping properties aids in better absorption of the projectile's kinetic energy.

In the case of flexible composites, an increase in impact velocity leads to an increase in energy absorption attributing to higher strain rates where the response of rubber varies. During impact loading, the mechanical strain rate dominates the segmental dynamics of rubber resulting in a changeover to glassy state and further failure leading to sufficiently great energy dissipation resulting in higher energy absorption by rubber at higher impact velocity. Thus, flexible composites absorb higher energy at higher impact velocity.

Among the proposed flexible composites, the energy absorption in case of JRRJ and JRJRJ stacking sequences are same at an impact velocity of 80 m/s in case of experimental and FE approach due to the fact that both the stacking sequences arrest the penetration of the projectile at this impact velocity providing a zero residual velocity. In other words, both these stacking sequences absorb the kinetic energy of the projectile completely at an impact velocity of 80 m/s. In the case of an analytical approach, both JRRJ and JRJRJ provide a negligible amount of residual velocity resulting in energy absorption of 31.8 J and 31.9 J respectively. The deviation of the energy absorbed obtained from the analytical approach is negligible compared to the experimental and FE approach. However, when the impact velocity is raised to 100 m/s and 120 m/s the JRJRJ absorbs better energy followed by JRRJ and JRJ. At an impact velocity of 80 m/s, the energy absorption of JRRJ and JRJRJ are equal and greater by 38% when compared to JRJ in case of experimental study and 29.13% in case of FE study. However, this increases drastically as the impact velocity increases.

The energy absorption of JRJRJ is 76.93% and 77.83% more compared to JRJ at an impact velocity of 100 m/s and 120 m/s respectively for experimental study owing to the more amount of resistance offered by the rubber layers in JRJRJ compared to JRJ. A similar trend is observed for FE and analytical studies.

However, the increase in energy absorption of JRJRJ when compared to JRRJ at 100 m/s and 120 m/s is merely 14% and 9.5% respectively for experimental study, as both JRRJ and JRJRJ stacking sequences has equal amount of rubber layers and addition of one more layer of jute in JRJRJ compared to JRRJ contributes to the marginal increase in energy absorption capability of JRJRJ. FE and analytical approaches follow a similar trend. Considering all these comparisons, it can be said that a flexible composite with the JRJRJ stacking sequence is the better energy absorber in a lower ballistic impact regime. The energy absorption percentage is calculated using Eq. 43 and tabulated in Table 4.27 at impact velocities of 80 m/s, 100 m/s and 120 m/s.

**Table 4.27** Energy absorption percentage of proposed flexible composites

Flexible Composite Configuration	Impact Velocity (m/s)	Energy Absorption Percentage		
		Analytical	FE	Experimental
JRJ	80	67.97	77.44	72.44
	100	52.00	60.32	49.60
	120	44.88	53.31	41.22
JRRJ	80	99.38	100.00	100.00
	100	80.50	84.00	76.96
	120	69.50	70.67	66.94
JRJRJ	80	99.69	100.00	100.00
	100	88.82	89.76	87.76
	120	73.31	75.83	80.11

The energy absorption percentage of the flexible composites increases in the order JRJRJ>JRRJ>JRJ. In case of an experimental study, at an impact velocity of 80 m/s, the energy absorption percentage of JRJRJ and JRRJ is 38 % more compared to JRJ. As the impact velocity increases to 100 m/s, JRJRJ absorbs 77% more energy compared to JRJ and 14 % more energy compared to JRRJ. This increase in energy absorption of JRJRJ is found to be 77.85 % and 9.5 % more than JRJ and JRRJ respectively at an impact velocity of 120 m/s. The addition of a layer of rubber to JRJ results in JRRJ configuration which provides 55.16 % and 62.39 % more energy absorption percentage at 100 m/s and 120 m/s respectively compared to JRJ. However, adding a single layer of jute to JRRJ results in JRJRJ configuration which exhibits 14 % and 9.5 % more energy absorption percentage capability at 100 m/s and 120 m/s respectively compared to JRRJ. This behaviour is due to the fact that JRRJ has an additional layer of rubber compared to JRJ which results in significant enhancement of energy absorption percentage compared to an addition of jute layer as in the case of JRRJ to JRJRJ. The same trend is followed for FE and analytical study

It can be seen that the energy absorption percentage reduces with an increase in impact velocity and as the number of rubber layers increases, the energy absorption percentage increases drastically. This shows that the number of rubber layers plays an important role in the energy absorption percentage. Thus it is evident that rubber plays a prominent role in deciding the energy absorption of the flexible composite and the role of jute when compared to rubber is negligible. Thus, at the lower ballistic impact regime considered in the present study, JRJRJ emerges as a better energy absorber compared to its counterparts. This is due to the more number of rubber layers in combination with the intermediate jute layer and more rubber-based matrix used.

Specific energy absorption (SEA) provides the energy absorption effectiveness of each stacking sequence of the flexible composite. SEA is calculated using Eq. 25. The areal density of the proposed flexible composites is calculated using Eq. 24 and tabulated in Table 4.28. The SEA of the proposed flexible composites is calculated

and tabulated in Table 4.29 for ballistic impact velocities and in Table 4.30 for impact velocity of 80 m/s, 100 m/s and 120 m/s.

**Table 4.28** The areal density of the flexible composite

<b>Flexible composite</b>	<b>Density (Kg/m<sup>3</sup>)</b>	<b>Thickness (m)</b>	<b>Areal Density (Kg/m<sup>2</sup>)</b>
JRJ	1159.64	0.01	11.59
JRRJ	1121.57	0.012	13.45
JRJRJ	1118.81	0.013	14.54

**Table 4.29** Specific energy absorption of the proposed flexible composites at the ballistic limit

<b>Flexible composite</b>	<b>SEA (Jm<sup>2</sup>/Kg)</b>		
	<b>Experimental</b>	<b>FE</b>	<b>Analytical</b>
JRJ	1.71	1.6	1.82
JRRJ	2.53	2.5	2.75
JRJRJ	2.6	2.48	2.91

It can be seen that the SEA of the proposed flexible composites increases in the order JRJRJ>JRRJ>JRJ. The SEA of JRJRJ at the ballistic limit obtained experimentally is enhanced by 52% and 2.7% compared to JRJ and JRRJ respectively.

The FE and analytical results follow the experimental trend with negligible variation in SEA of JRRJ and JRJRJ indicating that both these flexible composites exhibit nearly the same energy absorption capability. This is due to the fact that the dual-layer of rubber provides more resistance for projectile penetration thereby converting the most of the kinetic energy of the projectile into the absorbed energy of the flexible composite.

**Table 4.30** Specific energy absorption of the proposed flexible composites at impact velocity of 80 m/s, 100 m/s and 120 m/s

Stacking Sequence	Impact Velocity ( $v_i$ ) in m/s	SEA ( $\text{Jm}^2/\text{Kg}$ )		
		Experimental	FE	Analytical
JRJ	80	2.00	2.14	1.88
	100	2.14	2.60	2.24
	120	2.56	3.31	2.79
JRRJ	80	2.38	2.38	2.36
	100	2.86	3.12	2.99
	120	3.58	3.78	3.72
JRJRJ	80	2.20	2.20	2.19
	100	3.02	3.09	3.05
	120	3.63	3.76	3.97

SEA of the considered flexible composite increases with an increase in impact velocity above the ballistic limit. Above the ballistic limit, SEA of the flexible composites follows a similar trend as observed at the ballistic limits (JRJRJ>JRRJ>JRJ). The reason remains the same as explained for SEA at ballistic limit velocity. A good agreement of the SEA values can be observed between experimental, FE and analytical approaches.

#### 4.3.5.8 Damage mechanism for lower ballistic impact

The schematic of the proposed damage mechanism in each layer of the flexible composite is represented in Figure 4.41 along with damages from the experiment visualised through SEM. It is proposed that at the layer containing jute, the damage is dominated by fiber breakage and the mechanism of fiber pull out as seen in neat jute fabric is eliminated in the jute layer of the flexible composite due to the adherence of the jute to the rubber which is compliant in nature. Whereas, at the layer containing



rubber, the damage is dominated by tearing of the rubber where the resistive bands are generated due to compression of the rubber leading to maximum energy absorption and enhanced resistance to damage.

As the projectile strikes the front face of the flexible composite laminate, it encounters the jute layer which offers less resistance to the movement of the projectile and gets damaged through fiber breakage mode. As the projectile penetrates further, it encounters the rubber layer where maximum resistance is offered to the movement of the projectile due to their compliant nature. When the impact velocity is not sufficient to overcome the resistive forces induced by the proposed flexible composite, the movement of the projectile is arrested resulting in partial penetration. However, when the impact velocity overcomes the resistive forces, the complete penetration of projectile through the thickness of the proposed flexible composites takes place. The resistive forces are higher at the entry point of the rubber layer since the compliance offered due to the presence of a large amount of rubber and rubber-based matrix and this resistive force gradually reduces through the thickness of the rubber layer in the direction of impact as the tearing of rubber in the flexible composite takes place. The above-described mechanism can be visualized from Figure 4.40 where it can be seen that at the point of entry of projectile the resistance offered by rubber to the movement of the projectile is more compared to exit. Due to this resistance offered, the rubber stretches along the direction of movement of the projectile up to the point where the velocity of the projectile overcomes the resistance offered by the rubber. The proposed and experimental damage mechanism along with FE validation is shown in Figure 4.41.

The proposed flexible composites exhibit remarkably high-velocity impact response due to the high damping characteristics of the rubber. Figure 4.42 shows the comparison of the damage mechanism involved in the proposed flexible composites at ballistic impact velocity and at impact velocities of 80 m/s, 100 m/s and 120 m/s

obtained through experimentation and FE approach. The use of rubber matrix results in better attachment of the fabric and interleaving of NR provides better resistance against the movement of the projectile. It is also found that in the case of flexible composites, the main damage mechanisms involved are rubber tearing and fiber breakage. When the fabric reaches the maximum stress during an impact loading, the failure occurs through the fiber breakage mechanism which is shown at the point of impact of the projectile. Failure propagating further leads to tearing of rubber and rubber detachment in some cases.

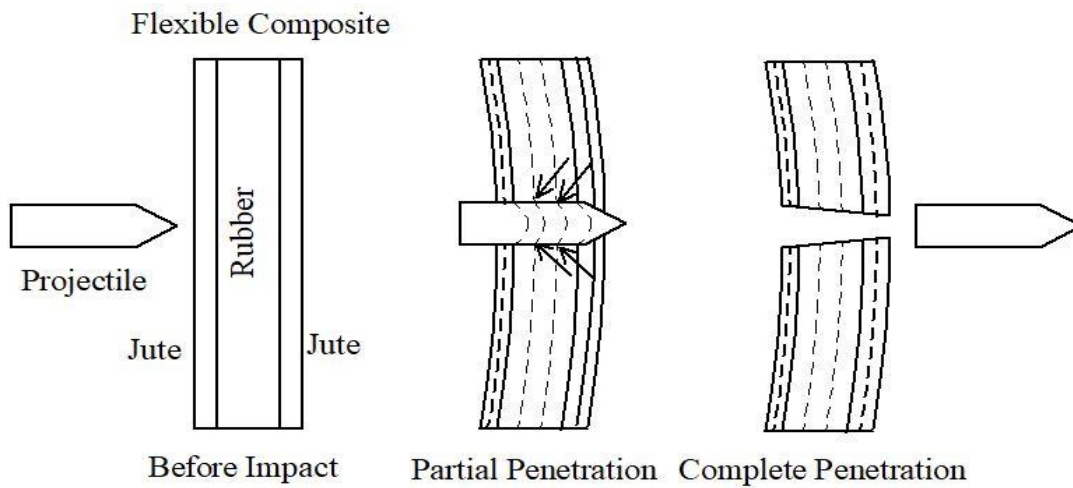


**Figure 4.40** Schematic of damage resistance distribution in flexible composite in case of lower ballistic impact

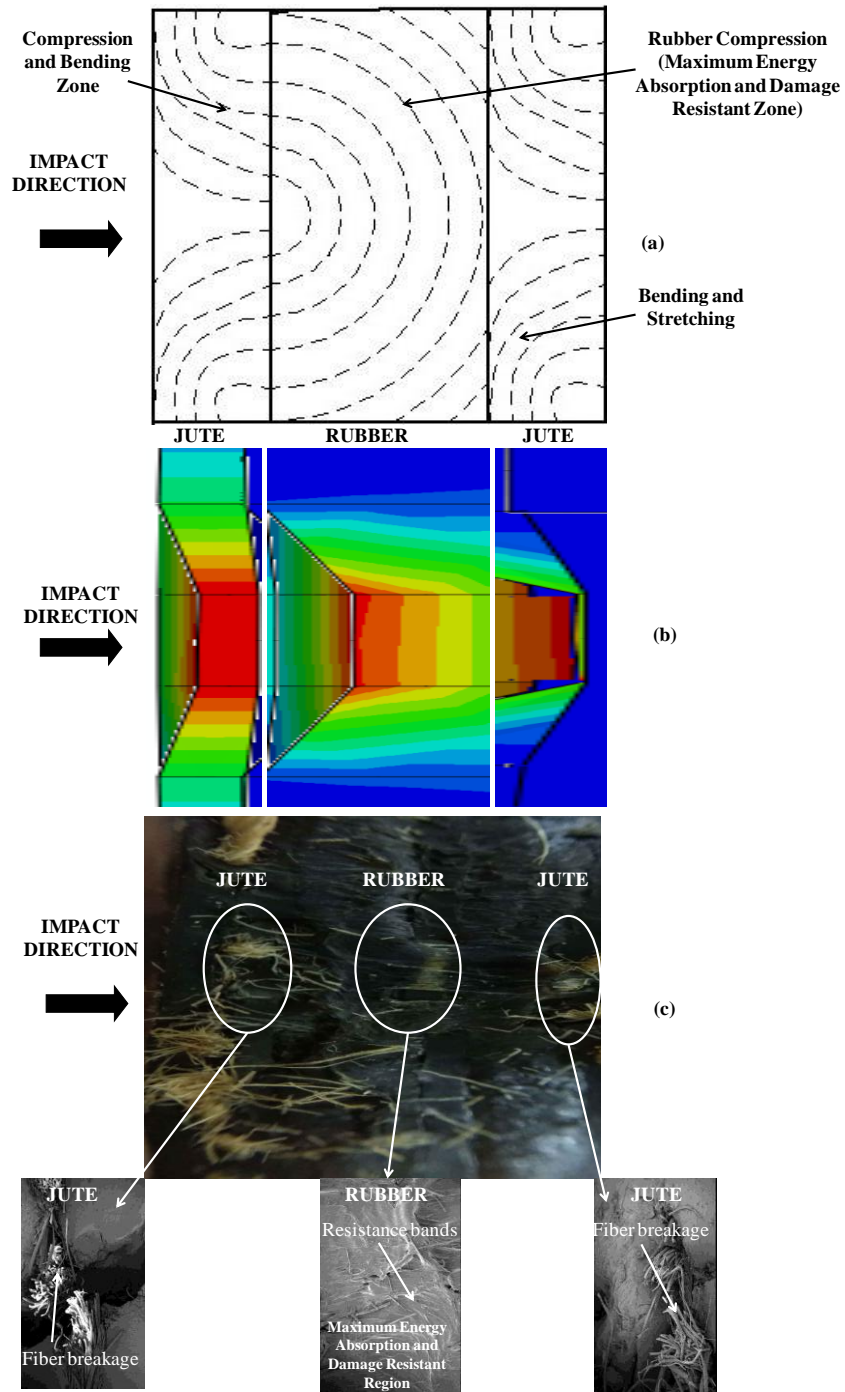


**Figure 4.41** Proposed damage mechanism validated with experimental and finite element approach

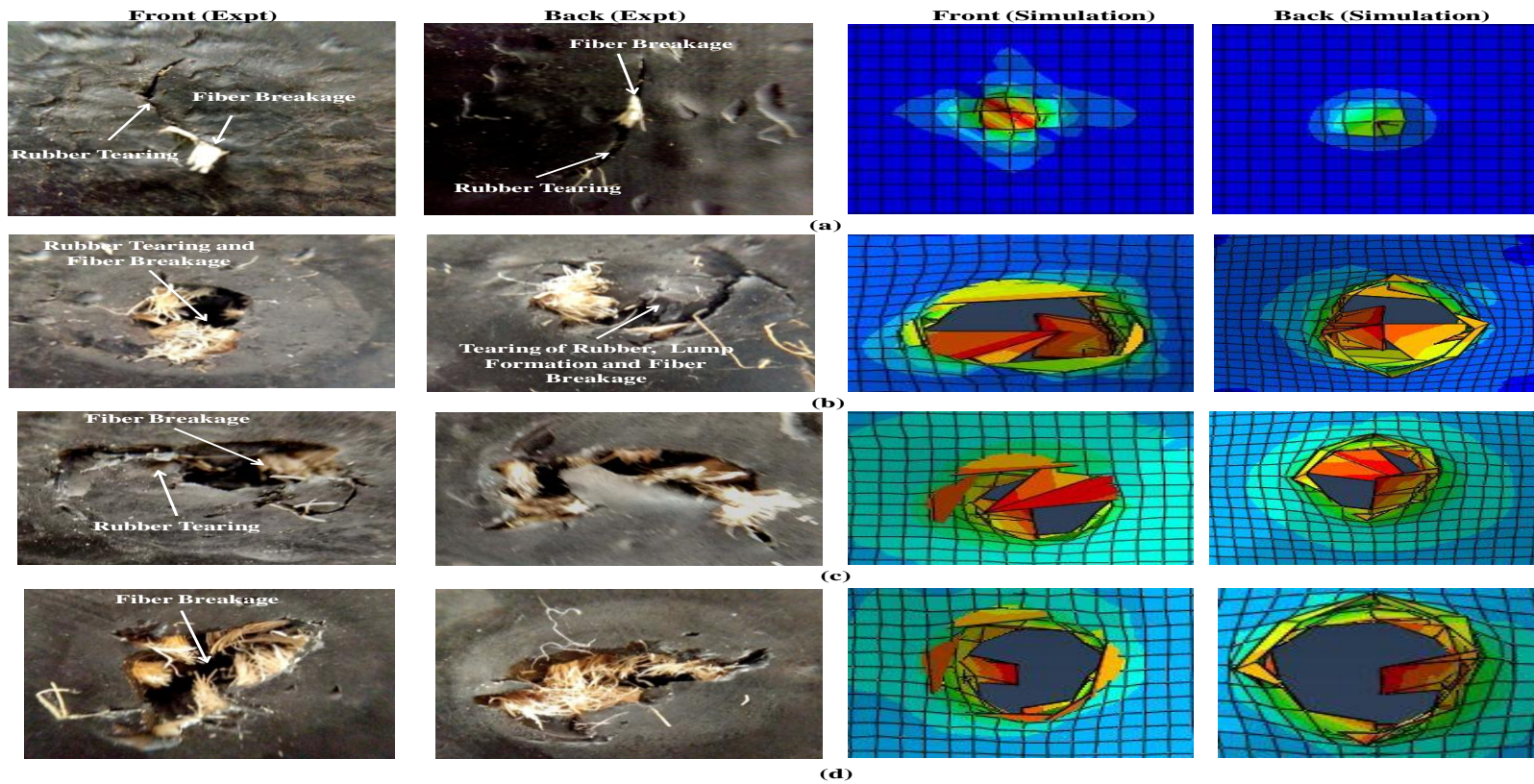


**Figure 4.42** Damage mechanism of flexible composites at (a) ballistic limit; (b) 80 m/s; (c) 100 m/s and (d) 120 m/s.

A clear distinction can be observed in the failure pattern of the proposed flexible composites at different impact velocities. At ballistic impact velocity, tearing of rubber and fiber breakage are the only patterns observed. However, as the impact velocity is increased lump formation of the torn out rubber is also observed in addition to tearing of rubber and fiber breakage. With further increase in the impact velocity, the rubber tearing and detachment of the rubber from the rear face of the flexible composite is observed. Thus it can be said that at lower impact velocity, rubber tearing is the only pattern that can be observed in the failed laminate and as the impact velocity increases, rubber tearing, lump formation and detachment are predominantly observed along with fiber breakage. The damage mechanisms explained above are exhibited by the scanning electron microscope images in Figure 4.43.

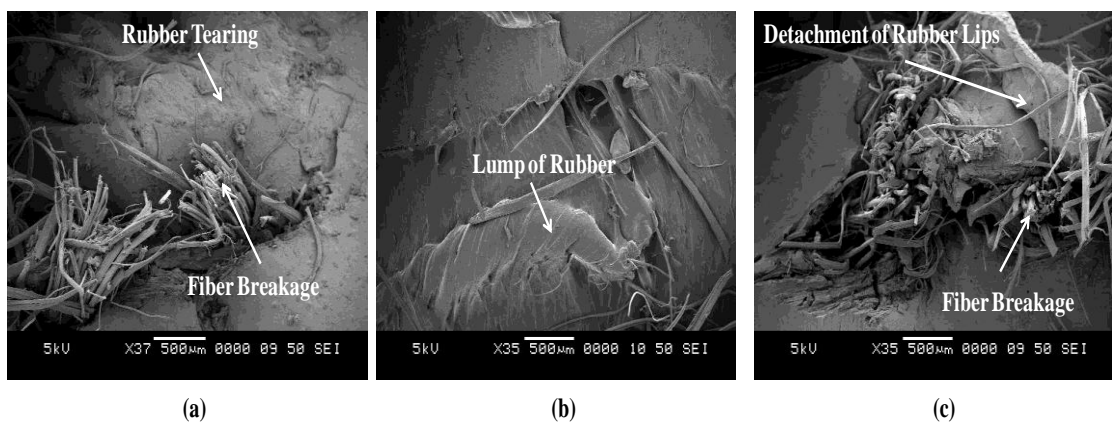


**Figure 4.43** Scanning electron microscope images exhibiting the damage mechanism involved

The damage mechanism involved in the proposed flexible composites for no complete penetration is shown in Figure 4.44. No complete penetration of the projectile through the proposed flexible composites result in complete kinetic energy absorption of the projectile by the flexible composites. The proposed flexible composites undergoes bending and compression with subsequent shear on the entry side and bending and

stretching on the exit side. The projectile penetrates the composite by tearing the rubber and fiber breakage. Further, as the projectile gets struck in the composite the pit formation as a result of bending and compression with subsequent shear can be observed at the front face of the composite. Whereas, at the rear face of the composite, tearing takes place due to bending and stretching.

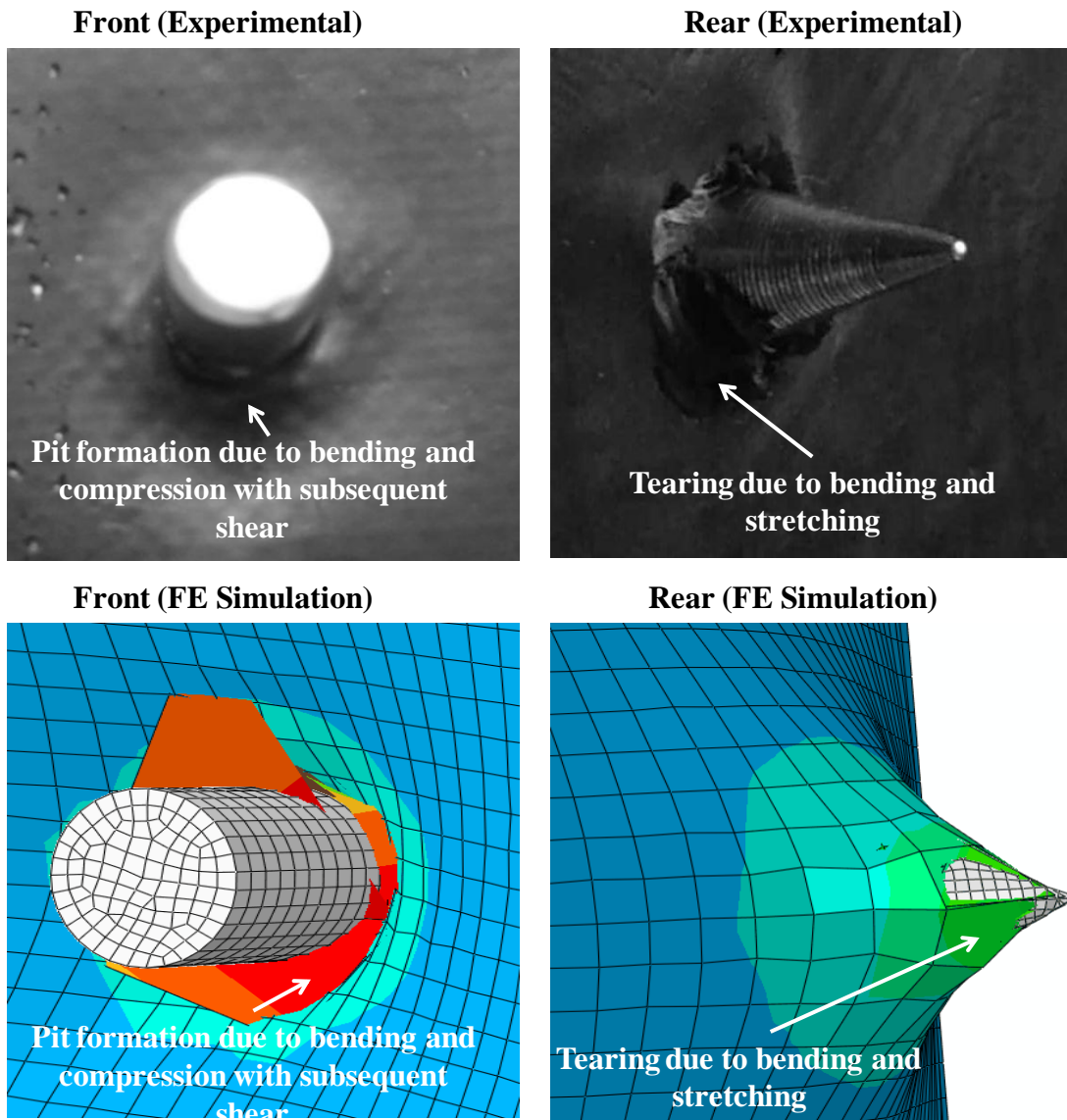


**Figure 4.44** Damage mechanism of flexible composites for no complete penetration

#### 4.4 Optimization using multi attribute decision making approach

The performance defining attributes description is provided in Table 4.31 and the optimization is carried out using VIKOR and PSI methods.

**Table 4.31** Performance defining attributes description used in MADM

<b>Performance defining attributes (PDA's)</b>	<b>PDA's Implication</b>
Tensile strength	Higher the better
Tear strength	Higher the better
ILSS	Higher the better
SEA of LVI	Higher the better
SEA of lower ballistic impact	Higher the better
Sp. Rate of Wear x 10 <sup>-7</sup>	Lower the better

##### 4.4.1 Results of VIKOR method

The three composite configurations JRJ, JRRJ, and JRJRJ are compared using the VIKOR method and ranking has been done accordingly. The decision matrix is developed based on the experimental results obtained and is presented in Table 4.32. Normalization is carried out in order to facilitate the comparison of the various different values of the properties obtained experimentally and is presented in Table 4.33.

**Table 4.32** Decision matrix for VIKOR

<b>Composite Configuration</b>	<b>Tensile Strength/ Thickness (MPa)</b>	<b>Tear Strength/ Thickness (N/mm)</b>	<b>ILSS (MPa)</b>	<b>SEA of LVI (Jm<sup>3</sup>/Kg)</b>	<b>SEA of lower ballistic impact (Jm<sup>2</sup>/Kg)</b>	<b>Sp. Rate of wear x 10<sup>-7</sup> (m<sup>3</sup>/Nm)</b>
JRJ	0.2	3.18	0.16	0.026	1.71	0.22
JRRJ	0.105	2.63	0.21	0.026	2.53	0.29
JRJRJ	0.09	2.38	0.44	0.024	2.6	0.35

**Table 4.33** Normalized matrix for VIKOR

<b>Composite Configuration</b>	<b>Normalized Tensile Strength</b>	<b>Normalized Tear Strength</b>	<b>Normalized ILSS</b>	<b>SEA of LVI</b>	<b>SEA of lower ballistic impact</b>	<b>Sp. Rate of wear x 10<sup>-7</sup></b>
JRJ	0.823	0.668	0.312	0.592	0.426	0.436
JRRJ	0.432	0.552	0.409	0.592	0.631	0.574
JRJRJ	0.370	0.500	0.857	0.547	0.648	0.693



The weights are calculated using the entropy method using Eq. 46-Eq. 50. The weights found are given in Table 4.34. The weighted normalized matrix is provided in Table 4.35.

**Table 4.34** Weights calculated from the entropy method

<b>Parameters</b>	<b>Weights (Calculated from Entropy Method)</b>
Tensile Strength	0.054
Tear Strength	0.006
ILSS	0.911
SEA of LVI	0.0006
SEA of lower ballistic impact	0.0136
Sp. Rate of Wear x $10^{-7}$	0.0144

The positive and negative ideal solution is determined according to Eq. 52 and Eq. 53 respectively and tabulated in Table 4.36.  $S_i$  and  $R_i$  values are found out using Eq. 54 and Eq. 55 respectively and are reported in Table 4.37. Eq. 56 is used to find the VIKOR index as a last step to rank the alternatives. Table 4.38 provides the VIKOR index and ranking provided to each of the alternative. The alternative having lowest VIKOR index is assigned with rank 1 and so on.

**Table 4.35** Weighted normalized matrix for VIKOR

<b>Composite Configuration</b>	<b>Normalized Tensile Strength</b>	<b>Normalized Tear Strength</b>	<b>Normalized ILSS</b>	<b>SEA of LVI</b>	<b>SEA of lower ballistic impact</b>	<b>Sp. Rate of wear x 10<sup>-7</sup></b>
JRJ	0.04423	0.00409	0.28418	0.00034	0.00583	0.00630
JRRJ	0.02322	0.00338	0.37299	0.00034	0.00863	0.00830
JRJRJ	0.01990	0.00306	0.78150	0.00032	0.00887	0.01002

**Table 4.36** Positive and negative ideal solution for VIKOR

<b>Parameters</b>	<b>Positive Ideal Solution</b>	<b>Negative Ideal Solution</b>
Normalized Tensile Strength	0.04423	0.01990
Normalized Tear Strength	0.00409	0.00306
Normalized ILSS	0.78150	0.28418
SEA of LVI	0.00034	0.00032
SEA of lower ballistic impact	0.00887	0.00583
Sp. Rate of Wear x 10 <sup>-7</sup>	0.00630	0.01002

**Table 4.37** Utility and regret measures for VIKOR

Alternative	$S_i$	$R_i$
JRJ	0.925	0.911
JRRJ	0.808	0.748
JRJRJ	0.074	0.053

**Table 4.38** Vikor index for  $\alpha = 0.5$ 

Alternative	$Q_i$	Ranking
JRJ	1	3
JRRJ	0.836	2
JRJRJ	0	1

The results indicate that JRJRJ has the lowest VIKOR index compared to JRRJ and JRJ. Thus, JRJRJ emerges as the optimal stacking sequence for the criteria considered in the present study based on the VIKOR method.

#### 4.4.2 Results of PSI method

The decision matrix for the current problem is represented as in Table 4.32. This decision matrix is normalized using Eq. 58 and Eq. 59. The mean value of normalized data is calculated according to Eq. 60 and is represented in Table 4.39.

The preference variation value, deviation in preference value and overall preference value calculated using Eq. 61, Eq. 62 and Eq. 63 respectively are tabulated in Table 4.40. The PSI values for each of the alternative is calculated using Eq. 64 and ranking based on PSI values are provided with the alternative having the highest PSI with rank 1 and so on. The same are tabulated in Table 4.41.

**Table 4.39** Normalized matrix and mean values of normalized data for PSI

<b>Composite Configuration</b>	<b>Normalized Tensile Strength</b>	<b>Normalized Tear Strength</b>	<b>Normalized ILSS</b>	<b>SEA of LVI</b>	<b>SEA of lower ballistic impact</b>	<b>Sp. Rate of wear x 10<sup>-7</sup></b>
JRJ	1.000	1.000	0.364	1.000	0.658	1.000
JRRJ	0.525	0.828	0.477	1.000	0.973	0.759
JRJRJ	0.450	0.749	1.000	0.923	1.000	0.629
Mean value	0.658	0.859	0.614	0.974	0.877	0.796

**Table 4.40** Preference variation value, deviation in preference value and overall preference value

<b>Composite Configuration</b>	<b>Normalized Tensile Strength</b>	<b>Normalized Tear Strength</b>	<b>Normalized ILSS</b>	<b>SEA of LVI</b>	<b>SEA of lower ballistic impact</b>	<b>Sp. Rate of wear x 10<sup>-7</sup></b>
Preference variation value	0.1779	0.0330	0.2304	0.0039	0.0725	0.0710
Deviation in preference value	0.822	0.967	0.770	0.996	0.928	0.929
Overall preference value	0.152	0.179	0.142	0.184	0.171	0.172

**Table 4.41** PSI values and ranking of alternatives

<b>Alternative</b>	<b>PSI values</b>	<b>Ranking</b>
JRJ	0.957	3
JRRJ	1.004	2
JRJRJ	1.012	1

**Table 4.42** Results of VIKOR and PSI methods

<b>Alternatives</b>	<b>VIKOR</b>	<b>PSI</b>
JRJ	3	3
JRRJ	2	2
JRJRJ	1	1

The results obtained through the VIKOR and PSI methods used in the present study are provided in Table 4.42. In the case of VIKOR method, the ranking is provided based on the ascending order of VIKOR index ( $JR_J=1 > JRR_J=0.836 > JRJR_J=0$ ) Aggregate functions, in case of the VIKOR method, are always nearer to ideal values. For example, in the case of the VIKOR method, JRJRJ is assigned with rank 1 and it has an aggregate function of 1 (1-0). This is equal to the ideal value of 1. In the case of the PSI method, the ranking is provided based on higher PSI values ( $JR_J=0.957 < JRR_J=1.004 < JRJR_J=1.012$ ). It can be seen that the order of ranking in both the MADM methods remains the same and thus can be said that JRJRJ stacking sequence is preferred over JRJ and JRRJ.

In this chapter, the results obtained from the analytical, FE and experimentation methods for various tests are discussed. The next chapter deals with the major conclusion drawn from the obtained results along with scope for future work with an intention to explore the possibilities of further research.

## CHAPTER 5

### 5 CONCLUSION AND FUTURE SCOPE

#### 5.1 Conclusion

In the present study, the role of rubber in a composite subjected to LVI loading is studied using FE approach and based on the outcome, a comparative study between the stiff and flexible composites is studied using FE approach. Various possible stacking sequences of the jute/rubber base flexible ‘green’ composite are proposed for impact applications and these proposed stacking sequences are studied for their impact response using FE simulation and the three best stacking sequences of flexible ‘green’ composite are chosen for further study. The optimal curing characteristics of the NR based rubber gum used as matrix is found out. Also, the peel strength of the constituents of the composite when bonded with NR based B stage cured pre peg is studied. Further, the selected three best stacking sequences of flexible ‘green’ composite are characterized for their physical, mechanical and tribological (Abrasive and Slurry erosive wear) properties along with their interlaminar shear stress characterization. MADM approach is adopted to select the optimal stacking sequence. The impact response in terms of energy absorption and resistance to damage is studied for the three stacking sequences of the proposed flexible ‘green’ composite. Based on these studies, following conclusions are drawn:

The FE based comparative study of the JE and JE-R-JE composites shows that JE-R-JE composite outstands the JE composite in terms of both energy absorption and resistance to damage. The presence of rubber as a constituent in the composite enhances the energy absorption of the composite along with minimizing the damage. Thus rubber is found to be the potential material for impact applications.

It is found from the FE based comparative study between the stiff and flexible composites that JRJ flexible composite absorbs nearly 62% more energy compared to stiff JE composite. JE is brittle in nature; it absorbs lesser energy and provides higher residual velocity to the impactor as opposed to JRJ which is ductile in nature. JE

composite will exhibit brittle behaviour whereas JRJ will exhibit ductile behaviour due to inclusion of rubber. Proposed flexible composite is expected to provide better energy absorption and reduce damage propagation under low velocity impact.

It is found that out of the six different stacking sequences of the flexible 'green' composite considered, JRJRJ configuration provides maximum contact force followed by JRJ, JRRJ, RJRJR, RJRJ and RJR indicating that JRJRJ provides better resistance to damage compared to its counterparts and the stacking sequences JRJ, JRRJ and JRJRJ are chosen for further study based on the contact force.

The complete and proper curing of the NR based B stage cured pre peg is found to happen at temperature of 138.7 °C and at time of 6.31 minutes and the adhesive study revealed that the rubber matrix system is compatible with jute as it provides good interfacial compatibility by demonstrating more and deeper marks left after the fibers are pulled out. Considering the compatibility with rubber sheet, it is found that the peel strength is much higher than the peel strength with jute as higher peel force is required to separate the rubber from rubber matrix. It is found that the peel strength and strain energy release rate of rubber is 5 times and 2.91 times more than jute when bonded with rubber gum due to the higher tackiness provided by the rubber which results in more amount of force being needed to separate the rubber from the rubber gum.

The mechanical characterization revealed that flexible composite with stacking sequence JRJ provided better properties. The tensile strength of JRJ is found to be 57.7% and 64.47% higher compared to JRRJ and JRJRJ respectively. The tear strength of JRJ is found to be 0.4% and 2.38% higher than JRRJ and JRJRJ respectively. Tensile properties of the composite are found to be in between that of jute and natural rubber. The ultimate strength of JRJ, JRRJ and JRJRJ is enhanced by 40, 25.36 and 24.32 times compared to natural rubber. Similarly modulus of JRJ, JRRJ and JRJRJ is enhanced by 68.1, 66.82 and 62.53 times compared to natural rubber. This enhancement is due to the addition of jute as a fiber. It was found that flexible composites mainly fail due to matrix tearing and subsequently fiber breakage and they are free from matrix cracking which is found in conventional stiff



composites. ILSS study reveals that the load carrying capacity of proposed flexible composites vary in the order JRJRJ > JRRJ > JRJ indicating that JRJRJ is less prone to damage compared to JRJ and JRRJ. Higher ILSS of JRJRJ results in higher load requiring for causing smaller delamination. Whereas, lower ILSS of JRJ causes delamination at lower load. Adoption of natural rubber sheets and addition of fiber enhances the ILSS of the flexible composites. Maximum ILSS is obtained for stacking sequence of JRJRJ with increase in 2.75 and 2.09 times compared to JRJ and JRRJ. It was found that ILSS of flexible composites does not only depend on the void content and fiber weight percentage, but also depends on the thickness of the laminate. The short beam failure behavior on the tension and compression side of the flexible composite exhibited same pattern for all the variants with no visible failure on compression side and matrix peeling with minimal fiber exposure on the tension side. However, in case of flexible composite with JRJ and JRJRJ stacking sequences separation of the layers was observed due to shear loading and in case of JRRJ stacking sequence, in addition to separation of layers, failure at neutral axis was also found.

Slurry erosive behaviour of the flexible green composite is studied along with the factors influencing the erosive behaviour. Analysing the means and SN ratio through Taguchi's L9 orthogonal array, optimum conditions for minimised weight loss is stacking sequence of JRJ, rotation speed of 500 rpm and sand concentration of 50 g/L. Through ANOVA, it was concluded that sand concentration is the main factor affecting the weight loss of composite. Regression model is developed and it was found that the developed model is adequate and feasible to predict the weight loss due to slurry erosion within the range of experimental conditions. The response optimization shows that for minimum weight loss of the proposed composite is obtained for optimum stacking sequence of JRJ (level 1) with minimum rotation speed of 500 rpm and sand concentration of 50 g/L. JRJ results in minimum weight loss compared to other two stacking sequences. It is found that the flexible composites being elastic in nature dissipates the kinetic energy of the abrasive particle exhibiting excellent erosion resistance.

An experimental study of the two body wear behavior of three different configurations of the flexible composites is carried out using two bodywear at varied abrading distance and load. Based on the experimental investigations, it is found from the responses of SN ratio and ANOVA that, abrading distance is the significant factor influencing the specific wear rate compared to composite configuration and load. The regression model developed is found to acceptable and feasible to predict the wear rate within the range of experimental conditions. Increase in the abrading distance and reducing the load, the volumetric wear loss of the proposed composites with abrading distance being the significant factor affecting wear loss. The volumetric wear loss and specific wear rate of the composite is significant when jute is exposed to abrading surface compared to rubber. The inclusion of rubber enhances the wear resistance of the polymeric composites under dry wear condition. The specific wear rate of all the proposed composites reduces with increased abrading distance and reduced load. Specific wear rate of JRJ is least followed by JRRJ and JRJRJ indicating JRJ has better wear resistance compared to JRRJ and JRJRJ for the chosen range of abrading distance and load. The wear mechanism of the rubber involves the development of wave-like pattern where the waves represent the stressed asperities. The rupturing of the uppermost part, the “tongue” takes place with continued stretching of the asperities. This ultimately leads to material loss. On the other hand, fiber breakage dominates the wear mechanism of the composite, when jute is being abraded. Flexible composites are dominated by rubber and thus characterized with better resistance against abrasive wear making them a potential candidate for sacrificial structural applications such as claddings.

JRJ stacking sequence is found suitable for use as a sacrificial structure to protect the primary structure from LVI, as JRJ absorbs more energy by undergoing maximum damage in the impact energy range considered in the present study. JRJRJ stacking sequence can also be used as a sacrificial structure as it provides better damage resistance. But, it leads to a rebound of the projectile since CoR is more for JRJRJ. Thus, this can be a potential material for absorbing energy and acting as a sacrificial structure like cladding to protect the primary structural components like the bumper of

an automobile, the body of armor vehicle and so on. However, it is found that there is no appreciable variation in the SEA of the proposed flexible composites.

The ballistic limit of JRJ, JRRJ and JRJRJ are found to be 63m/s, 83m/s and 88m/s respectively indicating that inclusion of additional layer of rubber (JRJ to JRRJ) enhances the ballistic limit by 32 % and the inclusion of additional layer of jute (JRRJ to JRJRJ) enhances the ballistic limit by 6 %. This shows that the rubber layer can significantly enhance the ballistic limit of flexible composite compared to jute layer. The energy absorption at ballistic limit of JRJRJ is more compared to JRJ and JRRJ by 97.7% and 12.7% respectively. The energy absorption of JRRJ is enhanced by 75.5% compared to JRJ. The SEA of JRJRJ is enhanced by 52% and 2.7% compared to JRJ and JRRJ respectively. The damage mechanism study pertaining to flexible composites reveals that the proposed flexible composites offers higher resistance to the movement of the projectile at the initial stage of impact event compared to later stage. The presence of rubber layers and the rubber based matrix offers resistance to the movement of the projectile due to their compliant nature leading to better energy absorption and reduced damage leading to tearing of matrix as opposed to matrix cracking in conventional stiff composites and thus eliminating catastrophic failure which is the major concern in composites subjected to impact. Thus the proposed flexible composite can be a potential material for secondary sacrificial structural application such as claddings which are used to protect the primary structural components.

Successful application of MADM approaches like VIKOR and PSI have shown that JRJRJ stacking sequence has emerged as the better stacking sequence among its counterparts. Also, it is clearly seen that the Hybrid Entropy-VIKOR and PSI models significantly support the selection of optimum stacking sequence and can be extended to the selection of suitable compositions for the composite for any intended engineering application. Also, these models are easily understood, marked by exactness and very efficient tools which can be conveniently used to aid the engineers and designers in selecting appropriate material among the alternatives available.

## **5.2 Future scope**

The basic purpose of this thesis has been fulfilled by the contributions presented in the preceding chapters. However, there is still a scope for future work to enhance the performance of the proposed flexible composite such as:

1. An analytical approach can be adopted to find the impact behavior of the proposed flexible composites which will serve as basis for any such flexible composites developed in future.
2. A study of the behavior of the flexible composites under the influence of temperature, hygro-thermal and other environmental conditions is still an overlooked area.
3. An extended study on the higher ballistic impact behaviour of the proposed flexible composites can be carried out for bullet proof applications.

## REFERENCE

Abali, F., Pora, A., and Shivakumar, K. (2003). "Modified short beam shear test for measurement of interlaminar shear strength of composites." *J. Compos. Mater.*, 37(5), 453.

Abo Sabah, S. H., Kueh, A. B. H., and Al-Fasih, M. Y. (2017). "Comparative low-velocity impact behavior of bio-inspired and conventional sandwich composite beams." *Compos. Sci. Technol.*, 149, 64–74.

Abrate, S. (1991). "Impact on Laminated Composite Materials." *Appl. Mech. Rev.*, 44(4), 155–190.

Abrate, S. (1998). *Impact on Composite Structures*. Cambridge: Cambridge University Press.

Abrate, S. (2011). *Impact engineering of composite structures*. Wien New York: Springer.

Adhikary, S. Das, and Li, B. (2018). "Simplified Analytical Models to Predict Low-Velocity Impact Response of RC Beams." *Pract. Period. Struct. Des. Constr.*, 23(2), 1–10.

Afendi, M., Teramoto, T., Bin, H., and Yh, A. L. (2011). "Strength prediction of epoxy adhesively bonded scarf joints of dissimilar adherends." *Int. J. Adhes. Adhes.*, 31(6), 402–411.

AG, J. (2017). "Biopolymers Strive to Meet Price/Performance Challenge." <https://www.ptonline.com/articles/biopolymers-strive-to-meet-price-performance-challenge>.

Akinci, A., Ercenk, E., Yilmaz, S., and Sen, U. (2011). "Slurry erosion behaviors of basalt filled low density polyethylene composites." *Mater. Des.*, 32(5), 3106–3111.

Akshaj, K. V., Vishwas, C. K., Balaganesan, G., and Sivakumar, M. S. (2016). "Low Velocity Impact Behavior of SiC/PU/GFRP Laminates." *Key Eng. Mater.*, 725, 122–

126.

AL-Oqla, F. M., and Sapuan, S. M. (2014). "Natural fiber reinforced polymer composites in industrial applications: feasibility of date palm fibers for sustainable automotive industry." *J. Clean. Prod.*, 66(1), 347–354.

Alemi-Ardakani, M., Milani, A. S., Yannacopoulos, S., and Shokouhi, G. (2016). "On the effect of subjective, objective and combinative weighting in multiple criteria decision making: A case study on impact optimization of composites." *Expert Syst. Appl.*, 46, 426–438.

Algbory, A. (2011). "Wear rate behaviour of carbon/epoxy composite materials at different working conditions." *Iraqi J. Mech. Mater. Eng.*, 11(3), 475–485.

Ali, M., Joshi, S. C., and Sultan, M. T. H. (2017). "Palliatives for Low Velocity Impact Damage in Composite Laminates." *Adv. Mater. Sci. Eng.*, 2017, 16 pages.

Aly, M. F., Attia, H. A., and Mohammed, A. M. (2013). "Integrated Fuzzy ( GMM ) - TOPSIS Model for Best Design Concept and Material Selection Process." *Int. J. Innov. Res. Sci. Eng. Technol.*, 2(11), 6464–6486.

Andre. (1945). *Scientific progress of manufacturing rubber units for the requirements of the engineeirng and ship building industries*. England.

Angrizani, C. C., Ornaghi, H. L., Zattera, A. J., and Amico, S. C. (2017). "Thermal and Mechanical Investigation of Interlaminare Glass/Curaua Hybrid Polymer Composites." *J. Nat. Fibers*, 14(2), 271–277.

Anojkumar, L., Ilangkumaran, M., and Sasirekha, V. (2014). "Comparative analysis of MCDM methods for pipe material selection in sugar industry." *Expert Syst. Appl.*, 41(6), 2964–2980.

Anojkumar, L., Ilangkumaran, M., and Vignesh, M. (2015). "A decision making methodology for material selection in sugar industry using hybrid MCDM techniques." *Int. J. Mater. Prod. Technol.*, 51(2), 102–126.

Ansari, M. M., and Chakrabarti, A. (2016a). "Impact behavior of FRP composite plate under low to hyper velocity impact." *Compos. Part B Eng.*, 95, 462–474.

Ansari, M. M., and Chakrabarti, A. (2016b). "Behaviour of GFRP composite plate under ballistic impact: Experimental and FE analyses." *Struct. Eng. Mech.*, 60(5), 829–849.

Ansari, M. M., and Chakrabarti, A. (2017a). "Ballistic Performance of Unidirectional Glass Fiber Laminated Composite Plate under Normal and Oblique Impact." *Procedia Eng.*, 173, 161–168.

Ansari, M. M., and Chakrabarti, A. (2017b). "Impact behaviour of GFRP and Kevlar/epoxy sandwich composite plate: Experimental and FE analyses." *J. Mech. Sci. Technol.*, 31(2), 771–776.

Anuar, H., and Zuraida, A. (2011). "Improvement in mechanical properties of reinforced thermoplastic elastomer composite with kenaf bast fibre." *Compos. Part B Eng.*, 42(3), 462–465.

Arib, R. M. N., Sapuan, S. M., Ahmad, M. M. H. M., Paridah, M. T., and Khairul Zaman, H. M. D. (2006). "Mechanical properties of pineapple leaf fibre reinforced polypropylene composites." *Mater. Des.*, 27(5), 391–396.

Arya, P. K., Tupkari, S., Satish, K., Thakre, G. D., and Shukla, B. M. (2016). "DME blended LPG as a cooking fuel option for Indian household: A review." *Renew. Sustain. Energy Rev.*, 53, 1591–1601.

Aryaei, A., Hashemnia, K., and Jafarpur, K. (2010). "Experimental and numerical study of ball size effect on restitution coefficient in low velocity impacts." *Int. J. Impact Eng.*, 37(10), 1037–1044.

*ASM Handbook*. (1992). Materials Park, USA: ASM International.

Autar K. Kaw. (2006). *Mechanics of Composite Materials*. New York: CRC Press.

Azghan, M. A., and Eslami-farsani, R. (2018). "The effects of stacking sequence and

thermal cycling on the flexural properties of laminate composites of aluminium-epoxy / basalt-glass fibres The effects of stacking sequence and thermal cycling on the flexural properties of laminate composites of alum.” *Mater. Res. Express*, 5(2).

Baarle, V. (2003). *Natural Rubber for Fashion*. *Nutuurrubber* 32(4th Quarter).

Bakare, I. O., Okieimen, F. E., Pavithran, C., Abdul Khalil, H. P. S., and Brahmakumar, M. (2010). “Mechanical and thermal properties of sisal fiber-reinforced rubber seed oil-based polyurethane composites.” *Mater. Des.*, 31(9), 4274–4280.

Baker, D., Bridges, D., Hunter, R., Johnson, G., Krupa, J., Murphy, J., and Sorenson, K. (2002). *Guide book to decision making methods*. NASA.

Balasubramani, V., Rajendra Boopathy, S., and Vasudevan, R. (2013). “Numerical analysis of low velocity impact on laminated composite plates.” *Procedia Eng.*, 64, 1089–1098.

Bandaru, A. K., Chavan, V. V., Ahmad, S., Alagirusamy, R., and Bhatnagar, N. (2016a). “Ballistic impact response of Kevlar® reinforced thermoplastic composite armors.” *Int. J. Impact Eng.*, 89, 1–13.

Bandaru, A. K., Patel, S., Sachan, Y., Alagirusamy, R., Bhatnagar, N., and Ahmad, S. (2016b). “Low velocity impact response of 3D angle-interlock Kevlar/basalt reinforced polypropylene composites.” *Mater. Des.*, 105, 323–332.

Basak, G. C., Bandyopadhyay, A., and Bhowmick, A. K. (2010). “International Journal of Adhesion & Adhesives Effect of tackifier compatibility and blend viscoelasticity on peel strength behavior of vulcanized EPDM rubber co-cured with unvulcanized rubber.” *Int. J. Adhes. Adhes.*, 30(6), 489–499.

Basavarajappa, S., Arun, K. V, and Davim, J. P. (2009). “Effect of Filler Materials on Dry Sliding Wear Behavior of Polymer Matrix Composites – A Taguchi Approach.” *Mater. Charact.*, 8(5), 379–391.



- Bax, B., and Müssig, J. (2008). "Impact and tensile properties of PLA/Cordenka and PLA/flax composites." *Compos. Sci. Technol.*, 68(7–8), 1601–1607.
- Belton, V. (1986). "A comparison of the analytic hierarchy process and a simple multi-attribute value function." *Eur. J. Oper. Res.*, 26(1), 7–21.
- Bensadoun, F., Depuydt, D., Baets, J., Verpoest, I., and Vuure, A. W. van. (2017). "Low velocity impact properties of flax composites." *Compos. Struct.*, 176, 933–944.
- Bhowmick, A., and Gent, A. (1984). "Effect of Interfacial Bonding on the Self-Adhesion of SBR and Neoprene." *Rubber Chem. Technol.*, 57(1), 216–226.
- Bhowmick, A. K., Loha, P., and Chakravarty, S. N. (1989). "Studies on adhesion between natural rubber and polybutadiene rubber." *Int. J. Adhes. Adhes.*, 9(2), 95–102.
- Bhushan, N. (2004). *Strategic decision making: applying the analytic hierarchy process*. London: Springer.
- Bienias, J., Jakubczak, P., and Dadej, K. (2016). "Low-velocity impact resistance of aluminium glass laminates - Experimental and numerical investigation." *Compos. Struct.*, 152, 339–348.
- Biron, M. (2007). *Thermoplastics and thermoplastic composites: technical information for plastics users*. Amsterdam: Butterworth-Heinemann.
- Blackley, D. (1997). *Polymer Lattices: Science and technology-Application of lattices*. London: Chapman and Hall.
- Bledzki, A. K., Jaszkiwicz, A., and Scherzer, D. (2009). "Mechanical properties of PLA composites with man-made cellulose and abaca fibres." *Compos. Part A Appl. Sci. Manuf.*, 40(4), 404–412.
- Bledzki, A. K., Mamun, A. A., Jaszkiwicz, A., and Erdmann, K. (2010). "Polypropylene composites with enzyme modified abaca fibre." *Compos. Sci. Technol.*, 70(5), 854–860.

Bloch, R. (1976). “Viscoelastic behaviour of filled and unfilled elastomers in moderately large deformations.” California institute of technology.

Bogenfeld, R., Kreikemeier, J., and Wille, T. (2018). “Review and benchmark study on the analysis of low-velocity impact on composite laminates.” *Eng. Fail. Anal.*, 86(December 2017), 72–99.

Børvik, T., Olovsson, L., Dey, S., and Langseth, M. (2011). “Normal and oblique impact of small arms bullets on AA6082-T4 aluminium protective plates.” *Int. J. Impact Eng.*, 38(7), 577–589.

Braga, F. de O., Bolzan, L. T., Lima, É. P., and Monteiro, S. N. (2017). “Performance of natural curaua fiber-reinforced polyester composites under 7.62 mm bullet impact as a stand-alone ballistic armor.” *J. Mater. Res. Technol.*, 6(4), 323–328.

Briggs, GAD; Briscoe, B. (1976). “Effect of roughness on rubber friction when waves of detachment are present.” *Nature*, 262, 381–382.

Brouwer, W. (1990). “Foam forming: a promising technology for the volume manufacture of ac sandwich components.” *6th Annu. ASM/ESD Adv. Compos. Conf.*, Detroit, USA.

Brown, K., Brooks, R., and Williamson, P. (2008). “Development of a novel thermoplastic composite sandwich structure for a rail application.” *SAMPE Eur. - 29th Int. Conf. Forum*, Paris, France, 220–225.

Byrd, L. W., and Birman, V. (2006). “Effectiveness of z-pins in preventing delamination of co-cured composite joints on the example of a double cantilever test.” *Compos. Part B Eng.*, 37(4–5), 365–378.

Cabrera, N. O., Alcock, B., and Peijs, T. (2008). “Design and manufacture of all-PP sandwich panels based on co-extruded polypropylene tapes.” *Compos. Part B Eng.*, 39(7–8), 1183–1195.

Callister, W. (2006). *Fundamentos da ciência e engenharia de materiais: uma*

*abordagem integrada*. Rio de Janeiro: LTC.

Caprino, G., Carrino, L., Durante, M., Langella, A., and Lopresto, V. (2015). "Low impact behaviour of hemp fibre reinforced epoxy composites." *Compos. Struct.*, 133, 892–901.

Carvelli, V., Gramellini, G., Lomov, S. V, Bogdanovich, A. E., Mungalov, D. D., and Verpoest, I. (2010). "Fatigue behavior of non-crimp 3D orthogonal weave and multi-layer plain weave E-glass reinforced composites." *Compos. Sci. Technol.*, 70(14), 2068–2076.

Céline, A., Fréour, S., Jacquemin, F., and Casari, P. (2014). "The hygroscopic behavior of plant fibers: A review." *Front. Chem.*, 1, 1–12.

Cerbu, C., and Botiș, M. (2017). "Numerical Modeling of the Flax / Glass / Epoxy Hybrid Composite Materials in Bending." *Procedia Eng.*, 181, 308–315.

Chakraborty, S., Chatterjee, P., and Prasad, K. (2018). "An Integrated DEMATEL – VIKOR Method-Based Approach for Cotton Fibre Selection and Evaluation." *J. Inst. Eng. Ser. E*, 99(1), 63–73.

Chan, W., Rogers, C., and Aker, S. (1986). "American Society for Testing and Materials." 266.

Chandra, R., and Mishra, S. (1995). *Rubber and Plastic Technology*. Denmark: CBS Press and Distributors.

Chandramohan, D., and Bharanichandar, J. (2013). "Natural Fiber Reinforced Polymer Composites for Automobile Accessories." *Am. J. Environ. Sci.*, 9(6), 494–504.

Chang, I. Y., and Lees, J. K. (1988). "Development in Thermoplastic Composites : A Review of Matrix Systems and Processing Methods Recent." *J. Thermoplast. Compos. Mater.*, 1, 277–296.

Charrier, J. (1990). *Polymer Materials and Processing*. Munich, Hanser Verlag.

Chatterjee, A. (1997). "Rigid body collisions: Some general considerations, new collision laws and some experimental data." Cornell University.

Chatterjee, P., Athawale, V. M., and Chakraborty, S. (2009). "Selection of materials using compromise ranking and outranking methods." *Mater. Des.*, 30(10), 4043–4053.

Chen, T. (2012). "Comparative analysis of SAW and TOPSIS based on interval-valued fuzzy sets: Discussions on score functions and weight constraints." *Expert Syst. Appl.*, 39(2), 1848–1861.

Chin, C. W., and Yousif, B. F. (2009). "Potential of kenaf fibres as reinforcement for tribological applications." *Wear*, 267(9–10), 1550–1557.

Chittineni, K. (2009). "Functionally gradient syntactic foams." Master of Science Thesis, Graduate Faculty of the Louisiana State University and Agricultural and Mechanical College, Louisiana.

Chou, T.-W. (1989). "Review Flexible Composites." *J. Mater. Sci.*, 24, 761–783.

Chou, T.-W., and Takahashi, K. (1987). "Non-linear elastic behaviour of flexible fibre composites." *Composites*, 18(1), 25–34.

Christensen, R. (1982). *Theory of viscoelasticity: An introduction*. New York: Academic press.

Christoforou, A. P., and Yigit, A. S. (1998). "Effect of flexibility on low velocity impact response." *J. Sound Vib.*, 217(3), 563–578.

D.H. Champ, E. Southern, A. G. T. (1974). "Fracture mechanics applied to rubber abrasion." *Am. Chem. Soc. Coat. Plast. Div. Prepr.*, 34(1), 237.

D'Almeida, A. L. F. S., Calado, V., Barreto, D. W., and D'Almeida, J. R. M. (2011). "Effect of surface treatments on the dynamic mechanical behavior of piassava fiber-polyester matrix composites." *J. Therm. Anal. Calorim.*, 103(1), 179–184.

- Dan, M., Yong, L., Tao, S., Lin, F., Peng, W., and Jun, X. (2011). "Tensile properties of Z-pins reinforced laminates." *Polym. Polym. Compos.*, 19(4–5), 251–258.
- Dang, C. Y., Tang, B. L., Zeng, X. L., Xu, J., Feng, M. J., Jiang, Y., and Shen, X. J. (2019). "Improved interlaminar shear strength of glass fiber/epoxy composites by graphene oxide modified short glass fiber." *Mater. Res. Express*.
- Daniels, B. K., Harakas, N. K., and Jackson, R. C. (1971). "Short beam shear tests of graphite fiber composites." *Fibre Sci. Technol.*, 3(3), 187–208.
- Desai, S., Bidanda, B., and Lovell, M. R. (2012). "Material and process selection in product design using decision-making technique (AHP)." *Eur. J. Ind. Eng.*, 6(3), 322–346.
- Dey, S., and Karmakar, A. (2014). "Effect of oblique angle on low velocity impact response of delaminated composite conical shells." *Proc. Inst. Mech. Eng. Part C J. Mech. Eng. Sci.*, 228(15), 2663–2677.
- Dhakal, H. N., Skrifvars, M., Adekunle, K., and Zhang, Z. Y. (2014). "Falling weight impact response of jute/methacrylated soybean oil bio-composites under low velocity impact loading." *Compos. Sci. Technol.*, 92, 134–141.
- Dhakal, H. N., Zhang, Z. Y., Bennett, N., and Reis, P. N. B. (2012). "Low-velocity impact response of non-woven hemp fibre reinforced unsaturated polyester composites: Influence of impactor geometry and impact velocity." *Compos. Struct.*, 94(9), 2756–2763.
- Doan, T. T. L., Brodowsky, H., and Mäder, E. (2007). "Jute fibre/polypropylene composites II. Thermal, hydrothermal and dynamic mechanical behaviour." *Compos. Sci. Technol.*, 67(13), 2707–2714.
- Duc, F., Bourban, P. E., and Månson, J. A. E. (2014a). "Dynamic mechanical properties of epoxy/flax fibre composites." *J. Reinf. Plast. Compos.*, 33(17), 1625–1633.

Duc, F., Bourban, P. E., Plummer, C. J. G., and Månson, J. A. E. (2014b). “Damping of thermoset and thermoplastic flax fibre composites.” *Compos. Part A Appl. Sci. Manuf.*, 64, 115–123.

Düring, D., Weiß, L., Stefaniak, D., Jordan, N., and Hühne, C. (2015). “Low-velocity impact response of composite laminates with steel and elastomer protective layer.” *Compos. Struct.*, 134, 18–26.

Dwivedi, U., Ghosh, A., and Chand, N. (2007). “Abrasive wear behaviour of bamboo (*dendrocalamus strictus*) powder filled polyester composites.” *BioResources*, 2(4), 693–698.

El-Sayed, a. a., El-Sherbiny, M. G., Abo-El-Ezz, a. S., and Aggag, G. a. (1995). “Friction and wear properties of polymeric composite materials for bearing applications.” *Wear*, 184(1), 45–53.

El-Tayeb, N. S. M. (2007). “A study on the potential of sugarcane fibers/polyester composite for tribological applications.” *Wear*, 265(1–2), 223–235.

Elias, A., Laurin, F., Kaminski, M., and Gornet, L. (2017). “Experimental and numerical investigations of low energy/velocity impact damage generated in 3D woven composite with polymer matrix.” *Compos. Struct.*, 159, 228–239.

Essabir, H., Achaby, M. E. I., Hilali, E. M., Bouhfid, R., and Qaiss, A. Ei. (2015). “Morphological, Structural, Thermal and Tensile Properties of High Density Polyethylene Composites Reinforced with Treated Argan Nut Shell Particles.” *J. Bionic Eng.*, 12(1), 129–141.

Essabir, H., Elkhaoulani, A., Benmoussa, K., Bouhfid, R., Arrakhiz, F. Z., and Qaiss, A. (2013). “Dynamic mechanical thermal behavior analysis of doum fibers reinforced polypropylene composites.” *Mater. Des.*, 51, 780–788.

Etaati, A., Mehdizadeh, S. A., Wang, H., and Pather, S. (2014a). “Vibration damping characteristics of short hemp fibre thermoplastic composites.” *J. Reinf. Plast. Compos.*, 33(4), 330–341.

Etaati, A., Pather, S., Fang, Z., and Wang, H. (2014b). "The study of fibre/matrix bond strength in short hemp polypropylene composites from dynamic mechanical analysis." *Compos. Part B Eng.*, 62, 19–28.

Fahim, M., and Chand, N. (2008). "Introduction to tribology of polymer composites." *Tribol. Nat. Fiber Polym. Compos.*, Woodhead Publishing, 59–83.

Fahmi, I., Abdul Majid, M., Afendi, M., Helmi, E., and Haameem, J. (2016). "Low velocity impact responses of Napier fibre/polyester composites." *Int. J. Automot. Mech. Eng.*, 13(1), 3226–3237.

Fan, Z., Santare, M. H., and Advani, S. G. (2008). "Interlaminar shear strength of glass fiber reinforced epoxy composites enhanced with multi-walled carbon nanotubes." *Compos. Part A Appl. Sci. Manuf.*, 39(3), 540–554.

Farahmand, P., Frosell, T., and Mcgregor, M. (2015). "Comparative study of the slurry erosion behavior of laser clad Ni-WC coating modified by nanocrystalline WC and La<sub>2</sub>O<sub>3</sub>." *Int. J. Adv. Manuf. Technol.*, 79, 1607–1621.

Fatt, H., and Park, K. (2001). "Dynamic models for low velocity impact damage of composite sandwich panels – Part A: deformation." *Compos. Struct.*, 52, 335–351.

Fawaz, Z., Zheng, W., and Behdinin, K. (2004). "Numerical simulation of normal and oblique ballistic impact on ceramic composite armours." *Compos. Struct.*, 63(3–4), 387–395.

Feraboli, P., and Kedward, K. T. (2006). "A new composite structure impact performance assessment program." *Compos. Sci. Technol.*, 66(10), 1336–1347.

Ferrante, L., Sarasini, F., Tirillò, J., Lampani, L., Valente, T., and Gaudenzi, P. (2016). "Low velocity impact response of basalt-aluminium fibre metal laminates." *Mater. Des.*, 98, 98–107.

Ferringo, T. (1978). *Handbook of fillers and reinforcements for plastics*. New York: Van Nostrand Reinhold.

Flynn, J., Amiri, A., and Ulven, C. (2016). “Hybridized carbon and flax fiber composites for tailored performance.” *Mater. Des.*, 102, 21–29.

Freitas, S. T. De, Zarouchas, D., and Poulis, J. A. (2018). “The use of acoustic emission and composite peel tests to detect weak adhesion in composite structures.” *J. Adhes.*, 00(00), 1–24.

Friedrich, K. (2018). “Polymer composites for tribological applications.” *Adv. Ind. Eng. Polym. Res.*, 1(1), 3–39.

Friedrich, K., Lu, Z., and Hager, A. M. (1995). “Recent advances in polymer composites’ tribology.” *Wear*, 190(2), 139–144.

Friedrich, K., Reinicke, R., and Zhang, Z. (2002). “Wear of polymer composites.” *Proc. Inst. Mech. Eng. , Part J J. Eng. Tribol.*, 216, 415–426.

Gangil, M., and Pradhan, M. K. (2018). “Optimization the machining parameters by using VIKOR Method during EDM process of Titanium alloy.” *Mater. Today Proc.*, 5(2), 7486–7495.

Garg, M., Sharma, S., and Mehta, R. (2015). “Pristine and amino functionalized carbon nanotubes reinforced glass fiber epoxy composites.” *Compos. Part A Appl. Sci. Manuf.*, 76, 92–101.

Geethamma, V. G., Kalaprasad, G., Groeninckx, G., and Thomas, S. (2005). “Dynamic mechanical behavior of short coir fiber reinforced natural rubber composites.” *Compos. Part A Appl. Sci. Manuf.*, 36(11), 1499–1506.

Gent, A. (1996). “A new constitutive relation for rubber.” *Rubber Chem. Technol.*, 69(4), 59–61.

George, J., Bhagawan, S. S., and Thomas, S. (1996). “Thermogravimetric and dynamic mechanical thermal analysis of pineapple fiber reinforced polyethylene composites.” *J. Therm. Anal.*, 47, 1121–1140.

Gilardi, G., and Sharf, I. (2002). “Literature survey of contact dynamics modelling.”



*Mech. Mach. Theory*, 37, 1213–1239.

Gopinath, G., Zheng, J. Q., and Batra, R. C. (2012). “Effect of matrix on ballistic performance of soft body armor.” *Compos. Struct.*, 94(9), 2690–2696.

Grosch, KA and Schallamach, A. (1965). “Relation between abrasion and strength of rubber.” *Trans. Inst. Rubber Ind*, 41, 80–82.

Grosch, K. (1990). *The abrasion of rubber, in: K. Anil, S.K.De Bhowmick (Eds.), Fractography of Rubbery Materials*. London: Elsevier Ltd.

Guo, C., Song, Y., Wang, Q., and Shen, C. (2006). “Dynamic-mechanical analysis and SEM morphology of wood flour/polypropylene composites.” *J. For. Res.*, 17(4), 315–318.

Guo, Q., Cheng, B., Kortschot, M., Sain, M., Knudson, R., Deng, J., and Alemdar, A. (2010). “Performance of long Canadian natural fibers as reinforcements in polymers.” *J. Reinf. Plast. Compos.*, 29(21), 3197–3207.

Gupta, N. (2003). “Characterization of syntactic foams and their sandwich composites: modelling and experimental approaches.” Graduate faculty of the Louisiana state university and Agricultural and Mechanical college, Louisiana.

Gupta, N., and Woldeesenbet, E. (2009). “Microscopic Studies of Syntactic Foams Tested Under Three-Point Bending Conditions.” *Eng. Technol. Conf. energy*, Texas, USA: ASME, 147–152.

Gupta, N., Ye, R., and Porfiri, M. (2010). “Comparison of tensile and compressive characteristics of vinyl ester/glass microballoon syntactic foams.” *Compos. Part B Eng.*, 41(3), 236–245.

Habibi, M., Laperrière, L., and Hassanabadi, H. M. (2018). “Influence of low-velocity impact on residual tensile properties of nonwoven flax/epoxy composite.” *Compos. Struct.*, 186(May 2017), 175–182.

Hajiha, H., and Sain, M. (2015). “High toughness hybrid biocomposite process

optimization.” *Compos. Sci. Technol.*, 111, 44–49.

Hammiche, D., Boukerrou, A., Djidjelli, H., Corre, Y., Grohens, Y., and Pillin, I. (2013). “Hydrothermal ageing of alfa fiber reinforced polyvinylchloride composites.” *Constr. Build. Mater.*, 47, 293–300.

Hancox, N. (2000). “An overview of the impact behavior of fibre-reinforced composites.” *Impact Behav. fiber-reinforced Compos. Mater. Struct.*, S. Reid and G. Zhou, eds., CRC Press.

Haque, M. M., Islam, M. S., and Islam, M. N. (2012). “Preparation and characterization of polypropylene composites reinforced with chemically treated coir.” *J. Polym. Res.*, 19(5).

Haro, E. E., Szpunar, J. A., and Odeshi, A. G. (2018). “Dynamic and ballistic impact behavior of biocomposite armors made of HDPE reinforced with chonta palm wood ( *Bactris gasipaes* ) microparticles.” *Def. Technol.*, 14(3), 238–249.

Herrera-Franco, P. J., and Valadez-González, A. (2005). “A study of the mechanical properties of short natural-fiber reinforced composites.” *Compos. Part B Eng.*, 36(8), 597–608.

Holbery, J., and Houston, D. (2006). “Natural-fibre-reinforced polymer composites in automotive applications.” *J. Miner. Met. Mater. Soc.*, 58(11), 80–86.

Hossain, M. R., Islam, M. a, Vuurea, a V, and Verpoest, I. (2013). “Effect of Fiber Orientation on the Tensile Properties of Jute Epoxy Laminated Composite.” *J. Sci. Res.*, 5, 43.54.

Huang, H., Liu, Z., Zhang, L., and Sutherland, J. W. (2009). “Materials selection for environmentally conscious design via a proposed life cycle environmental performance index.” *Int. J. Adv. Manuf. Technol.*, 44(11–12), 1073–1082.

Husain, A., Ansari, R., and Khan, A. H. (2017). “Experimental and numerical investigation of perforation of thin polycarbonate plate by projectiles of different nose

shape.” *Lat. Am. J. Solids Struct.*, 14(2), 357–372.

Hutchings, I. M. (1992). *Tribology; Friction and Wear of Engineering Materials*. London: CRC Press.

Ibrahim, A. H. (2014). “Imece2012-86016 Finite Element Modeling and Analysis of Low Velocity Impact on.” 1–12.

Ishai, O., and Cohen, L. J. (1967). “Elastic properties of filled and porous epoxy composites.” *Int. J. Mech. Sci.*, 9, 539–546.

Ivančević, D., and Smojver, I. (2016). “Explicit multiscale modelling of impact damage on laminated composites - Part I: Validation of the micromechanical model.” *Compos. Struct.*, 145, 248–258.

Ivañez, I., Barbero, E., and Sanchez-Saez, S. (2014). “Analytical study of the low-velocity impact response of composite sandwich beams.” *Compos. Struct.*, 111(1), 459–467.

Ivañez, I., Moure, M. M., Garcia-Castillo, S. K., and Sanchez-Saez, S. (2015). “The oblique impact response of composite sandwich plates.” *Compos. Struct.*, 133, 1127–1136.

Jackson, C., and Pascual, R. (2008). “Optimal maintenance service contract negotiation with aging equipment.” *Eur. J. Oper. Res.*, 189(2), 387–398.

Jagtap, K. R., Ghorpade, S. Y., Lal, A., and Singh, B. N. (2017). “Finite Element Simulation of Low Velocity Impact Damage in Composite Laminates.” *Mater. Today Proc.*, 4(2), 2464–2469.

Jahan, A., Ismail, M. Y., Sapuan, S. M., and Mustapha, F. (2010). “Material screening and choosing methods – A review.” *Mater. Des.*, 31(2), 696–705.

Jawaid, M., Abdul Khalil, H. P. S., Hassan, A., Dungani, R., and Hadiyane, A. (2013). “Effect of jute fibre loading on tensile and dynamic mechanical properties of oil palm epoxy composites.” *Compos. Part B Eng.*, 45(1), 619–624.

Jeya Girubha, R., and Vinodh, S. (2012). “Application of fuzzy VIKOR and environmental impact analysis for material selection of an automotive component.” *Mater. Des.*, 37, 478–486.

Jia, J., Du, X., Chen, C., Sun, X., Mai, Y. W., and Kim, J. K. (2015). “3D network graphene interlayer for excellent interlaminar toughness and strength in fiber reinforced composites.” *Carbon N. Y.*, 95, 978–986.

Johnson, S., Kang, L., and Akil, H. M. (2016). “Mechanical behavior of jute hybrid bio-composites.” *Compos. Part B Eng.*, 91, 83–93.

Joseph, S., Sreekumar, P., Kenny, J., Puglia, D., Thomas, S., and Joseph, K. (2010a). “Dynamic mechanical analysis of oil palm microfibril-reinforced acrylonitrile butadiene rubber composites.” *Polym. Compos.*, 31(2), 236–244.

Joseph, S., Sreekumar, P., Kenny, J., Puglia, D., Thomas, S., and Joseph, K. (2010b). “Dynamic mechanical properties of oil palm microfibril-reinforced natural rubber composites.” *J. Appl. Polym. Sci.*, 117(5), 1298–1308.

Joshi, A. G., Kumar, M. P., and Basavarajappa, S. (2014). “Influence of Al<sub>2</sub>O<sub>3</sub> Filler on Slurry Erosion Behavior of Glass/Epoxy Composites.” *Procedia Mater. Sci.*, 5, 863–872.

Jost, H. (2009). *The Presidential address.*, In: *World tribology congress*. Japan.

Jover, N., Shafiq, B., and Vaidya, U. (2014). “Ballistic impact analysis of balsa core sandwich composites.” *Compos. Part B Eng.*, 67, 160–169.

Judawisastra, H., Sitohang, R. D. R., and Rosadi, M. S. (2017). “Water absorption and tensile strength degradation of Petung bamboo ( *Dendrocalamus asper* ) fiber — reinforced polymeric composites.” *Mater. Res. Express*, 4(July).

Kabir, M., Wang, H., Aravinthan, T., Cardona, F., and Lau, K. (2011). “Effects of Natural Fibre Surface on Composite Properties: A Review.” *1st Int. Postgrad. Conf. Eng. Des. Dev. Built Environ. Sustain. Wellbeing*, Brisbane, Australia.

Karaduman, Y., Sayeed, M. M. A., Onal, L., and Rawal, A. (2014). “Viscoelastic properties of surface modified jute fiber/polypropylene nonwoven composites.” *Compos. Part B Eng.*, 67, 111–118.

Karas, K. (1939). “Plates under lateral impact.” *Arch. Appl. Mech.*, 10, 237–250.

Kärger, L., Baaran, J., Gunnion, A., and Thomson, R. (2009). “Evaluation of impact assessment methodologies. Part I: Applied methods.” *Compos. Part B Eng.*, 40(1), 65–70.

Karus, D. M., Ortmann, D. S., Gahle, D. C., and Pendarovski, D. C. (2006). *Use of natural fibres in composites for the German automotive production from 1999 till 2005*.

Ketabchi, M. R., Khalid, M., Ratnam, C. T., and Walvekar, R. (2016). “Mechanical and thermal properties of polylactic acid composites reinforced with cellulose nanoparticles extracted from kenaf fibre.” *Mater. Res. Express*, 3(12).

Khalil, A. H. P. S., Masri, M., Saurabh, C. K., Fazita, M. R. N., Azniwati, A. A., Sri Aprilia, N. A., Rosamah, E., and Dungani, R. (2017). “Incorporation of coconut shell based nanoparticles in kenaf/coconut fibres reinforced vinyl ester composites.” *Mater. Res. Express*, 4(3).

Khan, S. U., and Kim, J. (2012). “Interlaminar Shear Properties of CFRP Composites with CNF- Bucky Paper Interleaves.” *18th Int. Conf. Compos. Mater.*, 1–6.

Khodadadi, A., Liaghat, G., Ahmadi, H., Bahramian, A. R., and Razmkhah, O. (2019a). “Impact response of Kevlar/rubber composite.” *Compos. Sci. Technol.*, 184(October), 107880.

Khodadadi, A., Liaghat, G., Reza, A., Ahmadi, H., Anani, Y., Asemiani, S., and Razmkhah, O. (2019b). “High velocity impact behavior of Kevlar / rubber and Kevlar / epoxy composites : A comparative study.” *Compos. Struct.*, 216, 159–167.

Khodadadi, A., Liaghat, G., Vahid, S., Sabet, A. R., and Hadavinia, H. (2019c).

“Ballistic performance of Kevlar fabric impregnated with nanosilica / PEG shear thickening fluid.” *Compos. Part B*, 162, 643–652.

Kim, E. H., Rim, M. S., Lee, I., and Hwang, T. K. (2013). “Composite damage model based on continuum damage mechanics and low velocity impact analysis of composite plates.” *Compos. Struct.*, 95, 123–134.

Kim, J. K., and Mai, Y. wing. (1991). “High strength, high fracture toughness fibre composites with interface control-A review.” *Compos. Sci. Technol.*, 41(4), 333–378.

Kim, J. W., and Lee, J. S. (2016). “Influence of interleaved films on the mechanical properties of carbon fiber fabric/polypropylene thermoplastic composites.” *Materials (Basel)*, 9(5), 1–12.

Kling, S., and Czigány, T. (2014). “Damage detection and self-repair in hollow glass fiber fabric-reinforced epoxy composites via fiber filling.” *Compos. Sci. Technol.*, 99, 82–88.

Koskela, K., Lindgren, M., and Serna-guerrero, R. (2017). “Slurry erosion resistance of polyethylene under conditions relevant for mineral processing.” *Wear*, 392–393(September), 1–7.

Kozłowski, R., and Władyska-Przybylak, M. (2008). “Flammability and Fire Resistance of Composites Reinforced by Natural Fibers.” *Polym. Adv. Technol.*, 19, 446–453.

Krishan K Chawla. (2012). *Composite Materials*. Springer.

Kuan, H. T. N., Lee, M. C., Khan, A. A., and Sawawi, M. (2017). “The Low Velocity Impact Properties of Pandanus Fiber Composites.” *Mater. Sci. Forum*, 895, 56–60.

Kulandaivel, P. (2006). “Manufacturing and performance of thermoplastic composite sandwich structures.” University of Nottingham, UK.

Kulandaivel, P., Brooks, R., and Dunmore, M. (2005). “Processing and performance of thermoplastic composite sandwich beams for automotive applications.” *37th Int.*

*SAMPE Tech. Conf.*, Seattle, USA.

Kulkarni, S. M. (2002). "Processing, microstructural and mechanical behavior aspects of flyash-epoxy composites." Indian institute of Science, Bengaluru.

Kumar, R., and Singal, S. K. (2015). "Penstock material selection in small hydropower plants using MADM methods." *Renew. Sustain. Energy Rev.*, 52, 240–255.

Kumar, S., Kuriachen, B., Kumar, N., and Nateriya, R. (2018a). "The slurry abrasive wear behaviour and microstructural analysis of A2024- SiC-ZrSiO<sub>4</sub> metal matrix composite." *Ceram. Int.*, 44(6), 6426–6432.

Kumar, S., Nateriya, R., Kuriachen, B., and Pratap, V. (2018b). "Slurry abrasive wear , microstructural and morphological analysis of titanium carbide and zirconium sand aluminium alloy ( A5052 ) metal matrix composite." *Mater. Today Proc.*, 5(9), 19790–19798.

Kwakernaak, A., Hofstede, J., Poulis, J., and Benedictus, R. (2012). "Improvements in bonding metals for aerospace and other applications." *Weld. Join. Aerosp. Mater.*, Woodhead Publishing Limited, 235–287.

Laly, A. P., Zachariah, O., and Sabu, T. (2003). "Dynamic mechanical analysis of banana fiber reinforced polyester composites." *Compos. Sci. Technol.*, 63, 283–293.

Langhorst, A. E., Burkholder, J., Long, J., Thomas, R., Kiziltas, A., and Mielewski, D. (2018). "Blue-agave fiber-reinforced polypropylene composites for automotive applications." *BioResources*, 13(1), 820–835.

Lau, K. tak, Hung, P. yan, Zhu, M. H., and Hui, D. (2018). "Properties of natural fibre composites for structural engineering applications." *Compos. Part B Eng.*, 136(October 2017), 222–233.

Lee, B. L., Walsh, T. F., Won, S. T., Patts, H. M., Song, J. W., and Mayer, A. H. (2001). "Penetration Failure Mechanisms of Armor-Grade Fiber Composites under

Impact.” *J. Compos. Mater.*, 35(18), 1605–1633.

Lee, S.-Y., Kang, I.-A., Park, B.-S., Doh, G.-H., and Park, B.-D. (2009). “Effects of Filler and Coupling Agent on the Properties of Bamboo Fiber-Reinforced Polypropylene Composites.” *J. Reinf. Plast. Compos.*, 28(21), 2589–2604.

Levy, A. V., and Crook, P. (1991). “The erosion properties of alloys for the chemical processing industries.” *Wear*, 151(2), 337–350.

Li, X., He, L., Zhou, H., Li, W., and Zha, W. (2012). “Influence of silicone oil modification on properties of ramie fiber reinforced polypropylene composites.” *Carbohydr. Polym.*, 87(3), 2000–2004.

Li, Z., Khennane, A., Hazell, P. J., and Brown, A. D. (2017). “Impact behaviour of pultruded GFRP composites under low-velocity impact loading.” *Compos. Struct.*, 168, 360–371.

Lindgren, M., and Perolainen, J. (2014). “Slurry pot investigation of the influence of erodant characteristics on the erosion resistance of titanium.” *Wear*, 321, 64–69.

Liu, C., Zhang, Y. X., and Ye, L. (2017). “High velocity impact responses of sandwich panels with metal fibre laminate skins and aluminium foam core.” *Int. J. Impact Eng.*, 100, 139–153.

Liu, F., Chen, G., Li, L., and Guo, Y. (2012). “Study of impact performance of rubber reinforced concrete.” *Constr. Build. Mater.*, 36, 604–616.

Liu, F., Kong, X., Zheng, C., Xu, S., Wu, W., and Chen, P. (2018a). “The influence of rubber layer on the response of fluid-filled container due to high-velocity impact.” *Compos. Struct.*, 183(1), 671–681.

Liu, H., Wu, Q., and Zhang, Q. (2009). “Preparation and properties of banana fiber-reinforced composites based on high density polyethylene (HDPE)/Nylon-6 blends.” *Bioresour. Technol.*, 100(23), 6088–6097.

Liu, M. (2010). *Constitutive equations for the dynamic response of rubber*. Akron.



- Liu, M., and Hoo Fatt, M. S. (2011). "A constitutive equation for filled rubber under cyclic loading." *Int. J. Non. Linear. Mech.*, 46(2), 446–456.
- Liu, Y., Ma, Y., Che, J., Duanmu, L., Zhuang, J., and Tong, J. (2018b). "Natural fibre reinforced non-asbestos organic non-metallic friction composites: Effect of abaca fibre on mechanical and tribological behaviour." *Mater. Res. Express*, 5(5).
- Loha, P., Bhowmick, A. K., and Chakravarty, S. N. (1987). "Modification of the Peel Test for Testing of Rubber- to-Rubber Joints." *Polym. Test.*, 7, 153–163.
- Long, S., Yao, X., and Zhang, X. (2015). "Delamination prediction in composite laminates under low-velocity impact." *Compos. Struct.*, 132, 290–298.
- Madeed-Al, M., and Labidi, S. (2014). "Recycled polymers in natural fibre-reinforced polymer composites." *Nat. fibre Compos.*, A. Hodzic and R. Shanks, eds., Woodhead Publishing Limited, 103–114.
- Madjidi, S., Arnold, W. S., and Marshall, I. H. (1996). "Damage tolerance of CSM laminates subject to low velocity oblique impacts." *Compos. Struct.*, 34(1), 101–116.
- Mahendra, K. V, and Radhakrishna, K. (2007). "Fabrication of Al – 4 . 5 % Cu alloy with fly ash metal matrix composites and its characterization." *Mater. Sci. - Pol.*, 25(1), 57–68.
- Mahesh, V., Joladarashi, S., and Kulkarni, S. M. (2019). "Development and mechanical characterization of novel polymer-based flexible composite and optimization of stacking sequences using VIKOR and PSI techniques." *J. Thermoplast. Compos. Mater.*, 1–23.
- Mahesh, V., Mahesh, V., and Puneeth, K. (n.d.). "Influence of Areca Nut Nano Filler on Mechanical and Tribological Properties of Coir Fiber Reinforced Epoxy Based Polymer Composite." *Sci. Iran. Trans. Mech. Eng.*
- Mahmood, N., and Busse, K. (2006). "Investigations on the Adhesion and Interfacial Properties of Polyurethane Foam / Thermoplastic Materials." *J. Appl. Polym. Sci.*,

104, 479–488.

Maio, L., Monaco, E., Ricci, F., and Lecce, L. (2013). “Simulation of low velocity impact on composite laminates with progressive failure analysis.” *Compos. Struct.*, 103, 75–85.

Maity, S. R., and Chakraborty, S. (2013). “Grinding wheel abrasive material selection using fuzzy TOPSIS method.” *Mater. Manuf. Process.*, 28(4), 408–417.

Majid, D. L., Mohd Jamal, Q., and Manan, N. H. (2018). “Low-velocity Impact Performance of Glass Fiber, Kenaf Fiber, and Hybrid Glass/Kenaf Fiber Reinforced Epoxy Composite Laminates.” *BioResources*, 11(4), 8839–8852.

Malekzadeh, K., Khalili, M. R., and Mittal, R. K. (2006). “Analytical prediction of low-velocity impact response of composite sandwich panels using new TDOF spring-mass-damper model.” *J. Compos. Mater.*, 40(18), 1671–1689.

Mamivand, M., and Liaghat, G. H. (2010). “A model for ballistic impact on multi-layer fabric targets.” *Int. J. Impact Eng.*, 37(7), 806–812.

Mamtaz, H., Fouladi, M. H., Al-Atabi, M., and Namasivayam, S. N. (2016). “Acoustic absorption of natural fiber composites.” *J. Eng.*, 2016, 1–11.

Manikandan Nair, K. C., Thomas, S., and Groeninckx, G. (2001). “Thermal and dynamic mechanical analysis of polystyrene composites reinforced with short sisal fibres.” *Compos. Sci. Technol.*, 61(16), 2519–2529.

Maniya, K., and Bhatt, M. G. (2010). “A selection of material using a novel type decision-making method: Preference selection index method.” *Mater. Des.*, 31(4), 1785–1789.

Manoj, M. K., Galgali, R. K., Nath, S. K., and Ray, S. (2008). “Synthesis, characterization and effect of microstructure on slurry erosion resistance of cast Fe-TiC composites.” *J. Nav. Archit. Mar. Eng.*, 5, 19–26.

Mardani, A., Jusoh, A., Nor, K. M. D., Khalifah, Z., Zakwan, N., and Valipour, A.

(2015). “Multiple criteria decision-making techniques and their applications - A review of the literature from 2000 to 2014.” *Econ. Res. Istraz.* , 28(1), 516–571.

Margem, F. M., Monteiro, S. N., Neto, J. B., Jesus, R., and Rodriguez, S. (2010). “The dynamic-mechanical behavior of epoxy matrix composites reinforced with ramie fibers.” *Rev. Mater.*, 15(2), 164–171.

Mark, J. (1999). *Polymer Data Hand Book*. Newyork: Oxford University Press.

Martínez-Hernández, A. L., Velasco-Santos, C., de-Icaza, M., and Castaño, V. M. (2007). “Dynamical-mechanical and thermal analysis of polymeric composites reinforced with keratin biofibers from chicken feathers.” *Compos. Part B Eng.*, 38(3), 405–410.

Mateo, J. (2011). *Multi-Criteria Analysis in the Renewable Energy Industry*. New York: Springer London.

Mathivanan, N. R., and Jerald, J. (2010). “Experimental Investigation of Woven E-Glass Epoxy Composite Laminates Subjected to Low-Velocity Impact at Different Energy Levels.” *J. Miner. Mater. Charact. Eng.*, 09(07), 643–652.

Mazuki, A. A. M., Akil, H. M., Safiee, S., Ishak, Z. A. M., and Bakar, A. A. (2011). “Degradation of dynamic mechanical properties of pultruded kenaf fiber reinforced composites after immersion in various solutions.” *Compos. Part B Eng.*, 42(1), 71–76.

Mazumdar, S. (2002). *Composites Manufactuirng: Materials, Product and Process Engineeirng. Science (80-. )*, Boca Raton, London, New York, Washington DC: CRC Press.

McGarva, L. D., and Åström, B. T. (1999). “Experimental investigation of compression moulding of glass/PA 12-PMI foam core sandwich components.” *Compos. Part A Appl. Sci. Manuf.*, 30(10), 1171–1185.

Mei, H., Han, D., Farhan, S., Cheng, L., Xu, H., and Liu, Y. (2016). “Impact behavior of different cross-ply laminated carbon fiber-reinforced silicon carbide composites

under the low velocity.” *J. Compos. Mater.*, 50(8), 1137–1142.

Meybodi, M., Mohammadkhani, H., and Bagheri, M. (2016). “Oblique Low-Velocity Impact on Fiber-Metal Laminates.” *Appl. Compos. Mater.*, 24(3), 611–623.

Minamoto, H., and Kawamura, S. (2009). “Effects of material strain rate sensitivity in low speed impact between two identical spheres.” *Int. J. Impact Eng.*, 36(5), 680–686.

Mir, A., Aribi, C., and Bezzazi, B. (2014). “Study of the green composite jute/epoxy.” *Int. J. Mater. Metall. Eng.*, 8(2), 182–186.

Mishra, A. (2012). “Dry Sliding Wear Behavior of Epoxy-Rubber Dust Composites.” *Int. J. Mech. Mechatronics Eng.*, 6(7), 1218–1223.

Mishra, P., and Acharya, S. K. (2010). “Anisotropy abrasive wear behavior of bagasse fiber reinforced polymer composite.” *Int. J. Eng. Sci. Technol.*, 2(11), 104–112.

MJ, J., and Anandjiwala, R. (2008). “Recent Developments in Chemical Modification and Characterization of Natural Fiber-Reinforced Composites.” *Polym. Compos.*, 29, 187–207.

Mohammed, L., Ansari, M. N. M., Pua, G., Jawaid, M., and Islam, M. S. (2015). “A Review on Natural Fiber Reinforced Polymer Composite and Its Applications.” *Int. J. Polym. Sci.*, 2015, 1–15.

Mohanty, A. K., Misra, M., and Drzal, L. T. (2005). *Natural Fibers, Biopolymers, and Biocomposites*. CRC Press.

Mohanty, S., and Nayak, S. K. (2010). “Short bamboo fiber-reinforced HDPE composites: Influence of fiber content and modification on strength of the composite.” *J. Reinf. Plast. Compos.*, 29(14), 2199–2210.

Mohanty, S., Verma, S. K., and Nayak, S. K. (2006). “Dynamic mechanical and thermal properties of MAPE treated jute/HDPE composites.” *Compos. Sci. Technol.*, 66(3–4), 538–547.

- Monteiro, S. N., Lopes, F. P. D., Ferreira, A. S., and Nascimento, D. C. O. (2009). "Natural-fiber polymer-matrix composites: Cheaper, tougher, and environmentally friendly." *Jom*, 61(1), 17–22.
- Mooney, M. (1940). "A theory of large elastic deformation." *J. Appl. Phys.*, 11(9), 582–592.
- Morada, G., Ouadday, R., Vadean, A., and Boukhili, R. (2017). "Low-velocity impact resistance of ATH/epoxy core sandwich composite panels: Experimental and numerical analyses." *Compos. Part B Eng.*, 114, 418–431.
- Mullins, L. (1947). "Studies in absorption of energies by rubber- 1 introductory survey mullin." *J. rubber Res.*, 16(1), 180–185.
- Muzzy, J., Pfaendter, J., and Shaw, B. (2001). "Thermoplastic composite sandwich panels." *Automot. Compos. Conf.*, Troy, USA.
- Mwaikambo, L. (2009). "Tensile Properties of Alkalised Jute Fibres." *BioResources*, 4, 566–588.
- Mylsamy, K., and Rajendran, I. (2011). "The mechanical properties, deformation and thermomechanical properties of alkali treated and untreated Agave continuous fibre reinforced epoxy composites." *Mater. Des.*, 32(5), 3076–3084.
- Naik, N. K. Ā., Shrirao, P., and Reddy, B. C. K. (2006). "Ballistic impact behaviour of woven fabric composites : Formulation." *Int. J. impact Eng.*, 32, 1521–1552.
- Nalla Mohamed, M., Ananthapadmanaban, D., and Selvaraj, M. (2016). "Numerical Modeling of Energy Absorption Behaviour of Aluminium Foam Cored Sandwich Panels with Different Fibre Reinforced Polymer (FRP) Composite Facesheet Skins." *Appl. Mech. Mater.*, 852, 66–71.
- Nash, N. H., Young, T. M., McGrail, P. T., and Stanley, W. F. (2015). "Inclusion of a thermoplastic phase to improve impact and post-impact performances of carbon fibre reinforced thermosetting composites - A review." *Mater. Des.*, 85, 582–597.

Nasir Hussain, N., Prakash Regalla, S., and Daseswara Rao, Y. V. (2017). “Low velocity Impact Characterization of Glass Fiber Reinforced Plastics for Application of Crash Box.” *Mater. Today Proc.*, 4(2), 3252–3262.

Navarro, P., Aubry, J., Marguet, S., Ferrero, J. F., Lemaire, S., and Rauch, P. (2012). “Experimental and numerical study of oblique impact on woven composite sandwich structure: Influence of the firing axis orientation.” *Compos. Struct.*, 94(6), 1967–1972.

Nirmal, U., Hashim, J., and Low, K. O. (2012). “Adhesive wear and frictional performance of bamboo fibres reinforced epoxy composite.” *Tribol. Int.*, 47, 122–133.

Nirmal, U., Hashim, J., and Megat Ahmad, M. M. H. (2015). “A review on tribological performance of natural fibre polymeric composites.” *Tribol. Int.*, 83, 77–104.

Nisini, E., Santulli, C., and Liverani, A. (2017). “Mechanical and impact characterization of hybrid composite laminates with carbon, basalt and flax fibres.” *Compos. Part B Eng.*, 127, 92–99.

Nordin, A., Sakamoto, K., Azhari, H., Goda, K., Okamoto, M., Ito, H., and Endo, T. (2017). “Size Effect of Oil Palm Fibers on Tensile Properties of Oil Palm Fiber-Reinforced Polypropylene Composites.” *Proc. ICCM-21*, China.

Nurazzi, N. M., Khalina, A., Sapuan, S. M., and Rahmah, M. (2018). “Development of sugar palm yarn / glass fibre reinforced unsaturated polyester hybrid composites Development of sugar palm yarn / glass fibre reinforced unsaturated polyester hybrid composites.” *Mater. Res. Express*, 5(4).

Odgen, R. (1997). *Non linear elastic deformations*. New York: Dover, Mineola.

Offringa, A., and Davies, C. (1996). “Gulfstream V floors – primary aircraft structure in advanced thermoplastics.” *J. Adv. Mater.*, 27(2).

Oksman, K., Mathew, A. P., Långström, R., Nyström, B., and Joseph, K. (2009). “The influence of fibre microstructure on fibre breakage and mechanical properties of

natural fibre reinforced polypropylene.” *Compos. Sci. Technol.*, 69(11–12), 1847–1853.

Onut, S., Kara, S. S., and Mert, S. (2009). “Selecting the suitable material handling equipment in the presence of vagueness.” *Int. J. Adv. Manuf. Technol.*, 44(7–8), 818–828.

Otani, L. B., Pereira, A. H. A., Melo, J. D. D., and Amico, S. C. (2014). *Elastic moduli characterization of composites using the impulse excitation technique*.

P.K. Mallik. (2008). *Fiber Reinforced Composites*. New York: CRC Press.

Pal, R. (2005). “New models for effective Young’s modulus of particulate composites.” *Compos. Part B Eng.*, 36(6–7), 513–523.

Palta, E., Gutowski, M., and Fang, H. (2018). “A numerical study of steel and hybrid armor plates under ballistic impacts.” *Int. J. Solids Struct.*, 136–137, 279–294.

Pandya, K. S., Akella, K., Joshi, M., and Naik, N. K. (2012). “Ballistic impact behavior of carbon nanotube and nanosilica dispersed resin and composites.” *J. Appl. Phys.*, 112(113522), 1–8.

Panettieri, E., Fanteria, D., Montemurro, M., and Froustey, C. (2016). “Low-velocity impact tests on carbon/epoxy composite laminates: A benchmark study.” *Compos. Part B Eng.*, 107, 9–21.

Papa, I., Lopresto, V., Simeoli, G., Langella, A., and Russo, P. (2017). “Ultrasonic damage investigation on woven jute/poly (lactic acid) composites subjected to low velocity impact.” *Compos. Part B Eng.*, 115, 282–288.

Pappada, S., Rametta, R., and Passaro, A. (2010). “Processing, mechanical properties, and interfacial bonding of a thermoplastic core foam/composite-skin sandwich panel.” *Adv. Polym. Technol.*, 29(3), 137–145.

Park, H. (2017). “Investigation on low velocity impact behavior between graphite/epoxy composite and steel plate.” *Compos. Struct.*, 171, 126–130.

Park, Y., Kim, Y. H., Baluch, A. H., and Kim, C. G. (2015). “Numerical simulation and empirical comparison of the high velocity impact of STF impregnated Kevlar fabric using friction effects.” *Compos. Struct.*, 125, 520–529.

Pasquali, M., Terra, C., and Gaudenzi, P. (2015). “Analytical modelling of high-velocity impacts on thin woven fabric composite targets.” *Compos. Struct.*, 131, 951–965.

Passaro, A., Corvaglia, P., Manni, O., Barone, L., and Maffezzoli, A. (2004). “Processing-properties relationship of sandwich panels with polypropylene-core and polypropylene-matrix composite skins.” *Polym. Compos.*, 25(3), 307–318.

Patel, V. K., Chauhan, S., and Katiyar, J. K. (2018). “Physico-mechanical and wear properties of novel sustainable sour-weed fiber reinforced polyester composites.” *Mater. Res. Express*, 5(4).

Patel, V. K., and Dhanola, A. (2016). “Influence of CaCO<sub>3</sub>, AL<sub>2</sub>O<sub>3</sub> and TiO<sub>2</sub> microfillers on physico-mechanical properties of *Luffa cylindrica* / polyester composites.” *Eng. Sci. Technol. an Int. J.*, 19(2), 676–683.

Patel, V. K., and Rawat, N. (2017). “Physico-mechanical properties of sustainable Sagwan-Teak Wood Flour / Polyester Composites with / without gum rosin.” *Sustain. Mater. Technol.*, 13(May), 1–8.

Patil, S. (2006). “Experimental design analysis of sandwich structures with functionally graded compliant core.” M.Tech Thesis National Institute of Technology Karnataka, Surathkal.

Peças, P., Carvalho, H., Salman, H., and Leite, M. (2018). “Natural Fibre Composites and Their Applications: A Review.” *J. Compos. Sci.*, 2(4), 66.

Peel, L. D., and Jensen, D. W. (2001). “Response of fiber-reinforced elastomers under simple tension.” *J. Compos. Mater.*, 35(2), 96–137.

Pegoretti, A., Fabbri, E., Migliaresi, C., and Pilati, F. (2004). “Intraply and interply



hybrid composites based on E-glass and poly(vinyl alcohol) woven fabrics: Tensile and impact properties.” *Polym. Int.*, 53(9), 1290–1297.

Pernas-Sánchez, J., Artero-Guerrero, J. A., Varas, D., and López-Puente, J. (2014a). “Experimental analysis of normal and oblique high velocity impacts on carbon/epoxy tape laminates.” *Compos. Part A Appl. Sci. Manuf.*, 60, 24–31.

Pernas-Sánchez, J., Artero-Guerrero, J. A., Zahr Viñuela, J., Varas, D., and López-Puente, J. (2014b). “Numerical analysis of high velocity impacts on unidirectional laminates.” *Compos. Struct.*, 107, 629–634.

Pflug, J., Fan, X. Y., Vangrimde, B., Verpoest, I., Bratfisch, P., and Vanderpitte, D. (2002). “Development of a sandwich material with polypropylene/natural fiber skins and paper honeycomb core.” *Proc. 10th Eur. Conf. Compos. Mater.*, (January).

Pilato, L. (2010). *Phenolic resins: a century of progress*. Newyork: Springer.

Plummer, C., Bourban, P., and Manson, J. (2016). “Polymer Matrix Composites: Matrices and Processing.” *Ref. Modul. Mater. Sci. Mater. Eng.*, 1–9.

Prabhu, B. K., Dudse, S., and Kulkarni, S. M. (2014). “Statistical analysis of flexural modulus of cenospheres-reinforced, recycled poly(ethylene terephthalate) using Taguchi method.” *J. Elastomers Plast.*, 46(7), 611–622.

Provo Kluit, P. (1997). “The development of in-situ foamed sandwich panels.” TU Delft, Netherlands.

Pulford, C. T. R. (1983). “Antioxidant effects during blade abrasion of natural rubber.” *J. Appl. Polym. Sci.*, 28(2), 709–713.

Purnima, D., Maiti, S. N., and Gupta, A. K. (2006). “Interfacial Adhesion Through Maleic Anhydride Grafting of EPDM in PP / EPDM Blend.” *J. Appl. Polym. Sci.*, 102(December 2005), 5528–5532.

Quaresimin, M., Salviato, M., and Zappalorto, M. (2012). “Fracture and interlaminar properties of clay-modified epoxies and their glass reinforced laminates.” *Eng. Fract.*

*Mech.*, 81, 80–93.

Rahman, M., Jayaraman, K., and Mace, B. (2017). “Impact Energy Absorption of Flax Fiber-Reinforced Polypropylene Composites.” *Polym. Compos.*, 39(11), 4165–4175.

Rahman, M. R., Hasan, M., Huque, M. M., and Islam, M. N. (2010). “Physico-mechanical properties of jute fiber reinforced polypropylene composites.” *J. Reinf. Plast. Compos.*, 29(3), 445–455.

Rahman, S., Odeyinka, H., Perera, S., and Bi, Y. (2012). “Product-cost modelling approach for the development of a decision support system for optimal roofing material selection.” *Expert Syst. Appl.*, 39(8), 6857–6871.

Rajesh, S., Rajakarunakaran, S., and Pandian, R. S. (2012). “Modelling and optimization of sliding specific wear and coefficient of friction of aluminum based red mud metal matrix composite using taguchi and response surface methodology.” *Mater. Phys. Mech.*, 15, 150–166.

Ramachandra, M., and Radhakrishna, K. (2006). “Sliding wear, slurry erosive wear, and corrosive wear of aluminium/SiC composite.” *Mater. Sci.*, 24(2), 333–349.

Ramakrishnan, K. R., Shankar, K., Viot, P., and Guerard, S. (2012). “A comparative study of the impact properties of sandwich materials with different cores.” *EPJ Web Conf.*

Rana, A. K., Mitra, B. C., and Banerjee, A. N. (1999). “Short jute fiber-reinforced polypropylene composites: Dynamic mechanical study.” *J. Appl. Polym. Sci.*, 71(4), 531.

Rana, R. S., Kumre, A., Rana, S., and Purohit, R. (2017). “Characterization of Properties of epoxy sisal / Glass Fiber Reinforced hybrid composite.” *Mater. Today Proc.*, 4(4), 5445–5451.

Rao, C. H. C., Madhusudan, S., Raghavendra, G., International, E. V. R., Rao, C. H.

- C., Madhusudan, S., Raghavendra, G., and Rao, V. (2012). "Investigation in to Wear behavior of coir Fiber Reinforced Epoxy Composites with the Taguchi Method." *Int. J. Eng. Res. Appl.*, 2(5), 371–374.
- Rao, K. V. S., Girisha, K. G., and Rakesh, Y. D. (2016). "Evaluation of slurry erosion wear characteristic of plasma sprayed TiO<sub>2</sub> coated 410 steel." *IOP Conf. Ser. Mater. Sci. Eng.*, 149(1).
- Rao, R. V. (2006). "A material selection model using graph theory and matrix approach." *Mater. Sci. Eng.*, 431(1–2), 248–255.
- Rao, R. V. (2008). "A decision making methodology for material selection using an improved compromise ranking method." *Mater. Des.*, 29, 1949–1954.
- Rao, R. V., and Davim, J. P. (2008). "A decision-making framework model for material selection using a combined multiple attribute decision-making method." *Int. J. Adv. Manuf. Technol.*, 35(7–8), 751–760.
- Rasmussen, L. (2011). "Controlled Enzyme Catalysed Heteropolysaccharide Degradation: Xylans." Ph.D. Thesis, Technical University of Denmark, Denmark.
- Rathod, M. K., and Kanzaria, H. V. (2011). "A methodological concept for phase change material selection based on multiple criteria decision analysis with and without fuzzy environment." *Mater. Des.*, 32(6), 3578–3585.
- Ravandi, M., Teo, W. S., Tran, L. Q. N., Yong, M. S., and Tay, T. E. (2017). "Low velocity impact performance of stitched flax/epoxy composite laminates." *Compos. Part B Eng.*, 117, 89–100.
- Ray, D., Sarkar, B. K., Das, S., and Rana, A. K. (2002). "Dynamic mechanical and thermal analysis of vinyl ester-resin-matrix composites reinforced with untreated and alkali-treated jute fibres." *Compos. Sci. Technol.*, 62(7–8), 911–917.
- Reddy, P. R. S., Reddy, T. S., Madhu, V., Gogia, A. K., and Rao, K. V. (2015). "Behavior of E-glass composite laminates under ballistic impact." *Mater. Des.*, 84,

79–86.

Reddy, T. S., Reddy, P. R. S., and Madhu, V. (2017). “Response of E-glass/Epoxy and Dyneema® Composite Laminates Subjected to low and High Velocity Impact.” *Procedia Eng.*, 173, 278–285.

Remennikov, A., Kong, S. Y., and Uy, B. (2011). “Response of foam- and concrete-filled square steel tubes under low-velocity impact loading.” *J. Perform. Constr. Facil.*, 25(5), 373–381.

Ren, Z. H., Jin, P., Cao, X. M., Zheng, Y. G., and Zhang, J. S. (2015). “Mechanical properties and slurry erosion resistance of SiC ceramic foam / epoxy co-continuous phase composite.” *Compos. Sci. Technol.*, 107, 129–136.

Reyes, G., and Rangaraj, S. (2009). “Interfacial fracture properties of novel carbon foam structures.” *41st SAMPE Fall Tech. Conf.*, Wichita, USA.

Reyes, G., and Sharma, U. (2010). “Modeling and damage repair of woven thermoplastic composites subjected to low velocity impact.” *Compos. Struct.*, 92(2), 523–531.

Ricciardi, M. R., Papa, I., Langella, A., Langella, T., Lopresto, V., and Antonucci, V. (2018). “Mechanical properties of glass fibre composites based on nitrile rubber toughened modified epoxy resin.” *Compos. Part B Eng.*, 139(July 2017), 259–267.

Rivlin, R. (1992). “The elasticity of rubber.” *Rubber Chem. Technol.*, 65(2), 51–66.

Rojo, E., Alonso, M. V., Oliet, M., Saz-Orozco, B. Del, and Rodriguez, F. (2015). “Effect of fiber loading on the properties of treated cellulose fiber-reinforced phenolic composites.” *Compos. Part B Eng.*, 68, 185–192.

Rong, M., Zhang, M., Liu, Y., Yang, G., and Zeng, H. (2001). “The Effect of fiber Treatment on the Mechanical Properties of Unidirectional Sisal- Reinforced Epoxy Composites.” *Compos. Sci. Technol.*, 61, 1437–1447.

Rosa, I. M. De, Santulli, C., and Sarasini, F. (2010). “Mechanical and thermal

characterization of epoxy composites reinforced with random and quasi-unidirectional untreated Phormium tenax leaf fibers.” *Mater. Des.*, 31(5), 2397–2405.

Rosselli, F., and Santare, M. H. (1997). “Comparison of the short beam shear (SBS) and interlaminar shear device (ISD) tests.” *Compos. Part A*, 28(A), 587–594.

Rout, J., Misra, M., Tripathy, S. S., Nayak, S. K., and Mohanty, A. K. (2001). “The influence of fibre treatment of the performance of coir-polyester composites.” *Compos. Sci. Technol.*, 61(9), 1303–1310.

Roylance, D., and Wang, S. (1979). *Penetration mechanics of textile structures*. Cambridge.

Rozant, O., Bourban, P., and Ma, J. E. (2001). “Manufacturing of three dimensional sandwich parts by direct thermoforming.” *Compos. Part A Appl. Sci. Manuf.*, 32, 1593–1601.

S. Thomas, S. A. Paul, A. Pothan, B. D. (2011). “Natural Fibres: Structure, Properties and Applications.” *Cellul. Fibers Bio- Nano-Polymer Compos.*, I. K. Susheel Kalia, B. S. Kaith, ed., Springer, Berlin, Heidelberg, 3–42.

Sa, L., Balart, R., Sanchis, R., Fenollar, O., and Garcı, D. (2008). “Improved adhesion of LDPE films to polyolefin foams for automotive industry using low-pressure plasma.” *Int. J. Adhes. Adhes.*, 28, 445–451.

Safri, S. N. A., Sultan, M. T. H., Jawaid, M., and Jayakrishna, K. (2018). “Impact behaviour of hybrid composites for structural applications: A review.” *Compos. Part B Eng.*, 133, 112–121.

Saghafi, H., Ghaffarian, S. R., and Yademellat, H. (2019). “Finding the best sequence in flexible and stiff composite laminates interleaved by nanofibers.” *J. Compos. Mater.*, 53(28–30), 4065–4076.

Saha, A. K., Das, S., Bhatta, D., and Mitra, B. C. (1999). “Study of Jute Fiber Reinforced Polyester Composites by Dynamic Mechanical Analysis.” *J. Appl. Polym.*

*Sci.*, 71(9), 1505–1513.

Sahu, P., and Gupta, M. K. (2017). “Sisal (*Agave sisalana*) fibre and its polymer-based composites: A review on current developments.” *J. Reinf. Plast. Compos.*, 36(24), 1759–1780.

Saidane, E. H., Scida, D., Assarar, M., Sabhi, H., and Ayad, R. (2016). “Hybridisation effect on diffusion kinetic and tensile mechanical behaviour of epoxy based flax-glass composites.” *Compos. Part A Appl. Sci. Manuf.*, 87, 153–160.

Sakly, A., Laksimi, A., Kebir, H., and Benmedakhen, S. (2016). “Experimental and modelling study of low velocity impacts on composite sandwich structures for railway applications.” *Eng. Fail. Anal.*, 68, 22–31.

Salleh, F. M., Hassan, A., Yahya, R., and Azzahari, A. D. (2014). “Effects of extrusion temperature on the rheological, dynamic mechanical and tensile properties of kenaf fiber/HDPE composites.” *Compos. Part B Eng.*, 58, 259–266.

Sandeep Kumar, Patel V K, Mer KKS, Fekete Gusztav, T. S. (2018). “Influence of woven bast-leaf hybrid fiber on the physio-mechanical and sliding wear performance of epoxy based polymer composites.” *Mater. Res. Express*, 5, 1–13.

Sangamesh, R., Kumar, N., Ravishankar, K. S., and Kulkarni, S. M. (2018). “Mechanical Characterization and Finite Element Analysis of Jute-Epoxy Composite.” *MATEC Web Conf.*, 144, 02014.

Sanjay K, M. (2002). *Composites Manufacturing*. New York: CRC Press.

Sanjay, M. R., Arpitha, G. R., Naik, L. L., Gopalakrishna, K., and Yogesha, B. (2016). “Applications of Natural Fibers and Its Composites : An Overview.” *Nat. Resour.*, 7, 108–114.

Sanjay, M. R., Jawaid, M., Naidu, N. V. R., and Yogesha, B. (2019). *TOPSIS method for selection of best composite laminate. Model. Damage Process. Biocomposites, Fibre-Reinforced Compos. Hybrid Compos.*, Elsevier.

Sapiai, N., Jumahat, A., and Mahmud, J. (2018). “Mechanical properties of functionalised CNT filled kenaf reinforced epoxy composites.” *Mater. Res. Express*, 5(4).

Sapuan, S. M. (2001). “A knowledge-based system for materials selection in mechanical engineering design.” *Mater. Des.*, 22, 687–695.

Sarasini, F., Tirillò, J., D’Altilia, S., Valente, T., Santulli, C., Touchard, F., Chocinski-Arnault, L., Mellier, D., Lampani, L., and Gaudenzi, P. (2016). “Damage tolerance of carbon/flax hybrid composites subjected to low velocity impact.” *Compos. Part B Eng.*, 91.

Sarasini, F., Tirillò, J., Ferrante, L., Valente, M., Valente, T., Lampani, L., Gaudenzi, P., Cioffi, S., Iannace, S., and Sorrentino, L. (2014). “Drop-weight impact behaviour of woven hybrid basalt-carbon/epoxy composites.” *Compos. Part B Eng.*, 59, 204–220.

Sare, I. R., Mardel, J. I., and Hill, A. J. (2001). “Wear-resistant metallic and elastomeric materials in the mining and mineral processing industries — an overview.” 250, 1–10.

Satapathy, A., Kumar Jha, A., Mantry, S., Singh, S. K., and Patnaik, A. (2010). “Processing and characterization of jute-epoxy composites reinforced with SiC derived from rice husk.” *J. Reinf. Plast. Compos.*, 29(18), 2869–2878.

Sathishkumar, T., Naveen, J., and Satheeshkumar, S. (2014). “Hybrid fiber reinforced polymer composites-a review.” *J. Reinf. Plast. Compos.*, 33(5), 454–471.

Sathishkumar, T. P., Navaneethakrishnan, P., Shankar, S., Rajasekar, R., and Rajini, N. (2013). “Characterization of natural fiber and composites - A review.” *J. Reinf. Plast. Compos.*, 32(19), 1457–1476.

Saxena, M., Pappu, A., Haque, R., and Sharma, A. (2011). “Sisal Fiber Based Polymer Composites and Their Applications.” *Cellul. Fibers Bio- Nano-Polymer Compos.*, Springer, Berlin, Heidelberg, 589–659.

- Scarponi, C., Sarasini, F., Tirillò, J., Lampani, L., Valente, T., and Gaudenzi, P. (2016). “Low-velocity impact behaviour of hemp fibre reinforced bio-based epoxy laminates.” *Compos. Part B Eng.*, 91(2016), 162–168.
- Schallamach, A. (1952). “Abrasion pattern on rubber,” *Trans. Inst. Rubber Ind.*, 256–258.
- Schallamach, A. (1963). *Abrasion and tyre wear*. London: MacLaren.
- Schapery, R. (1969). “On the Characterization of Nonlinear Viscoelastic Materials.” *Polym. engineerirng Sci.*, 9(4), 295–310.
- Sen, S., Jamal M, N. Bin, Shaw, A., and Deb, A. (2019). “Numerical investigation of ballistic performance of shear thickening fluid (STF)-Kevlar composite.” *Int. J. Mech. Sci.*, 164(March), 105174.
- Senol, M. (2012). “Shear Behavior of Glass Fabric/Epoxy Resin Composite Prepared by Surface Treatments.” *Aatcc Rev.*, 12(2), 73–79.
- Seymour, R. (1990). *Engineering Polymer Source Book*. (McGraw-Hill, ed.), Newyork.
- Shaktivesh, Nair, N. S., Sessa Kumar, C. V., and Naik, N. K. (2013). “Ballistic impact performance of composite targets.” *Mater. Des.*, 51, 833–846.
- Shanian, A., Milani, A. S., Vermaak, N., Bertoldi, K., Scarinci, T., and Gerendas, M. (2012). “A combined finite element-multiple criteria optimization approach for materials selection of gas turbine components.” *J. Appl. Mech. Trans. ASME*, 79(6), 1–8.
- Shanian, A., and Savadogo, O. (2006). “A material selection model based on the concept of multiple attribute decision making.” *Mater. Des.*, 27(27), 329–337.
- Shim, V. P. W., Guo, Y. B., and Tan, V. B. C. (2012). “Response of woven and laminated high-strength fabric to oblique impact.” *Int. J. Impact Eng.*, 48, 87–97.



Shinoj, S., Visvanathan, R., Panigrahi, S., and Varadharaju, N. (2011). "Dynamic mechanical properties of oil palm fibre (OPF)-linear low density polyethylene (LLDPE) biocomposites and study of fibre-matrix interactions." *Biosyst. Eng.*, 109(2), 99–107.

Shivamurthy, B., Siddaramaiah, and Prabhuswamyc, M. S. (2009). "Influence of SiO<sub>2</sub> Fillers on Sliding Wear Resistance and Mechanical Properties of Compression Moulded Glass Epoxy Composites." *J. Miner. Mater. Charact. Eng.*, 08(07), 513–530.

Shuhimi, F. F., Abdollah, M. F. Bin, Kalam, M. A., Hassan, M., Mustafa, A., and Amiruddin, H. (2016). "Tribological characteristics comparison for oil palm fibre/epoxy and kenaf fibre/epoxy composites under dry sliding conditions." *Tribol. Int.*, 101, 247–254.

Siegfried, M., Tola, C., Claes, M., Lomov, S. V., Verpoest, I., and Gorbatiikh, L. (2014). "Impact and residual after impact properties of carbon fiber/epoxy composites modified with carbon nanotubes." *Compos. Struct.*, 111(1), 488–496.

Sikarwar, R. S., Velmurugan, R., and Gupta, N. K. (2014). "Influence of fiber orientation and thickness on the response of glass/epoxy composites subjected to impact loading." *Compos. Part B Eng.*, 60, 627–636.

Silva, R. V., Ueki, M. M., Spinelli, D., Bose Filho, W. W., and Tarpani, J. R. (2010). "Thermal, mechanical, and hygroscopic behavior of sisal fiber/polyurethane resin-based composites." *J. Reinf. Plast. Compos.*, 29(9), 1399–1417.

Singh, N., Yousif, B. F., and Rilling, D. (2011). "Tribological characteristics of sustainable fiber-reinforced thermoplastic composites under wet adhesive wear." *Tribol. Trans.*, 54(5), 736–748.

Singleton, A. C. N., Baillie, C. A., Beaumont, P. W. R., and Peijs, T. (2003). "On the mechanical properties, deformation and fracture of a natural fibre/recycled polymer composite." *Compos. Part B Eng.*, 34(6), 519–526.

Siow, Y., and Shim, V. (1998). "An experimental study of low velocity impact damage in woven fibre composites." *J. Compos. Mater.*, 32(12), 1178–1202.

Smith, J. C., Mccrackin, F. L., and Schiefer, H. F. (1958). "Stress-Strain Relationships in Yarns Subjected to Rapid Impact Loading:Part V: Wave Propagation in Long Textile Yarns Impacted Transversely." *Text. Res. J.*, 28(4), 288–302.

Sonia, A., Priya Dasan, K., and Alex, R. (2013). "Celluloses microfibrils (CMF) reinforced poly (ethylene-co-vinyl acetate) (EVA) composites: Dynamic mechanical, gamma and thermal ageing studies." *Chem. Eng. J.*, 228, 1214–1222.

Sorrentino, L., Aurilia, M., and Iannace, T. (2009). "Effects of the thermoforming on the cell morphology of a thermoplastic core." *17th Int. Conf. Compos. Mater.*, Edinburgh, Scotland.

Sparnins, E. (2009). "Mechanical Properties of Flax Fibers and Their Composites." Ph.D. Thesis, Luleå University of Technology, Luleå.

Sreekantha Reddy, T., Rama Subba Reddy, P., and Madhu, V. (2019). "Low velocity impact studies of E-glass/epoxy composite laminates at different thicknesses and temperatures." *Def. Technol.*, 15(6), 897–904.

Sreenivasan, V. S., Rajini, N., Alavudeen, A., and Arumugaprabu, V. (2015). "Dynamic mechanical and thermo-gravimetric analysis of *Sansevieria cylindrica*/polyester composite: Effect of fiber length, fiber loading and chemical treatment." *Compos. Part B Eng.*, 69, 76–86.

Stachowiak, G., and Batchelor, A. (2011). *Engineering Tribology*. London: Butterworth-Heinemann.

Stelldinger, E., Kuhhorn, A., and Kober, M. (2016). "Experimental evaluation of the low-velocity impact damage resistance of CFRP tubes with integrated rubber layer." *Compos. Struct.*, 139, 30–35.

Stuart, L. (1992). *Handbook of Composite Reinforcement*. California: Wiley

## Publications.

Sudhir Sastry, Y. B., Budarapu, P. R., Krishna, Y., and Devaraj, S. (2014). “Studies on ballistic impact of the composite panels.” *Theor. Appl. Fract. Mech.*, 72(1), 2–12.

Suresh Kumar, S. M., Duraibabu, D., and Subramanian, K. (2014). “Studies on mechanical, thermal and dynamic mechanical properties of untreated (raw) and treated coconut sheath fiber reinforced epoxy composites.” *Mater. Des.*, 59, 63–69.

Sy, B. L., Fawaz, Z., and Bougherara, H. (2019). “Numerical simulation correlating the low velocity impact behaviour of flax/epoxy laminates.” *Compos. Part A Appl. Sci. Manuf.*, 126(July), 105582.

Tajvidi, M., Motie, N., Rassam, G., Falk, R. H., and Felton, C. (2010). “Mechanical performance of hemp fiber polypropylene composites at different operating temperatures.” *J. Reinf. Plast. Compos.*, 29(5), 664–674.

Tan, K. T., Watanabe, N., and Iwahori, Y. (2010). “Effect of stitch density and stitch thread thickness on low-velocity impact damage of stitched composites.” *Compos. Part A*, 41(12), 1857–1868.

Tan, W., Falzon, B. G., Chiu, L. N. S., and Price, M. (2015). “Predicting low velocity impact damage and Compression-After-Impact (CAI) behaviour of composite laminates.” *Compos. Part A Appl. Sci. Manuf.*, 71, 212–226.

Tansel, Y. (2012). “An experimental design approach using TOPSIS method for the selection of computer-integrated manufacturing technologies.” *Robot. Comput. Integr. Manuf.*, 28(2), 245–256.

Thurston, R. M., Clay, J. D., and Schulte, M. D. (2007). “Effect of atmospheric plasme treatment on polymer surface energy and adhesion.” *J. Plast. Film Sheeting*, 23, 63–78.

Tong, Y., Zhao, S., Ma, J., Wang, L., Zhang, Y., Gao, Y., and Xie, Y. M. (2014). “Improving cracking and drying shrinkage properties of cement mortar by adding

chemically treated luffa fibres.” *Constr. Build. Mater.*, 71, 327–333.

Topac, O. T., Gozluclu, B., Gurses, E., and Coker, D. (2017). “Experimental and computational study of the damage process in CFRP composite beams under low-velocity impact.” *Compos. Part A Appl. Sci. Manuf.*, 92, 167–182.

Towo, A. N., and Ansell, M. P. (2008). “Fatigue evaluation and dynamic mechanical thermal analysis of sisal fibre-thermosetting resin composites.” *Compos. Sci. Technol.*, 68(3–4), 925–932.

Tuzkaya, G., Gülsün, B., Kahraman, C., and Özgen, D. (2010). “An integrated fuzzy multi-criteria decision making methodology for material handling equipment selection problem and an application.” *Expert Syst. Appl.*, 37(4), 2853–2863.

Tzanakis, I., Hadfield, M., Thomas, B., Noya, S. M., Henshaw, I., and Austen, S. (2012). “Future perspectives on sustainable tribology.” *Renew. Sustain. Energy Rev.*, 16(6), 4126–4140.

Ude, A. U., Ariffin, A. K., and Azhari, C. H. (2013). “Impact damage characteristics in reinforced woven natural silk/epoxy composite face-sheet and sandwich foam, coremat and honeycomb materials.” *Int. J. Impact Eng.*, 58, 31–38.

VanderKlok, A., Stamm, A., Dorer, J., Hu, E., Auvenshine, M., Pereira, J. M., and Xiao, X. (2018). “An experimental investigation into the high velocity impact responses of S2-glass/SC15 epoxy composite panels with a gas gun.” *Int. J. Impact Eng.*, 111(May 2017), 244–254.

Vignesh, K. (2018). “Mercerization treatment parameter effect on coir fiber reinforced polymer matrix composite Mercerization treatment parameter effect on coir fiber reinforced polymer matrix composite.” *Mater. Res. Express*, 5.

Vinson, J. (1999). *The Behavior of Sandwich Structures of Isotropic and Composite Materials*. USA: CRC Press.

Vishwanath, B., Verrnab, A. P., and Raoc, C. V. S. K. (1993). “Effect of

reinforcement polymer composites on friction and wear of fabric reinforced.” 167, 93–99.

Vu-quoc, L., Zhang, X., and Lesburg, L. (2001). “Normal and tangential force-displacement relations for frictional elasto-plastic contact of spheres.” *Int. J. Solids Struct.*, 38, 6455–6489.

Vu-Quoc, L., Zhang, X., and Lesburg, L. (2016). “A Normal Force-Displacement Model for Contacting Spheres Accounting for Plastic Deformation: Force-Driven Formulation.” *J. Appl. Mech.*, 67(June 2000), 363–371.

Walsh, J., Kim, H. I., and Suhr, J. (2017). “Low velocity impact resistance and energy absorption of environmentally friendly expanded cork core-carbon fiber sandwich composites.” *Compos. Part A Appl. Sci. Manuf.*, 101, 290–296.

Wambua, P., Ivens, J., and Verpoest, I. (2003). “Natural fibres: Can they replace glass in fibre reinforced plastics?” *Compos. Sci. Technol.*, 63(9), 1259–1264.

Wan, Y., Luo, H., Wang, T., Huang, Y., Li, Q., and Zhou, F. (2005). “Friction and wear behavior of three-dimensional braided carbon fiber / epoxy composites under.” *J. Mater. Sci.*, 40(17), 4475–4481.

Wang, F., Drzal, L. T., Qin, Y., and Huang, Z. (2016a). “Size effect of graphene nanoplatelets on the morphology and mechanical behavior of glass fiber/epoxy composites.” *J. Mater. Sci.*, 51(7), 3337–3348.

Wang, H., Hazell, P. J., Shankar, K., Morozov, E. V, and Escobedo, J. P. (2017a). “Impact behaviour of Dyneema ® fabric-reinforced composites with different resin matrices.” *Polym. Test.*, 61, 17–26.

Wang, H., Ramakrishnan, K. R., and Shankar, K. (2016b). “Experimental study of the medium velocity impact response of sandwich panels with different cores.” *Mater. Des.*, 99, 68–82.

Wang, R.-M., Zheng, S.-R., and Zheng, Y.-P. (2011). “Matrix materials.” *Polym.*

*Matrix Compos. Technol.*, Woodhead Publishing Series in Composites Science and Engineering, 101–548.

Wang, X., Zhao, X., Wu, Z., Zhu, Z., and Wang, Z. (2016c). “Interlaminar shear behavior of basalt FRP and hybrid FRP laminates.” *J. Compos. Mater.*, 50(8), 1073–1084.

Wang, Z., Xu, L., Sun, X., Shi, M., and Liu, J. (2017b). “Fatigue behavior of glass-fiber-reinforced epoxy composites embedded with shape memory alloy wires.” *Compos. Struct.*, 178, 311–319.

Weir, G., and Tallon, S. (2005). “The coefficient of restitution for normal incident , low velocity particle impacts.” *Chem. Eng. Sci.*, 60, 3637–3647.

Wetzel, E., Wagner, P., and Lee, Y. (2004). “Protective fabrics utilizing shear thickening fluids (STFs).” *4th Int. Conf. Saf. Prot. Fabr.*, Pittsburgh, 1–23.

Whisler, D., and Kim, H. (2012). “Effect of impactor radius on low-velocity impact damage of glass/epoxy composites.” *J. Compos. Mater.*, 46(25), 3137–3149.

Wong, C. X. ã., Daniel, M. C., and Rongong, J. A. (2009). “Energy dissipation prediction of particle dampers.” *J. Sound Vib.*, 319, 91–118.

Wong, D. W. Y., Zhang, H., Bilotti, E., and Peijs, T. (2017). “Interlaminar toughening of woven fabric carbon/epoxy composite laminates using hybrid aramid/phenoxy interleaves.” *Compos. Part A Appl. Sci. Manuf.*, 101, 151–159.

Wong, K. W., and Truss, R. W. (1994). “Effect of flyash content and coupling agent on the mechanical properties of flyash filled polypropylene.” *Compos. Sci. Technol.*, 52, 361–368.

Wool, R. P. (2006). “Adhesion at polymer – polymer interfaces : a rigidity percolation approach.” *Comptes Rendus Chim.*, 9, 25–44.

Xanthos, M. (2010). *Functional Fillers for Plastics*. Weinheim: Wiley-VCH.

- Xie, W., Zhang, W., Kuang, N., Li, D., Huang, W., Gao, Y., Ye, N., Guo, L., and Ren, P. (2016). "Experimental investigation of normal and oblique impacts on CFRPs by high velocity steel sphere." *Compos. Part B Eng.*, 99, 483–493.
- Xie, Y., Jiang, J. (Jimmy), Tufa, K. Y., and Yick, S. (2015). "Wear resistance of materials used for slurry transport." *Wear*, 332–333, 1104–1110.
- Xu, C., Wang, Y., Wu, J., Song, S., Cao, S., Xuan, S., Jiang, W., and Gong, X. (2017). "Anti-impact response of Kevlar sandwich structure with silly putty core." *Compos. Sci. Technol.*, 153, 168–177.
- Xu, X., Zhou, Z., Hei, Y., Zhang, B., Bao, J., and Chen, X. (2014). "Improving compression-after-impact performance of carbon – fiber composites by CNTs / thermoplastic hybrid film interlayer." *Compos. Sci. Technol.*, 95, 75–81.
- Yablokov, M., Piskarev, M., and Kendall, K. (2015). "Towards enhancing peel strength of adhesively bonded joints Towards enhancing peel strength of adhesively bonded joints." *IOP Conf. Ser. Mater. Sci. Eng.*, 87, 1–12.
- Yadav, S., Pathak, V. K., and Gangwar, S. (2019). "A novel hybrid TOPSIS-PSI approach for material selection in marine applications." *Sādhanā*, 44(58), 1–12.
- Yahaya, R., Sapuan, S., Jawaid, M., Leman, Z., and Zainudin, E. (2015). "Effect of layering sequence and chemical treatment on the mechanical properties of woven kenaf/aramid hybrid laminated composites." *Mater. Des.*, 67, 173–179.
- Yahaya, R., Sapuan, S. M., Jawaid, M., Leman, Z., and Zainudin, E. S. (2014). "Quasi-static penetration and ballistic properties of kenaf-aramid hybrid composites." *Mater. Des.*, 63, 775–782.
- Yan, L., Chou, N., and Jayaraman, K. (2014). "Flax fibre and its composites - A review." *Compos. Part B Eng.*, 56, 296–317.
- Yang, Y., and Chen, X. (2016). "Study of energy absorption and failure modes of constituent layers in body armour panels." *Compos. Part B*, 98, 250–259.

Yousif, B. F. (2009). “Frictional and wear performance of polyester composites based on coir fibres.” *Proc. Inst. Mech. Eng. Part J J. Eng. Tribol.*, 223(1), 51–59.

Yousif, B. F. (2013). “Design of newly fabricated tribological machine for wear and frictional experiments under dry/wet condition.” *Mater. Des.*, 48, 2–13.

Zaheer, U., Zulfiqar, U., Khurram, A. A., and Subhani, T. (2018). “Improving the performance of conventional glass fiber epoxy matrix composites by incorporating nanodiamonds.” *Compos. Interfaces*, 25(11), 1005–1018.

Zahid, S., Nasir, M. A., Nauman, S., Karahan, M., Nawab, Y., Ali, H. M., Khalid, Y., Nabeel, M., and Ullah, M. (2019). “Experimental analysis of ILSS of glass fibre reinforced thermoplastic and thermoset textile composites enhanced with multiwalled carbon nanotubes.” *J. Mech. Sci. Technol.*, 33(1), 197–204.

Zanini, S., Orlandi, M., Colombo, C., Grimoldi, E., and Riccardi, C. (2009). “Plasma-induced graft-polymerization of polyethylene glycol acrylate on polypropylene substrates.” *Eur. Phys. J. D*, 164, 159–164.

Zhang, C., Duodu, E. A., and Gu, J. (2017a). “Finite element modeling of damage development in cross-ply composite laminates subjected to low velocity impact.” *Compos. Struct.*, 173, 219–227.

Zhang, D., Fei, Q., and Zhang, P. (2017b). “Drop-weight impact behavior of honeycomb sandwich panels under a spherical impactor.” *Compos. Struct.*, 168, 633–645.

Zhang, H., Peng, Y., Hou, L., Tian, G., and Li, Z. (2019a). “A hybrid multi-objective optimization approach for energy-absorbing structures in train collisions.” *Inf. Sci. (Ny)*, 481, 491–506.

Zhang, J., and Zhang, X. (2015). “An efficient approach for predicting low-velocity impact force and damage in composite laminates.” *Compos. Struct.*, 130, 85–94.

Zhang, S., Pedersen, P. T., and Villavicencio, R. (2019b). “Damaged material volume



method.” *Probab. Mech. Sh. Collis. Grounding*, Butterworth-Heinemann, 271–323.

Zhou, D. W., and Stronge, W. J. (2008). “Ballistic limit for oblique impact of thin sandwich panels and spaced plates.” *Int. J. Impact Eng.*, 35(11), 1339–1354.

Žmindák, M., Pelagić, Z., Pastorek, P., Močilan, M., and Vyboštok, M. (2016). “Finite element modelling of high velocity impact on plate structures.” *Procedia Eng.*, 136, 162–168.

Zuhudi, N. Z. M., Lin, R. J. T., and Jayaraman, K. (2016). “Flammability, thermal and dynamic mechanical properties of bamboo-glass hybrid composites.” *J. Thermoplast. Compos. Mater.*, 29(9), 1210–1228.

**LIST OF PUBLICATIONS BASED ON PH.D. RESEARCH WORK**

<b>Sl No.</b>	<b>Title of Paper</b>	<b>Authors ( In the same order as in the paper, underline the Research Scholar's name)</b>	<b>Name of the Journal / Conference /Symposium, Vol., No., Pages</b>	<b>Month &amp; Year of Publication</b>	<b>Category*</b>
1	Experimental Investigation on Slurry Erosive Behaviour of Biodegradable Flexible Composite and Optimization of Parameters using Taguchi's Approach	<u>Vishwas Mahesh</u> , Sharnappa Joladarashi and Satyabodh M Kulkarni	Journal of Composite and Advanced Materials (Revue des Composites et des Matériaux Avancés), <b>28</b> (3), 345-355	September, 2018	<b>1</b>
2	Physio-Mechanical and Wear Properties of Novel Jute Reinforced Natural Rubber Based Flexible Composite	<u>Vishwas Mahesh</u> , Sharnappa Joladarashi and Satyabodh M Kulkarni	Material Research Express, <b>6</b> (5), 055503, 1-16	February, 2019	<b>1</b>
3	Investigation on effect of using rubber as core material in sandwich composite plate subjected to low velocity normal and oblique impact loading	<u>Vishwas M.</u> Sh. Joladarashi and S M Kulkarni	Scientia Iranica, Transaction on Mechanical Engineering B, <b>26</b> (2), 897-907	April, 2019	<b>1</b>
4	Experimental study on abrasive wear behaviour of flexible green composite intended to be used as protective cladding for structures	<u>Vishwas Mahesh</u> , Sharnappa Joladarashi and Satyabodh M Kulkarni	International Journal of Modern Manufacturing Technologies (IJMMT), <b>11</b> (1), 69-76	June, 2019	<b>1</b>

SI No.	Title of Paper	Authors ( In the same order as in the paper, underline the Research Scholar's name)	Name of the Journal / Conference /Symposium, Vol., No., Pages	Month & Year of Publication	Category*
5	Development and mechanical characterization of novel polymer-based flexible composite and optimization of stacking sequences using VIKOR and PSI techniques	<u>Vishwas Mahesh</u> , Sharnappa Joladarashi and Satyabodh M Kulkarni	Journal of Thermoplastic Composite Materials	Online Since July 2019	1
6	An Experimental Investigation on Low-Velocity Impact Response of Novel Jute/ Rubber Flexible Bio-Composite	<u>Vishwas Mahesh</u> , Sharnappa Joladarashi and Satyabodh M Kulkarni	Composite Structures, <b>225</b> , 111190, 1-12	October, 2019	1
7	An experimental study on adhesion, flexibility, interlaminar shear strength, and damage mechanism of jute/rubber-based flexible “green” composite	<u>Vishwas Mahesh</u> , Sharnappa Joladarashi and Satyabodh M Kulkarni	Journal of Thermoplastic Composite Materials	Online Since October 2019	1

SI No.	Title of Paper	Authors ( In the same order as in the paper, underline the Research Scholar's name)	Name of the Journal / Conference /Symposium, Vol., No., Pages	Month & Year of Publication	Category*
8	Comparative Study on Damage Behaviour of Synthetic and Natural Fiber Reinforced Brittle Composite and Natural Fiber Reinforced Flexible Composite Subjected to Low Velocity Impact	<u>Vishwas M.</u> , Sh. Joladarashi and S M Kulkarni	Scientia Iranica, Transaction on Mechanical Engineering B, 27 (1), 341-349	February, 2020	1
9	Damage Mechanics and Energy Absorption Capabilities of Natural Fiber Reinforced Elastomeric Based Bio Composite for Sacrificial Structural Applications	<u>Vishwas Mahesh.</u> , Sharnappa Joladarashi and Satyabodh M Kulkarni	Defence Technology	Online Since February 2020	1
10	Influence of Thickness and Projectile Shape on Penetration Resistance of the Compliant Composite	<u>Vishwas Mahesh.</u> , Sharnappa Joladarashi and Satyabodh M Kulkarni	Defence Technology	Online Since March 2020	1

SI No.	Title of Paper	Authors ( In the same order as in the paper, underline the Research Scholar's name)	Name of the Journal / Conference /Symposium, Vol., No., Pages	Month & Year of Publication	Category*
11	A Comprehensive Review on Material Selection for Polymer Matrix Composites Subjected to Impact Load	<u>Vishwas Mahesh</u> , Sharnappa Joladarashi and Satyabodh M Kulkarni	Defence Technology	Online Since April 2020	1
12	Evaluation of Tensile Strength and Slurry Erosive behaviour of Jute Reinforced Natural Rubber Based Flexible Composite	<u>Vishwas Mahesh</u> , Sharnappa Joladarashi and Satyabodh M Kulkarni	Journal of Composite and Advanced Materials (Revue des Composites et des Matériaux Avancés), 30(2), 77-82	April, 2020	1
13	Tribo-Mechanical Characterization and Optimization of Green Flexible Composite	<u>Vishwas Mahesh</u> , Sharnappa Joladarashi and Satyabodh M Kulkarni	Emerging Materials Research	Online Since August 2020	1
14	Behaviour of Natural Rubber in Comparison with Structural Steel, Aluminium and Glass Epoxy Composite under Low Velocity Impact Loading	<u>Vishwas Mahesh</u> , Sharnappa Joladarashi and Satyabodh M Kulkarni	International Conference on Advanced Materials, Manufacturing, Management and Thermal Sciences 2016 (AMMMT 2016), SIT Tumkur	---	3

SI No.	Title of Paper	Authors ( In the same order as in the paper, underline the Research Scholar's name)	Name of the Journal / Conference /Symposium, Vol., No., Pages	Month & Year of Publication	Category*
15	Modelling and Analysis of Material Behaviour under Normal and Oblique Low Velocity Impact	<u>Vishwas M.</u> Sharnappa Joladarashi and S M Kulkarni	International Conference on Emerging Trends in Materials and Manufacturing Engineering-2017 (IMME17), NIT Trichy	---	3
16	Finite element simulation of low velocity impact loading on a sandwich composite	<u>Vishwas M.</u> Sharnappa Joladarashi and Satyabodh M Kulkarni	International conference on Research in Mechanical Engineering Sciences (RiMES 2017), MIT Manipal	---	3
17	Suitability Study of Jute-Epoxy Composite Laminate for Low and High Velocity Impact Applications	<u>Vishwas Mahesh.</u> Sharnappa Joladarashi and Satyabodh M Kulkarni	International conference on Design, Materials and Manufacture (IcDEM 2018), NITK Surathkal	---	3

SI No.	Title of Paper	Authors ( In the same order as in the paper, underline the Research Scholar's name)	Name of the Journal / Conference /Symposium, Vol., No., Pages	Month & Year of Publication	Category*
18	Comparative Study on Energy Absorbing Behavior of Stiff and Flexible Composites under Low Velocity Impact	<u>Vishwas Mahesh</u> , Sharnappa Joladarashi and Satyabodh M Kulkarni	2nd International Conference on Polymer Composites (ICPC 2018), NITK Surathkal	---	3
19	Study on Stacking Sequence of Plies in Green Sandwiches for Low Velocity Impact Application	<u>Vishwas Mahesh</u> , Sharnappa Joladarashi and S M Kulkarni	4th International Conference on Composite Materials and Material Engineering, 2019 (ICCMME 2019), Tokyo, Japan	---	3
20	Slurry Erosive Study and Optimization of Material and Process Parameters of Single and Hybrid Matrix Flexible Composites using Taguchi Approach	<u>Vishwas Mahesh</u> , Sharnappa Joladarashi and Satyabodh M Kulkarni	2 <sup>nd</sup> International Conference on Emerging Research in Civil, Aeronautical and Mechanical Engineering (ERCAM 2019), NMIT Bangalore	---	3

SI No.	Title of Paper	Authors ( In the same order as in the paper, underline the Research Scholar's name)	Name of the Journal / Conference /Symposium, Vol., No., Pages	Month & Year of Publication	Category*
21	Influence of Laminate Thickness and Impactor Shape on Low Velocity Impact Response of Jute-Epoxy Composite: FE Study	<u>Vishwas Mahesh</u> , Sharnappa Joladarashi and Satyabodh M Kulkarni	2nd International Conference on Recent Advances in Materials and Manufacturing Technologies (IMMT 2019), BITS Pilani, Dubai Campus, UAE	---	3

\*Category: 1: Journal paper, full paper reviewed 2: Journal paper, abstract reviewed  
3: Conference/Symposium paper, full paper reviewed 4: Conference/Symposium paper, abstract reviewed  
5: others (including papers in Workshops, NITK Research Bulletins, Short notes etc.)

**Research Scholar**



(VISHWAS M)

Date: 26/08/2020

Place:Surathkal

**Research Guide(s)**



27/08/2020

(Dr. SHARNAPPA JOLADARASHI)



27/08/2020

(Dr. S M KULKARNI)



**BIO-DATA**

1	Name	VISHWAS M
2	Father's Name	T G Mahesh
3	Date of Birth	August 12, 1985
4	Nationality	Indian
5	Permanent Address	#128, "SAMARPANE", Behind Kailash Ashram, Shettyhally Road, Saptagiri Extension, Tumakuru 572102, Karnataka, India
6	Mobile Number	+91-9986644944
7	Email-ID	<a href="mailto:vishwasmahesh@gmail.com">vishwasmahesh@gmail.com</a> , <a href="mailto:vishwasm@sit.ac.in">vishwasm@sit.ac.in</a>

**Educational Qualifications:**

Sl No.	Qualification	University	College	Period	Performance
1.	Ph.D.	NITK, Surathkal	NITK, Surathkal	2017-2020	8.92 (Course Work)
2.	M.Tech, Product Design and Manufacturing	VTU, Belagavi	NIE, Mysuru	2009-2011	8.02
3.	B.E Mechanical	VTU, Belagavi	SIT, Tumakuru	2003-2007	79.28

I declare that above information is true and correct to best of my knowledge.



26/08/2020

**(VISHWAS M)**